

AD-A151 623

(2) 472

DNA-TR-82-156

**USER'S GUIDE AND HISTORY OF ANFO AS A
NUCLEAR WEAPONS EFFECT SIMULATION
EXPLOSIVE**

J. Petes
R. Miller
F. McMullan
Kaman Tempo
2560 Huntington Avenue
Alexandria, Virginia 22303

31 March 1983

Technical Report

CONTRACT No. DNA 001-82-C-0044

Reproduced From
Best Available Copy

APPROVED FOR PUBLIC RELEASE;
DISTRIBUTION UNLIMITED.

THIS WORK WAS SPONSORED BY THE DEFENSE NUCLEAR AGENCY
UNDER RDT&E RMSS CODE B337082466 P99QAXDE00019 H2590D.

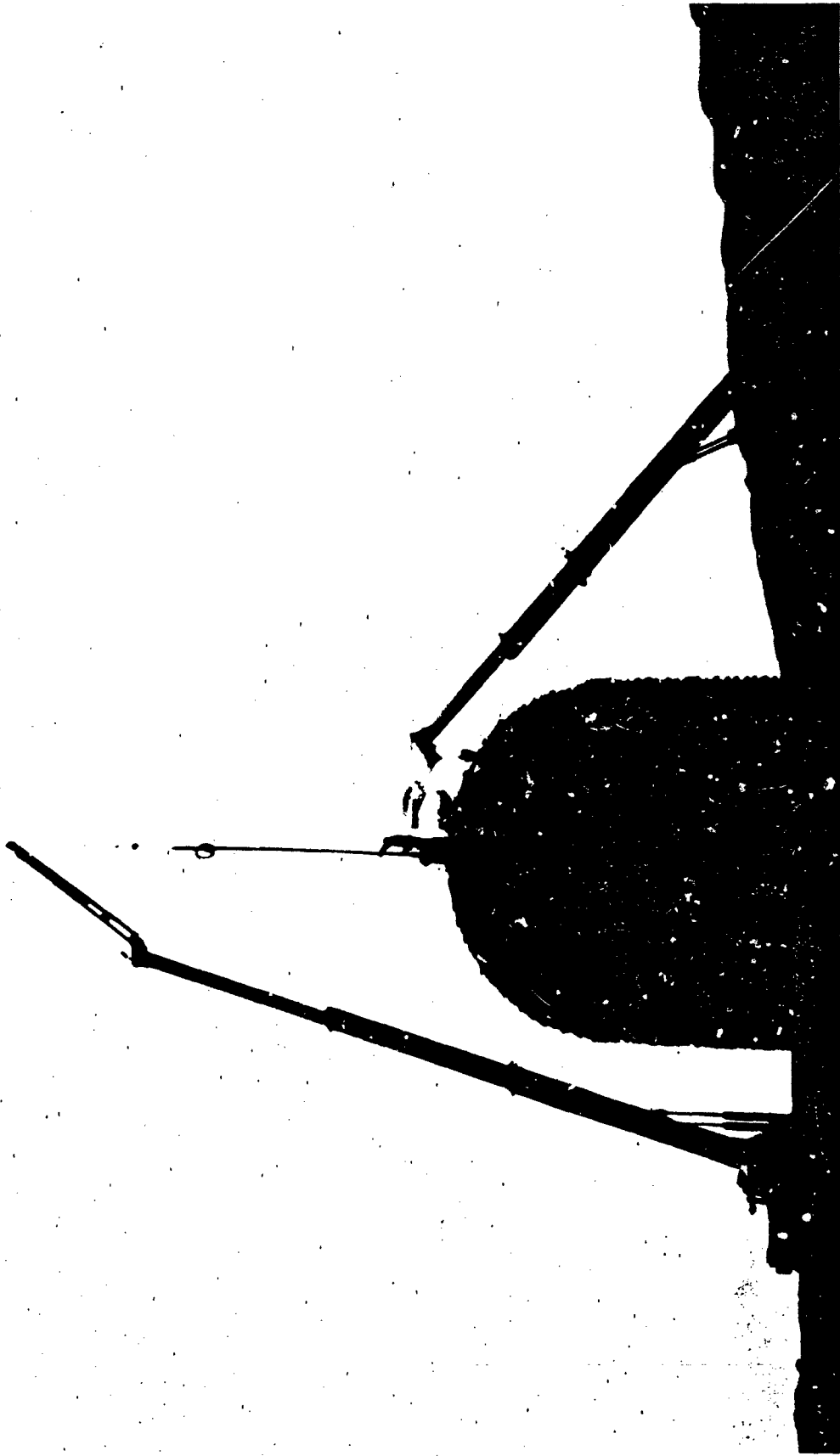
FILE COPY

Prepared for
Director
DEFENSE NUCLEAR AGENCY
Washington, DC 20305

DTIC
ELECTE
MAR 25 1985
S D
B

20000807026

85 01 15 125



FRONTPIECE - DICE THROW - 620 TON ANFO CHARGE BEING ARMED ON SHOT MORNING

UNCLASSIFIED

SECURITY CLASSIFICATION OF THIS PAGE (When Data Entered)

REPORT DOCUMENTATION PAGE		READ INSTRUCTIONS BEFORE COMPLETING FORM
1. REPORT NUMBER DNA-TR-82-156	2. GOVT ACCESSION NO. AD-A151623	3. RECIPIENT'S CATALOG NUMBER
4. TITLE (and Subtitle) USER'S GUIDE AND HISTORY OF ANFO AS A NUCLEAR WEAPONS EFFECT SIMULATION EXPLOSIVE		5. TYPE OF REPORT & PERIOD COVERED Technical Report
		6. PERFORMING ORG. REPORT NUMBER KT-83-012(R)
7. AUTHOR(s) Joseph Petes Robert Miller Frank McMullan		8. CONTRACT OR GRANT NUMBER(s) DNA 001-82-C-0044
9. PERFORMING ORGANIZATION NAME AND ADDRESS Kaman Tempo 2560 Huntington Ave. Alexandria, VA 22303		10. PROGRAM ELEMENT, PROJECT, TASK AREA & WORK UNIT NUMBERS Task P99QAXDE-00019
11. CONTROLLING OFFICE NAME AND ADDRESS Director Defense Nuclear Agency Washington, D.C. 20305		12. REPORT DATE 31 March 1983
14. MONITORING AGENCY NAME & ADDRESS (if different from Controlling Office)		13. NUMBER OF PAGES 334
		15. SECURITY CLASS. (of this report) UNCLASSIFIED
16. DISTRIBUTION STATEMENT (of this Report) Approved for public release; distribution unlimited.		15a. DECLASSIFICATION/DOWNGRADING SCHEDULE N/A since UNCLASSIFIED
		17. DISTRIBUTION STATEMENT (of the abstract entered in Block 20, if different from Report)
18. SUPPLEMENTARY NOTES This work was sponsored by the Defense Nuclear Agency under RDT&E RMSS Code B337082476 P99QAXDE00019 H2590D.		
19. KEY WORDS (Continue on reverse side if necessary and identify by block number) Ammonium Nitrate-Fuel Oil Airblast ANFO Craters High Explosives Explosive Charge Construction Nuclear Weapons Effects Simulation HE Test Operations		
20. ABSTRACT (Continue on reverse side if necessary and identify by block number) The history of the development and use of ANFO as a nuclear weapons blast, cratering, and ground shock simulation source, is traced from 1966 to 1976 when the first full scale target testing operation was conducted on DICE THROW with a 600-ton ANFO charge. The results of the development tests, of DICE THROW, and of subsequent tests with ANFO through PRE-DIRECT COURSE in 1982, are given and analyzed in terms of explosive charge performance. The results indicate that ANFO is a safe, economical and reliable explosive source for effects simulation purposes. The details presented serve as a guide for utilization of ANFO for future		

UNCLASSIFIED

SECURITY CLASSIFICATION OF THIS PAGE(When Data Entered)

20. ABSTRACT (Continued)

similar and more demanding simulation purposes.

Accession For	
NTIS GRA&I	<input checked="" type="checkbox"/>
DTIC TAB	<input type="checkbox"/>
Unannounced	<input type="checkbox"/>
Justification	
By	
Distribution/	
Availability Codes	
Dist	Avail and/or Special
A-1	

Page 32 does not contain proprietary information per Ms. Jarret, DNA/Tech. Library



UNCLASSIFIED

SECURITY CLASSIFICATION OF THIS PAGE(When Data Entered)

USER'S GUIDE AND HISTORY OF ANFO AS A NUCLEAR WEAPONS
EFFECTS SIMULATION EXPLOSIVE.

Preface

This document has two purposes: 1) to record the history of the use of ammonium nitrate/fuel oil (ANFO) as an explosive for use on Defense Nuclear Agency (DNA) sponsored large scale military target response testing operations, and 2) to serve as a user's guide for persons faced with the task of preparing ANFO explosive charges for use on future tests.

Section 1 deals primarily with the history of the use of ANFO. As the Earl of Chesterfield said back in the 18th century, "History is only a confused heap of facts." The ANFO facts are scattered in many documents reporting the results of tests, progress reports on the development of ANFO as a nuclear weapons effects simulation explosive, and undocumented incidents and information pertaining to the subject available in the "corporate memory." Out of this "confused heap of facts," we attempt to make sense and an understandable story. More than that, though, we hope that the history itself will serve partly as a user's guide. George Santayana said, "Those who cannot remember the past are condemned to repeat it." In this history there are many lessons learned which should serve as guides for future operations, and many mistakes made and paths taken which should not be duplicated. Hopefully, the good and the bad will be self evident.

To assure that the good is properly and completely presented for user guidance, Sections 2 and 3 deal with the specifics of ANFO; Section 2 with the physical and chemical characteristics, Section 3 with the design and construction techniques for ANFO charges in several geometries. Section 2 is perhaps the most erudite of all the sections because explosives and explosions by their very nature require highly technical discussions of chemistry, hydrodynamics and thermodynamics to describe their properties. But this section, notwithstanding the detail--or maybe because of it--is the one generating the most unanswered questions.

ANFO has been used by the mining and excavating industries since about 1956--ten years before the concept of using ANFO for simulation purposes and twenty years before it was accepted for large scale test operations. ANFO properties relevant to uses by these industries are adequately documented. However, the properties and characteristics of ANFO in unconfined multi-ton charges as used on DNA test operations have not been studied in any great depth. With more than two dozen variables of ANFO physical and chemical properties to consider, the task, indeed, is complex and formidable. Such things as shock front and fireball anomalies--jets, spikes, protuberances--are observed but no conclusive reasons are available to explain their occurrence. Detonation pressures and velocities as computed using equation-of-state data and as measured in field tests show wide variations, again with no certain reason for the variations. Even equation-of-state formulations show significant differences. Obviously, these known uncertainties need further investigation in future research programs if we want to describe ANFO and its effects in a satisfactory manner. For now, the information in Section 2, a distillation of available information, will have to do.

Section 3 is straightforward; it describes what has been done in the past in designing and constructing hemispherical, spherical, cylindrical, and other charge shapes. These procedures can be continued into the future.

Section 4 presents data obtained on all the major large charge ANFO shots. These data cover mainly airblast, ground shock, craters, and detonation velocity; some data are presented as measured, others are reduced to standard conditions so that comparisons can be made readily between the results of different shots.

The last section of the report, Section 5, looks to the future. It describes ways of tailoring ANFO charge configurations to meet specific objectives for air, underground, or underwater tests. It is hoped that with the information provided in this report, the reader will be in position to create new and innovative uses to better meet the needs of the military target testing community.

Acknowledgements

There is a fine line between plagiarism and research; someone once defined plagiarism as stealing from one author, research as stealing from many. We hope we have not plagiarized but, rather, have been involved in research. Certainly, the bibliography and list of references indicate that we consulted many documents with many authors. We are deeply indebted to these authors for the wealth of information they presented. In our efforts to abstract the data and correlate them, we strove to do more than repeat and paraphrase the information and remarks. We hope we added a cohesion, a continuity, and a clarity that, indeed, makes this report an accurate history of ANFO development and a sound and practical guide for nuclear weapons effects simulation operations.

We would be remiss not to single out Michael M. Swisdak, Naval Surface Weapons Center, White Oak, Maryland, for the many reports and original photographs he provided for use in this report.

And always last but never least, the mechanics of getting the report completed is attributable to exemplary staff support. Nancy Parnell provided graphics and publications support, Becky Lopez typing support, and Carol Seeley typed and edited poorly hand-scripted drafts and the final camera-ready copy. Bouquets, even if only figurative, to all.

Joe Petes
Robert Miller
Frank McMullan

NOTE: In this report both U.S. customary and S.I. units of measurements are used. This is so because some of the reports and documents referred to in the text use U.S. units, others S.I. units, and still others, both. By repeating the original units used in the referenced material it should be easier for the reader to check the references when greater detail is required. However, in our report, we do make conversions between units when it simplifies data correlation among references. A table of conversion factors is included in this report to permit ready conversions when and where the reader desires to do so.

CONVERSION FACTORS

To Convert From	to	Multiply By
atmospheres (standard)	kilopascals (kPa)	101.325
bar	kilopascals (kPa)	100.000
bär	atmosphere	0.9869
bar	pounds/in ² (psi)	14.50
caloric (thermochemical)	joule (J)	4.184
cubic centimeter (cm ³)	cubic feet (ft ³)	3.531 x 10 ⁻⁵
cubic feet (ft ³)	cubic centimeter (cm ³)	28,320.0
feet (ft)	centimeter (cm)	30.48
feet/second (ft/sec)	meters/sec (m/s)	0.3048
inch (in)	centimeters (cm)	2.540
kilograms (kg)	pounds (lb)	2.2046
meters/second (m/s)	feet/second	3.281
pounds (lb)	kilograms (kg)	0.4536
pounds/ft ³	grams/cm ³	0.01602
pounds/inch ² (psi)	kilopascal (kPa)	6.894757
pounds/inch ² -sec (psi-sec)	kilopascals-sec (kPa-s)	6.894757
pounds (mass) (lb)	kilogram (kg)	0.4536
temperature (°C + 17.78)	temperature (°F)	1.8
temperature (°F - 32)	temperature (°C)	0.5556
temperature (°C + 273.16)	temperature Kelvin (K)	1.0
temperature (°F + 459.69)	temperature Rankine (R)	1.0
ton (short 2,000 lb)	kilogram (kg)	907.1847

TABLE OF CONTENTS

	<u>PAGE</u>
PREFACE	1
ACKNOWLEDGEMENTS	3
CONVERSION FACTORS	4
LIST OF ILLUSTRATIONS	9
LIST OF TABLES	15
<u>Section</u>	
1 A HISTORY OF THE USE OF ANFO FOR NUCLEAR WEAPONS BLAST AND SHOCK SIMULATION	17
1.1 Background	17
1.1.1 The Origins of a Concept	17
1.1.2 ...And Questions	18
1.1.3 Bootleg Tests	19
1.1.4 Navy Interests	21
1.1.5 ...And DNA Requirements	22
1.1.6 TNT for Simulation	22
1.1.7 TNT Problems	25
1.1.8 Detonable Gases for Simulation	29
1.2 ANFO Development for Airblast Tests	31
1.2.1 Why Commercial ANFO?	32
1.2.2 Phase I, Small Scale Tests	37
1.2.3 ...And Results	39
1.2.4 Phase II, Test Proposals	45
1.2.5 ...ANFO Events I, II, and III	45
1.2.6 20 Ton and 100 Ton ANFO Test Results	50
1.3 ANFO for Sea Trials or Ground Motion Tests?	59
1.3.1 ANFO Development for Ground Motion Tests	60
1.3.2 Cylindrical ANFO Charges?	60
1.3.3 CHEST	62
1.3.4 ANFO Spheres	64
1.3.5 HEST, DIHEST, etc.	67

CONTENTS (continued)

<u>Section</u>	<u>Page</u>
1.4 ANFO for DICE THROW?	69
1.4.1 Pre-DICE THROW I	69
1.4.2 Phase 1	73
1.4.3 Phase 2	78
1.4.4 Phase 3	79
1.4.5 Pre-DICE THROW II	84
1.5 And Finally, DICE THROW!	95
1.5.1 ...Results	100
1.6 ANFO Epilogue	105
References	107
Appendix 1-A Chronology of ANFO Use for Nuclear Blast and Shock Simulation	109
2 PROPERTIES AND CHARACTERISTICS	111
2.1 General	111
2.2 Ammonium Nitrate	112
2.3 Number 2 Diesel Oil	115
2.4 Ammonium Nitrate - Fuel Oil (ANFO)	116
2.4.1 Production	116
2.5 Detonation Properties	117
2.5.1 Chemical Reaction and ANFO Composition	117
2.5.2 Calculated Detonation Parameters	119
2.5.3 Empirical Detonation Equations	121
2.6 Physical Characteristics of ANFO	123
2.6.1 Fuel Oil Content	125
2.6.2 Prill Size and Bulk Density	128
2.6.3 Detonation Velocity	131
2.7 Large Scale ANFO Detonations	136
2.7.1 Measured FO Content	136
2.7.2 Calculated Bulk Density	139

CONTENTS (continued)

<u>Section</u>	<u>Page</u>
2.7.3 Detonation Velocity measurements	145
2.7.3.1 NSMC Phase 1 Shots	146
2.7.3.2 ANFO I through V	149
2.7.3.3 Pre-DICE THROW I, Events 2, 3, and 4	151
2.7.3.4 Pre-DICE THROW II, Event 2	152
2.7.3.5 DICE THROW	156
2.7.3.6 Other Large Scale Operations	160
2.7.3.7 Detonation Velocity Summary	161
2.8 Environmental Factors (Reference 26)	162
2.8.1 General	162
2.8.2 Detonation Products (Reference 7)	162
2.8.3 Environmental Hazards	164
References	166
Appendix 2-A Steady-State Detonation	169
3 CHARGE DESIGN AND CONSTRUCTION	176
3.1 Introduction	176
3.1.1 ANFO Procurement	176
3.1.2 ANFO Safety	179
3.1.3 Bagged Versus Bulk ANFO	183
3.1.4 Handling ANFO	184
3.2 Charge Design	186
3.2.1 Bagged Design and Construction	186
3.2.2 Cased Bulk Design and Construction	191
3.2.3 Construction Times	200
3.3 Detonation Schemes	202
3.3.1 Booster Safety	210
3.4 Summary	215
References	217

CONTENTS (continued)

<u>Section</u>	<u>Page</u>	
4	EXPLOSION EFFECTS	218
4.1	Introduction	218
4.2	Airblast Results	219
4.2.1	Hemispherical ANFO Charges	220
4.2.2	Spherical ANFO Charge, Tangent to Surface	237
4.2.3	Spherical ANFO Charge, Half Buried	237
4.2.4	Domed Cylindrical ANFO Charges with L/D = 0.75/1	237
4.2.5	Airblast Summary	276
4.3	Crater Results	276
4.3.1	General	276
4.3.2	Craters From Hemispherical Charges	277
4.3.3	Craters From Spherical Charges	283
4.3.4	Craters From Domed Cylindrical Charges (L/D = 0.75/1)	283
4.3.5	Crater Summary	289
4.4	Anomalies	290
4.4.1	ANFO Homogeneity	291
4.4.2	Reentrant Corners	294
4.4.3	Multi-point Detonation	295
4.4.4	Anomaly Summary	299
References		301
5	FUTURE APPLICATIONS OF ANFO	303
5.1	"What is Past is Prologue"	303
5.1.1	"Conventional" Charge Shapes	304
5.2	Blast Directing	307
5.2.1	Horizontal Cylindrical Charges	308
5.3	Other Charge Constructions	318
5.4	ANFO Uses at Sea	319
5.5	ANFO Uses Underground	322
5.6	ANFO Future	322
References		324

LIST OF FIGURES

<u>Figure</u>		<u>Page</u>
1-1	Small ANFO Charge Setup to Determine Free Field Blast Pressure vs Distance	20
1-2	SNOWBALL Charge--500 Tons TNT, Block Built	23
1-3	Nuclear Environment Pertinent to Structure Hardness	24
1-4	MIXED COMPANY Charge--500 Tons TNT Sphere Tangent-to-the-Ground. Charge Supported by Polystyrene Foam Cradle	26
1-5	MIXED COMPANY Anomaly Growth as Viewed by Aerial Camera	27
1-6	MIXED COMPANY Shock Front vs Anomaly Arrival Times in 270° - 360° Quadrant	28
1-7	Prilled Ammonium Nitrate; Prill Diameter About 0.5 to 2 mm	34
1-8	Theoretical Energy of ANFO as Function of Fuel Oil Content	36
1-9	Schematic Diagram of ANFO Charge Assembly in Phase I Study	37
1-10	Completed 1000 lb ANFO Charge in Phase I Study	38
1-11	Mixing ANFO in a Cement Mixer	40
1-12	Pouring ANFO into Form for 1000 lb Charge	41
1-13	Airblast Pressures Form TNT and Field Mixed ANFO Fired on Ground, Scaled to Sea Level Conditions	42
1-14	Equivalent Weight vs Charge Weight for Unconfined ANFO	43
1-15	AN Being Augered From Railroad Hopper Car into ANFO Mixing Truck for Event I	47
1-16	Mixing Truck Augering ANFO into Bagging Truck for Event I	48
1-17	Tanker Truck Feeding AN into Mixing Truck: ANFO Augered into Fiberglass Container for Event III	49

ILLUSTRATIONS (continued)

<u>Figure</u>		<u>Page</u>
1-18	Event I - 20 ton ANFO Hemisphere	51
1-19	Event I - First Layer of Bags Completed with Loose ANFO Filling in Voids	52
1-20	Event III - 100 ton ANFO Charge in Fiberglass Container	53
1-21	Event III - Detonation of 100 ton ANFO Charge: Unperturbed Shock Wave Visible	55
1-22	Peak Pressure vs Scaled Distance for ANFO Events I, II, and III. Scaled to Sea Level Conditions	56
1-23	Equivalent Weight vs Pressure for Phase I ANFO Surface Bursts	57
1-24	Cratering High Explosive Simulation Technique	63
1-25	25 ton ANFO IV Tangent Sphere Charge	65
1-26	Sketch of HEST Facility	68
1-27	DIHEST Concept	70
1-28	Charge Geometries and Detonation Points	77
1-29	Cross Section of Bulk ANFO Capped Cylinder, (L/D = 0.84/1), pre-DICE THROW I, Event 2, 6 tons	80
1-30	Completed Bagged ANFO Charge, pre-DICE THROW I, Event 4	82
1-31	Design of Bagged ANFO Capped Cylinder (L/D = 0.75/1), pre-DICE THROW I, Event 4	83
1-32	Initial NSWC ANFO Stacking Plan, pre-DICE THROW II, Event 2	85
1-33	ANFO Charge Configuration - pre-DICE THROW, Event 2	87
1-34	Final NSWC ANFO Stacking Plan, pre-DICE THROW II, Event 2	88
1-35	Completed Charge for pre-DICE THROW II, Event 2, (L/D = 0.75), 120 tons	89

ILLUSTRATIONS (continued)

<u>Figure</u>		<u>Page</u>
1-36	Main Booster Assembly (MBA) - pre-DICE THROW II, Event 2	91
1-37	Booster Initiation System (BIS), pre-DICE THROW II, Event 2	92
1-38	Temperature-Time Record in ANFO Stack, pre-DICE THROW II, Event 2	94
1-39	Test Group Staff Organization	97
1-40	Site Location for DICE THROW (620 ton ANFO) and pre-DICE THROW II, Event 2 (120 ton ANFO)	98
1-41	DICE THROW Charge: Placing BIS into Position	99
1-42	Measured Incident Shock Overpressure vs Ground Range - DICE THROW - 620 ton ANFO Shot	101
1-43	Overpressure vs Ground Range, pre-DICE THROW II, Event I, 100 ton TNT Tangent Sphere, BRL Data	102
2-1	Activation Energy	114
2-2	ANFO (94.5/5.5) Detonation Pressure	124
2-3	ANFO (94.5/5.5) Detonation Velocity	124
2-4	Energy and Sensitivity vs Fuel Oil Content	126
2-5	Change in Initiation Sensitivity with Particle Sizing	129
2-6	Particle Size Distributions for Various ANFO Events	130
2-7	Change in Initiation Sensitivity with Density	131
2-8	Relationships of Several ANFO Variables (Reference 15)	133
2-9	ANFO Detonation Velocities vs Primer Type	135
2-10	ANFO Shots for Blast and Shock	137
2-11	ANFO Detonation Velocity vs Apparent Bulk Density	148

ILLUSTRATIONS (continued)

<u>Figure</u>		<u>Page</u>
2-12	ANFO I-IV Detonation Velocity Geometries	150
2-13	Pre-DICE THROW II, Event 2 Detonation Velocity Histories	153
2-14	DICE THROW ANFO Stack (cutaway)	157
2-15	DICE THROW Detonation Velocities	159
3-1	Filling Voids With Bulk ANFO (DICE THROW)	187
3-2	Stacking Plan for ANFO I	189
3-3	Plywood Form and Protective Housing for DICE THROW	190
3-4	DIRECT COURSE Sphere Design	194
3-5	Overall Tower Design, Pre-DIRECT COURSE	196
3-6	Charge Suspension Details, Pre-DIRECT COURSE	197
3-7	Conceptual Design of Pre-MINE THROW Charge	199
3-8	Detonation Designs for Cylindrical Charges	204
3-9	Firing System, Lawrence Livermore Laboratory Explosives Diagnostics	206
3-10	Booster Diagnostic Light Pipe System (MISERS BLUFF II-1 and 2)	207
3-11	ANFO II and III, Schematic Diagram	209
3-12	Segment of Octol Booster Ready for Emplacement, DICE THROW	211
3-13	Octol Booster Emplacement Being Completed, DICE THROW	212
3-14	Securing Booster to PVC Pipe With Tape, DICE THROW	213
3-15	Cross Section of Booster System, DICE THROW	214
4-1	Secondary Pressure Pulses on ANFO III	231
4-2	Times of Arrival vs Scaled Distance for ANFO At DRES (Scaled to Sea Level Conditions)	232

ILLUSTRATIONS (continued)

<u>Figure</u>		<u>Page</u>
4-3	Peak Secondary Shock Pressures vs Scaled Distances, ANFO Trials, DRES, August 1969 (Scaled to Sea Level Conditions)	233
4-4	Reduced Pressure-Distance for ANFO I, II, and III, Scaled to Sea Level Conditions	234
4-5	Reduced Time of Arrival (TOA') - Distance for ANFO I, II, and III Scaled to Sea Level Conditions	235
4-6	Reduced Positive Phase Duration (τ') - Distance for ANFO I, II, and III Scaled to Sea Level Conditions	236
4-7	Reduced Impulse (I') - Distance for ANFO I, II, and III Scaled to Sea Level Conditions	236
4-8	Reduced Airblast Parameters for ANFO IV Scaled to Sea Level Conditions	240
4-9	Reduced Airblast Parameters for ANFO V Scaled to Sea Level Conditions	242
4-10	Reduced Pressure for Domed Cylinders (L/D = 0.75/1)	267
4-11	Reduced Time of Arrival for Domed Cylinders (L/D = 0.75/1)	268
4-12	Reduced Positive Duration for Domed Cylinders (L/D = 0.75/1)	269
4-13	Reduced Impulse for Domed Cylinders (L/D = 0.75/1)	271
4-14	Reduced Dynamic Pressure for Domed Cylinders (L/D = 0.75/1)	273
4-15	Reduced Dynamic Pressure Impulse for Domed Cylinders (L/D = 0.75/1)	274
4-16	Typical Crater Profile	278
4-17	Mean Apparent Crater Profiles for 20 Ton Hemispherical Shots	281
4-18	Mean Apparent Crater Profiles for 100 Ton Hemispherical Shots	282

ILLUSTRATIONS (continued)

<u>Figure</u>		<u>Page</u>
4-19	Mean Apparent Crater Profiles for 20 Ton TNT Equivalent Surface Tangent Spherical Shots	284
4-20	Mean Apparent Crater Profiles for 20 Ton TNT Equivalent Half Buried Spherical Shots	285
4-21	MILL RACE Surface Breakout Profile Along Radial 178 ⁰	298
5-1	Pressure and Positive Duration from Surface Burst ANFO Charges (Scaled to Standard Conditions)	305
5-2	Cylindrical Charge L/D Effects on Pressure	306
5-3	Blast Directing Scheme	309
5-4	Two Ton Blast Directing System for DIAL PACK	310
5-5	Plan View of Azimuthal Blast Lines	311
5-6	Pressure vs Azimuthal Angle for L/D = 1 Cylindrical Charge	312
5-7	Pressure vs Azimuthal Angle for L/D = 5 Cylindrical Charge	314
5-8	Impulse vs Azimuthal Angle for L/D = 1 Cylindrical Charge	316
5-9	Impulse vs Azimuthal Angle for L/D = 5 Cylindrical Charge	317
5-10	Natural Slumping Shaped Charge	318
5-11	Sea Trial Concept - At Anchor or Underway	320

LIST OF TABLES

<u>Table</u>	<u>Page</u>
1-1 Particle Size Distribution of a Representative 50-lb Bag of Prilled Ammonium Nitrate	35
1-2 ANFO Charge Development Program Participants	71
1-3 Pre-DICE THROW Charge Development Program	74
1-4 Pre-DICE THROW II, Event 2 Booster System Details	90
1-5 Detonation Velocities of ANFO Charges	95
2-1 Properties of Fuel Oil and Red Dye	116
2-2 Manufacturers' Data on ANFO	118
2-3 Detonation Properties of ANFO	120
2-4 C-J Parameters for ANFO	121
2-5 Large ANFO Charge Bulk Densities and Fuel Oil Content	127
2-6 Stacking Data for MISERS BLUFF II-22	140
2-7 Stacking Data for MISERS BLUFF II-26	142
2-8 ANFO Large Charge Summary	147
2-9 ANFO Detonation Product Composition (Moles/kg of ANFO)	163
2-10 Toxic Products From a 120-Ton ANFO Explosion	164
3-1 Test Method Used to Determine Amount of No. 2 Diesel Fuel in AN/FO Mixture	180
3-2 Certification of Fuel Oil and Particle Size Analysis	181
3-3 Charge Construction Times	201
3-4 Boosters Used on Selected Large ANFO Charges	203
3-5 Booster Detonation Times	205

TABLES (continued)

<u>Table</u>	<u>PAGE</u>
4-1 ANFO I Airblast Data	221
4-2 ANFO II Airblast Data	224
4-3 ANFO III Airblast Data	227
4-4 ANFO IV Airblast Data	237
4-5 ANFO V Airblast Data	241
4-6 Pre-DICE THROW I-4 Airblast Data	243
4-7 Pre-DICE THROW II-2 Airblast Data	244
4-8 MISERS BLUFF II-I Airblast Data	248
4-9 DICE THROW Airblast Data	250
4-10 MILL RACE Airblast Data	260
4-11 Crater Dimensions for Hemispherical and Spherical Charges (Reference 18)	280
4-12 Crater Dimensions for Domed Cylindrical ANFO Charges with L/D = 0.75/1	286
4-13 Crater Dimensions for Charges with Energy Release of 20 Tons TNT Equivalent	289

SECTION 1

A HISTORY OF THE USE OF ANFO FOR NUCLEAR WEAPON BLAST AND SHOCK SIMULATION

1.1 BACKGROUND

On 6 October, 1976, a short bright flash, a long, loud bang, and a large gray mushroom cloud ushered in a new era for nuclear weapon blast and shock wave simulation. A 628-ton domed cylindrical ANFO (ammonium nitrate-fuel oil) charge was detonated at the White Sands Missile Range, New Mexico, as part of Operation DICE THROW, a test to determine the vulnerability of military hardware and targets to nuclear weapon proportioned airblast and ground shock. Six foreign countries, 28 U.S. agencies, and all the U.S. military services participated in this Operation which involved the largest single explosive charge of ANFO ever detonated under controlled conditions.

1.1.1 The Origins of a Concept

The start of this era came ten years, almost to the month, after the concept for using ANFO for nuclear weapon effects simulation first was conceived. In August 1966, two NSWC (Naval Surface Weapons Center, formerly Naval Ordnance Laboratory) scientists were discussing the general subject of nuclear weapon blast simulation, and in particular, the forthcoming large-scale field tests (to which they had been invited as official observers), of a new simulation technique. This new method used detonable gases as the explosion source. One of the men, L. D. Sadwin, had some experience with ANFO and knowledge of its uses by the mining industry; the other, J. Petes, was familiar with the Navy's and DNA's (Defense Nuclear Agency, formerly Defense Atomic Support Agency) requirements and endeavors to find an adequate replacement for TNT, the then current explosive used for large-scale nuclear weapon blast simulation tests. They knew of the problems associated with the use of TNT, and they were aware of the July 1966 attempt to detonate 20 tons of an oxygen-propane mixture in a hemispherical balloon which test was aborted when the balloon suffered structural failure.

"Why not use ANFO?" they reasoned. "ANFO is inexpensive, relatively safe, and cost-effective in terms of energy output - the very reasons that the mining industry uses it in ever-increasing amount. It is readily available; basically 'AN' is commercial fertilizer made by industry in millions of pounds per day quantities, and the 'FO' is ordinary #2 diesel oil, easily available throughout the country. Also, the ANFO may have hydrodynamic advantages over the block built TNT charges then being used on major military hardware tests. Perhaps detonation front and blast anomalies would be minimized in the ANFO charges (as they were shown to be in the gas balloon simulation technique) because of the greater homogeneity of the prilled explosive material compared to the discontinuities encountered between TNT blocks."

1.1.2 . . . And Questions

Their enthusiasm, however, was moderated by many questions, answers to which were not immediately available, nor indeed, were they to be found at all later in the literature. Will ANFO detonate reliably with predictable blast output in large unconfined piles? Mining industry experience was limited to ANFO charges heavily confined in relatively small diameter bore holes and most loads were primed with dynamite placed every ten feet along the column length to sustain detonation. Such confinement and multiple and time-sequenced detonation points would never do for ANFO charges designed to produce ideal airblast fields. For one, charge confinement was deemed inappropriate; the confining case could produce fragments that could jeopardize test targets directly, and depending on the size of the fragments, they could produce airblast anomalies through the bow waves associated with the fast moving fragments. For another, single point initiation of the charges (as used for hemispherical and spherical TNT charges) was considered necessary to assure a constantly advancing symmetrical detonation front so that the blast field could be predicted reliably.

Would large ANFO charges in the hundreds of tons size be safe - chemically and thermally stable over a period of time, say a month - or would there be some reactions taking place generating heat or chemical products which would lead to auto-detonation? The Texas City explosion in 1947 was remembered in

which two shiploads of ammonium nitrate fertilizer caught fire for some undetermined reason and detonated with disastrous results--hundreds killed, thousands injured, and millions of dollars worth of damage.

Would the fuel oil settle out of the ANFO mixture during the days or weeks it may take to construct the charge and fire it? The mining industry seldom, if ever, faced this problem; they would mix the AN and FO on site just before filling the bore holes, or would use premixed ANFO freshly delivered from a nearby manufacturer.

Assuming detonation of a large charge of ANFO, say 500 tons, would its blast output be similar to that of a 500-ton TNT charge? It was realized that the density of bulk ANFO was considerably less than that of TNT and thus, its detonation velocity and pressure would be less. This would mean that the peak airblast output of an ANFO charge should be less than for TNT, but at the pressure levels of most concern to target studies, about 2000 to 3000 psi and less, would the ANFO blast be adequate? This could not be answered at the time.

These questions and answers, pros and cons, doubts and concerns--and hopes--were batted back and forth by Petes and Sadwin, and a little later, with their colleagues. It was felt that before a real case could be made to the Navy and DNA for support to investigate the merits of the ANFO concept, some basic information on the detonability of unconfined ANFO would be required.

1.1.3 Bootleg Tests

The Air-Ground Explosions Division of NSWC was heavily engaged in experimental field work with military high explosives. It was a relatively simple, although unorthodox, matter to introduce several ANFO shots between authorized work at its remote Stump Neck, Maryland Airblast Facility. J. F. Pittman conducted these bootleg tests in mid-August 1966 with 8-lb, 20-lb, and 64-lb charges of ANFO contained in thin plastic paint buckets and garbage cans which were considered to be essentially non-confining (Figure 1-1).

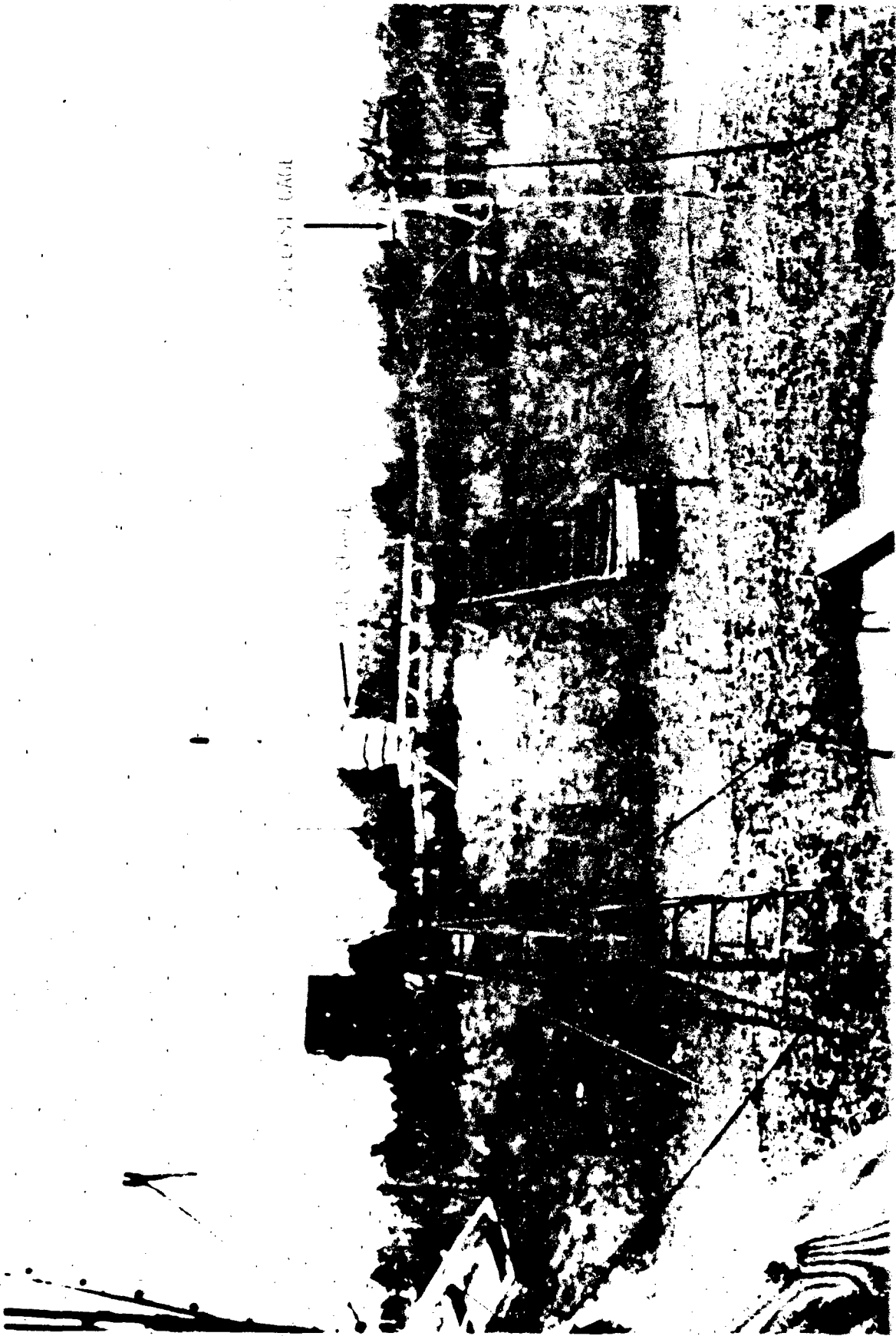


FIGURE 1-1. SMALL ANFO CHARGE SETUP TO DETERMINE FREE FIELD BLAST PRESSURE VS DISTANCE.

The test results were encouraging. The charges detonated reliably; repetitive shots with the same weight charges produced the same pressure-distance curves in the range of pressures measured, from 5 to 100 psi. But the outputs of the different weight charges, as evaluated in terms of TNT equivalence, were different. The 8-lb charges had a TNT equivalence of about 0.47, the 20-lb charges 0.51, and the 64-lb charges about 0.75. This increasing output (or TNT equivalence) with increasing charge weight was interpreted to mean that the critical size--the minimum diameter required to attain a steady state detonation velocity through the explosive--was greater than that realized in the small charges used; hence, the full explosive energy of the charges was not realized. Of course, the 64-lb charges may have attained full output, but this could not be established from the data. The hope was that, in fact, full output was not attained, that larger ANFO charges would produce blast output more nearly approaching that of TNT.

Data obtained by R. W. Van Dolah in Bureau of Mines tests investigating the sensitivity of ANFO showed that for 1500-lb charges, the TNT equivalence of ANFO was 1.0 for pressures up to 10 psi (Reference 1). Larger charges than those fired in the bootleg program would have to be fired to check this out. But larger charges could not be bootlegged; they would have to be tested under some authorized, funded, and planned program. The Navy and DNA were logical places to seek the necessary support; both had compelling reasons for seeking nuclear weapon blast and shock simulation techniques.

1.1.4 Navy Interests . . .

The Navy had but recently (1965) fielded at Kahoolawe, Hawaii, Operation SAILOR HAT, a three event airblast program in which 500-tons of TNT were fired on each event. Fully operational combatant ships and naval structures, weapons, and equipment located on a floating platform (a converted aircraft carrier hull) were subjected to long duration blast waves with amplitudes up to about 10 psi. These tests were designed to establish the vulnerability/-survivability of these navy ships and items and to provide guidelines for hardening in a nuclear weapon blast environment. Much valuable information was obtained on the tests, information not available through analysis or other

simulation techniques. The Navy looked forward to doing more such tests, but the costs were staggering; it was estimated that the cost of each 500-ton charge was about \$1,000,000. The Navy was in the market for a cheaper explosion simulation source.

1.1.5 . . . And DNA Requirements

DNA, as a Department of Defense agency, had similar and broader reasons for seeking nuclear weapons blast and shock simulation techniques; the use of nuclear weapons and devices in the atmosphere was prohibited by the first test moratorium of October 1958 and by its successor, the Nuclear Test Ban Treaty of 1963. Yet, the Department of Defense had the continuing requirement to obtain nuclear weapons effects data on military equipment and targets. Techniques to simulate airblast and ground shock of nuclear weapon proportions were obvious alternatives. DNA supported and encouraged the pursuit of many such alternatives.

1.1.6 TNT For Simulation

Initially, interest was in the response of targets primarily to airblast. In 1959, DNA initiated a joint program with DRES (Defence Research Establishment, Suffield) Canada, to develop TNT as the explosion source for long duration airblast waves. This program continued, expanded, and accelerated DRES's earlier efforts investigating the properties of TNT in various forms for field applications. Using 12x12x4 inch blocks of TNT weighing 33 lbs each, charges were constructed on the ground in a hemispherical shape with single point initiation occurring at the ground in the center of the equatorial plane. This development culminated in 1964 on Operation SNOWBALL when a 500-ton hemispherical charge was detonated successfully (Figure 1-2). Additional 500-ton TNT hemispheres were fired on Operation SAILOR HAT in 1965.

As time went on, the interests of the military services extended to subsurface facilities, structures, and targets; ground motion as well as airblast became a matter of concern to the military scientific community (Figure 1-3). Analyses and progressively larger scaled experimentation showed that a spherical charge built on and tangent to the ground would produce airblast, ground shock, and cratering energies in the same relative

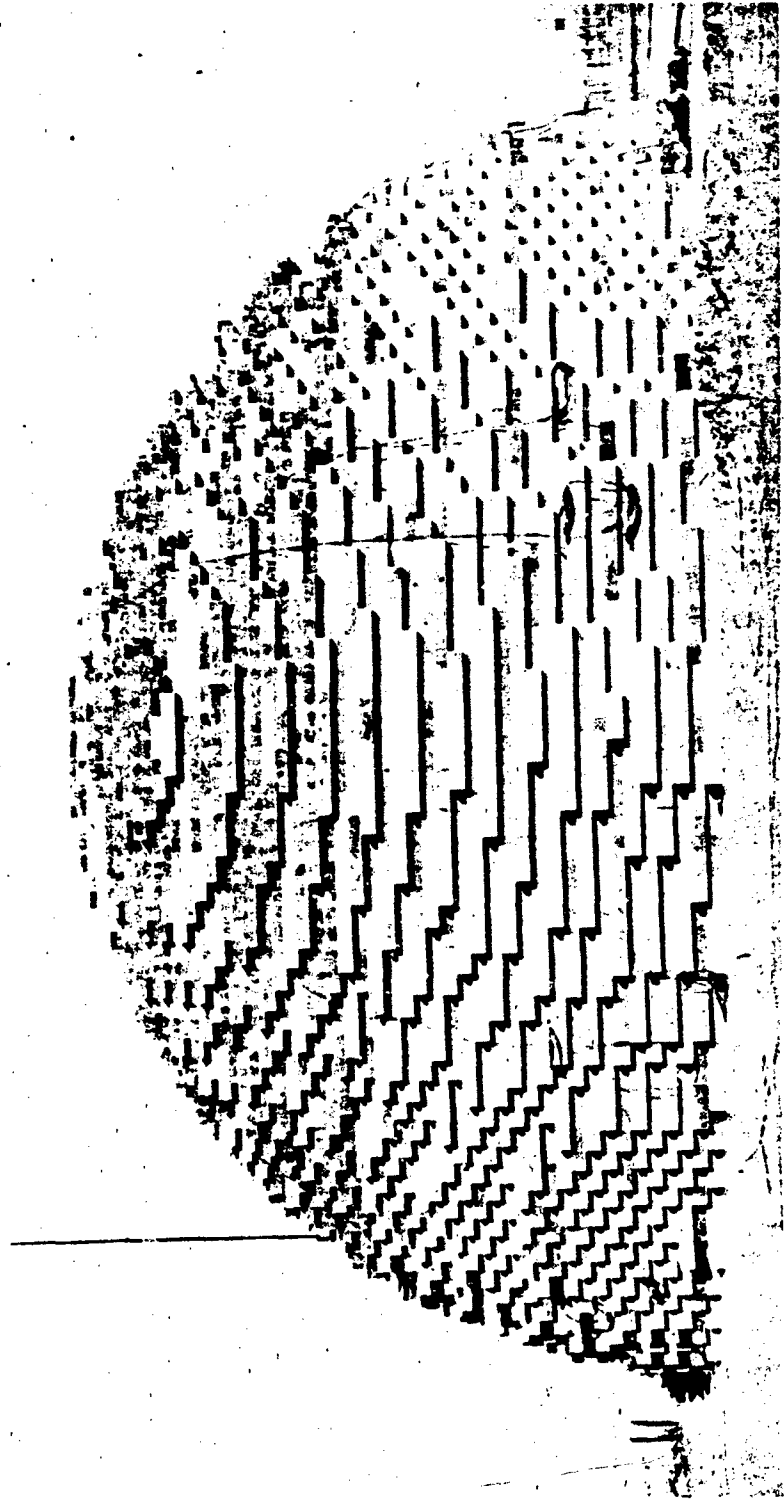


FIGURE 1-2. SNOWBALL CHARGE - 500 TONS TNT, BLOCK BUILT.

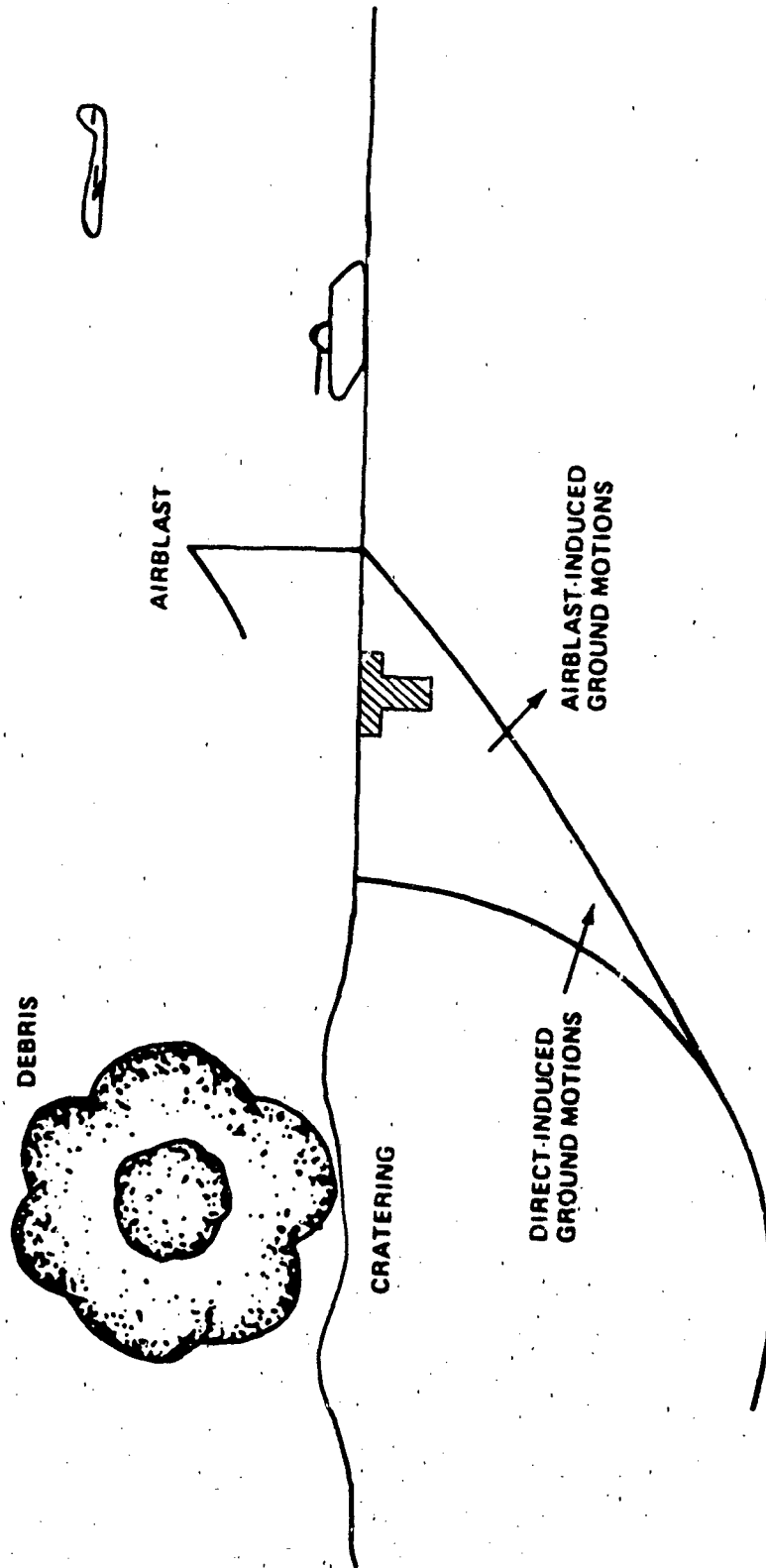


FIGURE 1-3. NUCLEAR ENVIRONMENT PERTINENT TO STRUCTURE HARDNESS.

proportions as a surface burst nuclear weapon. This relationship of effects was deemed important so as to best satisfy, on a single shot, the requirements of the military scientists and analysts interested in blast, craters, and ground shock. Block built charges were now stacked in this geometry. A number of such 500-ton charges were detonated on military test operations, namely PRAIRE FLAT (1968), DIAL PACK (1970), and MIXED COMPANY (1972) (Figure 1-4).

1.1.7 TNT Problems

As useful as the TNT block built charges were, they presented problems. For one, as the Vietnam War continued, TNT was becoming available in ever shorter supply; the World War II surplus was about exhausted and the TNT manufacturing plants were nearing the end of their productive lives. For another, the cost of processing the TNT into 33-lb blocks and placing the charge in the field ready for test was high--up to \$1,000,000 for a 500-ton charge.

A third problem surfaced early in the use of these large, block built charges--the airblast front was plagued with large, unpredictable anomalies (Figure 1-5). These manifest themselves generally as ahead running spikes, jets, and protuberances on the main shock front (Figure 1-6). Some of these anomalies extended 1,000 ft from the explosion source and perturbed the pressure field within a 30° sector measured from the origin. Three such major anomalies, not uncommon on some of the tests, could adversely influence 25% of the area in which targets were located and thus invalidate expensive and important target response studies.

An extended and detailed study of anomalies was initiated by a working group of American, British, and Canadian scientists under the auspices of TTCP (The Technical Coordinating Program) soon after J. M. Dewey of DRES, in 1965, reported the occurrence of serious blast front perturbations on operation SNOWBALL (Reference 2). The report of the working group (Reference 3), published in 1970, found that anomalies were, in fact, characteristic to explosions of solid high explosives; evidence was found for jets, spikes, and perturbations from charge sizes ranging from gram weights up to the 500-ton charges of immediate interest. They concluded that one of the major reasons



FIGURE 1-4. MIXED COMPANY CHARGE - 500 TONS TNT SPHERE TANGENT-TO-THE-GROUND.
CHARGE SUPPORTED BY POLYSTYRENE FOAM CRADLE.

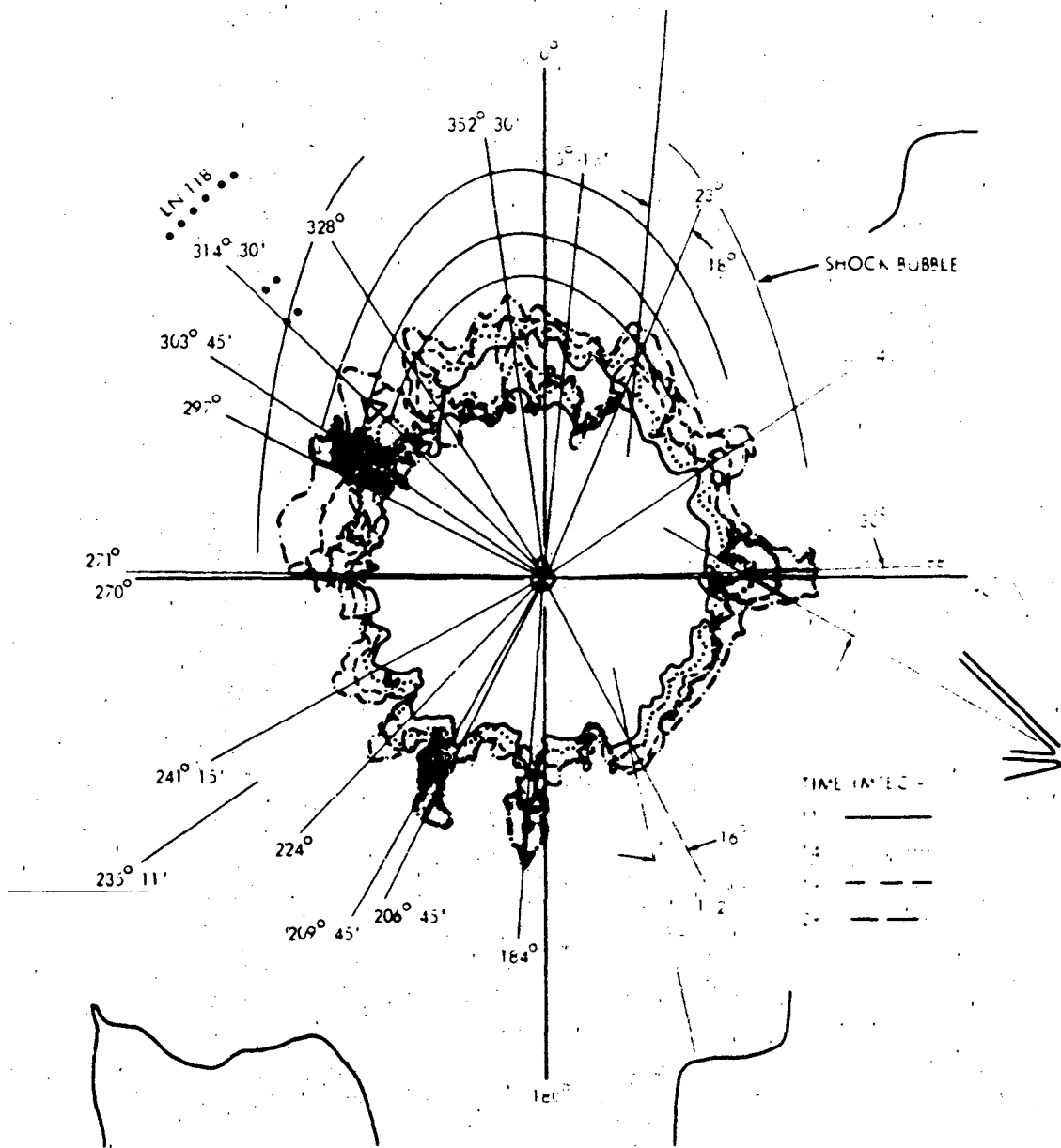


FIGURE 1-5. MIXED COMPANY ANOMALY GROWTH AS VIEWED BY AERIAL CAMERA.

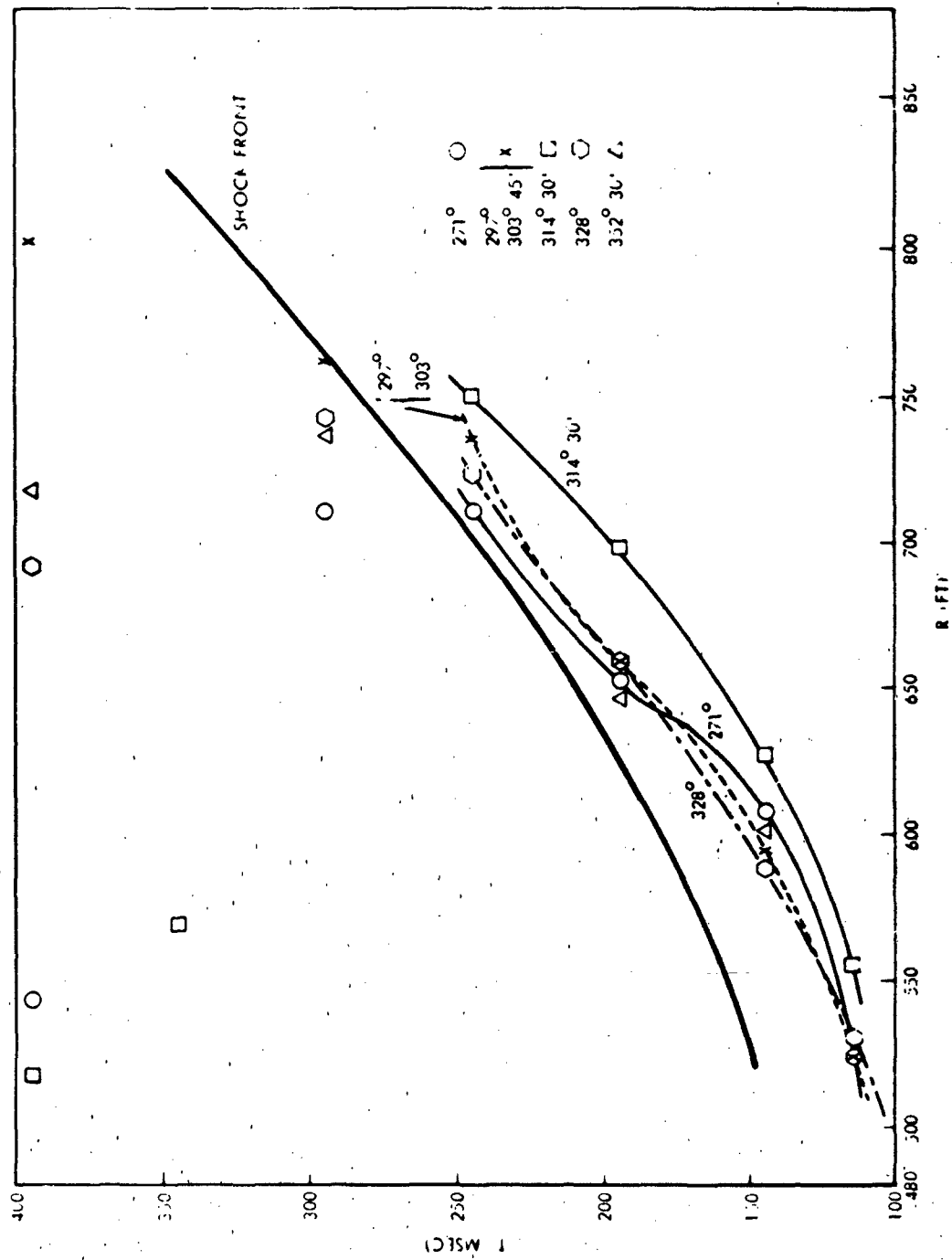


FIGURE 1-6. MIXED COMPANY SHOCK FRONT VS ANOMALY ARRIVAL TIMES IN 270°-360° QUADRANT.

for the anomalies arises from the very unstable nature of the detonation process as it progresses from explosive grain to explosive grain on a microscale; this is particularly true for cast TNT with its relatively large and irregular granular structure. In block built TNT charges, the instabilities are accentuated on a larger scale because of the significant reduction in detonation velocity as it progresses across the somewhat irregular interfaces between blocks.

The TTCF working group suggested ways to reduce the number and severity of the anomalies that were explosive dependent but offered little hope for eliminating them so long as the 12x12x4 inch block built construction was used. (All the anomalies identified by the TTCF working group are not explosive oriented; some arise along paths of ground surface discontinuities, e.g., roads and trenches, and occur regardless of the high explosive used.) Significantly, they recommended the study of other explosive materials for nuclear weapon blast simulation--detonable gases, slurries, and ANFO.

1.1.8 Detonable Gases for Simulation

DNA was already supporting efforts to determine the merits of detonable gases; in 1965, project SLEDGE (Simulating Large Explosive Detonable Gas Experiment) was initiated (Reference 4). Detonable gases had the promise of attractive features: 1) if the gas mixture was lighter than air, then a balloon filled with the gases would permit conducting large scale, i.e., multi-ton, blast tests at high altitudes to help determine the response of in-flight missiles and aircraft in a realistic environment; 2) the microscale homogeneity of the gas mixture should be better than that of TNT, thus leading to better detonation properties and, hence, better blast fields without serious anomalies as compared to TNT shots; and 3) the low density of the detonable gas mixture would match the density of the surrounding air better than TNT, and thus, reduce the Taylor instabilities which were advanced as another source of anomalies for TNT charges.

The fact that detonable gases would produce peak pressures considerably lower in magnitude than those generated by TNT was of minimum concern. Most military targets of interest were usually exposed at less than the 600 psi

maximum expected from detonable gases. In fact, this low peak pressure had an advantage: for surface bursts, with the gas charge resting on the ground, cratering with its deleterious ejecta of crater material would be reduced or even eliminated.

Analyses, small-scale experiments with oxygen-methane and oxygen-propane mixtures, and a large test of a surface burst with 20-tons of oxygen-propane in a 125-ft diameter hemispherical balloon (Operation DISTANT PLAIN, Event 2a, 1966, Reference 5), showed that, indeed, the promises could be realized. On none of the tests were anomalies observed. The 20-ton surface test produced a slight surface depression under the charge with no crater ejecta, and a 1000-lb mixture of oxygen and methane could fly and be detonated.

However, serious operational problems faced the gas balloon endeavor. The very construction of large balloons, 100-ft in diameter and more, was itself a challenge which was only partially met; on one test with a 110-ft diameter balloon, the balloon material failed, aborting the experiment. Additionally, the cost of fabrication for a large balloon and filling it with the detonable gases was estimated to be rather high, perhaps \$500,000 for a 380-ft diameter balloon necessary to contain 500-tons of detonable gases. Handling and filling the balloon were difficult. Long filling times were required for large quantities of gases. The balloon was susceptible to wind damage during the filling procedure even though an airfilled ballonet was used to achieve some structural rigidity of the balloon while the slow oxygen and methane or propane filling was taking place.

The most serious problem was the one concerned with safety. Static charges could build up on the balloon material through wind action even though attempts were made to cover the balloon material with a conductive coating. The hazards of discharging static charges through arcing in an atmosphere of detonable gases is, of course, well known. It was on 22 October 1966, while observing the premature static discharge ignition of a 110-ft diameter balloon filled with oxygen and about half of its quota of methane, that gave Petes and Sadwin strengthened reasons for considering ANFO as a nuclear weapon blast simulation source.

1.2 ANFO DEVELOPMENT FOR AIRBLAST TESTS

Early in November 1966, Petes and Sadwin disclosed their thoughts on the use of ANFO as a nuclear weapon blast simulant explosive to J. Kelso, DNA, and Y. Park, NAVSEC (Naval Ships Engineering Center, then Naval Ships Systems Command) (Reference 6). Many discussions were held. All the information in hand on ANFO was presented and discussed; the merits of ANFO--its documented low cost, about five cents per pound delivered to any continental test site; the controlled and repeatable detonability of unconfined ANFO as demonstrated in Pittman's tests; the ready availability of ANFO on the commercial market from dozens of manufacturers; and, the safety and ease of handling as evidenced by its increased acceptance and use (approaching one million tons per year) by the mining and quarrying industries. The unresolved questions and doubts originally and subsequently raised by Petes and Sadwin were reviewed also, so that the technical and financial risks involved in exploring ANFO as a suitable blast simulation source could be put in perspective. Would large charges, 500-tons, detonate reliably? Would self-heating of such large charges be a hazard? Would the known hygroscopicity of ANFO preclude its use for Navy purposes in a sea or near sea environment? Would the fuel oil settle out of the ANFO? Questions and more questions which had no ready answers. The apparent merits of ANFO and the enthusiastic and persistent (and, perhaps, overstated) salesmanship of the NSWC personnel outweighed the doubts: Kelso and Park agreed to fund a small experimental study to determine the feasibility of using ANFO. An official proposal was submitted by NSWC to NAVSEC in March 1967 (Reference 7); reprogrammed DNA funds were provided via NAVSEC in December 1967.

The principal objectives of this new task were to determine the blast yield for hemispherical ANFO charges weighing up to 4000-lbs and to demonstrate, on this scale, the predictability of the airblast field. Depending on the results of this task, a follow-on program would be recommended with the goal of eventually constructing and testing up to 500-ton charges.

1.2.1 Why Commercial ANFO?

At the very start of this project, the fundamental decision was made to use commercially developed and available material, such as Gulf Oil Corporation* Spen-C-N-1 premixed ANFO and N-IV prilled AN. The project specifically avoided the attractive research task of developing a new AN-based explosive or even exploring the many AN-based explosives described in the literature and patent disclosures. Such an investigation would be time consuming, costly, and probably would have been counter-productive by compromising the demonstrated virtues of commercial ANFO--low cost, safety, and ready availability. It was recognized that additives such as aluminum and TNT would increase the blast output of AN-based mixtures but the greater sensitivity of these mixtures militated against advocating their pursuit and use. Water as an additive to make an AN slurry or gel was also discussed as an alternative but the idea was dismissed from further consideration because of the obvious requirement for a case to contain the mixture; casing, particularly heavy casing, could result in deleterious fragment effects on the blast field and the test targets.

The selection of ANFO and AN was made with some trepidation: safety was of paramount concern. After all, single quantities of up to 500 tons of ANFO were envisioned for test purposes; an accidental explosion was unthinkable. Neither industry nor the military had experience with such large quantities. Industry uses ANFO loaded into relatively small diameter (1" to 12") columns set in a pattern of bore holes optimized for rock break-up. Any one hole could hold up to about 1,000 lbs of ANFO. The military has used AN in relatively small, one-man deployable cratering and demolition charges (AN 86.6%, dinitrotoluene 7.6%, non-explosive ingredients 5.8%), and in mixtures with TNT for use as the explosive fill for ammunition. Amato 80-20 contained 80% AN and 20% TNT; amato 50-50 had 50% AN and 50% TNT. (It is interesting to note that just as a driving force for suggesting ANFO as a nuclear blast simulation source was the shortage of TNT in 1960-70, so the amato's were introduced as a military explosive during World War I in order to reduce the demand for TNT which was then in short supply.)

*Mention of proprietary items constitutes neither endorsement nor criticism.

Although AN is not classified under U.S. Department of Transportation regulations as an explosive, but rather as an oxidizer, AN can detonate and has detonated with catastrophic results (Reference 8). The most recent large accident was the aforementioned Texas City, Texas explosion on 16 April 1947. Two freighters loaded with commercial fertilizer grade AN detonated at the pier resulting in 454 deaths, 150 missing, 3,000 injured, and damage estimated at \$50,000,000. A fire in one of the ships has been attributed as the cause of the resulting explosion.

Twenty-six years prior to the Texas City explosion another large AN accident took place in what, in retrospect, appears like bizarre circumstances. The Badesche Company manufactured AN-based fertilizer at its plant at Oppau, Germany. Large masses of the material were stored outdoors where it was subject to the ravages of weather. The AN would cake because of its hygroscopicity and it could freeze. It had been the standard practice to break up the caked AN with explosives. On 29 September 1921, this procedure was used with disastrous results. An estimated 4,500 tons of AN detonated. More than 1,000 persons were killed, about 75% of the houses in Oppau were leveled or made uninhabitable, and a crater 400 feet in diameter and 90 feet deep was formed. The blast was felt in Munich, 175 miles away. The bizarre feature of this episode is that AN was considered to be so safe that explosives could be used to break it up, even though as early as 1867 the properties of AN as an explosive ingredient and indeed, as an explosive, were recognized in a Swedish patent issued to Ohlsson and Norbein. On second thought, perhaps it is not bizarre; even today industry finds it necessary to provide the following warning with the product, "We also stress that dynamite or any other explosive must not be used to break up caked ammonium nitrate" (Reference 9).

The selected ANFO was available in 50-lb bags ready mixed in the stoichiometric proportions of 94 to 6, by weight, of AN to FO respectively; prilled AN (Figure 1-7), which could be mixed with #2 diesel fuel oil at a test site, was available in bulk quantities and in 50-lb bags. This prilled AN was developed in the 1940's specifically for use as the base material for ANFO explosives. Untreated AN is highly hygroscopic leading to caking and

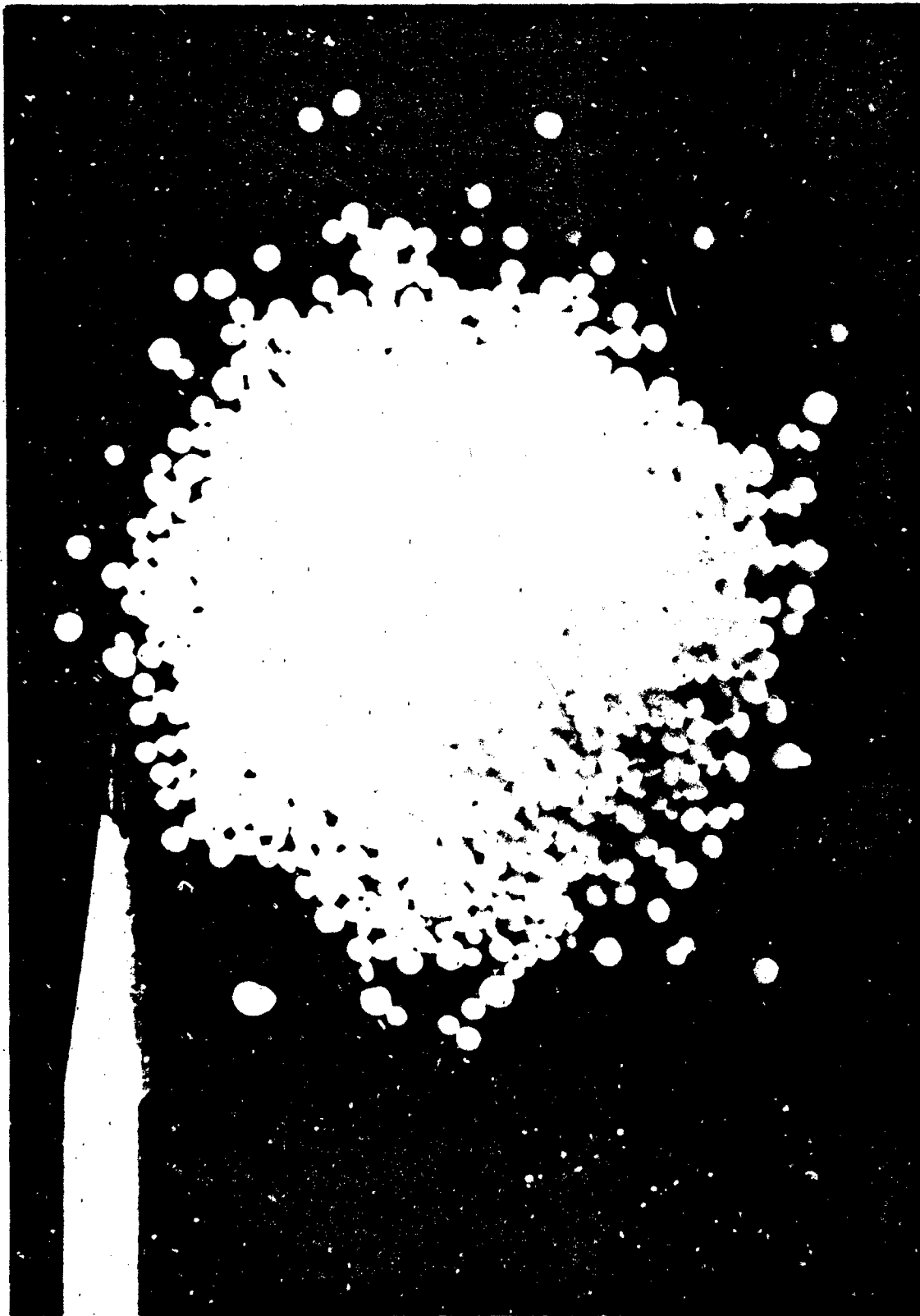


FIGURE 1-7. PRILLED AMMONIUM NITRATE; PRILL DIAMETER ABOUT 0.5 TO 2 mm.

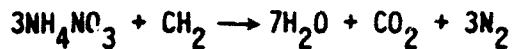
dissolution in humid or wet atmospheres. In fertilizer grade AN, the prills are normally coated with a diatomaceous earth which inhibits water absorption. In AN designed for ANFO applications, the diatomaceous earth is replaced with a surfactant which, in addition to inhibiting water absorption, permits uniform fuel oil absorption by the prill, resulting in an intimate and homogeneous ANFO mixture.

Prill size or AN bulk density is a parameter which influences ANFO sensitivity and explosive output; the higher the prill density, the lower the sensitivity and the output. The use of high density prills such as used in agricultural grade AN, results in an uneven distribution of fuel oil with most of the oil being concentrated on the surface of the prill rather than being uniformly distributed throughout the prill. This oil rich surface and the oil poor inner prill material upset the stoichiometric balance of the ANFO on a prill scale; this leads to low output. The AN used in both the premixed and field mixed ANFO had a bulk density of 0.88 g/cm^3 ; a typical particle size distribution is shown in Table 1-1.

TABLE 1-1 PARTICLE SIZE DISTRIBUTION OF A REPRESENTATIVE 50-LB BAG OF PRILLED AMMONIUM NITRATE

Retained on U.S. Standard Sieve	Percent
#10	13.5
#12	18.5
#14	8.6
#16	8.2
#20	18.3
#35	22.9
Tray	10.2

This type of prill--with a surfactant and a bulk density of about 0.88 g/cm³--was found by industry to be favorable for combining with fuel oil in stoichiometric proportions. This results in a balanced reaction with all the reactants being consumed. The reaction,



calls for 5.65% fuel oil. Analyses and experiments indicated that the optimum or near optimum explosive output of ANFO is obtained for a fuel oil content of from 5% to 7%. This leeway in oil content is fortunate because in practice it is difficult to maintain a precise 5.65% oil content without strict quality control. In fact, it is common practice to overfuel, i.e., approach the 7% limit, because the ANFO output is affected less by overfueling than under-fueling (Figure 1-8). This overfueling turns out to be an advantage for large charge simulation preparation; it compensates to some extent for the evaporation losses of FO that occur when the ambient temperature is high.

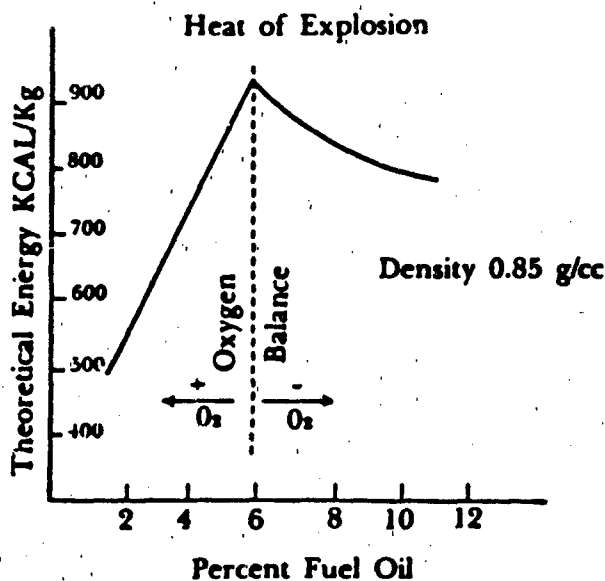


FIGURE 1-8. THEORETICAL ENERGY OF ANFO AS FUNCTION OF FUEL OIL CONTENT.

(FROM: Monsanto Blasting Products ANFO Manual, August 1, 1979)

1.2.2 Phase I - Small Scale Tests

With the selection of the ANFO and AN material decided, the plans for testing ANFO charges in sizes up to 4000-lbs continued. Realizing that both premixed and field mixed ANFO could be used but not having the experience or the foresight to know which method would be most adaptable to military testing requirements in the 500-ton range, both techniques were used. Sadwin, Pittman and a small field crew completed a 23-shot ANFO series in May 1968 in the Rattlesnake Flats area about 18 miles southwest of Hawthorne, Nevada (Reference 10).

Charges weighing 260-, 500-, 1000-, and 4000-lbs were fired. Again, with no guidance available, but to assure detonation of the ANFO, the charges were boosted with cast Pentolite cylinders weighing 8-, 15-, 24-, and 32-lbs respectively. The boosters were placed at the center of the ground plane of the charges (Figure 1-9). All but one of the charges used loose, unbagged ANFO piled on the ground in roughly hemispherical shape. A thin corrugated paper fence was used to retain the lower portion of the pile (Figure 1-10).

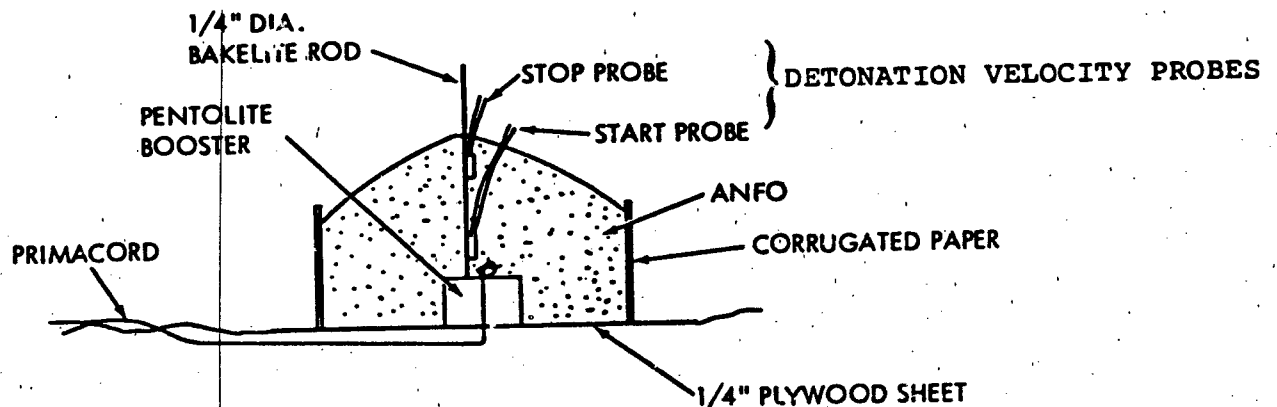


FIGURE 1-9. SCHEMATIC DIAGRAM OF ANFO CHARGE ASSEMBLY IN PHASE I STUDY.

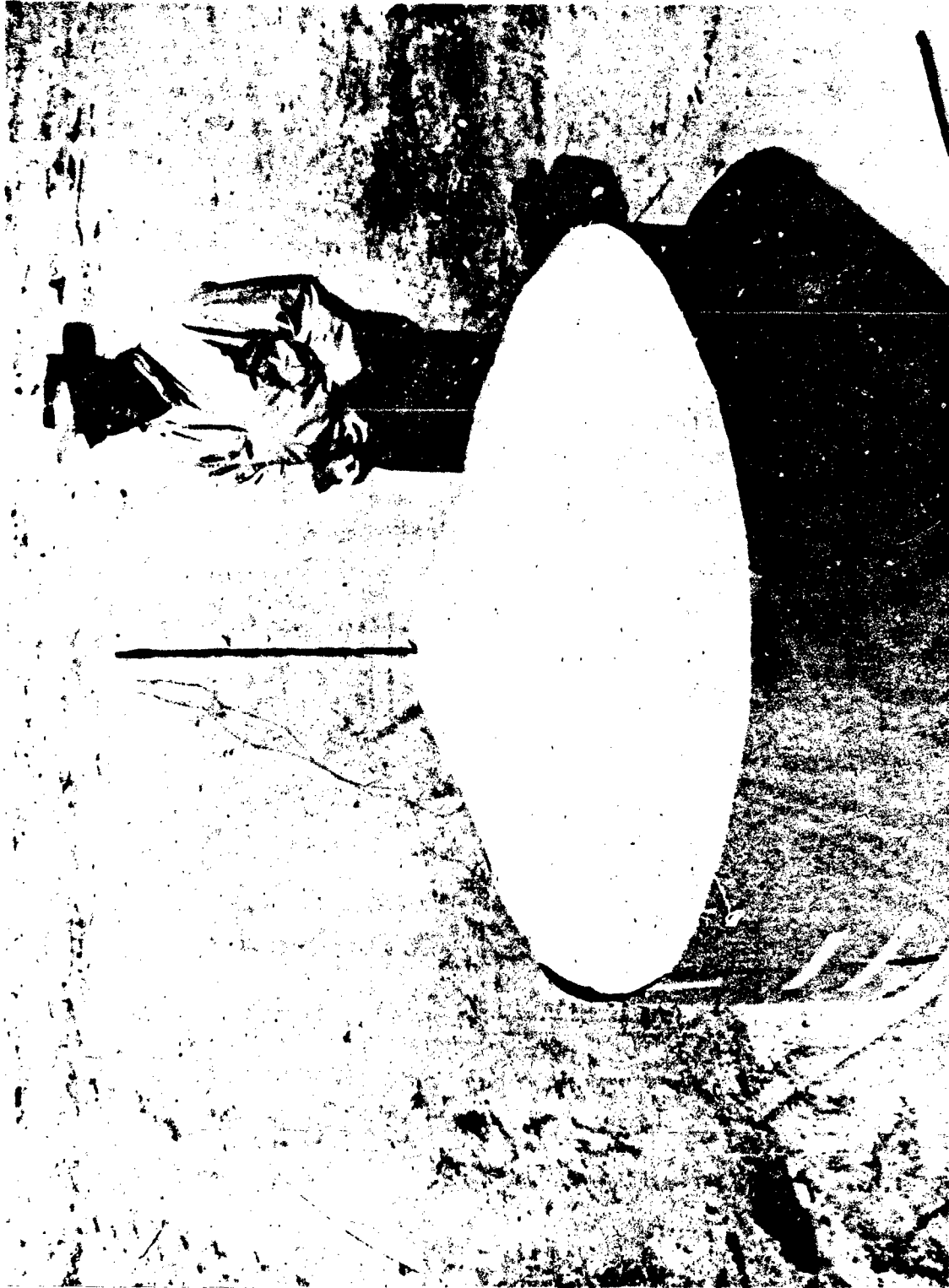


FIGURE 1-10. COMPLETED 1000 LB ANFO CHARGE IN PHASE I STUDY.

One 1000-lb charge was made by stacking the 50-lb bags of premixed ANFO in as close to a hemispherical shape as possible, (the 20 bags required made this stack resemble a cube more than a hemisphere). Five charges used the ready mixed ANFO; the other eighteen charges were made with field mixed ANFO with the mixing being done in a 4.5 cubic foot cement mixer (Figures 1-11 and 1-12). The emphasis on field mixing stemmed from the thought that in the 500-ton size, field mixing would be less expensive than buying ready mixed ANFO.

Three 238-lb hemispherical TNT shots were fired as part of the test program so that a basis would be available to judge the performance of the ANFO shots. The TNT shots also permitted a check on the operation of the airblast instrumentation.

The instrumentation used in the program was minimal but adequate. Airblast was measured in the range from about 1.0 psi to 30.0 psi. A two point probe was used to indicate detonation velocity within the charge. High speed, (4,000 and 7,000 frames per second) cameras were used to observe the explosion. And after each shot, crater size measurements were made.

1.2.3 . . . And Results

The results of the test program indicated that unconfined ANFO charges of about 260-lbs are required before stable detonation and blast conditions could be achieved. This was evidenced by the scalability of the pressure-distance data for charges weighing from 260 lbs to 4,000 lbs (Figure 1-13) and the leveling off of the TNT equivalence of ANFO for charges weighing more than 260 lbs (Figure 1-14). These results confirmed the suspicion (and hope), that the smaller charges used in the earlier bootleg tests were not sufficiently large in diameter or weight, to permit steady state conditions to be realized. The new data indicated that ANFO had an average detonation velocity of 4200 meters/second and an average equivalent weight, on a pressure basis, of 0.82 compared to TNT. The positive duration and impulse of the blast wave, although not stated in terms of equivalence, appeared to be somewhat less.



FIGURE 1-11. MIXING ANFO IN A CEMENT MIXER.



FIGURE 1-12. POURING ANFO INTO FORM FOR 1000 LB CHARGE.

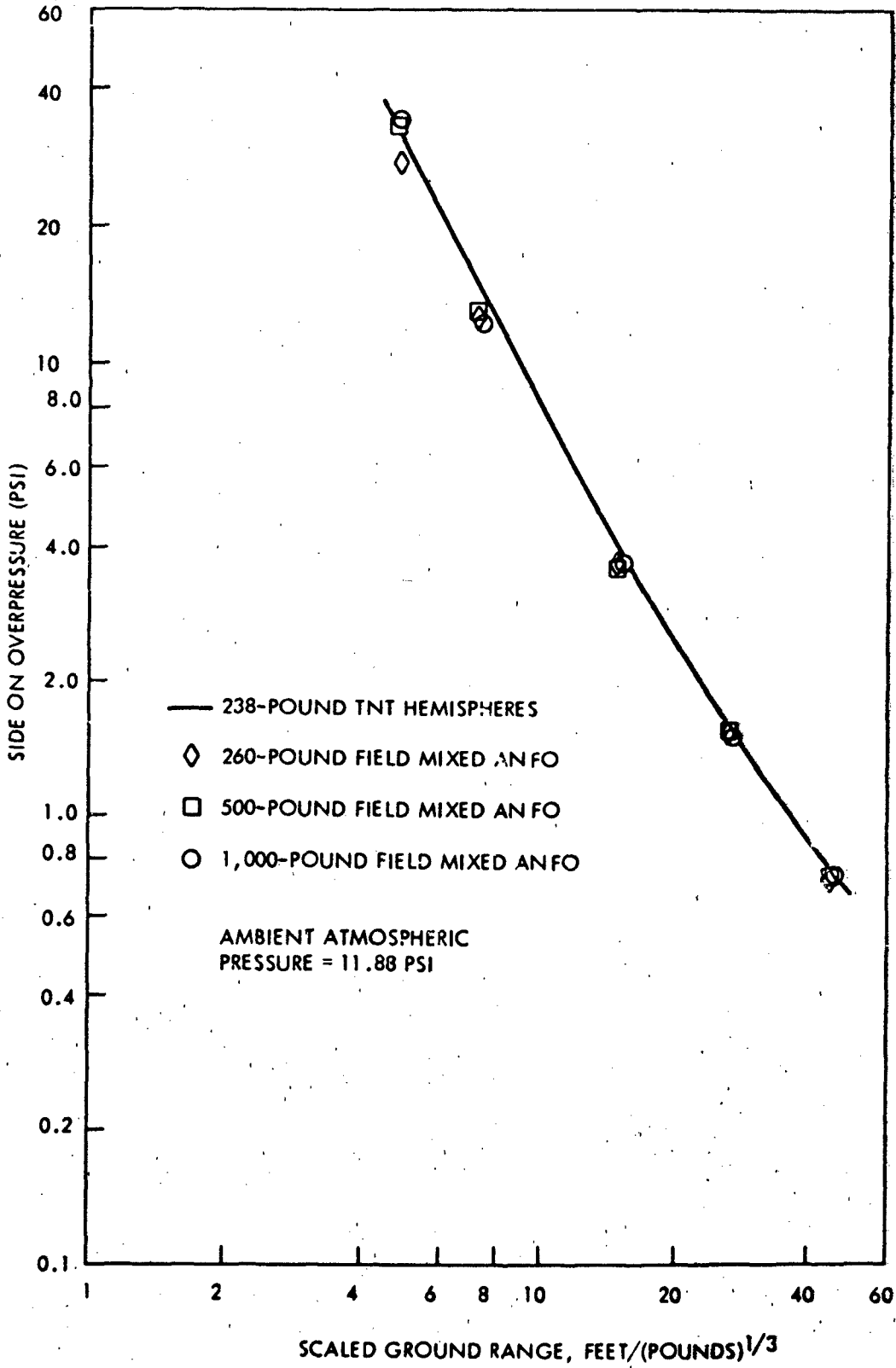


FIGURE 1-13. AIRBLAST PRESSURES FROM TNT AND FIELD MIXED ANFO FIRED ON GROUND, SCALED TO SEA LEVEL CONDITIONS.

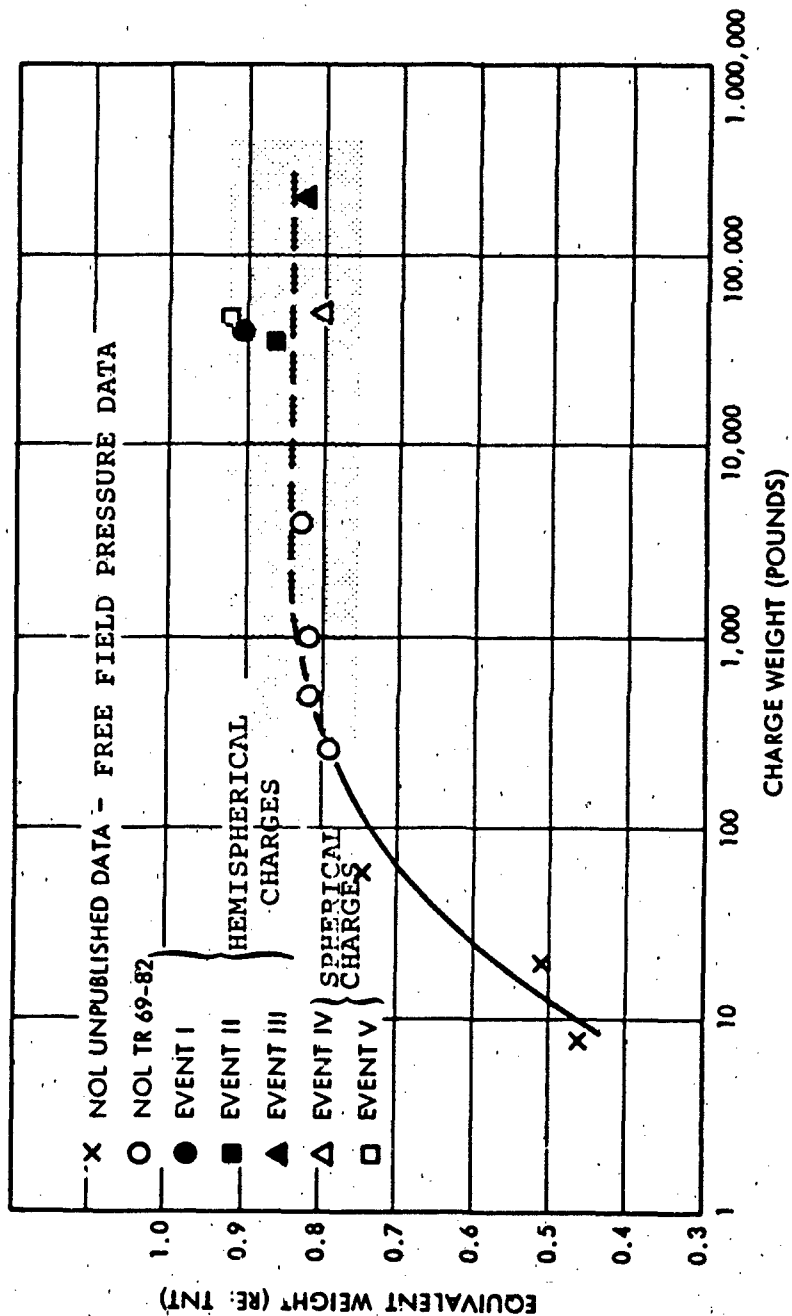


FIGURE 1-14. EQUIVALENT WEIGHT VS CHARGE WEIGHT FOR UNCONFINED ANFO.

The detonation velocity data was heartening; the literature gave the detonation velocity of stoichiometric ANFO, in heavy, confining steel pipes, as 4200 meters/second. The 0.82 TNT equivalence of ANFO, however, was a bit disappointing--a higher output would have been desirable. This relatively low output is attributable in large part to the fact that ANFO is in stoichiometric balance; it does not depend upon or utilize atmospheric oxygen in the explosion process as does TNT. TNT is extremely oxygen deficient; for maximum output, it depends on atmospheric oxygen to continue the combustion process. This afterburning leads to longer duration blast waves and higher impulses. Some thoughts again were given to the use of additives in the ANFO to increase output, but again, they were dismissed as being too costly, time consuming, and complicated.

The initial disappointment was soon mollified when it was considered that on one hand, there is nothing sacred about the size or yield or type of charges used on military tests; no matter which chemical explosive source is used and no matter how large a yield is realized, chemical explosions only simulate in a limited range some of the effects of nuclear weapons. Through knowledge of the explosion processes of both nuclear and HE sources, analysts can relate one to the other and utilize the simulated effects to advantage. And on the other hand, because of this analytical ability, whether the HE yield is 80 tons or 120 tons, test results can be interpreted as if the environment were produced by 100 tons. As a matter of fact, for charges with yields 18-20% different, at a given pressure level, the differences in distances at which this pressure occurs are less than 7%. The converse is almost true also; at a given distance, the pressure difference is about 7%. This is less than the scatter in measured data usually obtained in field operations. So, the chemistry of ANFO was accepted along with its reduced blast output, i.e., its 0.82 TNT equivalence.

The cratering performance of the 260 lb ANFO shots were compared to that of the TNT control shots. The ANFO crater radius was 7% smaller than that for TNT, its depth 9% greater, and its volume about 20% less. In light of the caliche material located about 1.5 ft below the surface, these comparisons were considered satisfactory.

1.2.4 Phase II - Test Proposals

NSWC was ready to move on to the follow-on tests suggested in its March 1967 proposal--to demonstrate the merits of still larger charges and to explore ways to utilize the charges for tests at sea as part of the Navy's hardening program. A Phase II ANFO proposal was submitted to NAVSEC in July 1968 (Reference 11).

It was proposed that the Phase II work consist of two 20 ton and one 100 ton ANFO shots with pressure-time and high speed photographic instrumentation providing the main measurements coverage. A one year program with six weeks in the field was contemplated. The estimated total cost for the program was to be \$115,000. It was pointedly noted that the cost of TNT alone for a 100 ton charge would be about \$200,000. The proposal suggested that a Phase III program with charges weighing up to 500 tons would be necessary (after the successful completion of Phase II) to adapt the ANFO simulation technique to sea trials for the Navy's ship hardening program and to other DNA uses.

NAVSEC heartily endorsed the proposal in October 1968 with the statement, "One important aspect of airblast hardening is testing and evaluation of equipment to determine if design specifications have been met and to locate areas of weakness. This may be accomplished for components by testing them in the conical shock tube and for complete systems and sub-systems by exposing them to simulated nuclear airblast from chemical energy explosion sources. Presently used energy sources (TNT, detonable gases) are expensive, over-sensitive, inconvenient, and impractical for specialized purposes such as sea operations. The Navy, however, has recently experienced a breakthrough in this area with the proposed utilization of ANFO--an inexpensive, insensitive, and versatile explosive--for this purpose" (Reference 12). They forwarded the proposal to DNA for direct funding. Kelso, who, of course, had been following the program of the ANFO endeavor, provided DNA funds for the task in January 1969.

1.2.5 . . . ANFO Events I, II, and III

A three shot program was undertaken with two 20 ton and one 100 ton ANFO charges (Reference 13). The field program, under the direction of Sadwin, was conducted at DRES, the site of the early TNT and detonable gas large-scale experiments and military equipment tests. The initial objectives of the DRES

ANFO program were to establish the scalability of ANFO charges from the 260-4000 lb range to the 20-100 ton range, and to gain experience in handling, mixing, and preparing large charges with the ultimate goal of fielding still larger charges, up to the 500 ton size considered useful for military tests.

By this time, i.e., early 1969, the demonstrated and potential merits and applications of ANFO were being recognized by an ever increasing number of military scientists. More information on the explosion effects of ANFO was being asked for than could be readily provided by NSWC itself. Four other U.S. agencies and DRES participated in the Phase II ANFO test program to help get this additional information.

DRES provided field support and made blastwave time-of-arrival, crater size, and photographic measurements on each of the shots. BRL (Ballistics Research Laboratories) made side-on and total head airblast measurements in the high, i.e., up to about 1000 psi, and moderate pressure regions. U.S.G.S. (U.S. Geological Survey) made cratering studies and NWC (Naval Weapons Center) and NCEL (Naval Civil Engineering Laboratory) made measurements on above ground and underground structures, respectively. NSWC, in addition to directing the over-all operation, was in charge of charge design and preparation, charge monitoring, e.g., determining the internal temperature, oil content and prill size of the ANFO charge, and low pressure blast measurements.

The ANFO used on all three events was supplied by a Canadian source located in Calgary, Canada. All mixing and bagging was performed on site using techniques and equipment developed by and for the mining industry. For the first two events, the 20 ton shots, AN was delivered to a Suffield railroad siding in a 70 ton capacity hopper car. The AN was augered into a mixing truck where the FO was introduced in correct and metered proportions (Figure 1-15). The 7 ton capacity mixing truck was driven to the GZ (ground zero) area where, for Event I, the ANFO was augered into a bagging unit (Figure 1-16), and for Event II, the ANFO was augered directly into a fiberglass hemispherical container. For Event III, the 100 ton shot, it was found more efficient to have the AN brought to the GZ area in 22 ton capacity tanker trucks, auger the AN into the mixing truck, and the ANFO directly into the fiberglass container (Figure 1-17). In the mixing operation the diesel

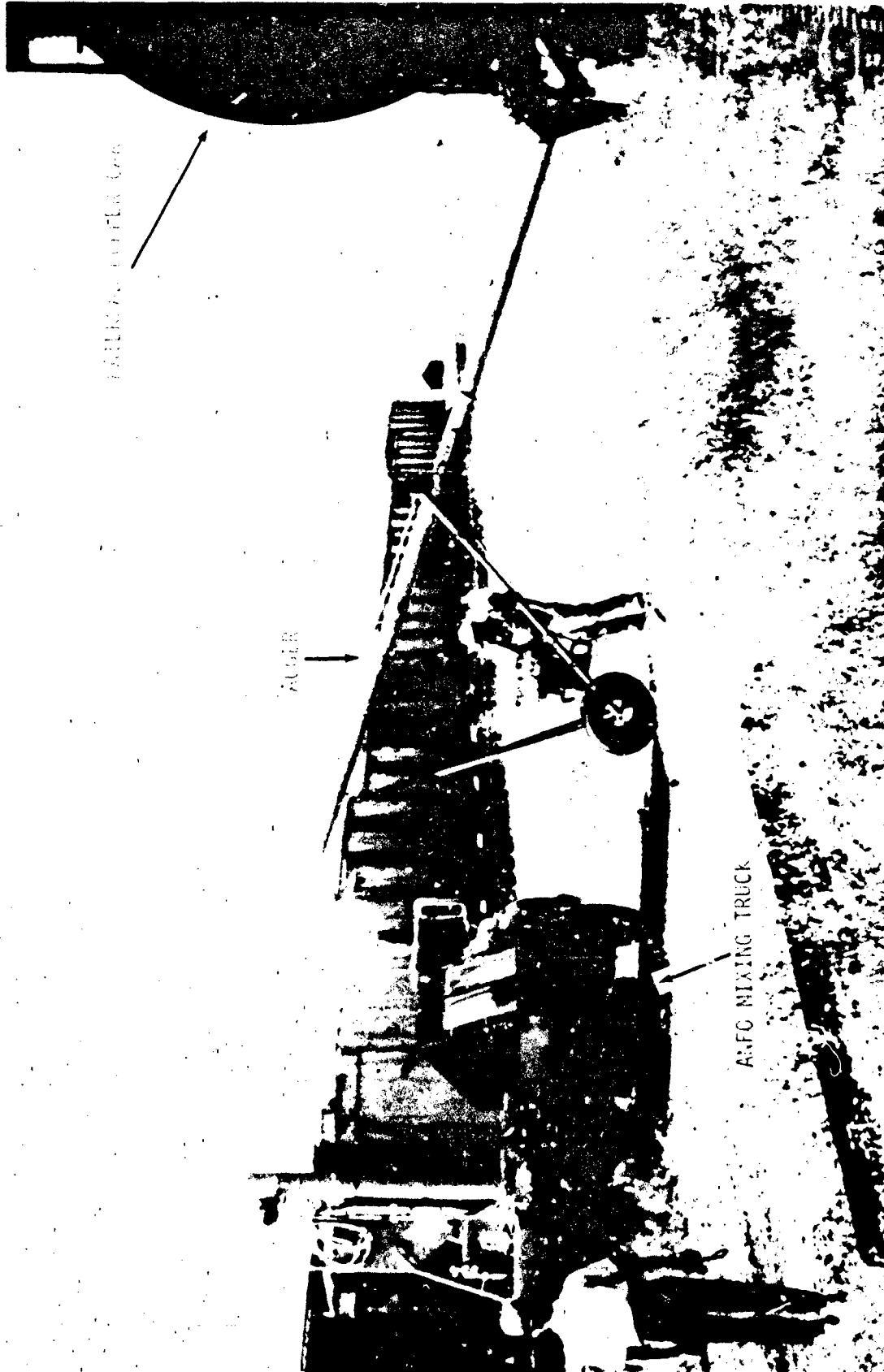


FIGURE I-15. AN BEING AUGERED FROM RAILROAD HOPPER CAR INTO ANFO MIXING TRUCK FOR EVENT I.

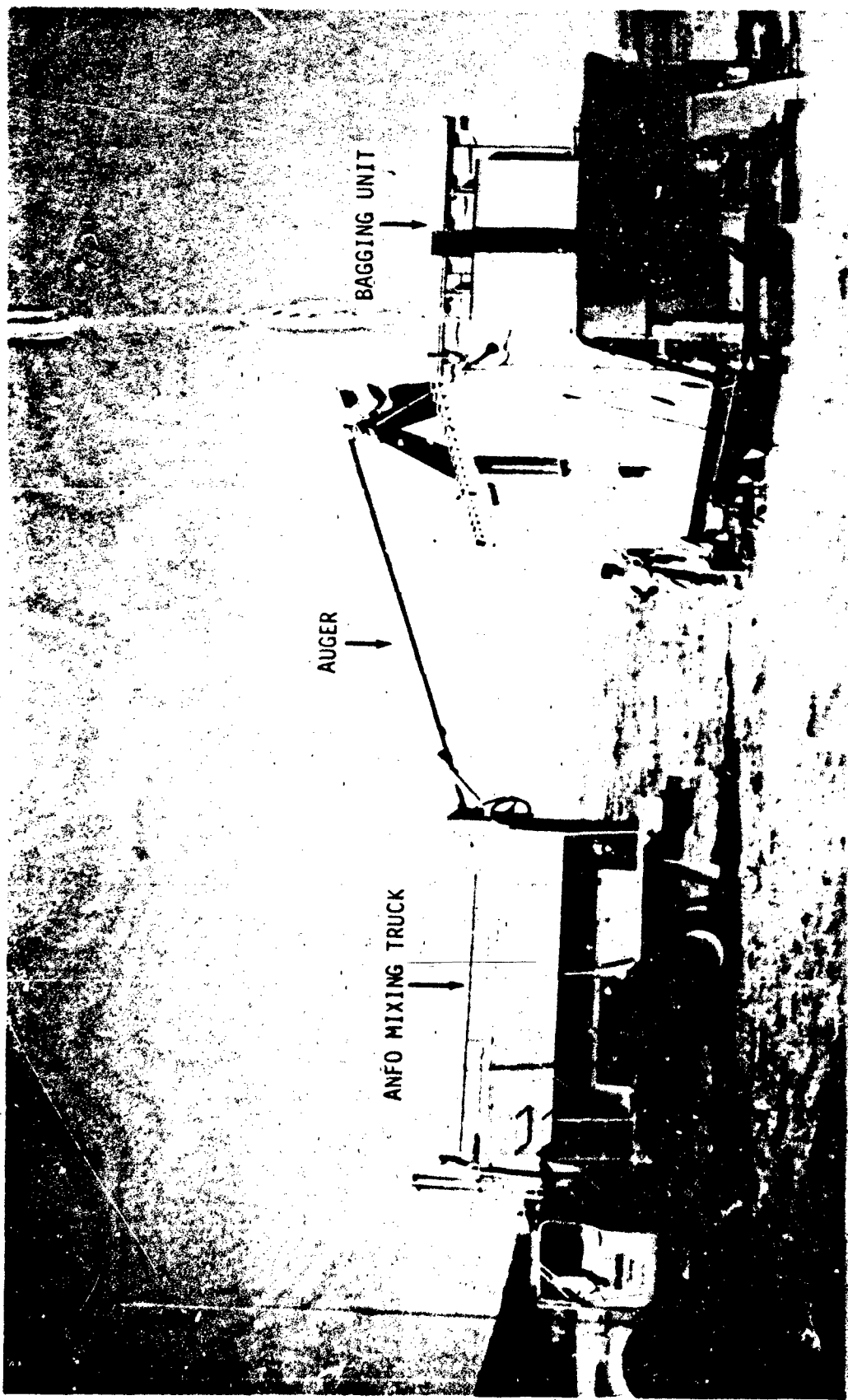


FIGURE 1-16. MIXING TRUCK AUGERING ANFO INTO BAGGING TRUCK FOR EVENT 1.

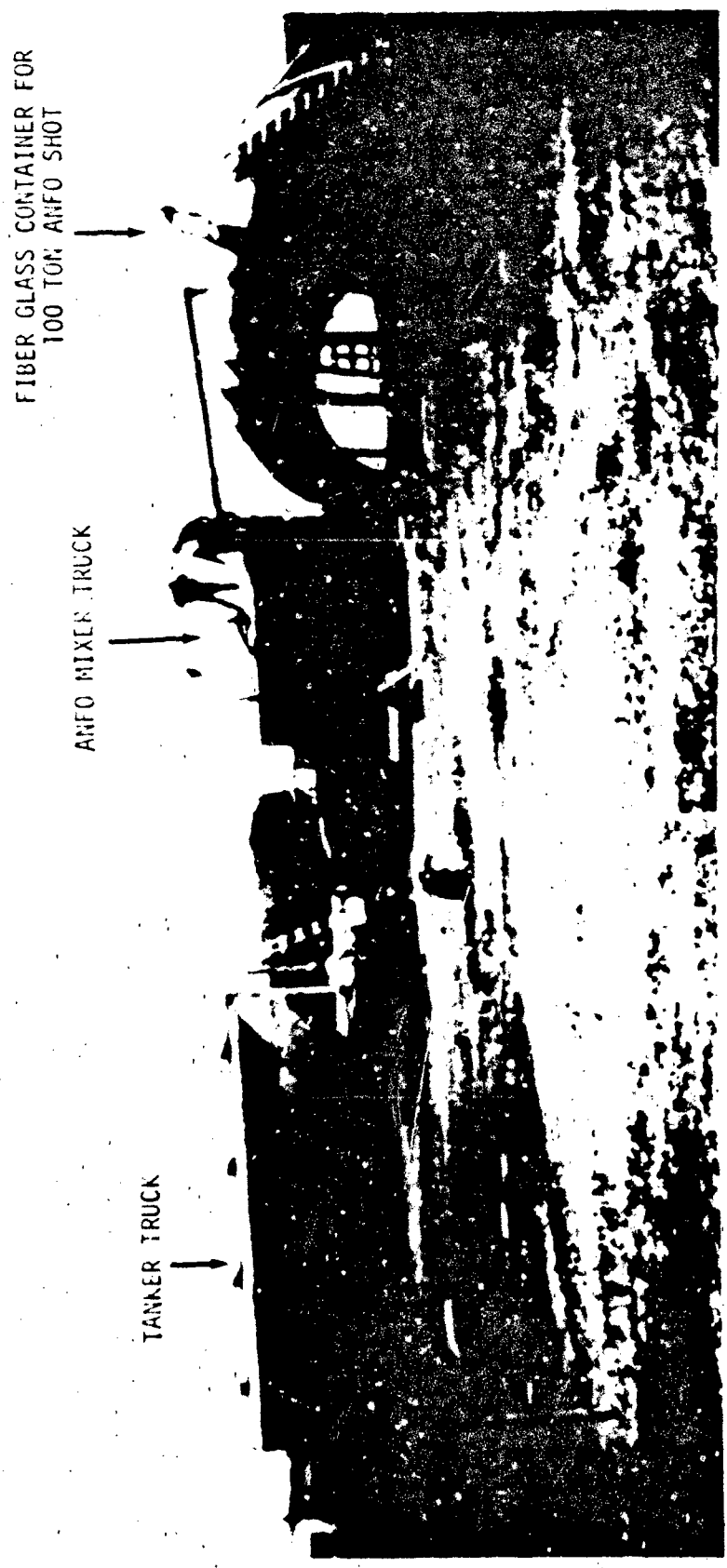


FIGURE 1-17. TANKER TRUCK FEEDING AN INTO MIXING TRUCK: ANFO AUGERED INTO FIBERGLASS CONTAINER FOR EVENT III.

fuel oil was colored with a red dye so that a continuous visual check could be made of the fuel oil content of the ANFO; a change in color tone of the ANFO would indicate a change in the FO proportion. The fuel oil content was periodically checked also by chemical analysis. For these three charges, the percentage of FO was found to vary from 5.85 to 5.95%, acceptable limits to provide a stoichiometric mixture of ANFO.

The 20 ton hemisphere for Event I was formed using the bagged ANFO (Figure 1-18). Note the rather smooth hemispherical surface contour that was formed by the pliant bags. This was considered to be an advantage over the reentry cornered surface of TNT block built charges as depicted in Figure 1-2; reentry corners and planer surfaces were considered to be a possible cause for blast anomalies (Reference 3). Eight hundred 50-lb bags were used in this charge. One hundred-fifty of these bags were opened and the loose ANFO used to fill the interstices between the full bags. This was done to provide as homogeneous mass of explosive material as possible (Figure 1-19). It is remembered that one postulated source of anomalies in TNT block charge construction was the nonhomogeneity of the charge, particularly at the interfaces between the blocks. The loose ANFO between the bags was aimed at reducing charge construction induced blast anomalies.

Event II used bulk ANFO contained in a thin fiberglass hemispherical envelope open at the top to permit filling. This construction was used to determine the merits of bulk loading, the effects of light containment, and the difference between field operations in terms of time, difficulty, and cost for bagged vs bulk ANFO charges. Event III, the 100 ton charge (Figure 1-20), was built similarly to the Event II charge; its primary objective was to establish the scalability of large charges of ANFO. Each charge was boosted by a 250-lb hemispherical TNT/pentolite charge placed at the bottom center of the main charge and initiated with 100 grain per foot primacord.

1.2.6 20 Ton and 100 Ton ANFO Test Results

Starting on 14 August and continuing on a weekly basis through 28 August 1969, the three ANFO shots were fired. Prior to the first firing, there was some speculation--even wagering--among the test participants and observers as to whether the charge would, in fact, successfully detonate or would succeed



FIGURE 1-18. EVENT I - 20 TON ANFO HEMISPHERE.

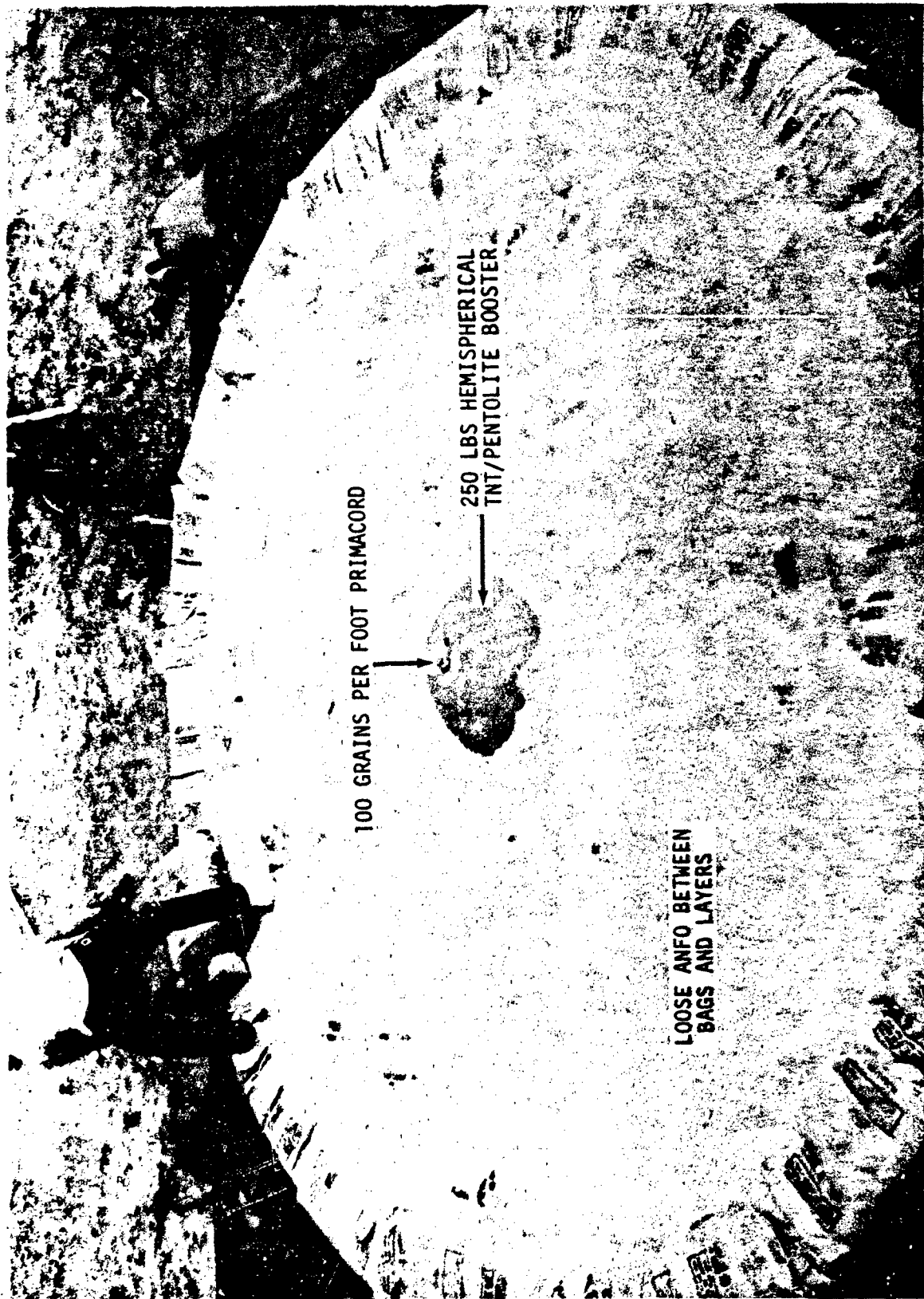


FIGURE 1-19. EVENT I - FIRST LAYER OF BAGS COMPLETED WITH LOOSE ANFO FILLING IN VOIDS.



FIGURE 1-20. EVENT III - 100 TON ANFO CHARGE IN FIBERGLASS CONTAINER.

instead only in spreading fertilizer over the DRES plains. DRES, for instance, remembered that in the late 1950s in its general studies of explosive materials, it had investigated briefly the properties of AN-based explosives; it could not reliably detonate the small charges used. Others were aware of the heavy and multi-point boosting used by the mining industry for ANFO confined in bore holes.

The first charge and the subsequent charges detonated successfully (Figure 1-21). Analysis of the test data by NSWC showed the reproducibility and scalability of the explosion effects (Figure 1-22). The NSWC blast data averaged over the 1 to 200 psi range indicated that the average TNT equivalence for the 20-100 ton ANFO shots was 0.94 for both the bagged and bulk charges. This is considerably higher than the 0.82 equivalence reported for the earlier 200-4000-lb shots.

As noted in Reference 13, there are several reasons for this apparent but not necessarily real discrepancy. The earlier 0.82 equivalence was established over a 1 to 30 psi range (using the only data available) and a linear weighting method was used. Because the linear method gives undue emphasis to the data at the higher pressures, and pressures up to 300 psi were recorded for the Phase II shots, a logarithmic weighting scheme was used for the Phase II data. Using a common system for both the Phase I and II shots, i.e., logarithmic averaging over the 1 to 30 psi range, the Phase I data gives an equivalent weight of 0.86, the Phase II data 0.87.

As discussed by Sadwin and Swisdak (Reference 13), equivalent weight determinations may be inappropriate not only for ANFO but for any explosive comparisons unless a statistically significant number of shots can be fired. For one, by quoting a single number, the illusion is given that (in the ANFO example), the ANFO pressure-distance curve is parallel to that of the reference TNT curve. As Figure 1-22 shows, this is not so over the whole pressure range of interest. Hence, depending on the pressure level of particular concern, different equivalencies can be calculated. This is dramatically illustrated in Figure 1-23 for the Phase I NSWC data. For another reason why equivalent weight numbers should be used with some trepidation, equivalent weights, as determined from pressure-distance



FIGURE 1-21. EVENT III - DETONATION OF 100 TON ANFO CHARGE: UNPERTURBED SHOCK WAVE VISIBLE.

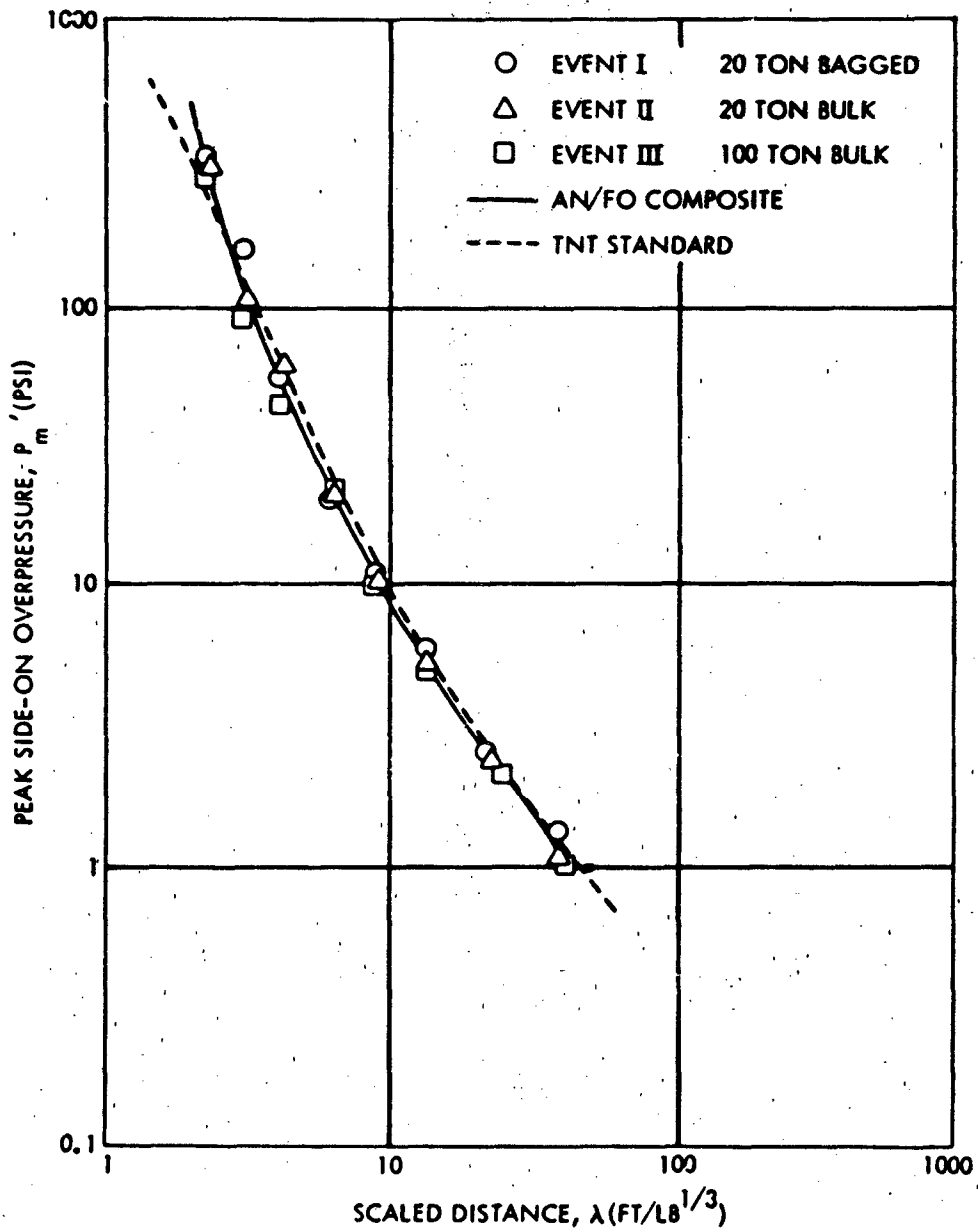


FIGURE 1-22. PEAK PRESSURE VS SCALED DISTANCE FOR ANFO EVENTS I, II, AND III. SCALED TO SEA LEVEL CONDITIONS.

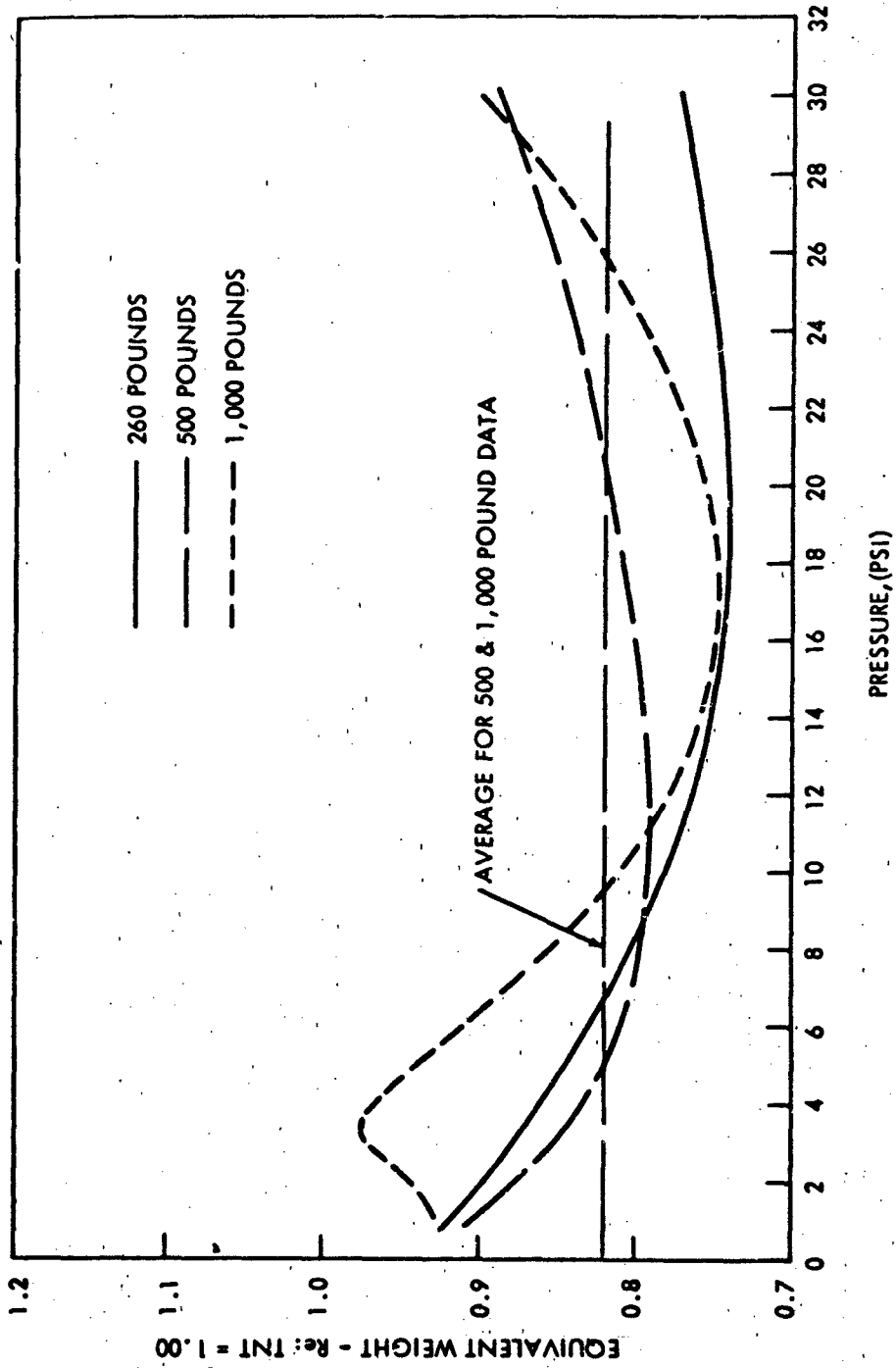


FIGURE 1-23. EQUIVALENT WEIGHT VS PRESSURE FOR PHASE I ANFO SURFACE BURSTS.

comparisons, are extremely sensitive measures of the merits or yields of one explosive compared to another. As discussed earlier (Section 1.2.3) a 20% difference in yield or equivalency leads to about a 7% difference in pressure at a given range. On a single shot or a small number of shots, this 7% difference is hardly discernible because of the scatter in the data. (And it is noted that in this Section of the report, full use is made of nominal charge weights at times rather than exact weights. The results of either calculations or measurements for a nominal 6-ton charge vs an 11,242 lb charge are hardly discernible and have little significance.)

Detonation velocity, deduced from DRES photographic measurements and ionization probes, indicated an average velocity of 4470 meters per second, about 5% higher than that obtained in the earlier 260- to 4000-lb Phase I Program. Crater measurements showed reproducibility in crater dimensions produced by the two 20 ton shots, and close agreement with the crater produced by a 20 ton hemisphere of TNT fired in the same area. A comparison between the 100 ton ANFO shot and a 100 ton TNT hemispherical charge indicated marked differences in crater radii and depths but only a 15% difference in estimated crater volumes; the TNT crater was wider, shallower, and had a larger volume. A major reason for these variations was attributed to the geologic formation underlying each shot; the TNT crater struck water while the ANFO one did not.

Photographic coverage of the explosions showed the presence of anomalies essentially only in the bulk loaded, fiberglass contained charges. The TTCF working group studying anomalies had access to the Phase II ANFO results. In its report (Reference 3) it concluded "An ANFO charge built with stacked bags produced no anomalies attributable to the charge material; however, some Type 5 anomalies attributable to charge construction were evident. (A Type 5 anomaly is one in which a fireball perturbation affects the shock front.) Some anomalies of all types were observed on the cased ANFO charges; these were considerably less in magnitude and extent than those observed on similar sized TNT charges."

The measurements of the internal temperature of the charges showed that there was no internally generated self-heat; only small variations in temperature occurred and these were associated with diurnal air temperature

changes. The ANFO was shown to be a stable mixture; there was no evidence of the fuel oil settling out of the mixture.

The field operations provided the sought after experience in handling large ANFO charges (Reference 14). The ease of charge preparation was demonstrated by the short span of time, fourteen days, required to prepare and fire three shots. The costs of bagged ANFO and fiberglass contained bulk ANFO charges were about the same, with the cost of the container equalling the cost of the additional manpower required for the bagging and stacking operations.

1.3 ANFO FOR SEA TRIALS OR GROUND MOTION TESTS?

The Phase II program was highly successful; speculation about the merits of ANFO for airblast tests was eliminated through hard, scientific, and operational data. NSWC was ready to go on to the Phase III program it had recommended earlier--to adopt ANFO to sea trials for Navy testing of surface ships and their components to airblast environments. But this Phase III program was not to be. Circumstances and the rearrangement of Navy priorities dictated another course.

On one hand, the Navy was reviewing and reevaluating its ship hardening program; until this was completed, the requirements for testing surface ships at sea could not be established. On the other hand, as indicated earlier, military interests were now heavily involved with underground structures as targets for tests; DNA had supported the development of spherical TNT charges to produce the required airblast, craters, and blast induced and direct ground shock induced environments on missile silos, command and personnel shelters, utilities, underground stores and other underground targets, as well as for surface and air targets. A wealth of information was obtained on Operations DISTANT PLAIN (1966-67), PRAIRIE FLAT (1968), and MINE SHAFT (1968-69) to guide design and determine survivability of these targets. Spherical charges ranging in size from 20 ton to 500 ton were used, and to meet the blast, ground motion, crater size requirements, charges were fired at different heights of burst from half buried to 85 ft altitude. A new operation, DIAL PACK, using a 500 ton TNT spherical charge tangent to the surface was in the planning stage for 1970.

Although Kelso supported Petes' suggestion that ANFO could readily be built in spherical shape and be used instead of TNT for underground shock effects, in truth, the ground shock effects of ANFO explosions had not been thoroughly established on the ANFO tests. The ground motion and underground structures scientists and engineers were not ready to commit multi-million dollar operations to ANFO. They argued that the underground motion investigations were difficult enough because of the variable soil and rock properties without switching to another, less powerful, less characterized explosion source. They argued, further, that data from the new source would have to be compared and correlated with the large body of data available from TNT operations and a ready means for this correlation was not immediately evident. Their views prevailed; before tests are committed to ANFO charges, the ground effects from such charges should be adequately studied and demonstrated.

1.3.1 ANFO Development for Ground Motion Tests

Instigated by Kelso, NSWC, starting in September 1969, made several proposals and unofficial estimates relative to the cost, construction, and use of ANFO in spherical configurations. Since airblast was of continuing interest to DNA, in November 1969, Petes at a TTCP meeting in Santa Barbara, California (Reference 15), disclosed a new approach to airblast simulation: use vertical, cylindrical charges of ANFO. It was reasoned that a cylindrical charge would be easier to build of bagged ANFO than either a hemisphere or a sphere. Moreover, the distribution of explosion energies would not be wasted with a cylindrical charge. In a test with a spherical or hemispherical charge, as much blast energy goes where there are no targets as where there are; cylindrical charges would give a larger proportion of the blast where it is needed--along the ground. And further, if a charge length to diameter ratio of 1 to 1 were used, perhaps, the crater size with its deleterious ejecta would be smaller than for the other charge geometries.

1.3.2 Cylindrical ANFO Charges?

This idea simmered for about a year. Operation DIAL PACK took place in July 1970 with the now predictable airblast results--extensive fireball and airblast anomalies which disrupted surface target studies. The simmering was

raised to a boil in the minds of NSWC personnel when a new thought was added to the idea for utilizing cylindrical ANFO charges: these charges could, it was hoped, provide the underground explosives engineers with the ratio of airblast, ground shock, and crater energies necessary to simulate nuclear weapon bursts, on one hand, and on the other, provide good blast fields for the surface target investigators. It was rationalized that it was the ratios that were important, not the absolute magnitudes of these energies. After all, TNT in the spherical tangent-to-the-ground geometry provided only the ratios and not the magnitudes of nuclear weapon bursts. In a proposal prepared in November 1970, it was stated "We know from free field experiments with cylindrical HE charges that airblast is enhanced in a mid-plane perpendicular to the longitudinal axis of the charge over that which is obtained from a spherical charge of the same weight at the same distance. The enhancement is a function of L/D (length/diameter). Thus, the simple way of changing ground coupled energy for a given yield cylindrical charge applies to changing the horizontal plane airblast output (peak pressure vs distance) from a cylindrical charge--vary L/D.

We propose to concentrate on a limited range of L/D cylindrical charges, perhaps 1/2 to 1/1 or 1.5/1. We believe that this range of L/D's will cover the underground and surface target effects requirements and give sufficient flexibility to get different airblast/ground shock/cratering relationships."

The proposal outlined a program in which initial investigations of the L/D relationship on cratering and ground shock would be investigated using 8-lb TNT or pentolite cylinders before proceeding up to 10,000-lb ANFO charges. Calculational efforts were deemed appropriate also and were proposed.

Simmering and boiling in one laboratory does not necessarily lead to an immediately marketable dish; the time for cylindrical ANFO charges for large scale test operations had not arrived as yet.

1.3.3 CHEST

However, DNA continued its pursuit for the utilization of ANFO for ground shock simulation through contractors and others better versed in underground shock phenomena than NSWC. F. Sauer, PI (Physics International Company) had a novel technique for simulating crater and direct-induced ground motions from a nuclear weapon surface burst (Reference 16). This technique, with the acronym CHEST (Cratering High Explosive Simulation Technique), is based on the following assumption: if the velocity field from a source of chemical energy can be made identical to the late-stage velocity field from a nuclear source, then the ensuing cratering and far-field ground motions will be identical also. The velocity fields can be made identical if a chemical energy source can be made to generate the same boundary conditions on a region of space that would be generated by a nuclear surface burst (Figure 1-24). ANFO was chosen as the explosive to be used because it could meet the required boundary conditions i.e., the work stresses in the test site soil, and because it was easy to emplace and its cost was low.

A large scale test, MINE THROW, was planned in which the crater and ground motions generated by JOHNNY BOY, a 500 ton TNT equivalent shallow-buried nuclear burst in alluvium, was to be duplicated with this technique. In pre-MINE THROW tests in 1970-1971, the technique was tried out on a small scale. In one test for instance, a hole approximately 9.6 ft in diameter and 6.1 ft in depth was dug. This excavation was lined with a 2-ft thickness of ANFO contained in 10 lb bags and totaling about 6 tons. The excavation size and ANFO quantity were selected on the basis of two dimensional computer (ELK) calculations which provided contours of constant peak stress; for the purpose of the experiment, the 55-kilobar stress contour was selected as the one of interest since it was expected that ANFO would generate approximately that pressure when reflecting off the alluvium interface.

The preliminary tests showed the feasibility of CHEST but it also indicated some problems. The detonation pressure was considerably higher than expected; the measured pressures were on the order of 90 to 100 kilobars. If normal density ANFO were to be used on MINE THROW, the initial excavation size would be so small that not enough ANFO could be used as the explosive liner to

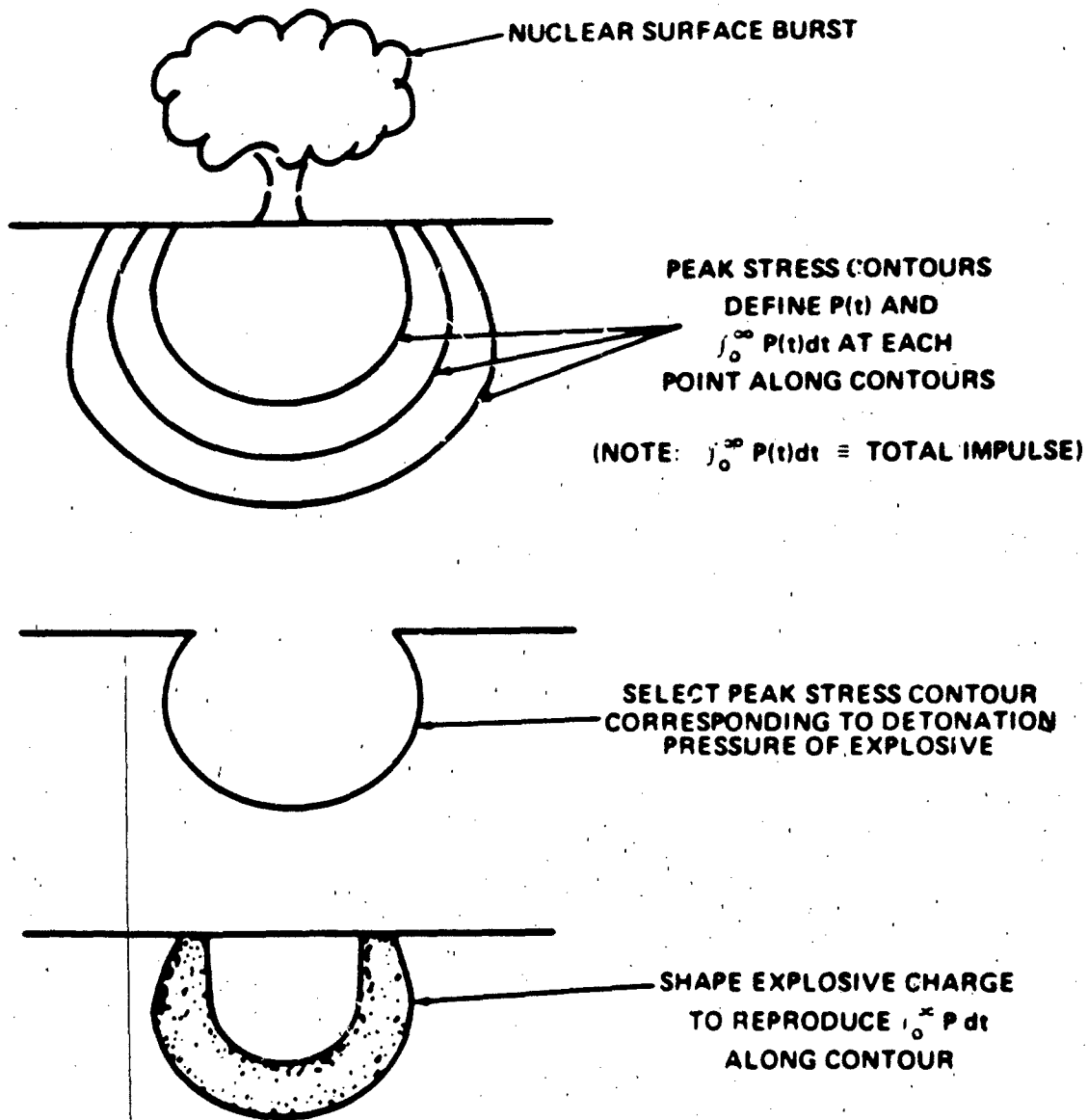


FIGURE 1-24. CRATERING HIGH EXPLOSIVE SIMULATION TECHNIQUE.

generate the required impulse. Hence, PI embarked on a program to develop low density ANFO, one with a detonation pressure of about 55 kilobars (Reference 17).

By adding low-density polystyrene beads to the normal ANFO, they achieved mixtures that exhibited stable detonations over the density range from 0.5 to 0.9 g/cm³. A mixture with a density of 0.75 g/cm³ and a calculated detonation pressure of 56 kilobars was selected for the MINE THROW I event which was not conducted.

1.3.4 ANFO Spheres

During this same time period, ANFO spheres were being investigated with DNA support for use as a direct counterpart for the TNT spheres. In October 1971, two 25 ton spherical ANFO charges were fired at DRES (Reference 18). These charges, designated ANFO IV and ANFO V (and considered to be follow-on to the 1969 three shot series at DRES) used bagged ANFO. One charge (ANFO IV) was constructed tangent to the ground, the other was half below-half above the surface. Limited by a particularly austere budget, it was not possible to make as extensive a measurement effort as was possible for the three earlier large ANFO shots, but airblast, crater size, and photographic measurements were made. The test data were sufficient to provide judgment on the performance of spherical ANFO shots. Comparison could be made directly with similarly configured TNT charges fired at the same site. It was found that ANFO IV and V, with their 0.82 TNT equivalence, produced the same blast as 20 ton TNT shots. Some blast anomalies were observed by DRES on ANFO IV, none on ANFO V. It was conjectured that the anomalies stemmed from the somewhat asymmetrical construction of the charge, the rough outer surface created by the bag construction, and the possibility of air pockets entrapped in the ANFO bags. In the 1969 series, the bags were contoured into a relatively smooth outer curve by butting the ends of the bags together; on the 1971 tests the outer bags touched only at the inside corners (Figure 1-25). The crater obtained on ANFO V matched very closely the dimensions of the DISTANT PLAIN crater produced by a 20 ton TNT spherical charge half buried while the ANFO IV crater dimensions fell half way between those of DISTANT PLAIN 5A and 6A, 20 ton spherical TNT charges tangent to the surface; the ANFO IV crater had a volume of 16,540 ft³, the DISTANT PLAIN 5A crater 24,087 ft³, and the

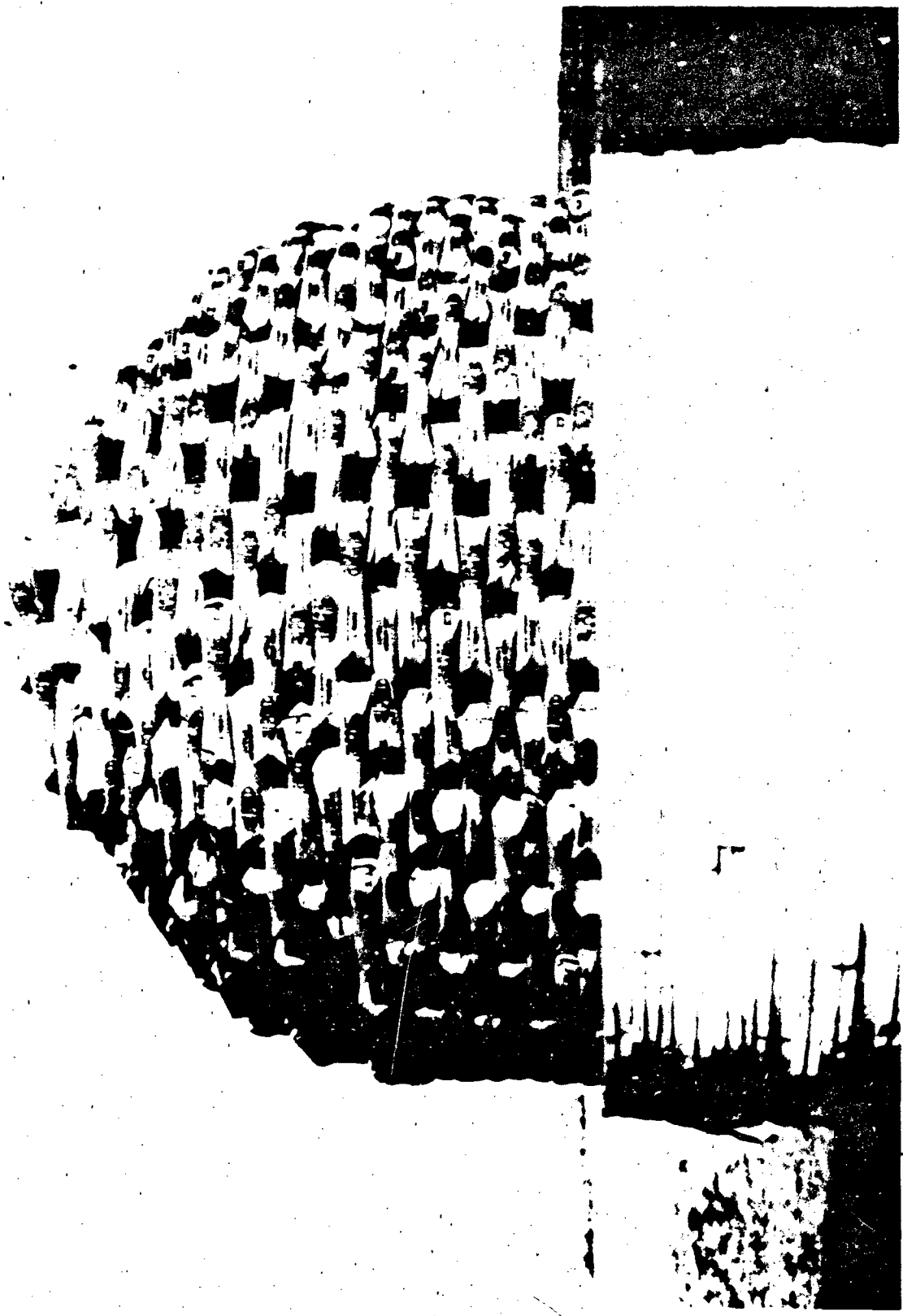


FIGURE 1-25. 25 TON ANFO IV TANGENT SPHERE CHARGE.

DISTANT PLAIN 6A crater 7,064 ft³. It is important to note that both DISTANT PLAIN shots were fired in the same area at DRES, the ANFO IV shot in another area. The difference in crater sizes for the similar TNT shots is an indication of the problems associated with crater (and ground motion) predictions: even small differences in geologic structure and materials can lead to large differences in actual test results.

These difficulties in ground motion and crater studies were stated by D. S. Randall, PI, after PI ran a four shot spherical ANFO test series in November 1971 (Reference 19). Each charge consisted of 1200 lbs of ANFO contained in a hollowed out styrofoam cube resting on the surface. Two shots were fired over a silty playa material; the other two over a 10-ft layer of clay above shale of unknown thickness. Each pair of ANFO shots was compared to a 1000-lb TNT shot of similar geometry fired at each site. Craters produced by the ANFO charges were neither consistently larger nor smaller than craters produced by TNT charges of the same yield. Essentially, this is the same result as obtained at DRES in ANFO IV and V. Hence, Randall's statement in November 1972, "Craters produced by equal energy charges of different explosives are so strongly influenced by the characteristics of the test bed that no general predictive relationship between charge mass and crater size can be generated at this time."

(Incidentally, PI was well aware of the airblast and fireball anomaly problem; significantly they note that on their 1200-lb ANFO sphere tests, "The fireballs expanded spherically without any evidence of anomalous behavior.")

The spherical ANFO tests conducted in October-November 1971 certainly did not provide data that could allay the concerns of the ground motion and cratering community. However, these data, in being compared with TNT results, did tend to bring into sharper focus than in the past, the whole ground effects problem i.e., the dependence of effects on ground geology and the difficulty of determining this ground geology with sufficient resolution to permit accurate predictions. Unfortunately, ground characteristics are not as easily defined as atmospheric characteristics. Another large scale military test operation was in the planning stage. What explosive to use on MIXED COMPANY?

NSWC, with the encouragement of Kelso, again submitted a proposal for using a spherical ANFO charge with a TNT equivalent yield of 500 tons. The reasoning was as follows: First, most of the targets for MIXED COMPANY were to be blast targets; the superior merits of ANFO over TNT for blast had been demonstrated with hemispherical charges weighing up to 100 tons, and spherical charges weighing up to 25 tons; it could be expected that the same superiority would be maintained on a 500 ton shot; and so, airblast targets would be subjected to a more predictable blast field than had been realized with TNT charges. (Remember DIAL PACK! Remember PRAIRIE FLAT! was the message.) And second, with the state-of-the-ground motion and cratering art being what it was, predicting the ground effects of ANFO shots probably would be no worse than for TNT shots. Besides, by measuring the ground effect phenomena, e.g., acceleration, displacement, crater dimensions, the observed response of targets should be relatable to the effects inputs, and, so, the objectives of the underground structure studies would be realized.

Again, the ANFO arguments and proposal were not accepted. MIXED COMPANY, fired in November 1972, used a 500 ton spherical TNT charge; and again, the now familiar airblast refrain--too many anomalies, too many airblast targets subjected to undesirably high (or low) pressures with distorted profiles. And the ground motion investigators again were finding that their predictions were not being realized adequately.

Persistence, as the study of almost any history of human events shows, has its merits. Or perhaps, it is frustration that leads to new challenges. In any case, now, the ground motion scientists joined forces with the airblast scientists in the search for a TNT replacement on military hardware tests dedicated to both sub-surface and surface target investigations.

1.3.5 HEST, DIHEST, etc.

During the years subsequent to the nuclear test treaty, the scientists interested in underground targets had not been at all idle in devising large scale simulation methods for their specific needs. AFWL (Air Force Weapons Laboratory), for instance, had designed HEST (High Explosives Simulation Technique) for simulating ground motions induced by airblast (Figure 1-26). Miles of explosive primacord wrapped on racks were arranged in the large area cavity formed by the ground surface and an earth overburden. A traveling

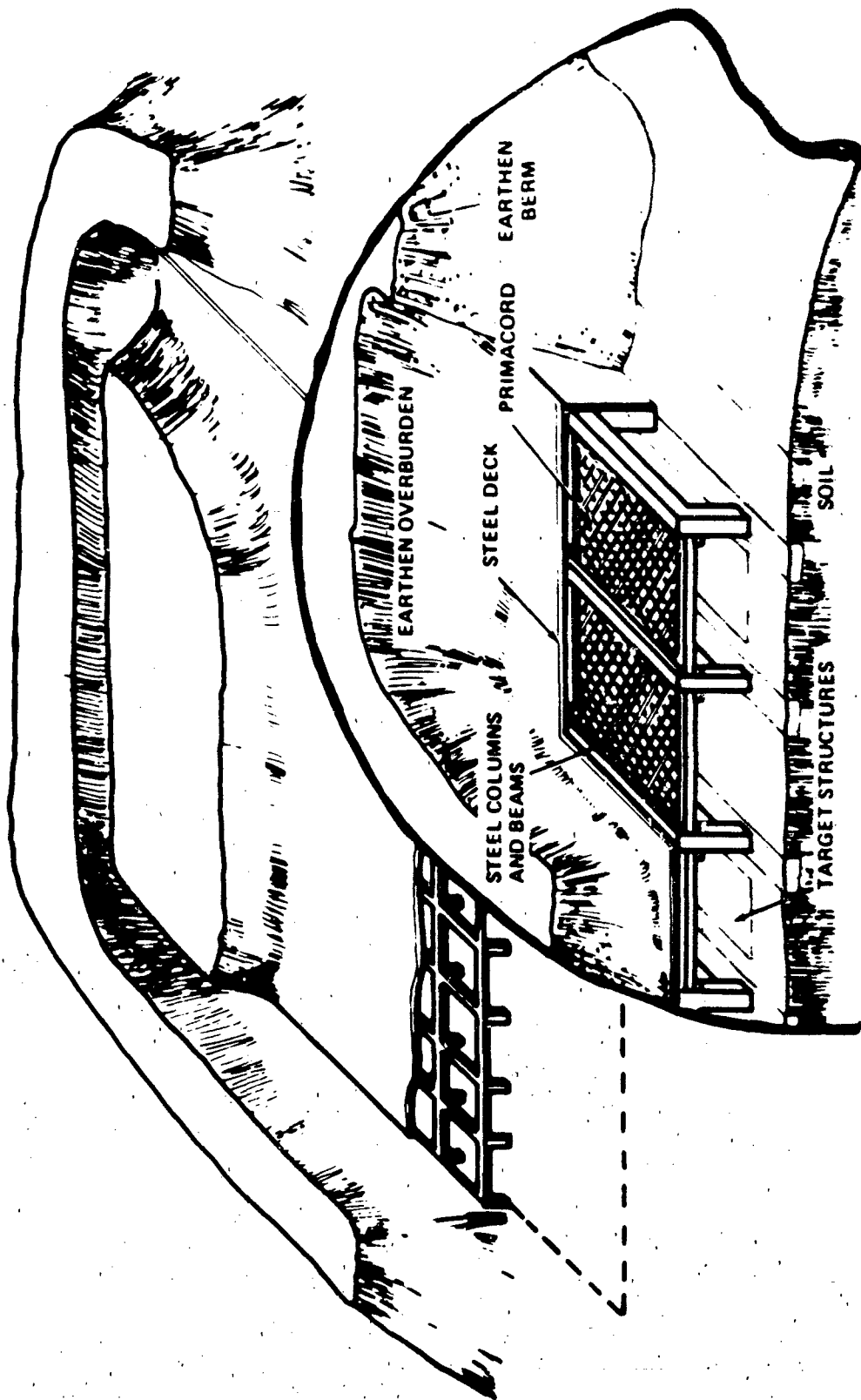


FIGURE 1-26. SKETCH OF HEST FACILITY.

blast wave was generated which coupled its energy to the ground and thus subjected the target, which was under the cavity, to ground stresses and motions. For other test objectives, AFML devised DIHEST (Direct Induced High Explosive Technique) (Figure 1-27) for generating directly induced ground shock. Many vertical holes filled with explosive were utilized to produce the required ground effects field. For still other tests, HEST and DIHEST were combined into a common system to generate both directly induced and airblast induced ground shock.

The previously described CHEST technique was still another method for producing ground shock. And, of course, the spherical TNT charge was yet another technique--and the one that found most application. It enjoyed this status because it could satisfy, basically, the requirements of both the underground and surface target testing communities.

1.4 ANFO FOR DICE THROW?

Now a new military hardware test was in the planning stage--Operation DICE THROW. After several meetings conducted by DNA in 1974, where target requirements and options for charge material and configuration were reviewed by representatives of the DoD test community, the decision was made to tentatively plan on using ANFO for the new test. And because of the intriguing possibility that cylindrical charges could satisfy ground motion requirements, DNA initiated an intensive program in 1975 to explore this charge shape and its application to the ANFO explosive. A program very similar to the one proposed by NSWC in November 1970 was started. The press of time--DICE THROW was scheduled for 1976--dictated quick action. If the ANFO cylindrical charge investigation did not prove successful, DICE THROW would have to revert to TNT; it took a long lead time to process the 500 tons required.

1.4.1 Pre-DICE THROW I

The program was multi-faceted with many agencies involved each in its own field of experience and competence (Table 1-2). The general objectives of this pre-DICE THROW effort was to design an ANFO charge that would provide a one-to-one correlation with the surface tangent sphere configuration (as used on DIAL PACK and MIXED COMPANY) in cratering and blast efficiency and would minimize blast anomalies (Reference 20).

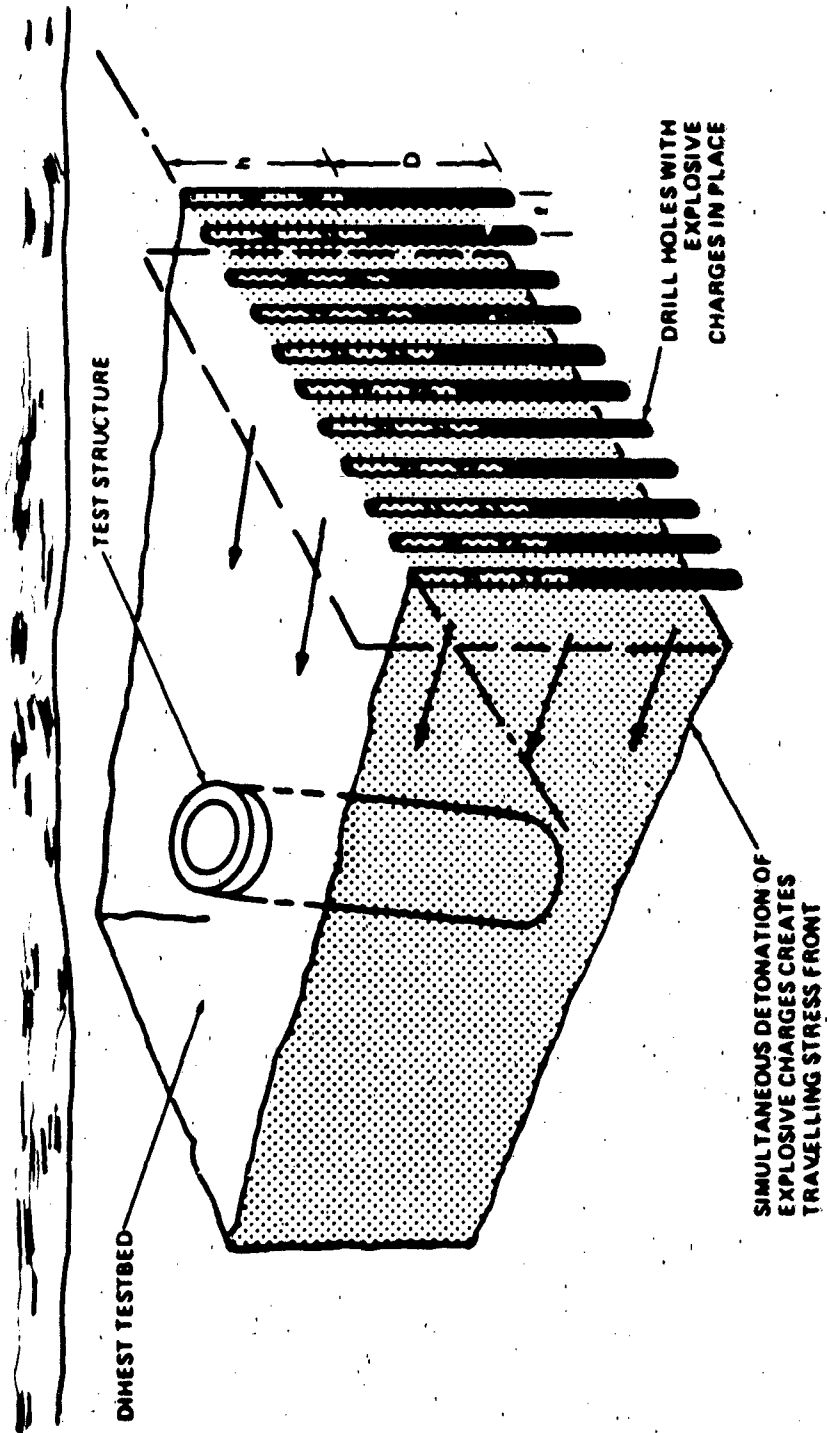


FIGURE 1-27. DIHEST CONCEPT.

TABLE 1-2. ANFO CHARGE DEVELOPMENT PROGRAM PARTICIPANTS

AGENCY	PROGRAM PHASE	PARTICIPATION
Air Force Weapons Laboratory (AFWL)	1, 2, 3, 4	Crater and Debris Measurements Technical Inputs Phases 1, 2, 3 Technical Supervision Seismic Measurements Ground-Motion Predictions Airblast Calculations Technical Photography
Ballistics Research Laboratory (BRL)	1, 2, 3, 4	Technical Consultation Airblast Measurements Airblast Predictions
University of New Mexico Civil Engineering Research Facility (CERF)	1, 2, 3, 4	Phases 1, 2, 3 Technical Supervision ANFO Charge Construction Crater and Debris Measurements Ground-Motion Measurements Airblast Measurements ANFO Detonation Diagnostics
General Electric Company TEMPO (DASIAC)	1, 2, 3, 4	Program Reporting Environmental Impact Assessment
Defense Research Establishment Suffield (DRES)	4	TNT Charge Construction Detonation Diagnostics
Denver Research Institute (DRI)	3, 4	Technical Photography
Defense Nuclear Agency (DNA)	1, 2, 3, 4	Program Supervision and Coordination
Lawrence Livermore Laboratory (LLL)	4	ANFO Detonation Characterization ANFO Detonation Diagnostics
Naval Surface Weapons Center (NSWC)	3, 4	Technical Inputs Consultant on ANFO Use ANFO Quality Control Booster Manufacturer for ANFO (including Testing)
R&D Associates (RDA)	1, 2, 3, 4	Technical Consultant
Stanford Research Institute (SRI)	4	Stress Measurements

TABLE 1-2. ANFO CHARGE DEVELOPMENT PROGRAM PARTICIPANTS (continued)

AGENCY	PROGRAM PHASE	PARTICIPATION
Science Systems and Software (SSS)	4	Stress Measurements Airblast Measurements
U.S. Geological Survey (USGS)	4	Aerial Technical Photography Cratering Consultant
Waterways Experiment Station (WES)	4	Ground-Motion Measurements Cratering Measurements Soil Sampling and Testing Timing and Firing
White Sands Missile Range (WSMR)	3, 4	Construction Support Program Coordination Technical Photography
Williams Aircraft Company	4	Aerial Technical Photography





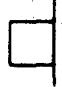



1.4.2 Phase 1

A three phase experimental program was planned and started in January 1975 using 1 lb to 5 ton charges. This development plan executed under the technical supervision of CERF (the Eric H. Wang Civil Engineering Facility, now named NWMERI--New Mexico Engineering Research Institute), is shown in Table 1-3. The immediate objective of the first phase with 1 lb charges was to determine a suitable cylindrical charge geometry in terms of length to diameter ratio. Plastic C-4 explosive was used for the charges because it could be molded easily into the various geometries under consideration. Because axial symmetry of the hydrodynamic effects of the explosion is required or, at least highly desirable, thought had to be given as to the location of the initiation point (or points, as it soon became evident); for a spherical charge single point detonation at the center of the charge provides this symmetry. Figure 1-28 depicts the initiation sites used in the program.

The use of these small charges required rather a controlled environment so that even small differences in explosion cratering effects could be related to the differences in charge geometries and detonation points. The CERF field facility provided this environment with a 14-ft diameter pit into which well characterized commercial grade concrete sand was placed to provide a uniform test bed for all tests (Reference 21).

Concurrent with the experimental program, hydrodynamic calculations were being made by C. Needham, AFWL, for predicting the blast effects of cylindrical charges. Swisdak, NSWC, provided detailed information on the physical characteristics of commercially available ANFO and AN prills to M. Finger, LLL (Lawrence Livermore Laboratory) who made equation-of-state calculations to characterize the detonation properties of the ANFO. This information provided the basis for Needham's calculations. His work and data available from an early 1960 study by J. Wisotski (Denver Research Institute) showed that the blast propagating off the sides of a right circular cylindrical charge is adversely affected by the rarefaction wave coming off the flat top of the charge. To prevent, or alleviate, these perturbations, the later shots of the Phase I program used cylindrical geometries with hemispherical caps.

Table 1-3. PRE-DICE THROW CHARGE DEVELOPMENT PROGRAM

Event	Date Fired	Test Site	Explosive Type	Charge Shape ^a	Radius mm(in)	Length: Diameter	Charge weight kg (lb)
CERF PDT I-A	1/15/75	CERF	C-4		41 (1.61)	NA	0.45 (1)
CERF PDT I-B	1/16/75	CERF	C-4		41 (1.61)	NA	0.45 (1)
CERF PDT I-C	1/22/75	CERF	C-4		41 (1.61)	NA	0.45 (1)
CERF PDT I-D	1/29/75	CERF	C-4		52 (2.03)	NA	0.45 (1)
CERF PDT I-E	2/12/75	CERF	C-4		NA	1.00:3	0.45 (1)
CERF PDT I-F	1/27/75	CERF	C-4		NA	1.00:1	0.45 (1)
CERF PDT I-G	2/7/75	CERF	C-4		NA	1.00:1	0.45 (1)
CERF PDT I-H	2/11/75	CERF	C-4		NA	2.00:1	0.45 (1)

^aKey:

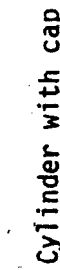
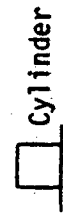


Table 1-3. PRE-DICE THROW CHARGE DEVELOPMENT PROGRAM (Continued)







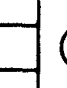











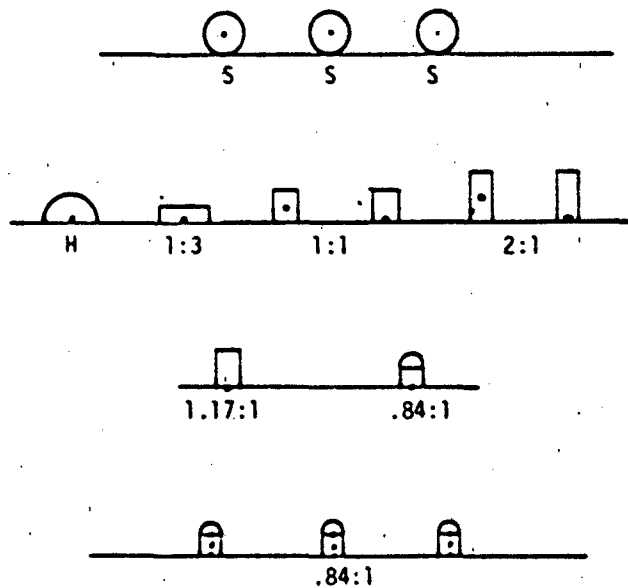
Event	Date Fired	Test Site	Explosive Type	Charge Shape	Radius mm(in)	Length: Diameter	Charge weight kg (lb)
CERF PDT I-I	2/6/75	CERF	C-4		NA	2.00:1	0.45 (1)
CERF PDT I-J	2/17/75	CERF	C-4		NA	1.17:1	0.45 (1)
CERF PDT I-K	2/18/75	CERF	C-4		NA	0.84:1	0.45 (1)
CERF PDT I-L	2/21/75	CERF	C-4		NA	0.84:1	0.45 (1)
CERF PDT I-M	2/25/75	CERF	C-4		NA	0.84:1	0.45 (1)
CERF PDT I-N	2/27/75	CERF	C-4		NA	0.84:1	0.45 (1)
CERF PDT I-O	6/3/75	CERF	C-4		NA	0.50:1	0.45 (1)
CERF PDT I-P	6/5/75	CERF	C-4		NA	0.50:1	0.45 (1)
CERF PDT I-Q	7/3/75	CERF	C-4		NA	0.75:1	0.45 (1)
CERF PDT I-R	7/8/75	CERF	C-4		NA	0.75:1	0.45 (1)
CERF PDT II-A	3/6/75	PICK AXE	TNT		338 (15.96)	NA	454 (1,000)

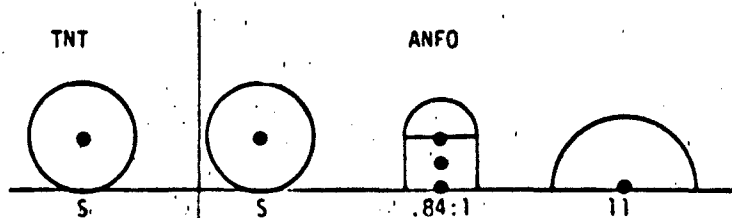
Table 1-3. PRE-DICE THROW CHARGE DEVELOPMENT PROGRAM (Continued)

Event	Date Fired	Test Site	Explosive Type	Charge Shape	Radius mm(in)	Length: Diameter	Charge weight kg (lb)
CERF PDT II-B	3/11/75	PICK AXE	ANFO		444 (21.00)	NA	552 (1,216)
CERF PDT II-C	3/18/75	PICK AXE	ANFO		NA	0.84:1	543 (1,197)
CERF PDT II-D	3/25/75	PICK AXE	ANFO		559 (26.40)	NA	562 (1,240)
PDT I-1	4/16/75	WSMR	TNT		721 (34.08)	NA	4,218 (9,300)
PDT I-2	4/30/75	WSMR	ANFO		NA	0.84:1	5,094 (11,230)
PDT I-3	5/14/75	WSMR	ANFO		NA	0.50:1	5,275 (11,630)
PDT I-4	7/31/75	WSMR	ANFO		NA	0.75:1	5,094 (11,242)

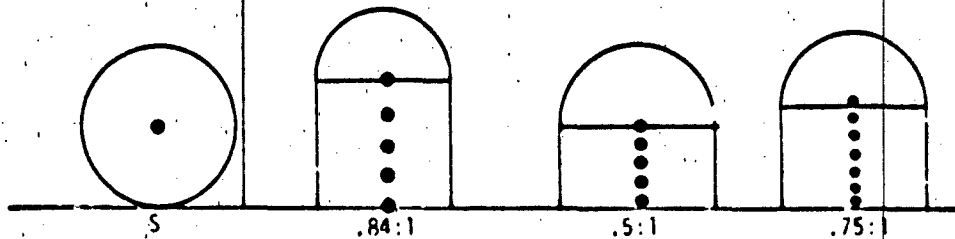
1 lb - C4
Phase 1



1000 lb
Phase 2



5 ton
Phase 3



Note: Not to scale.

FIGURE 1-28. CHARGE GEOMETRIES AND DETONATION POINTS.

"At the completion of the one-pound series, it was determined that for C4 charges a multiply-initiated, tangent-above, right circular cylinder with length-to-diameter ratio of .84 (measured on the cylindrical section) with hemispherical cap appeared to best meet the desired cratering and fireball shock-expansion program objectives. In addition, it was observed that apparent crater volumes exhibited a ± 10 -percent variation in reproducibility in a well-controlled test bed. Based on other field data, it is believed that this variation may be as large as 20 percent in a natural geologic medium. A nominal 20-percent variation in apparent crater volume was accepted as the uncertainty in determining cratering agreement for the remainder of the program" (Reference 20).

1.4.3 Phase 2

The second phase of the program with nominal 1000-lb TNT equivalent charges, was started and completed in March 1975. As part of this phase and based on calculations and the earlier phase results, a capped cylindrical ANFO charge with an L/D ratio of 0.84/1 and three point initiation was constructed. Bulk ANFO was used and contained in a thin case; the cylindrical portion of the charge was confined by a light cardboard form, the cap within a hemispherical styrofoam mold. Using the information developed on the earlier ANFO tests, i.e., ANFO I, II, and III, 1200-lbs of ANFO were used to give a 1000-lb TNT equivalence.

The shot was fired on 18 March. The cratering results essentially duplicated on a scaled basis the results of the similarly configured 1-lb C-4 charge. Significant differences were noted in the fireball characteristics of the ANFO explosion and the control tangent sphere 1000-lb TNT shot. The ANFO fireball was short lived and largely white in color whereas the TNT fireball was of long duration and fiery red. Although these differences were noteworthy to the experimenters, they were observed and explained on the earlier ANFO I-V series; they are attributable to the oxygen balance of the ANFO as contrasted to the oxygen deficiency of TNT. In an oxygen balanced explosive all the oxygen required to complete the combustion process is contained within the explosive compound or mixture. In an oxygen deficient explosive, the deficiency leads to afterburning, i.e., the utilization of atmospheric oxygen to continue and complete the detonation and combustion processes. Hence, the short, hot fireball for the ANFO explosion and the longer, cooler fireball for TNT.

The results of this phase of the program were indeed encouraging--a capped cylindrical charge of ANFO would replicate the effects of a surface tangent sphere of TNT if proper account is taken of the intrinsic differences in the explosive characteristics, charge geometries, and initiation points.

The requirement for the number and type of initiation points was studied further via hydrocodes by Needham. He found that the larger the number of points, the quicker would the detonation fronts within the charge coalesce to form a smooth outer contour before the front exited the charge; the smoother the front at this time, the more uniform would be the ensuing blast wave. So, for the Phase 3 shots with 5 ton TNT equivalencies, five and seven point initiation systems were used (Figure 1-28).

Multipoint initiation calls for special attention; to obtain the required smooth detonation front, all initiations have to take place simultaneously, lest skewed mach wave interactions between the several detonation fronts produce jetting within and outside the charge. Simultaneity was no mean feat, but it was successfully accomplished with the use of quick acting detonators and a well designed firing circuit.

1.4.4 Phase 3

Phase 3 operations started in the Spring of 1975 at the White Sands Missile Range, the prospective site for the main DICE THROW event. As indicated in Figure 1-28, three ANFO capped cylindrical charges were fired as well as a control, baseline-establishing TNT tangent spherical charge. Based on the Phase 2 results, the first ANFO charge had an L/D ratio of 0.84/1, and as suggested by the initiation studies of Needham, five detonation points were used. The design for the charge is shown in Figure 1-29. The cylindrical portion of the container was constructed from thin sheets of fiberglass and the hemispherical cap was formed from thin nylon parachute fabric. A nominal 12,000-lbs of bulk ANFO was rained into the containment vessel to provide a 10,000-lb TNT equivalent yield. Relatively extensive instrumentation coverage was used on the test.

The ground motion results, and the airblast measurements were satisfactory and well within the normal spread of data from single explosions. However, the crater volume was about 30% smaller than the TNT control and high speed photographs showed several airblast anomalies.

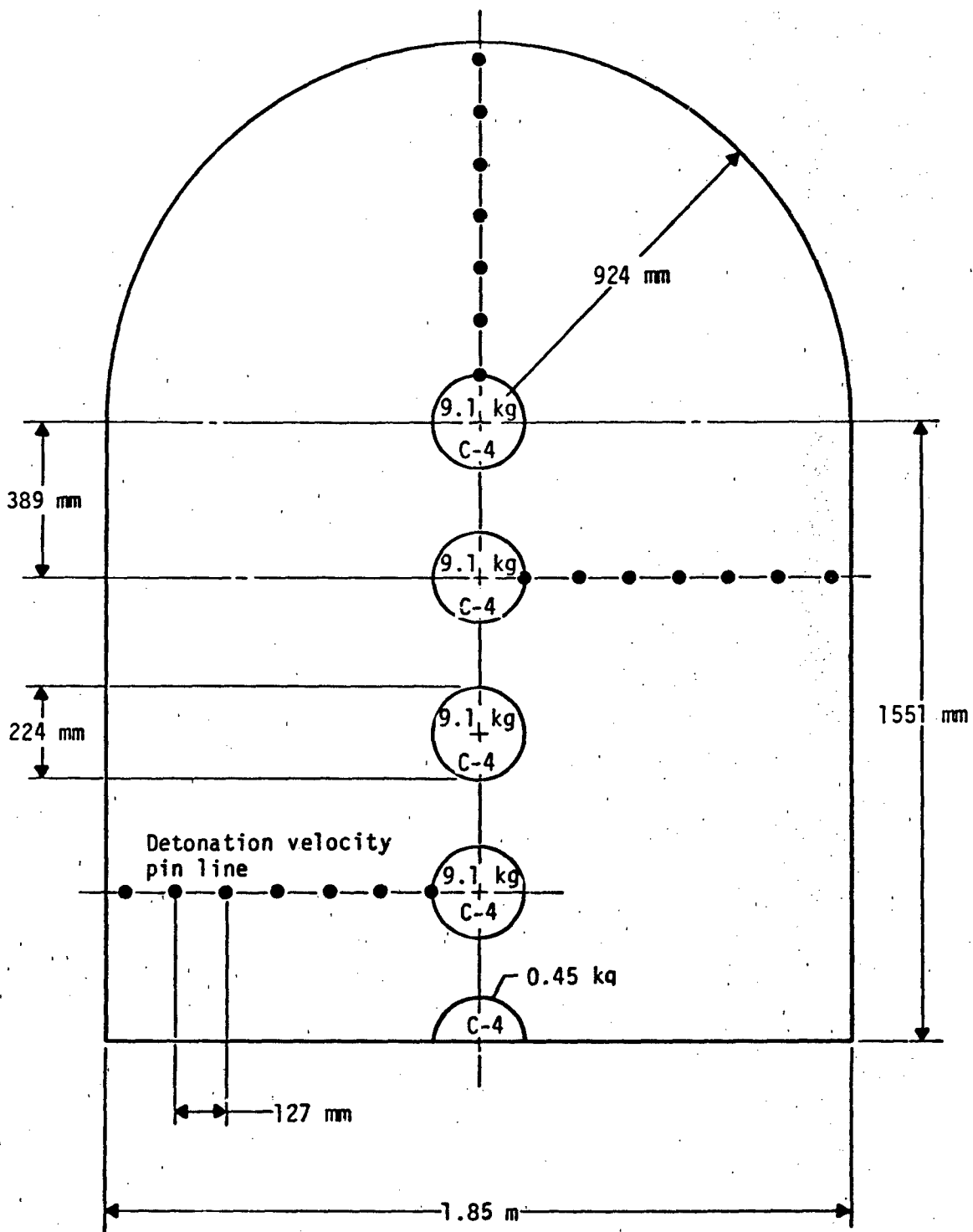


FIGURE 1-29. CROSS SECTION OF BULK ANFO CAPPED CYLINDER, (L/D = 0.84/1), PRE-DICE THROW 1, EVENT 2, 6 TONS.

A second capped cylinder was fired with an L/D ratio of 0.5/1. Again bulk ANFO was used to fill the form. This time, however, a heavy tarpaulin canvas was used to shape the hemispherical cap. The nylon used on the first shot of this series was flimsy so that a good hemispherical shape could not be attained; this was suggested as a cause for some of the anomalies. The charge exploded satisfactorily but because of the larger area of charge/ground contact with this 0.5/1 L/D ratio, a substantially larger crater resulted on this shot than on the control TNT surface tangent sphere or the previous L/D 0.84/1 ANFO geometry. Also, blast anomalies were present again.

In this iterative experimental search for the most suitable ANFO shot geometry, the third and last 12,000-lb ANFO charge had an L/D ratio of 0.75/1. Perhaps remembering past history where it was observed that even lightly cased ANFO charges produced more anomalies than bag built charges, this charge was constructed with bagged ANFO. Careful attention was paid to bag placement so that a smooth periphery was obtained for the charge (Figure 1-30) as on the 1970 ANFO I, II, and III series. In fact, because the relatively small diameter (6.28-ft) of the charge made it difficult to place the standard 50-lb bags of ANFO into a tight, bag-butted-against-bag, configuration, the ANFO was repackaged into 15-lb sizes in nylon bags. Nylon was selected because the paper, canvas, and burlap bags investigated absorbed oil, some to the extent that the bags deteriorated and disintegrated. Changes were made in the detonation scheme also. Seven-point initiation was used and instead of spherical boosters, cylindrical C-4 boosters were arrayed along the axis of the cylindrical portion of the charge as shown in Figure 1-31.

All these changes--new L/D, bagged ANFO, seven-point initiation--resulted in a very satisfactory charge performance and explosion effects. Crater size was close to the TNT standard crater, ground motions were well within the accepted standard scatter, airblast measurements were as predicted with little scatter and significantly, very few anomalies were evident. DNA and most of the testing community were ready to move on to DICE THROW, the 600 ton ANFO event. But prudence dictated an intermediate scale test first; a second series of tests was planned, pre-DICE THROW II.

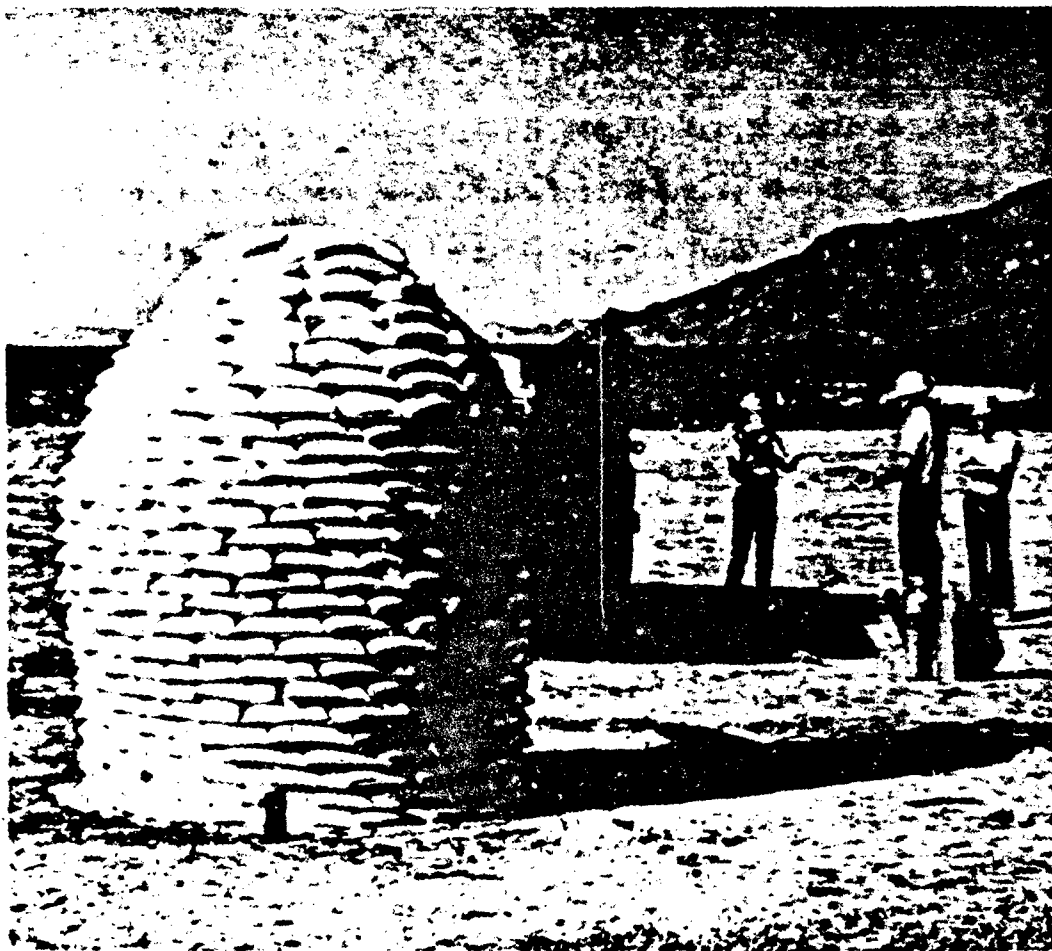


FIGURE 1-30. COMPLETED BAGGED ANFO CHARGE, PRE-DICE THROW I, EVENT 4.

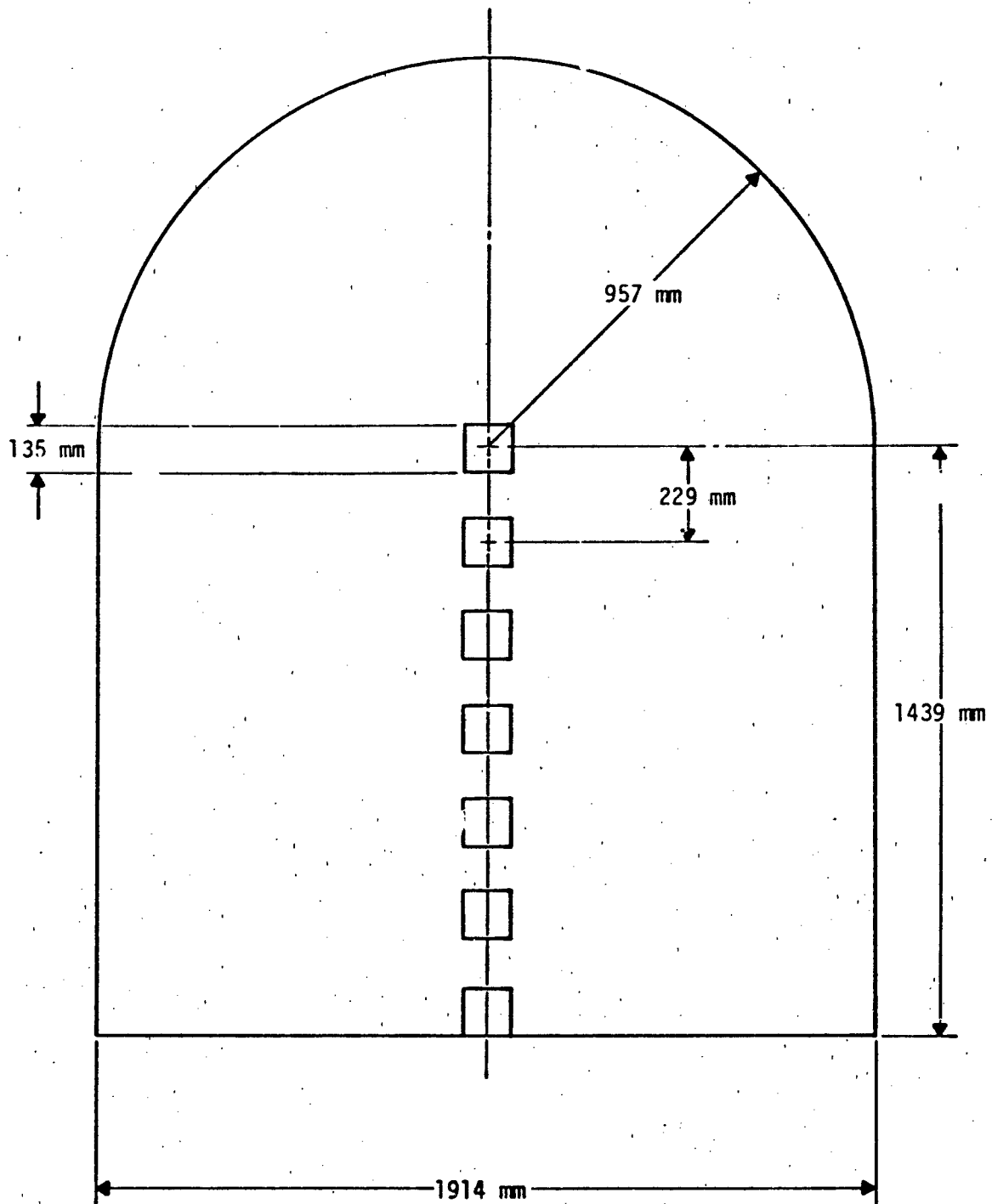


FIGURE 1-31. DESIGN OF BAGGED ANFO CAPPED CYLINDER ($L/D = 0.75/1$),
 PRE-DICE THROW I, EVENT 4.

1.4.5 Pre-DICE THROW II

Pre-DICE THROW II was arranged and conducted in August-September 1975. There were two shots, Event I, the control event for comparison purposes, a 100 ton block built TNT sphere tangent to the surface, and Event II, a 120 ton ANFO charge scaled to the highly successful pre-DICE THROW, Phase 3, Event 4 shot. (As with all the ANFO tests after the 0.82 TNT equivalence had been established, where direct comparisons are to be made between ANFO and TNT effects, the ANFO weight is approximately 1.2 larger than the TNT yield.)

Pre-DICE THROW II was a crucial operation; on the performance of this ANFO shot hinged the charge design selection for the main event, DICE THROW. The operation took on the aura and magnitude of the main event itself. Site selection was carefully made to meet the geologic requirements of the Air Force MX program; an area on the White Sands Missile Range, close to the pre-DICE THROW I, Phase 3 site, was chosen. There were twenty-two project agencies on the operation fielding twenty-eight different projects. Some projects dealt with charge construction, initiation, and diagnostics, air and ground shock measurements, gage development cratering, ejecta, ground displacements, technical photography, and prediction techniques for the phenomenology of concern. Other projects were directly concerned with military hardware items and detection systems. All in all, pre-DICE THROW II was a big show with many participants, a large audience, and a concerned angel, DNA (Reference 22).

The block built TNT spherical charge was constructed under the direction of DRES personnel in a manner similar to previously built large TNT charges. The Event II charge with the domed cylindrical geometry was constructed under the supervision of Swisdak with 50-lb bags of ANFO obtained locally in New Mexico. A bag stacking plan similar to the one used on ANFO I and pre-DICE THROW, Phase 3, Event 4, was used. As before, it was deemed important to obtain a smooth outer contour for the charge. Figure 1-32 shows the layout for one layer of bags; note the bag-against-bag arrangement to get that smooth outer contour. To obtain some structural strength to the construction each layer had its inner bags laid at about a 90° angle to the bags below and above.

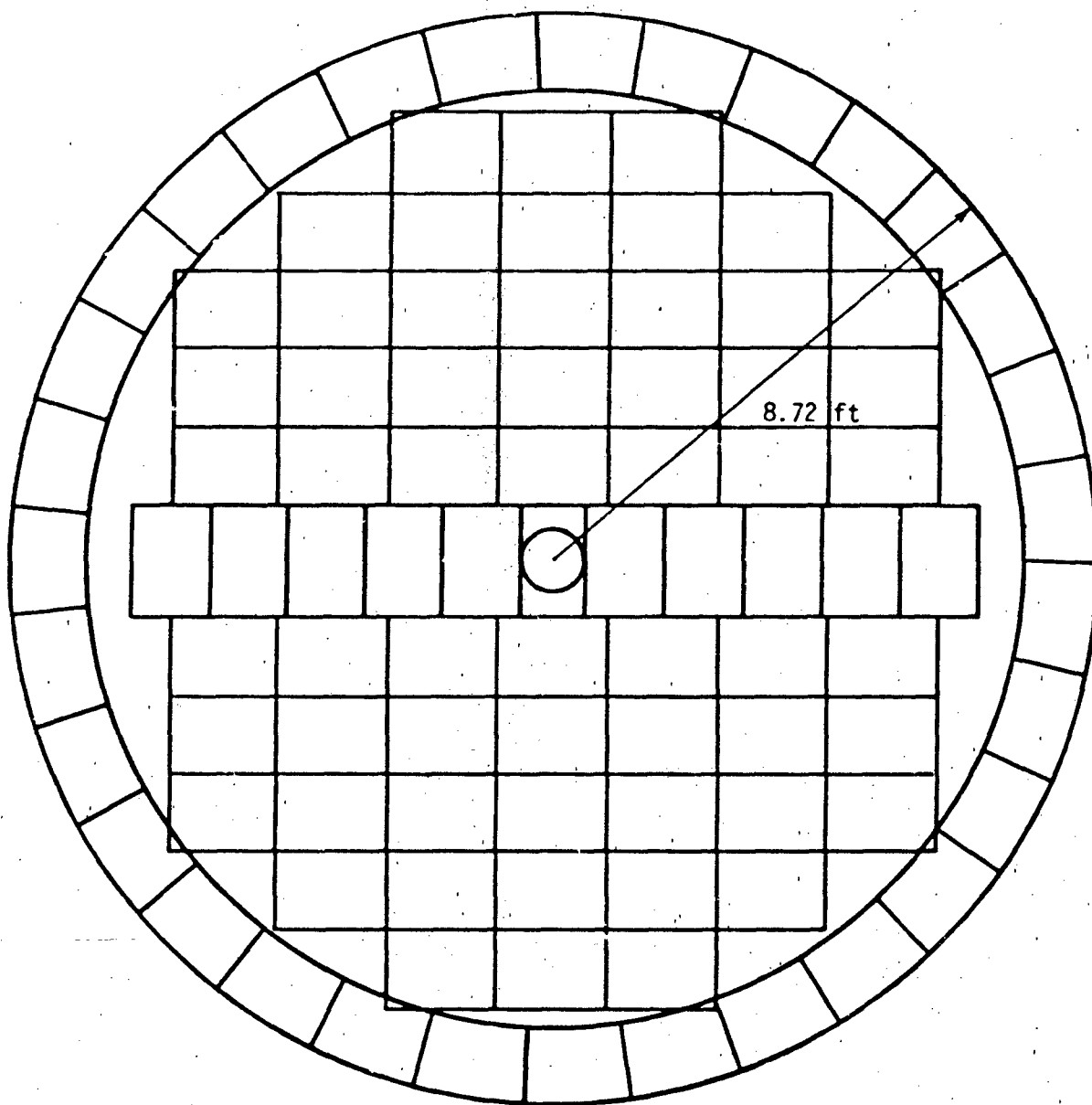


FIGURE 1-32. INITIAL NSWC ANFO STACKING PLAN, PRE-DICE THROW II, EVENT 2.

During construction of the stack, after about 40 tons had been emplaced, some of the dire concerns of DNA were realized; the stack collapsed partially during a heavy rainstorm. Although a tarpaulin had been used to protect the charge, rain water apparently penetrated to the ANFO resulting in a dissolution of some ANFO and a partial collapse of the charge. Also contributing to the collapse, it was postulated, was excessive personnel traffic on the rim of the charge during charge preparation and while emplacing the protective tarpaulin. And, the charge stacking plan was suspect. The outer bags particularly were essentially unsupported in the lateral direction and thus in a sort of unstable equilibrium; this design while successful for the smaller 12,000-lb charge, appeared untenable for the larger, almost 22-ft high, charge (Figure 1-33).

A new stacking plan was quickly fashioned, one which followed the pattern of the block TNT charge construction. All bags, including the peripheral ones, were interlocked to some extent (Figure 1-34), and additional structural strength to the stack was attained by rotating the bag stacking arrangement of each layer 90° with respect to the layer below. The smooth outer contour was sacrificed in this design; it was hoped that this variation from the ideal design could be tolerated--that it would not lead to the generation of an excessive number of anomalies. The significance of a smoothly contoured ANFO charge versus a rough one had not been established by experiment or analysis, although as indicated in Section 1.3.4 no anomalies were noted on ANFO V even though it had a rough outer contour. In any case, the charge had to be constructed if DICE THROW was to continue on schedule; the theme was brawn before beauty. The charge, indeed, was successfully built and completed in three days without further mishap (Figure 1-35).

As with the prototype 12,000-lb ANFO shot, a seven point detonation scheme was used on this pre-DICE THROW II-2 event. A new and sophisticated design was made by Swisdak in which arming, firing, and operational safety were the paramount considerations. The initiation and boosting system consisted of two parts, an MBA (Main Booster Assembly) emplaced along the axis of the stack during charge construction, and a BIS (Booster Initiation System) lowered into the MBA in order to arm the charge.

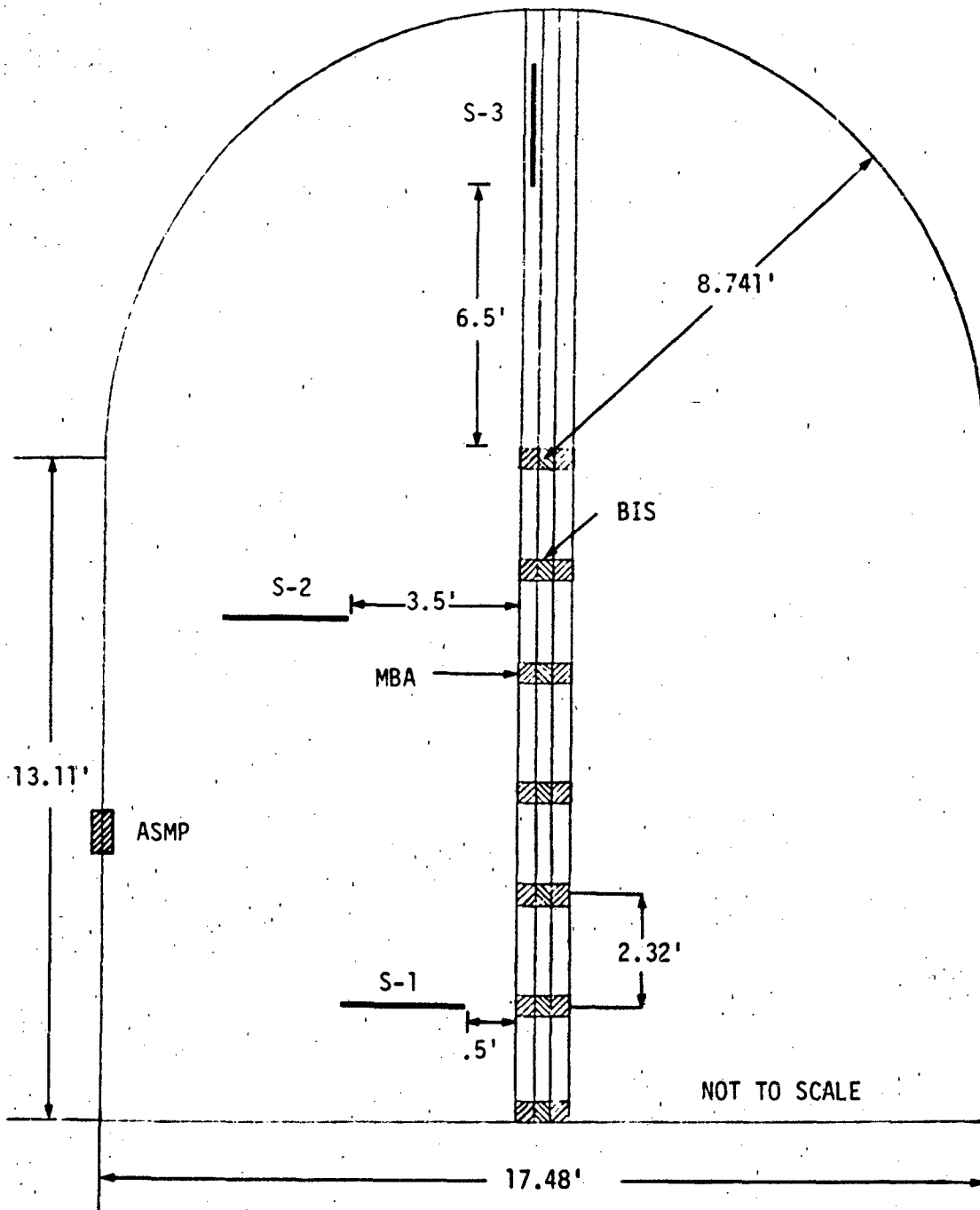


FIGURE 1-33. ANFO CHARGE CONFIGURATION - PRE-DICE THROW II - EVENT 2.

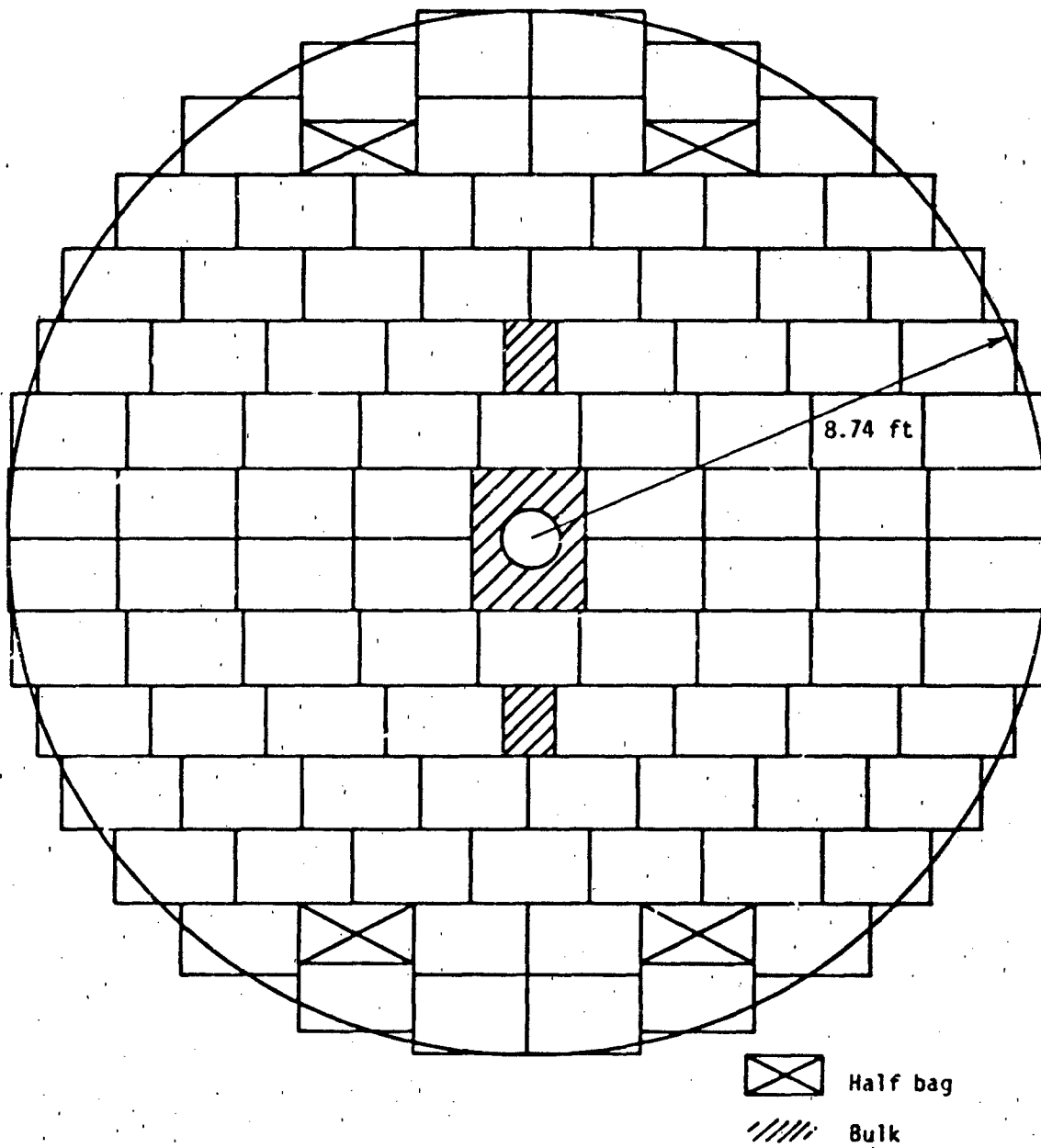


FIGURE 1-34. FINAL NSWC ANFO STACKING PLAN, PRE-DICE THROW II, EVENT 2.

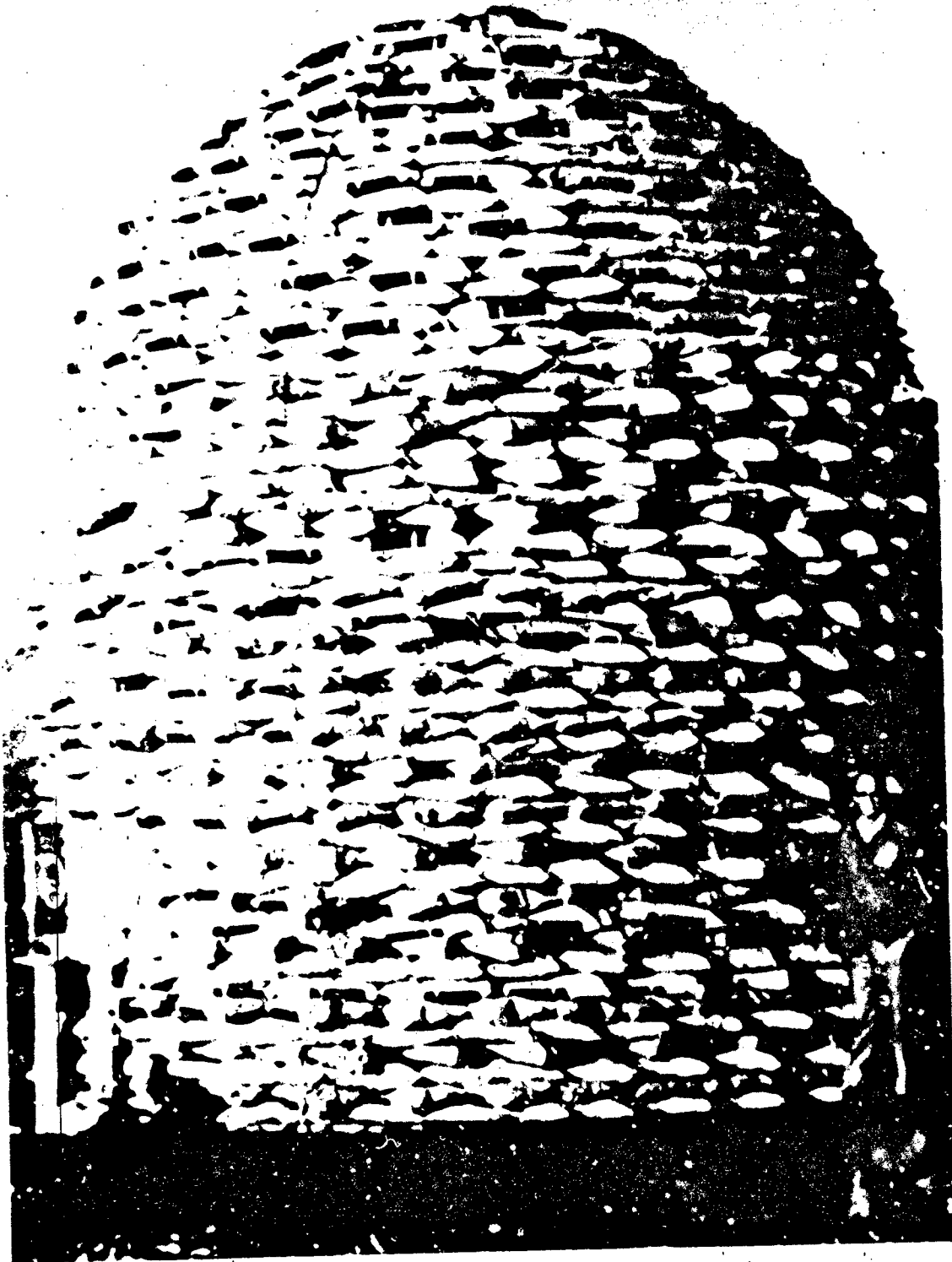


FIGURE 1-35. COMPLETED CHARGE FOR PRE-DICE THROW II, EVENT 2, ($L/D = 0.75$),
120 TONS.

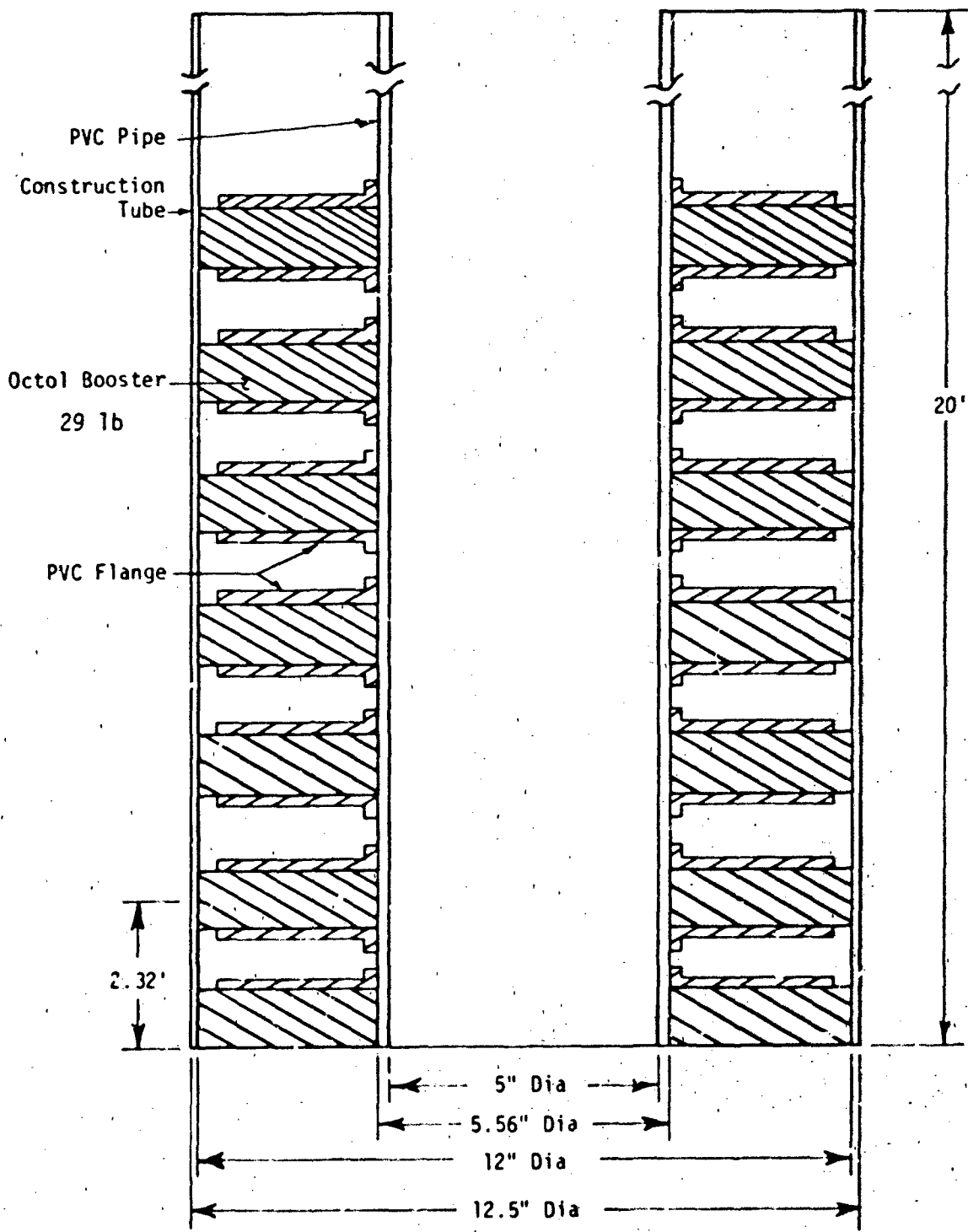
The MBA consisted of a 5-inch diameter (I.D.) PVC (Poly-vinyl-chloride) tube around which were afixed seven 29-1b, 5-inch thick, 12-inch diameter charges of 75/25 Octol, a rather insensitive explosive (Figure 1-36). The location of these booster charges are indicated in Table 1-4. A cardboard construction tube was placed around the MBA to protect it during ANFO bag stacking.

TABLE 1-4. PRE-DICE THROW II, EVENT 2 BOOSTER SYSTEM DETAILS

Location	Booster Center Height Above Base (Feet)	Octol Weight (Pounds)	Pentolite Weight (Pounds)
1	.21	28.54	1.99
2	2.32	28.73	1.99
3	4.44	28.78	1.98
4	6.55	29.00	1.98
5	8.67	29.05	1.98
6	10.78	29.16	1.98
7	12.90	29.22	1.98

The BIS (Figure 1-37) was the arming device. It consisted of a 4.5-inch diameter (O.D.) PVC tube into which were fixed seven pentolite explosive discs at spacings identical to the one of the Octol boosters (Table 1-4). Each pentolite initiator was provided with two exploding bridge wire detonators (Reynolds Industry type RD-1), one as the primary, the other for redundancy.

To arm the charge, the BIS is lowered into the MBA (with the help of a crane [see Frontispiece]) so that the pentolite and octol discs are aligned. Laboratory tests demonstrated the adequacy of this MBA/BIS system. The shock wave from the pentolite successfully bridged the air gap between the PVC tubes and through the tube wall thicknesses to detonate, high order, the octol boosters.



NOT TO SCALE

FIGURE 1-36. MAIN BOOSTER ASSEMBLY (MBA) - PRE-DICE THROW II - EVENT 2.

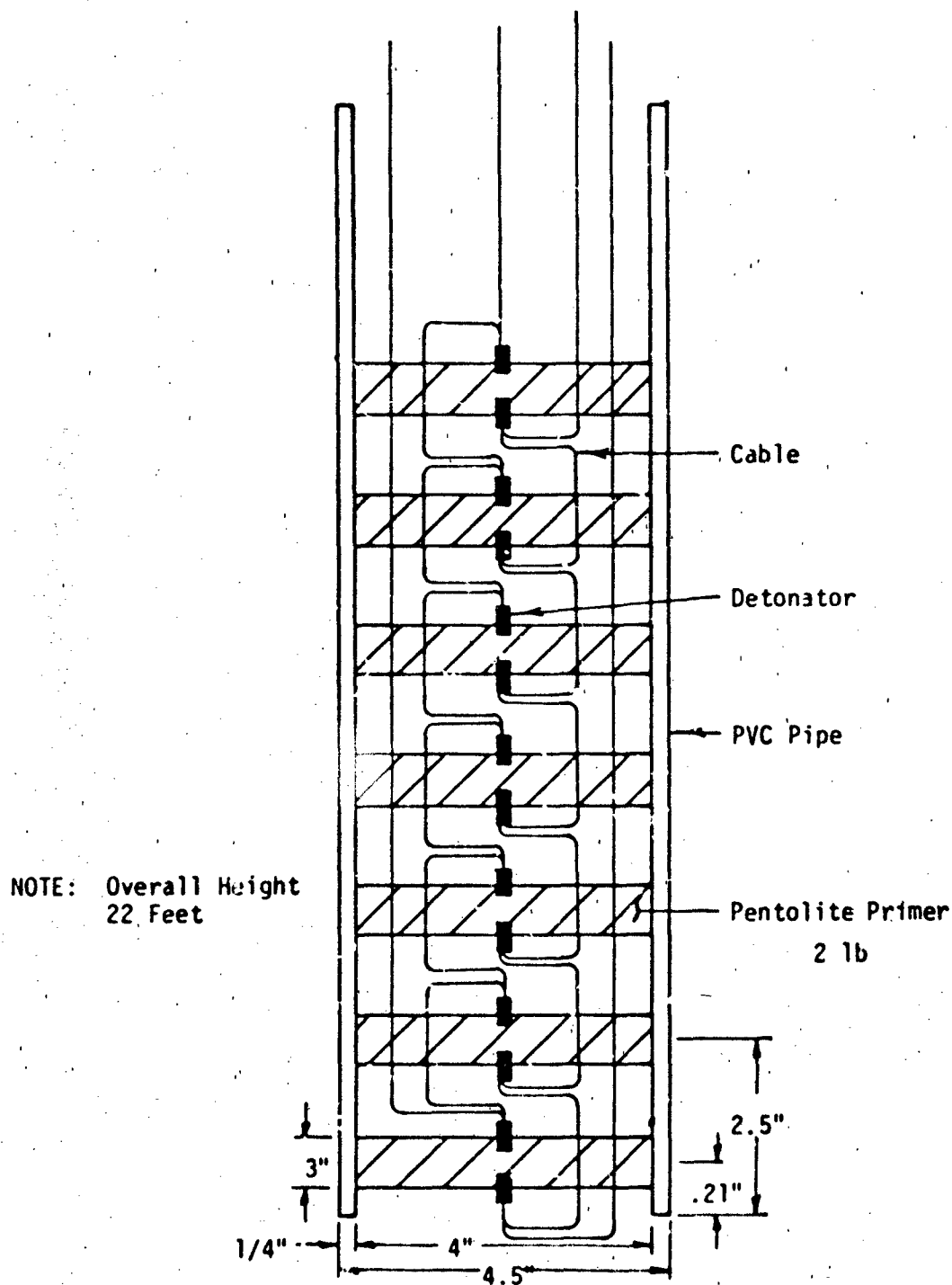


FIGURE 1-37. BOOSTER INITIATION SYSTEM (BIS) PRE-DICE THROW II, EVENT 2.

The somewhat flexible nature of the long PVC tubes presented a slight problem: difficulty was experienced at first in inserting fully the BIS into the MBA because the MBA PVC tube had a slight bend. With the help of a lot of grease and some little prayer, the BIS insertion was finally made satisfactorily.

On 12 August the Event I TNT charge was fired; on 22 September 1975, the Event II ANFO shot took place. The data obtained and their analyses resolved DNA's problems and questions relative to the selection of the charge for the DICE THROW main event; the 120 ton domed hemispherical bagged ANFO charge performed excellently, and in some important aspects, better than the control 100 ton block built spherical TNT charge. Both airblast measurements and fireball photography showed the absence of significant anomalies on the ANFO shot, while the TNT charge produced perhaps even more than its normal number of airblast perturbations. Ground motion particle velocities were similar in waveforms and amplitudes for the TNT and ANFO detonations. Adequate predictions could be made for blast and ground motion effects. The ANFO shot crater was larger than that of the TNT charge; this result was consistent with the results of the pre-DICE THROW I tests. The TNT crater, however, was unexpectedly larger than predicted; this again points up the difficulties of trying to predict effects in a medium as inhomogeneous as ground.

The measurements unique to the ANFO event provided valuable self consistent and comforting information. The internal temperature probes in the ANFO charge showed 70^o-75^oF temperatures (Figure 1-38). The variations followed diurnal air temperature changes; there was no self heating of the charge.

The average detonation velocity within the charge, as measured by LLL with three rate sticks was 4,790 meters/second. This is higher than that measured in earlier tests. There apparently is a direct correlation between detonation velocity and charge size as Table 1-5 shows.

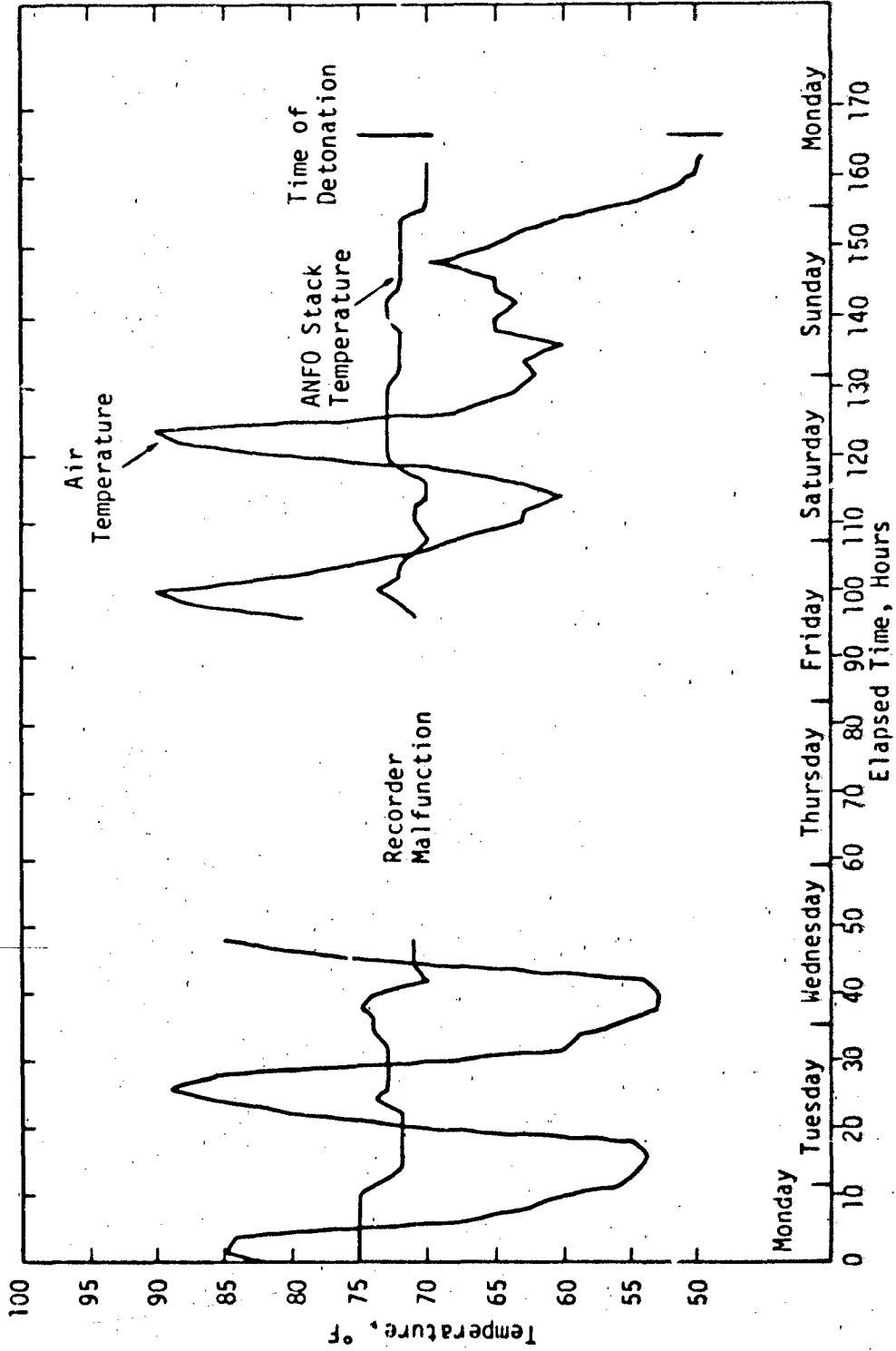


FIGURE 1-38. TEMPERATURE-TIME RECORD IN ANFO STACK, PRE-DICE THROW II, EVENT 2.

TABLE 1-5. DETONATION VELOCITIES OF ANFO CHARGES

Charge Wt	Shape	Average Detonation Velocity (m/sec)
260-4000 lbs	Hemisphere	4200
20 ton	Hemisphere	4410
20 ton	Sphere	4390
100 ton	Hemisphere	4600
120 ton	Cylinder	4790

It is probable that the bulk density of the ANFO in situ increases with the size of the charge: the larger, i.e., taller, the charge the more the lower layers of prills are compacted by the weight of the upper layers. Some prill break-up undoubtedly occurs; the fragmented prills fill the voids between the prills thus increasing the bulk density. With increased bulk density, increased detonation velocity can be expected as Finger's calculations indicate and earlier industry experiments have shown. (Note that the prill density need not change to get increased bulk density; it is the prill size distribution that determines to a large degree the bulk density. With prill density unchanged, the original stoichiometric ANFO proportions remain undisturbed on a prill basis.)

1.5 . . . AND FINALLY, DICE THROW!

Pre-DICE THROW II, Event II, the 120 ton ANFO shot, was an unqualified success. DNA and DNA/FC now proceeded in full gear on Operation DICE THROW with ANFO (Reference 23). This operation was, "designed to meet two primary objectives: 1) provide a simulated nuclear blast and shock environment for target response experiments that are vitally needed by the military services and defense agencies concerned with nuclear weapons effects, and 2) confirm empirical predictions and theoretical calculations for shock response of military structures, equipment, and weapons systems." All the U.S. military services, 28 agencies, and six foreign countries participated in DICE THROW.

A large field operation such as DICE THROW requires a large organization to plan, coordinate, and carry out all the activities. The Field Command/DNA had this responsibility. They assembled a knowledgeable and capable staff made up of experienced and dedicated persons (Figure 1-39). Field operations at the WSMR started in early 1976 with site preparation and continued through the ANFO charge construction and firing in October to the end of the year when post-shot data recovery and site clean-up were completed. The test site was at the Giant Patriot location about 25 miles northwest of the Queen 15 site where the 120 ton ANFO Pre-DICE THROW event took place (Figure 1-40).

The DICE THROW charge (Figure 1-41) was scaled to the pre-DICE THROW II 120 ton charge in all its significant features. The cylindrical portion of the DICE THROW charge had an $L/D = 0.75$ with a diameter of 29.8 ft and a length of 22.5 ft. This was capped with a 14.9 ft radius hemisphere so that the total height of the charge was 37.4 ft. The charge was constructed from 24,903 bags of premixed ANFO obtained locally in New Mexico. Of this total, 1,755 bags were opened and the loose ANFO used to fill the spaces between the other bags. The total weight of the ANFO in the charge was 621.77 tons. The paper bags, the booster explosives, and miscellaneous material in the charge brought the total weight to 628.27 tons.

The interlocking bag stacking plan developed on pre-DICE THROW II was again used but with an added feature; the outer bags of ANFO were glued together to increase the structural integrity of the charge.

One other feature was added to charge construction; a protective housing was built in which the charge stacking took place. Neither rains nor storms, nor winds, of which there were ample number at the White Sands Missile Range test site, deterred or harmed the stacking task. The housing was designed so that it could be removed easily prior to the shot, be stored, and be ready for use as needed for other charge stacking jobs.

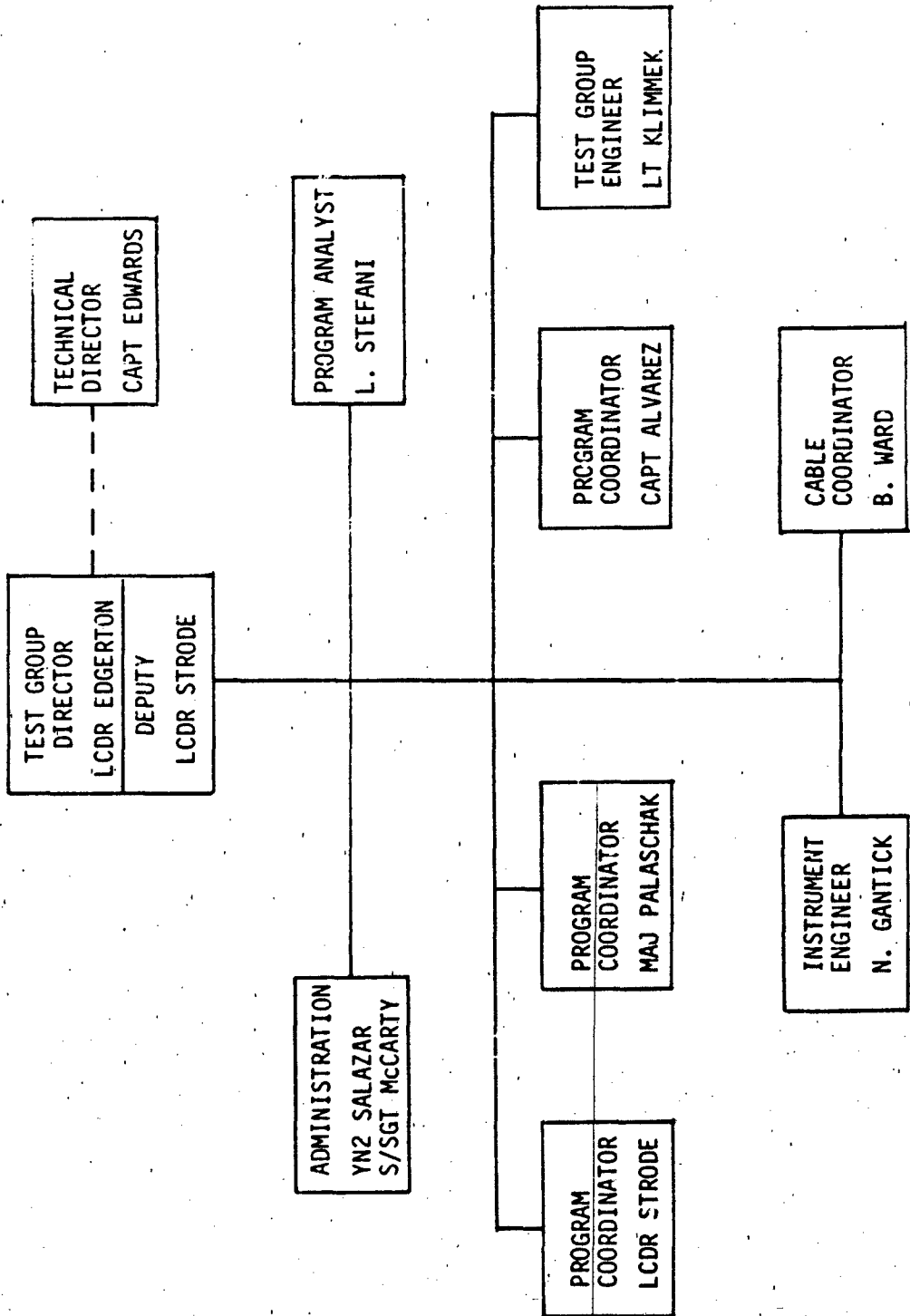


FIGURE 1-39. TEST GROUP STAFF ORGANIZATION

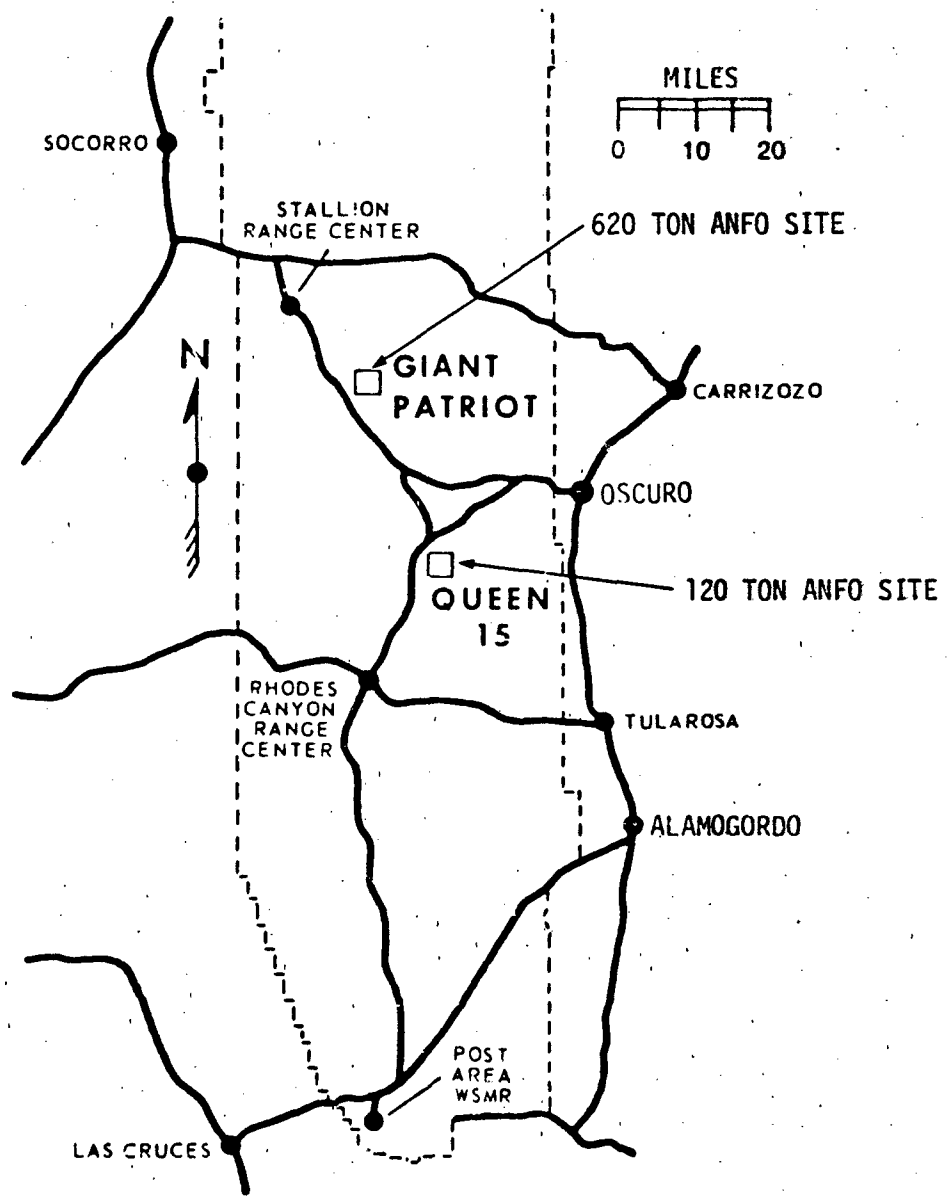


FIGURE 1-40. SITE LOCATION FOR DICE THROW (620 TON ANFO) AND PRE-DICE THROW II, EVENT 2 (120 TON ANFO).

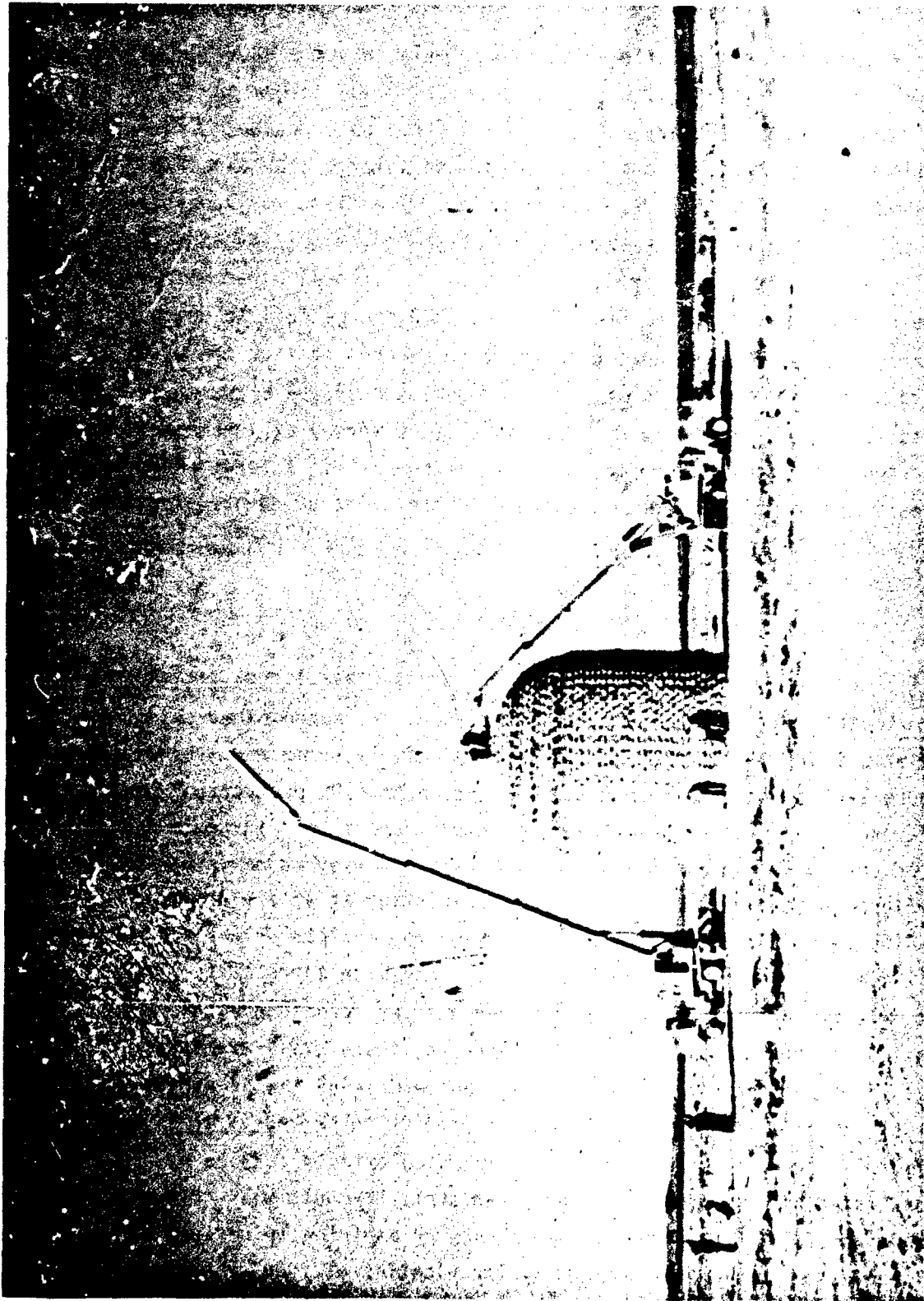


FIGURE 1-41. DICE THROW CHARGE: PLACING BIS INTO POSITION.

The seven point initiation/boosting design was the same as used on the 120 ton ANFO event except that the construction tube around the MBA was eliminated as not necessary. The shot was fired on 6 October 1976--a short duration bright flash, a long, loud bang, and a large gray cloud was all that was seen from the distant observation point. The flash was somewhat disappointing to many observers who had never before seen an ANFO explosion; missing was the red-orange roiling and boiling fireball mixed with dense black smoke so familiar on TNT shots. "Did the ANFO charge fail to detonate properly?" they wondered during the fifteen seconds it took the blast to arrive at the observation station. The magnitude of the blast that was felt put to rest these momentary doubts, and a later survey of the test site indicated that, indeed, the charge went off properly. A large crater was seen and many targets responded to the blast to the point of severe structural damage. The ANFO fireball was characteristic of stoichiometric explosives that have no afterburning.

1.5.1 . . . Results

Airblast measurements along three different blast lines, radiating approximately 120° apart from GZ, and at about two dozen other points in the test area indicate the propagation of a relatively symmetrical blast front (Figure 1-42); the data points scatter around the BRL prediction curve (Reference 23). (To put this scatter into perspective, Figure 1-43 is introduced to illustrate the spread normally experienced on large TNT shots. The figure presents data for the 100 ton TNT tangent sphere control shot of pre-DICE THROW II, Event 1; the scatter, where multiple data points are available, is considerably larger than for the much larger DICE THROW ANFO shot. It is interesting to note that even after more than a half dozen shots with 100 ton and 500 ton TNT tangent spheres, there still are two prediction curves for the event--and the data fall below each of the predictions. That the data scatter and do not fall on the prediction curves is interesting but not surprising. The long history of explosion effects studies has demonstrated amply that on any one given shot, the data will show scatter around (hopefully!) some hydrodynamic code or empirically derived curve. The real explosion is not constrained by the niceties of ideal, theoretical conditions postulated in the prediction schemes.)

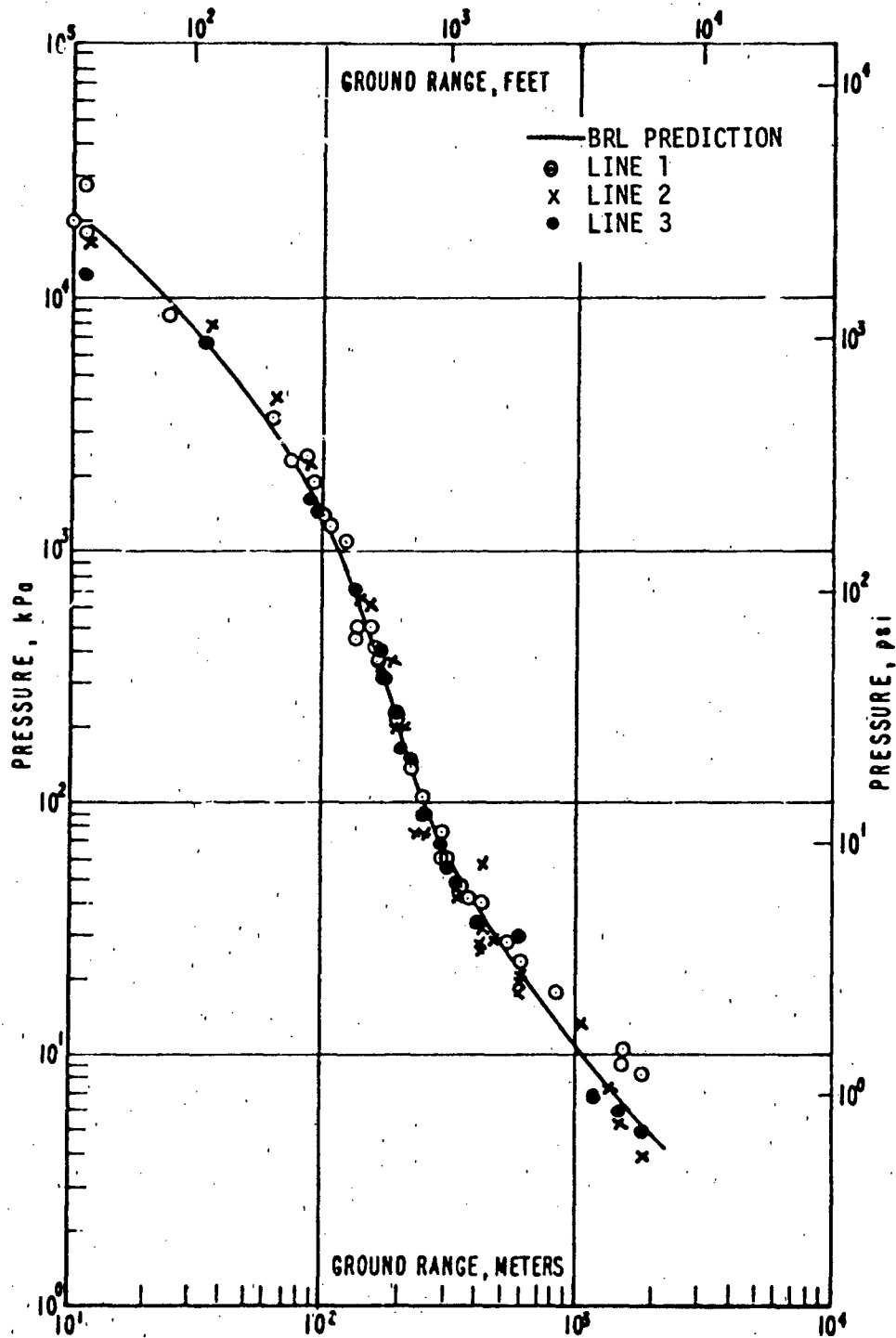


FIGURE 1-42. MEASURED INCIDENT SHOCK OVERPRESSURE VERSUS GROUND RANGE - DICE THROW - 620 TON ANFO SHOT.

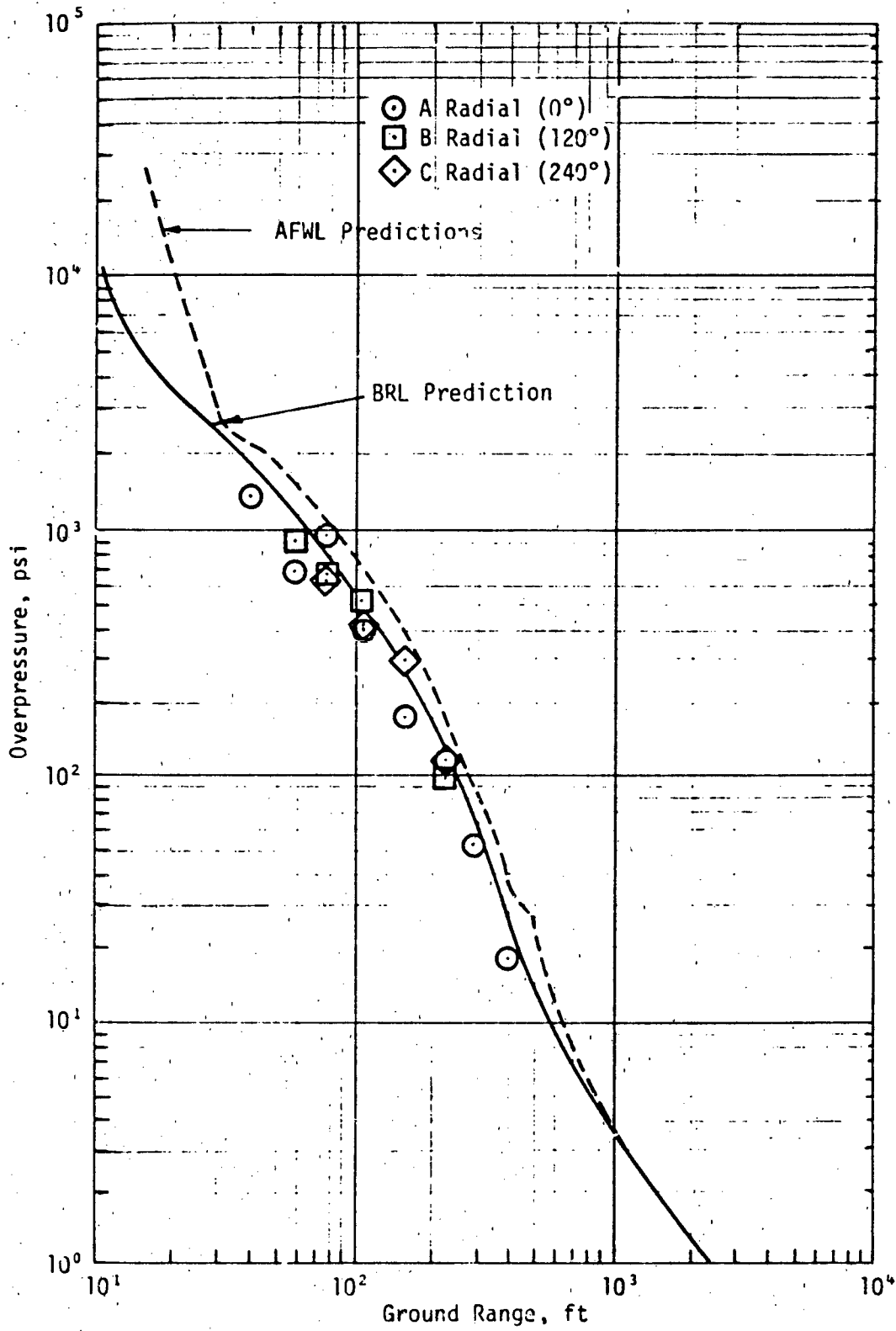


FIGURE 1-43. OVERPRESSURE VERSUS GROUND RANGE, PRE-DICE THROW II, EVENT I, 100 TON TNT TANGENT SPHERE, BRL DATA.

On DICE THROW scatter between 2 and 2,000 psi is well within that usually found in field experiments. The scatter around the 1 psi level may be attributable to the influence of local wind and temperature variations at the long distances where the low blast pressures occur. At the 3,000 psi level, the scatter may result from the difficulties of gages following a high transient pressure in an air field perturbed by detonation products and thermally induced air instabilities, or this scatter may be true representations of the pressure field close-in to the charge--real non-symmetries or anomalies. Although anomalies are not particularly discernible in the pressure-distance plots of Figure 1-42, the pressure-time records at several blast measuring stations and high speed photographs of the fireball and shock front do give evidence that some anomalies occurred.

The presence of these anomalies is disturbing even though they are less extensive and severe than those produced on the earlier employed block built TNT charges; no ready and conclusive explanations are available to account for them. Indeed, it may be that as stated earlier, there is evidence that most, if not all, condensed explosives produce anomalies such as jetting. If this is so, then the ANFO charge performance furthers this view, and it has to be lived with; c'est la vie. Or it may be that uneven fuel oil distribution and possible air pockets within the charge (resulting from inadequate filling of the inter-bag spaces with loose ANFO) may lead to a sufficiently inhomogeneous explosive charge so that non-symmetrical detonation occurs. Swisdak's measurements of fuel oil content made during charge construction shows average fuel oil percentages ranging from 4.96 to 7.02 in the layers, although the average for the whole charge is 6.12% (Reference 23).

Additional inhomogeneities within the charge could be caused by density variations of the ANFO. Again, Swisdak's data indicates that on a layer to layer basis, there were density differences (and that the average density for the whole charge was 0.914 g/cm^3 , a much higher value than normally encountered). Explosive diagnostic measurements by B. Hayes and R. Bost (Lawrence Livermore Laboratory) with rate sticks and time interval gages within the charge show that "while the explicit relationship for ANFO is not known, both the measured detonation velocity and pressure confirm there were density gradient regions within the stack. As a consequence, it is not

unreasonable to expect hydrodynamic instabilities to develop since the change in detonation velocity with respect to a change in density is like a factor of seven. This effect will lead to considerable internal turbulence which does not smooth out. More probably, cellular disturbances are generated fostering multiple interactions which disrupt the smooth isentropic expansion of the detonation products" (Reference 23).

Still another source of inhomogeneities within the charge may be the presence of the bags in which the ANFO is contained. The average weight of a bag is 0.54 lbs; this constitutes a little more than 1 percent of the total weight of a bag of ANFO. On the DICE THROW charge, this 1 percent translates into about 12,500 lbs of extraneous, non-explosive bag material.

Another reason for the anomalies may be the rather rough outer contour of the charge with reentrant-like corners noted earlier. And still another reason could be the non-simultaneous detonation of the seven boosters. Unfortunately, most of the probes for determining simultaneity did not function properly so no clue is available from this source. In short, blast anomalies were observed but their source or sources of origin are not evident.

Although in this section of the report much emphasis has been placed on the characteristics of the pressure-distance curve as a legitimate criteria to evaluate ANFO performance, the other hydrodynamic parameters of blast waves have been used also as criterion. As reported by G. Teel (BRL) in Reference 22, the measured blast arrival times, positive phase durations, positive phase impulses, horizontal dynamic pressures, and dynamic pressure impulses all compare with pre-test predictions. The predictions were based on the LLL developed equation-of-state for ANFO, AFWL HULL code calculations, and BRL data obtained from the Pre-DICE THROW II, Event 2, 120 ton ANFO shot. The predicted inflection points in the duration- and impulse-distance curves are not as pronounced on the DICE THROW event as predicted; this may be because a clear demarcation between fireball and shockwave separation for an ANFO explosion is either reduced or eliminated.

(The measured data obtained on DICE THROW and the earlier development shots are presented in Section 4.)

1.6 ANFO EPILOGUE

With the successful completion of the DICE THROW program, the history of the development of ANFO as a nuclear weapons effects simulation was concluded. Ten years of dedicated effort by many scientists and engineers and the faith of a few administrators have demonstrated the merits of ANFO for nuclear weapons blast and ground motion simulation. Almost all the original promises of ANFO have been realized. Charges up to the millions of pounds size can be constructed without confinement and be detonated reliably. There is no self-heating or fuel oil leakage in the charge. The detonation characteristics and the blast and ground motion effects of these charges can be predicted and scaled (provided charges larger than about 1000 lbs are used and proper account is taken of the increased bulk density of the larger charges). Blast anomalies are minimal with ANFO charges. The cost of ANFO in today's competitive market is considerably less than that of other explosives, and because of this competitive and large market, it is readily available throughout the country. ANFO is relatively safe; it is less sensitive to initiation than almost all military and commercial explosives. The low yield, i.e., TNT equivalence of ANFO, can be compensated for by using 20% more ANFO than if TNT were used as the explosive source. The still present hygroscopicity of ANFO can be minimized by the use of a protective structure as was done on DICE THROW.

All in all, ANFO is a good and proper replacement for TNT for use on military test operations requiring nuclear weapon proportioned blast and ground motions. As testimony to this statement it is noted that since DICE THROW all DNA test operations with charges larger than 100 tons have used ANFO. In 1973, on the MISERS BLUFF operation, seven 120 ton ANFO domed cylindrical charges were fired, six of them simultaneously. On MILL RACE in 1981, a 600-ton ANFO domed cylindrical charge was detonated. In the same year on Operation DISTANT RUNNER, two 120 ton domed cylinders were used. And for 1983, it is planned to fire a 600 ton ANFO spherical charge at an elevated height of burst in DIRECT COURSE.

To conclude this historical section of the report, a quotation inscribed at the entrance to the National Archives in Washington, DC is cited, "What is past is prologue." The history provides only a guide; the future uses of ANFO for simulation work will be limited only by the imagination of engineers and scientists. New shapes to produce enhanced unidirectional blast, new environments, e.g., underwater, for ship response tests, new sizes in the thousands of tons range to even better simulate nuclear weapon effects, all are possible. But just as TNT did not meet all test requirements, so ANFO cannot respond to all demands. New explosives and new techniques should be investigated. Until such replacements are found, ANFO will continue to do a bang-up job.

REFERENCES

1. Van Dolah, R.W., Gibson, F.C., and Murphy, J.N., "Sympathetic Detonation of Ammonium Nitrate and Ammonium Nitrate-Fuel Oil," U.S. Department of the Interior, Bureau of Mines, Report of Investigation 6746, 1966.
2. Dewey, J.M., Nature 205, 1306, 1965.
3. Patterson, A.M., Kingery, C.N., Rowe, R.D., Petes, J., Dewey, J.M., "Fireball and Shock Wave Anomalies," DASIAC Special Report No. 105, Panel N-2 Report N2-TR 1-70, 1970.
4. Balcerzak, M.J., Johnson, M.R., and Kurz, F.R., "Nuclear Blast Simulation, Part I, Detonable Gas Explosion," General American Research Division, General American Transportation Corporation, 1966.
5. Balcerzak, M.J., Johnson, M.R., and Lucole, S.W., "Nuclear Blast Simulation, Detonable Gas Explosion, Operation DISTANT PLAIN," 1967.
6. NOL ltr 241:JP:lnr 4330 Ser 5706 of 1 Nov 66 to DASA.
7. NOL ltr 241:JP:ee 3900 Ser 1216 of 10 Mar 67 to NSSC.
8. Kelso, Jr. R. and Choromokos, J. Jr., "Ammonium Nitrate/Fuel Oil Explosives," 3rd International Symposium on Military Applications of Blast Simulation, 1972.
9. "Everything You Always Wanted to Know About Ammonium Nitrate but Were Afraid to Ask," brochure of Atlas Powder Company, Dallas, Texas 75251.
10. Sadwin, L.D., and Pittman, J.F., "Airblast Characteristics of AN/FO, Phase I," U.S. Naval Ordnance Laboratory, White Oak, Md., NOLTR 69-82, 1969.
11. NOL ltr 241:JP:ee 3900 Ser 4482 of 31 Jul 68 to NSSC.
12. NSSC ltr 6105:SHM:mmm C-10342 Ser 0189 of 22 Oct 68 to DASA.
13. Sadwin, L.D., and Swisdak, M.M. Jr., "Blast Characteristics of 20- and 100-ton Hemispherical AN/FO Charges, NOL Data Report," U.S. Naval Ordnance Laboratory, White Oak, Md., NOLTR 70-32, 1970.
14. Sadwin, L.D., and Swisdak, M.M. Jr., "AN/FO Charge Preparation for Large Scale Tests," U.S. Naval Ordnance Laboratory, White Oak, Md., NOLTR 70-205, 1970.
15. The Technical Cooperation Program, Panel N-2, "Twelfth Meeting of Panel N-2 (Shock, Blast, and Thermal), Sub Group N, Part 1, Proceedings and Working Group Reports, 1969.

REFERENCES (continued)

16. Physics International Progress Reports, PIPR 274-1, 1970; PIPR 274-2, 1971; PIRP-274-3, 1971.
17. McKay, M.W., Hancock, S.L., and Randall, D. "Development of a Low-Density Ammonium Nitrate/Fuel Oil Explosive and Modeling of Its Detonation Properties," Physics International Corporation, DNA Report 3351 F, 1972.
18. Anderson, J.H.B., "Observations on the Blast Phenomenology of Unconfined Charges of Ammonium Nitrate/Fuel Oil Explosive (AN/FO IV and V--October 1971) DRES TN 315, 1972.
19. Randall, D.S., "Comparison of Craters Produced by TNT and ANFO Detonations," Physics International Company, PIFR-381, DNA 2893F, 1972.
20. Edwards, E.Y., "ANFO Charge Development Program, Program Summary," Field Command, DNA, June 1977.
21. Ostrower, M.J., "Pre-DICE THROW Charge Development Program," CERF, University of New Mexico, Albuquerque, NM, AFWL-TR-79-216, December 1979.
22. Edwards, T.Y., and Perry, G.L., "Middle North Series, Pre-DICE THROW II Events, Preliminary Results Summary," Field Command, DNA, Kirtland Air Force Base, NM, POR 6904, September 1976.
23. "Proceedings of the DICE THROW Symposium, 21-23 June 1977," GE Tempo, DNA 4377 P-1, July 1977.

APPENDIX 1-A

CHRONOLOGY OF ANFO USE FOR NUCLEAR BLAST & SHOCK SIMULATION

- 1659 - Ammonium nitrate first prepared by Glauber
- 1867 - Swedish patent granted to Ohlsson and Norrbein for use of ammonium nitrate as an explosive ingredient.
- 1940's - Ammonium nitrate formed as prills which when coated with diatomaceous earth (Kieselguhr) provided a free flowing product which could be used in explosive preparation for mining and excavation purposes.
- 1955 - Patent issued to Robert Akre who developed "Akremite," a blasting agent consisting of prilled ammonium nitrate and finely divided carbon.
- 1956 - ANFO--prilled ammonium nitrate mixed with #2 diesel fuel oil first used at an iron mine on the Mesabi Range.
- 1957-58 - Defence Research Establishment, Suffield (Canada) experimented with 60-lb spheres of ANFO as part of program studying airblast phenomenology. Switched to TNT because ANFO did not detonate satisfactorily.
- 1966 - Concept for use of ANFO for nuclear weapons blast simulation introduced by Sadwin and Petes at Naval Ordnance Laboratory (NOL). Tests with unconfined charges weighing 8-, 20-, and 64-lbs gave TNT equivalencies of 0.47, 0.51, and 0.75 respectively, indicating that critical charge diameter was not reached.
- 1968 - NOL fired hemispherical ANFO charges weighing 260-, 500-, and 1,000-lbs. A TNT equivalence of 0.82 was obtained on all shots, suggesting that the critical diameter was attained or exceeded.
- 1969 - Two 20-ton and one 100-ton unconfined hemispherical charges fired; 0.82 TNT equivalence was attained and pressure data from all charges from 260-lbs to 200,000-lbs scaled indicating reproducibility of detonations.
- 1970 - Use of ANFO in sub-surface hemispherical-like geometry (with diameter at surface) investigated by F. M. Søjer (Physics International Company) for simulating nuclear weapon ground shock.
- 1970 - Concept for use of cylindrical charges for nuclear weapon blast, ground shock, and cratering in energy ratios similar to those obtained from surface burst nuclear weapons was introduced by the Naval Surface Weapons Center (NSWC).

- 1971 - Two 25-ton unconfined ANFO spheres were fired. ANFO IV was constructed tangent to the ground, ANFO V was half buried. Results compared favorably with TNT shots of same geometries.
- 1975 - Intensive DNA program to develop an ANFO charge geometry which would produce blast and shock phenomena comparable to surface tangent sphere TNT charges. A domed cylinder with L/D = 0.75 for cylindrical section selected as proper geometry.
- 1976 - Event DICE THROW fired -- a 628-ton unconfined domed cylinder--for testing the response of military equipment and targets.
- 1978 - Event MISERS BLUFF -- six 120-ton domed cylinders in hexagonal pattern fired simultaneously for military effects test.
- 1981 - Event MILL RACE -- 600-ton domed cylinder for military effects test.
- 1981 - Event DISTANT RUNNER -- two 120-ton domed cylinders for testing the response of aircraft shelters.
- 1983 - Event DIRECT COURSE -- 600-ton sphere at height-of-burst = 166 ft for military effects test; scheduled.

SECTION 2 PROPERTIES AND CHARACTERISTICS

2.1 GENERAL

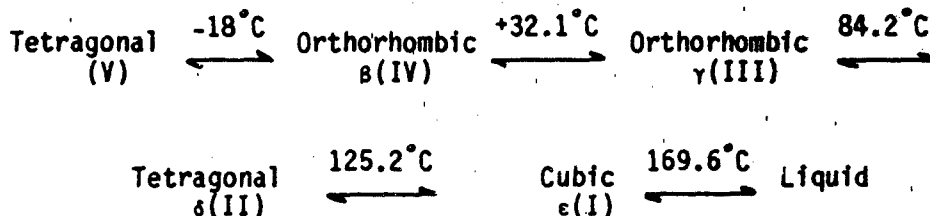
This section summarizes the physical and chemical properties of ANFO. Since ANFO is composed of ammonium nitrate (AN), produced by a rather unique process, and absorbed No. 2 diesel fuel oil (FO), each of these components is addressed independently, before ANFO itself is discussed in detail. ANFO is best characterized as a physical mixture of AN and FO. On the macroscale, the mixture approaches one of homogeneous composition; but on a particle basis, there is considerable inhomogeneity. Chemically, the explosive detonation of ANFO follows a reaction in which the FO provides the means to achieve an oxygen balance. Although there is a great difference in the physical properties of ANFO compared to AN, their chemical properties are quite similar.

For applications of ANFO as an explosive, there are two different regimes. One such application is by the mining industry wherein ANFO is used in a confined state such as borehole loading in bedrock or in pipe casings. The more recent application is its use in large open masses to simulate nuclear weapon blast and shock energy; this report is primarily oriented towards the latter. The research for this report has revealed that specific data on ANFO performance in large masses is relatively sparse compared to that from various mining industry sources. For this reason the information in this report includes both regimes. This section undertakes a presentation of the facts and data which have been extracted from numerous literature sources covering ANFO applications by the mining industry and by experimenters who detonated large amounts of the material in the open. A discussion of the physical properties centers around the results of rather detailed analytical methods employed during large scale ANFO detonation projects. The chemical properties are presented with emphasis on decomposition reactions and the ANFO detonation reaction. Some of the theoretical aspects necessary to model the ANFO detonation are summarized. Representative topical areas include Chapman-Jouget detonation parameters and their variance with ANFO composition and density, reaction zone dimension, application of various equations of state, etc.

Appendix 2-A contains a tutorial summary of modeling the steady-state detonation and a description of some equations of state. A compendium of the results, primarily from many large scale detonations of open stacks of ANFO, are presented on detonation velocity versus several ANFO variables. A separate subsection comprises a review and summary from an analytical viewpoint. In this subsection an attempt is made to tie together all the elements of information to characterize a modern description of ANFO from the viewpoint of its detonation properties and characteristics.

2.2 AMMONIUM NITRATE

Ammonium nitrate (NH_4NO_3) is a colorless solid with a crystal density of 1.725 g/cm^3 at 25°C and a molecular weight of 80.04 g/mole . The major use is an industrial fertilizer; its secondary use is in mining explosives. Its melting point is 169.6°C , and it is very soluble in water (118.3 g per 100 cm^3 at 0°C and 871 g per 100 cm^3 at 100°C). In moist air it becomes liquid owing to its hygroscopicity. Ammonium nitrate exists under five crystalline modifications below its melting point (References 1 and 2):



On rapid cooling ($2^\circ\text{C}/\text{min}$) of the liquid, form (II) changes directly to form (IV) at 50°C . This phenomenon has been observed only in cooling the liquid phase; otherwise, the transformations indicated above occur at their respective transition temperatures. Evidence exists which supports another crystalline form at cryogenic temperature (-170°C), but this form has not yet been fully characterized. The specific gravity of form (IV) is 1.72 , form (III) is 1.66 , and form (II) is 1.62 . The transition from IV to III is significant and has an exothermic effect (-5.0 cal/g); during this transition, the specific heat (C_p) changes by about -400 cal/mole (Reference 3).

Commercially, NH_4NO_3 is produced from multistep processes. In the Haber process, nitrogen (N_2) is reduced by hydrogen (H_2) to form ammonia (NH_3). The NH_3 is then oxidized to nitric oxide (NO) in the Ostwald process:



The NO reacts with O_2 and H_2O producing aqueous nitric acid (HNO_3) which is then neutralized by NH_3 in an acid-base reaction (Stengel process):

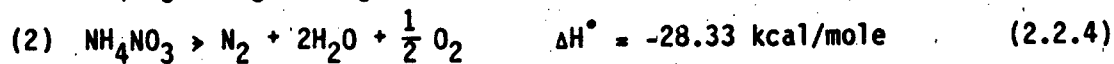


The product is an 83 percent aqueous solution of NH_4NO_3 from which the solid is obtained after dehydration (References 2, 3, 4, and 5)

Ammonium nitrate is commercially available in several forms, e.g., flaked, granular, crystals, and prills. For ANFO applications (and for agriculture), the prilled form is used. This form is produced by a special dehydration technique and is discussed in Section 2.4.1.

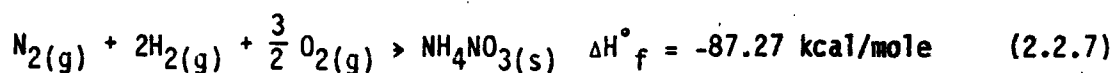
Ammonium nitrate is a strong oxidizing agent which decomposes rapidly at elevated temperatures yielding nitrogen or one of its oxides as one of the decomposition products. Fused NH_4NO_3 is regarded a high-temperature acid; it behaves as nitric acid and will dissolve many metal oxides and oxidize many metals. At ordinary temperatures NH_4NO_3 is quite stable except in the presence of oxidizable materials or reducing agents (Reference 2).

The more common decomposition equations for NH_4NO_3 and their heats of reaction (ΔH) are as follows:



The variation in decomposition processes is a function of different temperature conditions.

Other formulations are also possible for extreme conditions of temperature and pressure. Equation (2.2.3) is the only reaction at temperatures below 160°C explaining why NH_4NO_3 becomes acid during prolonged storage. Equation (2.2.4) is the operative reaction for the complete detonation of NH_4NO_3 while (2.2.5) and (2.2.6) correspond with incomplete explosions. The standard heat of formation (ΔH°_f) for NH_4NO_3 is -87.27 kcal/mole (References 3 and 6):



It should be noted that only equation (2.2.3) is endothermic, reversible, and nonexplosive. The other equations have a high activation energy but are explosive and are exothermic reactions meaning the enthalpy (H°) of the products is less than that of the reactants. Figure 2-1 depicts the relationship between the activation energy (E_a) and enthalpies for reactions of this nature. The activation energy forms a barrier in the reaction progress, but once overcome, the reaction proceeds spontaneously.

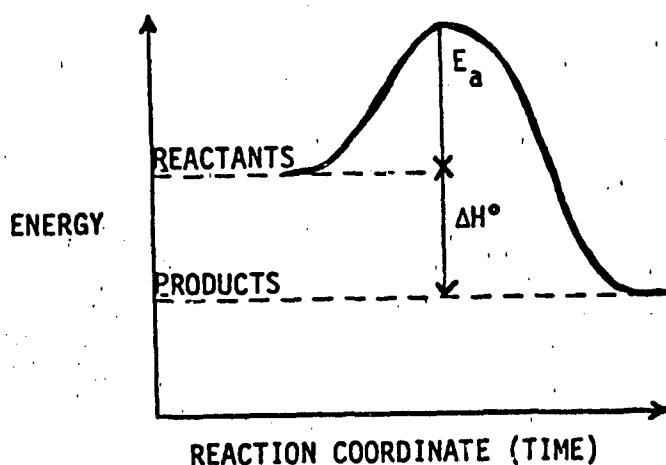


Figure 2-1. ACTIVATION ENERGY

Most investigators agree that the reaction mechanism for explosive decomposition of NH_4NO_3 is first order, or unimolecular. Various values have been reported for E_a (depending on conditions) and range between 31.4 and 40.5 kcal/mole. Equation (2.2.6) only starts above 170°C; equation (2.2.5) begins at about 220°C. Chemically pure, completely anhydrous NH_4NO_3 is reported to not decompose until 300°C but that a trace of H_2O will catalyze decomposition, according to equation (2.2.6), at 180°C. Thermal decomposition can be enhanced by adding a wide variety of compounds including organics; for example, the Texas City explosion in 1947 involved NH_4NO_3 containing 5 percent kaolin and 1 percent mineral oil (References 3 and 6).

2.3 NUMBER 2 DIESEL OIL (References 7 and 8)

The chemical composition of this fuel oil is very close to the methylene group ($-\text{CH}_2$). The methylene group has a carbon to hydrogen ratio of 1:2 and is a nonexistent species under normal conditions of temperature and pressure. A common representation for fuel oil is $\text{C}_{7.17}\text{H}_{14}$ although it is a considerably larger molecule.

For preparing ANFO a dye is added to the fuel oil in order to attain coloration. This dye is usually red and is a solution in xylene (C_8H_{10}). It is the same additive used in automotive and aviation petroleum products. For ANFO applications, the nominal amount is 12.5 ounces of dye solution per 100 gallons of fuel oil. The dye is not chemically operative in the ANFO reaction but does serve a very useful purpose. Absorption of the colored FO in AN produces a characteristic pink color to the resulting ANFO at about 6 percent by weight of FO. Color variations are indicative of too much FO (more color) or of insufficient FO (little coloration).

Table 2-1 summarizes some of the properties of the fuel oil and the dye.

TABLE 2-1. PROPERTIES OF FUEL OIL AND RED DYE

PROPERTY	FUEL OIL	DYE
Flash point (°C)	60	36
Pour point (°C)	-18	<-28
Boiling point (initial, °C)	160	141
Boiling point (final, °C)	358	--
Viscosity (centistokes @ 38°C)	2.70	39
Specific gravity (@ 15°C)	--	1.01
Visual strength (Hellige, percent)	--	45

2.4 AMMONIUM NITRATE - FUEL OIL (ANFO)

2.4.1 Production (Reference 5)

For explosive and agricultural applications, AN is produced in a prilled form. This is achieved by spraying a concentrated solution of NH_4NO_3 into the top of 100-200 foot prilling towers. During free fall in these towers, droplets of the concentrated solution are cooled and solidified into spherically shaped particles. These particles are subsequently dried, screened for size, and coated with a diatomaceous earth or other surfactant for moisture resistance (Reference 9).

The basic difference between prills for agricultural and explosive purposes is a result of the techniques used in the prilling towers and the amount and kind of surfactant used for moisture resistance. When manufacturing agricultural grade prills, the temperature of the concentrated solution of NH_4NO_3 is higher, and the towers are not as high. The resultant prill is hard with a bulk density generally over 0.88 g/cm^3 , a moisture content around 0.3 percent, and they receive about a 3 percent surfactant coating. Explosive grade prills are produced in higher prilling towers and are cooled at a slower rate. The resulting prill contains less moisture and is more

porous with a bulk density in the range of 0.78-0.92 g/cm³. Explosive grade prills receive a surfactant coating of 0.8 to 1.2 percent (Reference 4). The surfactant is added to inhibit moisture absorption (which adversely affects blast efficiency) and to deter caking which interferes with the free-flow pouring of the ANFO in field use. (Of late, i.e., MILL RACE and Pre DIRECT COURSE, a compromise prill somewhere between the characteristics of explosive grade and agricultural grade prills was used; explosive grade prills would have been a special order.)

The porosity of the explosive grade AN prills enables easy absorption of No. 2 diesel fuel oil. This product, ANFO, is usually packaged in 50 lb (22.7 kg) lots in multiwall paper sacks. The packaged density varies between 48-57 lbs/ft³ (0.77-0.91 g/cm³) depending on the manufacturer.

Although the AN prills are treated for moisture resistance, they are not insensitive to water. In essence, the poured product offers no resistance to water; in packaged form the resistance is largely dependent on the integrity of the package and the environment. High humidity and prolonged exposure can desensitize the material (References 4 and 9)

Table 2-2 contains manufacturers' data on ANFO. This table was extracted from Reference 10 and includes only those products formed from AN prills and No. 2 diesel fuel oil. All products are approximately 94/6 ANFO weight percentage ratio. As can be seen in this table, there are many products included under the generic name "ANFO" and they have different physical and chemical characteristics. These characteristics and differences as they apply to large ANFO charges used for nuclear weapons effects simulation, are main topics of this report.

2.5 DETONATION PROPERTIES

2.5.1 Chemical Reaction and ANFO Composition

The detonation of ANFO is by the following chemical reaction (Reference 7):



This reaction equation is a bit different from the simpler one given on page 1-20; it indicates the variations experienced in many chemical reactions.

TABLE 2-2. MANUFACTURERS' DATA ON ANFO

Product	Density (g/cm ³)	Detonation Velocity (m/s)	Detonation Pressure (kbar)	Energy (cal/g)
<u>DuPont</u>				
SP-2 AN	0.83	4500		
ANFO-p ^a	0.80	4700	48.2	
ANFO-HD ^a	0.85	4500	60	890
Tovite	1.12	4500		
<u>Hercules</u>				
Herco ^a	0.80	3840		
Hercomix 1 ^a	0.80	3840	30	771
<u>Atlas</u>				
Pellite	0.81	2730	16	944
<u>Trojan-U.S. Powder</u>				
TL-201	0.77	3150	19	
<u>Gulf</u>				
N-IV	0.80			
NCN-100	0.93	3660	31	700
<u>Monsanto</u>				
M-Pel	0.80	3300	21	400
M-Pak 100	0.90	3900		
M-Pak 500	1.00	3600		

^aPneumatically loaded to higher density than poured.

Equation 2.4.1 is an oxygen balanced reaction where the mass fraction of NH_4NO_3 (80.04 g/mole) to ANFO (84.74 g/mole) is 94.45 percent and the FO fraction is 5.55 percent. At higher weight percentages of AN, the composition is oxygen rich which increases the production of nitrogen oxides (NO , NO_2). Higher weight percentages of FO, conversely, represent an oxygen poor material which reduces the amount of CO_2 produced in favor of CO . From a thermodynamic viewpoint, both the oxygen rich and oxygen poor compositions degrade the amount of detonation energy available compared to the oxygen balanced reaction.

2.5.2 Calculated Detonation Parameters

The process of calculating detonation parameters for any explosive is highly complex and extremely specialized. One of the more critical elements in this process is the selection of a valid equation of state for the reaction products. Detailed calculations are usually performed on large computers with codes specially tailored for thermohydrodynamic principles of detonation equilibrium.

Some of the more commonly used equations of state for explosives are: Virial, Becker-Kistiakowsky-Wilson (BKW), Jones-Wilson-Lee (JWL) and Lennard-Jones-Devonshire (LJD). For the benefit of those who may not be familiar with equations of state and the principles of detonation equilibrium or steady state conditions, Appendix 2-A contains an overview of detonation theory. At this point it should suffice to mention that detonation equilibrium is known as the Chapman-Jouget (CJ) state and the calculated detonation parameters are referred to this state as the CJ parameters.

Calculations of ANFO detonation parameters were performed by Chaiken et al of the U.S. Bureau of Mines using the U.S. Army Ballistic Research Laboratory computer code called TIGER and were based on the reaction given by equation (2.4.1) for an ANFO density of 0.8 g/cm^3 . In addition, the investigators used the Virial equation of state for the gaseous products, $\Delta H_{\text{AN}}^\circ = -88 \text{ kcal/mole}$ and $\Delta H_{\text{FO}}^\circ = -45 \text{ kcal/mole}$. Some of the results of those calculations are presented in Table 2-3 and reflect the optimum properties of an oxygen balanced composition at about 6 percent FO by weight. (Note in particular that such calculations also predict the amount and species of

reaction products. Table 2-9 in Section 2.8.2 provides more complete data on calculated reaction product composition.) While these same investigators admit that the results for pressure and velocity are about 15 percent too low (a common condition from the search for an equation of state which approaches perfection), the relative results, i.e., the peaking of velocity, detonation pressure and energy at 6 percent FO, are significant (Reference 7).

TABLE 2-3. DETONATION PROPERTIES OF ANFO
(Reference 7)

Percent FO (By Weight)	Detonation Velocity (m/s)	Detonation Pressure (kbar)	Detonation Energy (cal/g)	Moles NO+NO ₂ (g of ANFO) ⁻¹	Moles CO (g of ANFO) ⁻¹
0	3030	20.5	365	0.326	--
1	3203	23.7	459	0.541	2 x 10 ⁻⁵
2	3410	26.6	554	0.747	3 x 10 ⁻⁴
3	3570	29.5	650	0.884	0.002
4	3720	32.2	749	0.877	0.008
5	3870	34.9	851	0.585	0.046
6	3980	36.6	898	5 x 10 ⁻⁵	0.761
7	3980	36.8	862	2 x 10 ⁻⁶	2.00
8	3970	36.7	728	4 x 10 ⁻⁷	2.96
9	3940	36.5	799	1 x 10 ⁻⁷	3.68
10	3910	36.2	772	4 x 10 ⁻⁸	4.23

It is emphasized that calculated parameters or properties are seldom, if ever, close to perfection. The results of such calculations are quite sensitive to numerous input variables such as density and specific energy of the explosive. The above is just one example; the velocity results appear, indeed, too low. Table 2-4 summarizes the results from five other cases to illustrate the sensitivity on input variables as well as the application of various equations of state.

TABLE 2-4. C-J PARAMETERS FOR ANFO

C-J Parameter	Equation of State				
	BKW ^a	LJD ^a	JWL ^b	BKW ^c	VIRIAL ^d
Detonation Velocity, D _{CJ} (m/s)	5440	4988	4650	4870	4100
Detonation Pressure, P _{CJ} (kbar)	73.4	61	60	68.5	48.8
Temperature, T (°K)	2252	2927	--	2360	3230
$\left(\frac{\delta \ln P}{\delta \ln V}\right)_s$, γ_{CJ}	2.55	2.61	2.063	--	--

^aDensity = 0.88 g/cm³, Energy = 933.8 cal/g, Reference 27.

^bDensity = 0.85 g/cm³, Energy = 913.8 cal/g, Reference 28.

^cDensity = 1.0 g/cm³, Energy = 904 cal/g, Reference 7.

^dDensity = 1.0 g/cm³, Energy = 908 cal/g, Reference 7.

As a final comment on the science of calculating explosive behavior, the reader should not be left with the impression that theoretical predictions have no useful purpose. A major element in the science is the application of the steady state condition which assumes ideal explosive behavior. ANFO, however, does not exhibit such ideal behavior. Therefore, observed performance more often than not will deviate significantly from predicted performance.

2.5.3 Empirical Detonation Equations

In this subsection we present an empirical relationship used by Kamlet et al (References 11, 12, 13, and 14). The empirical equations are relatively simple and easy to represent graphically. The ones presented here were developed for explosive materials containing C-H-N-O chemical elements as, for example, ANFO, among others. Empirical equations represent mathematical

relationships in terms of constants and variables derived from experimental data. Normally, a large amount of experimental data is used in order to derive the best value for constants.

The equations for detonation pressure (P) and velocity (D) are:

$$P = K\rho_0^2\phi \quad \text{kilobars} \quad (2.5.1)$$

$$D = A\phi^{1/2}(1 + B\rho_0) \quad \text{m/s} \quad (2.5.2)$$

In these empirical equations, K, A, and B are the constants determined from experimental data on the particular explosive. For ANFO their values are: $K = 15.58$, $A = 1.01 \times 10^3$ and $B = 1.30$. Density of the explosive is ρ_0 in g/cm^3 . The value for ϕ is based upon the chemical reaction of detonation and is given by:

$$\phi = NM^{1/2}Q^{1/2}$$

where N is the number of moles of gas produced per gram of explosive, M is the average molecular weight of the gaseous products, and Q is the negative of the reaction heat ($-\Delta H_0$).

Using the methylene group ($-\text{CH}_2$) to represent fuel oil, the chemical reaction is taken as



For 3 moles (254.16 g) of explosive, 11 moles of gas are produced with an average molecular weight (M) of 23.11 g/mole. The heat of reaction ($-Q$ or $-\Delta H^\circ$) used by Kamlet et al is 912 cal/g; therefore, ϕ is evaluated to be 6.283. Substituting K, A, B, and ϕ into equations (2.5.1) and (2.5.2) gives simple expressions for P and D:

$$P = 97.89\rho_0^2 \quad \text{kilobars} \quad (2.5.4)$$

$$D = 2532 + 3291\rho_0 \quad \text{m/s} \quad (2.5.5)$$

These equations are plotted in Figures 2-2 and 2-3 and indicate a pressure of 75.8 kilobars and velocity of 5428 m/s for a nominal ANFO density of 0.88 g/cm³.

These results appear too high. In a later subsection these relationships will be reviewed with the application of experimental data obtained from several large scale ANFO detonations.

2.6 PHYSICAL CHARACTERISTICS OF ANFO

There are some two dozen physical and chemical variables in what is commonly known as ANFO. For a variety of reasons, including proprietary rights of the manufacturer and lack of thorough quality control of the manufacturing process, there are no established and universally applied specifications for ANFO manufacture. The ANFO from one manufacturer will differ from that of another, and in fact, the ANFO from a given manufacturer may have differences between batches. In most instances, the manufacturer does not and is not about to do a detailed analysis of his product to quantify the variables; he doesn't have to since satisfactory explosive behavior in terms of rock breaking or earth moving, can be attained over a wide range of the variables

But what is satisfactory behavior for the military explosive scientist who wants to simulate nuclear weapons blast and shock? It is not enough to know that the explosive goes bang and creates a shockwave; he wants to know how the magnitude of the bang relates to the specific physical and chemical properties of the explosive. If these are known then, if need be, the output of the explosion can be varied by changing the explosive properties. Most military explosives have set and rigidly observed specifications and known properties - chemical composition, detonation wave properties, shockwave output; one batch of TNT will be the same as another batch within narrow limits.

In carrying over these traits and experiences of the military explosive scientists, the aforementioned problem is faced: there are no standards for ANFO in all the parameters that influence blast generation. As a result, one set of calculations or one set of experiments will not reproduce the data

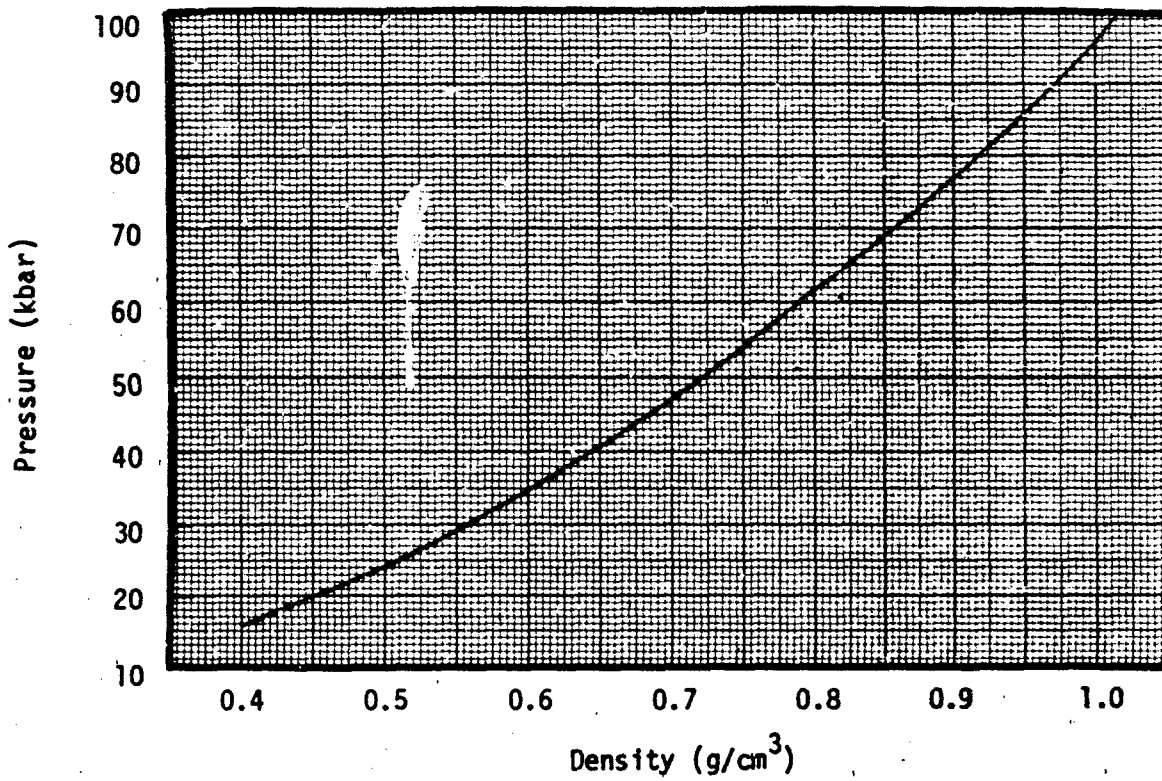


FIGURE 2-2. ANFO (94.5/5.5) DETONATION PRESSURE.

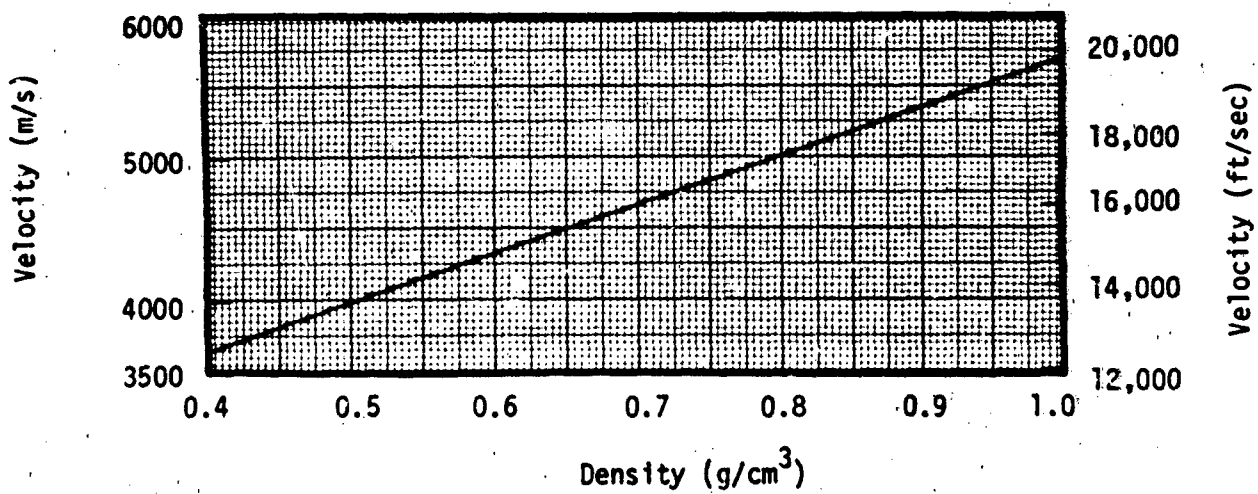


FIGURE 2-3. ANFO (94.5/5.5) DETONATION VELOCITY.

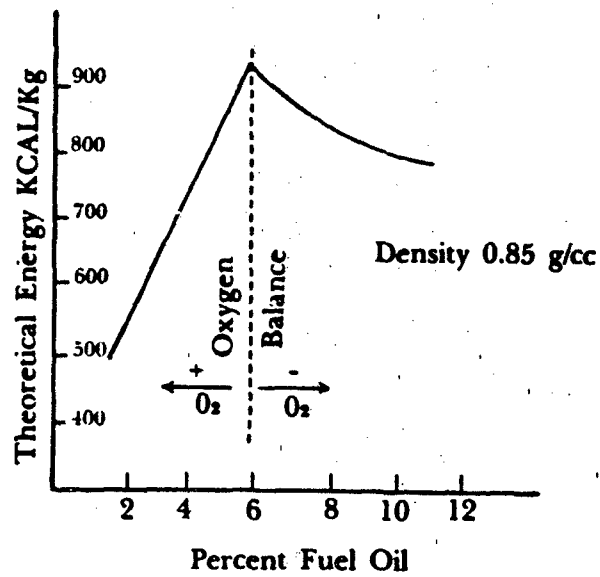
from another set of calculations or experiments because slightly different ANFOs are used. What follows will show these discrepancies in results as reported in the literature.

The situation is not really as bleak as it may appear. There is a great deal of information on ANFO and its characteristics; most of it is qualitatively self-consistent. And as we shall see, the small quantitative differences present problems only to the purist theoretician and analyst, not so much to the field experimenter. With the aforesaid as preamble, consider some of the more important variables such as percentage of fuel oil content in ANFO, prill size distribution, and bulk density. These determine to a large extent, the energy output of ANFO and its sensitivity to detonation.

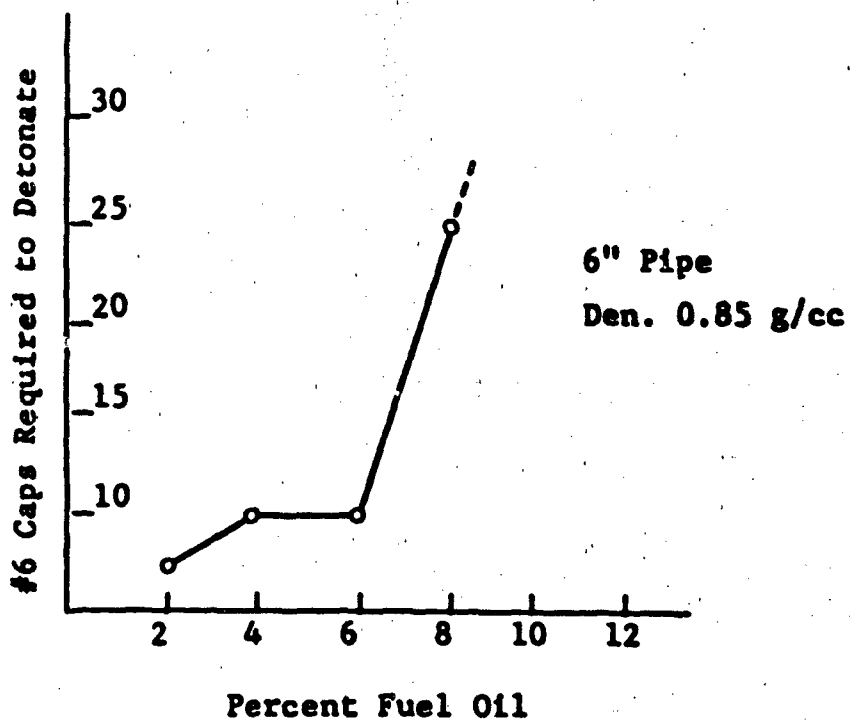
2.6.1 Fuel Oil Content

As Figures 2-4 a) and b) indicate (Reference 15), the energy output and sensitivity of ANFO are functions of the FO content. At about 6 percent, the ANFO is stoichiometric as discussed in Section 2.5.1, and full energy is attained in the detonation process. There is a rapid decrease in output as the FO percentage falls below this level and a somewhat lower rate of decrease if the FO content is greater than 6 percent. Depending on size and porosity, it is difficult for the AN prill to absorb more than about 10-12 percent FO; the excess oil just settles out of the bulk mixture after some little time. Overfueled ANFO is difficult to detonate using as a criterion the number of No. 6 caps required for initiation (Figure 2-4b); with less than optimum FO, the charge becomes more sensitive. So achieving and maintaining a 6 percent fuel oil content is important from two standpoints: obtaining maximum energy and safety in terms of detonation sensitivity.

Attaining a 6 percent FO content is predicated on proper quality control during the plant or field mixing of the AN and FO. Normally, there are two methods used to monitor fuel oil content - some analytical, the other visual. One analytical technique involves measuring the weight loss from an ANFO sample after repeated washings with a petroleum ether and subsequent oven drying. Another is based on measuring the volume of oil-clay mixture which separates in an aqueous ammonium nitrate-fuel oil mixture. With these analyses as a base, the red dye added to the FO provides a quick



a)



b)

FIGURE 2-4. ENERGY AND SENSITIVITY VS FUEL OIL CONTENT.

visual check for monitoring the FO content. At the proper FO percentage, the color of the bulk ANFO is pink; at lower percentages the color is almost white while at higher percentages it is bright red. As Table 2-5 indicates, an average 6 percent FO content has been attained on most of the large charge ANFO operations.

TABLE 2-5. LARGE ANFO CHARGE BULK DENSITIES AND FUEL OIL CONTENT

	Bag Weight	Number of Samples	Fuel Oil Content	Number of Samples	Density
	(lb)		(%)		(g/cm ³)
Pre-DICE THROW	50.8 ± 0.8	203	6.0 ± 0.4	51	0.880
DICE THROW	50.4 ± 1.0	480	6.1 ± 0.4	89	0.914
MISERS BLUFF II-1	49.3 ± 1.1	198	6.7 ± 1.3	50	0.900
MISERS BLUFF II-2					
STACK 1	46.9 ± 1.9	214	5.6 ± 1.1	81	0.914
STACK 2	49.3 ± 2.1	266	4.3 ± 1.3	82	0.923
STACK 3	48.8 ± 2.3	251	6.0 ± 1.7	76	0.886
STACK 4	47.8 ± 2.2	247	5.4 ± 0.7	73	0.904
STACK 5	43.8 ± 1.2	253	5.3 ± 1.2	71	0.908
STACK 6	47.8 ± 2.0	248	6.0 ± 1.2	71	0.910

ANFO I	50 ± 0.1	--	5.85	--	0.88*
ANFO II	BULK	--	5.90	--	0.839
ANFO III	BULK	--	5.95	--	0.865

*Estimated; volume not controlled for this bagged construction.

There is concern, however, about maintaining this 6 percent. Evaporation of the FO can and has taken place between the time of the initial assay when the ANFO is first prepared and the time when the charge is fired. Although the vapor pressure of No. 2 diesel oil is relatively low compared to most liquid petroleum fuels, evaporative losses can be expected over prolonged periods. On MISERS BLUFF, where test bed temperatures consistently ranged from 110°F to 120°F during the day, a simple experiment was conducted to collect data on evaporative losses (Reference 16). Bags of ANFO were laid out in the sun and weighed daily. Each day one bag was opened and analyzed for fuel content. Over a seven day period, it was found that bag weights decreased by about 0.3 lb. and the FO content decreased by about 23 percent from 5.3 percent to 4.1 percent. It was found that after about three days, the bag weights and FO content tended to stabilize. This could be due to some weak intermolecular bonding between AN and the absorbed fuel oil. For large stacks of ANFO, it is conjectured that evaporation on only the outer portions of the stack takes place to any significant degree; inner portions of the stack might contain sufficient fuel oil vapors to overcome the vapor pressure of the FO. Because of this evaporation problem, it may be judicious to slightly overfuel the ANFO to say 7 percent. Neither the energy output nor the sensitivity of the mixture would suffer unduly in the inner portion of the stack and the excess initial fueling would compensate to some extent the evaporative losses of the outer portions of the charge.

2.6.2 Prill Size and Bulk Density

The distribution of prill sizes is important in two ways: it affects the sensitivity and the bulk density of ANFO. Figure 2-5 shows that the larger prill diameters (2.36 to 0.85 mm corresponding to sieve mesh sizes 8 to 20) are more difficult to detonate than the smaller sizes; the smaller sizes, e.g., 150 μ m corresponding to mesh size 100, may be too sensitive for field operation safety. However, because the prills are friable to some extent, individual prills break up producing fines. So a range of prill sizes are the normal occurrence in bulk ANFO. Distributions such as shown in Figure 2-6 for several large charges used on test operations are found to be acceptable from both the sensitivity and energy output standpoints. With the majority of the prills in the #12 sieve size (about 1.70 mm), the desired oil absorption and homogeneity is attained.

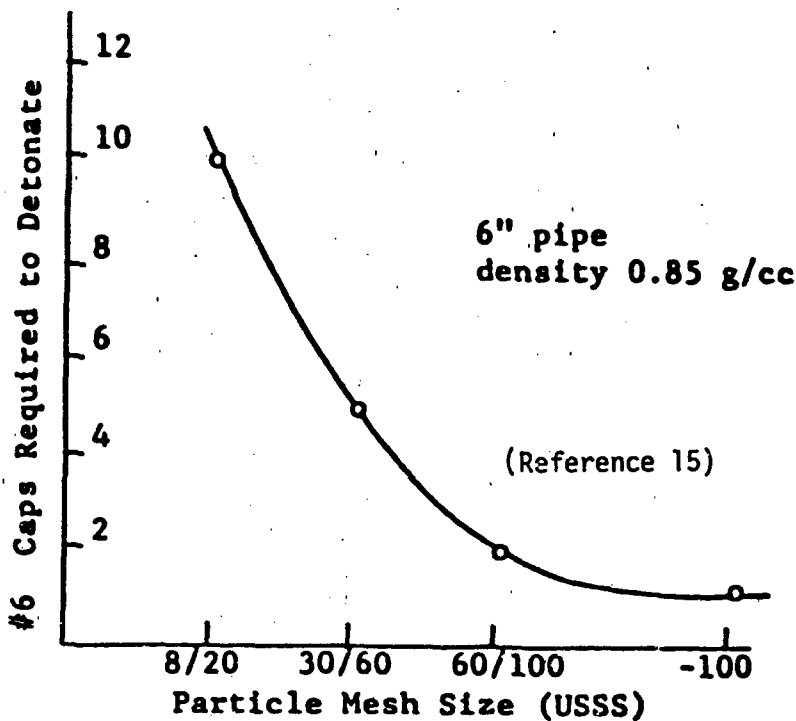


FIGURE 2-5. CHANGE IN INITIATION SENSITIVITY WITH PARTICLE SIZING.

The prill size distribution determines also, to a considerable degree, the bulk density of ANFO. With too many fines or small prills, the bulk density becomes high and as Figure 2-7 indicates, it is considerably more difficult to detonate than a lower density mixture such as about 0.80 to 0.85 g/cm³. In fact, as the bulk density approaches 1.00 g/cm³, it may be almost impossible to sustain a steady state detonation wave through the bulk ANFO.

To strike a reasonable balance between detonability and energy output as represented by detonation velocity (Figure 2-8b), ANFO for explosive blast generation, should have a bulk density of from 0.85 to 0.90 g/cm³ (Reference 8).

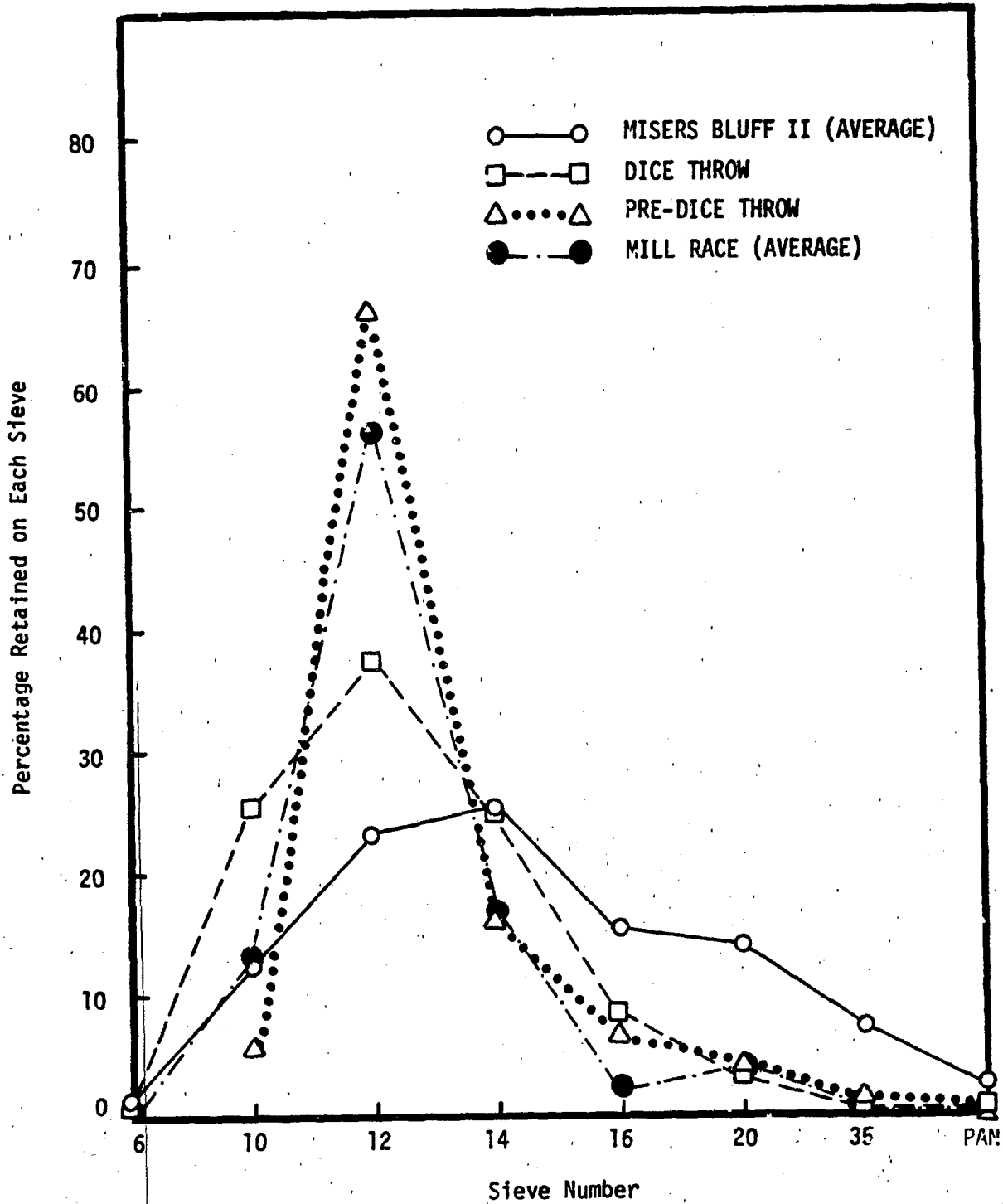
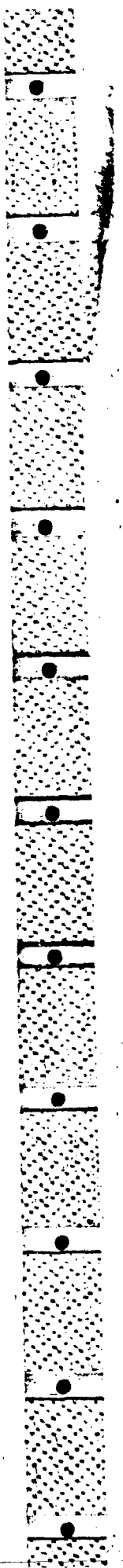


FIGURE 2-6. PARTICLE SIZE DISTRIBUTIONS FOR VARIOUS ANFO EVENTS.



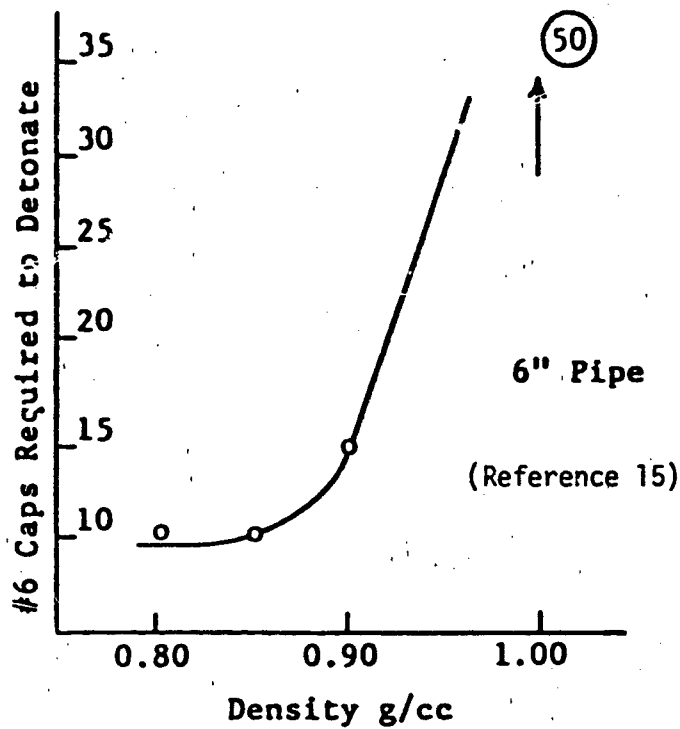


FIGURE 2-7. CHANGE IN INITIATION SENSITIVITY WITH DENSITY.

2.6.3 Detonation Velocity

Detonation wave velocity is an intrinsic characteristic of any explosive; it is an indication of the energy output of the material with the higher detonation velocities usually (but not always) giving the higher shock and blast outputs. Detonation velocity therefore is a useful criterion by means of which to evaluate energy yields and the performance of explosives. For ANFO, in particular, it is a useful measure because as is evident in much of the preceding sections, there is no "standard" ANFO in actuality, one in which all parameters are controlled or, at times, even known.

The detonation velocity in ANFO is influenced by many of the physical and chemical characteristics of this explosive. Figures 2-8a through 2-8f show some of these relationships. As the prill size decreases, the steady state detonation velocity asymptotically approaches a value of about 15,000 ft/sec (Figure 2-8a). This is in consonance with the data shown in Figure 2-8b; i.e., as the bulk density increases, the detonation velocity increases. (The fact that there is quite a disparity between the indicated ideal curve and the experimentally derived curve should not be too disturbing. Different sets of the ANFO variables are represented in the two curves. The problems associated with establishing even a theoretical ideal curve were discussed in Section 2.5.) For a given bulk density, the maximum detonation velocity is achieved for a stoichiometric ANFO as seen in Figure 2-8c. And as noted in Section 2.6.2, this figure shows that at about 12 percent FO content, the explosive limit is reached where a steady state velocity cannot be attained. Too much absorbed water in the ANFO, about 9 percent, also precludes detonation of the ANFO as seen in Figure 2-8d.

There are other factors that influence detonation velocity, for instance the confinement afforded the charge and the diameter of the charge. As Figure 2-8e shows, heavy confinement, as in a 6 inch diameter rock bore hole, leads to a high detonation velocity; an unconfined charge of this same diameter has a considerably lower velocity, hardly three quarters of the confined velocity. The charge size, too, has an influence on velocity. This is depicted in Figure 2-8f where it is seen that for a given ANFO density and a given booster charge, steady state detonation is achieved only for diameters larger than about 11 inches in a confined state.

As with theoretical and empirical detonation equations with their great variety and differences (discussed in Subsections 2.5.2 and 2.5.3) so the literature is rife with experimental determinations of the detonation velocity, energy output, and initiation sensitivity of ANFO. Very few of the experiments, for various practical reasons, use a common set of variables for ANFO properties; particularly variable is the bulk density used in the experiments. Therefore, slightly different results are often reported than those shown in earlier presented tables and figures. For example, take the

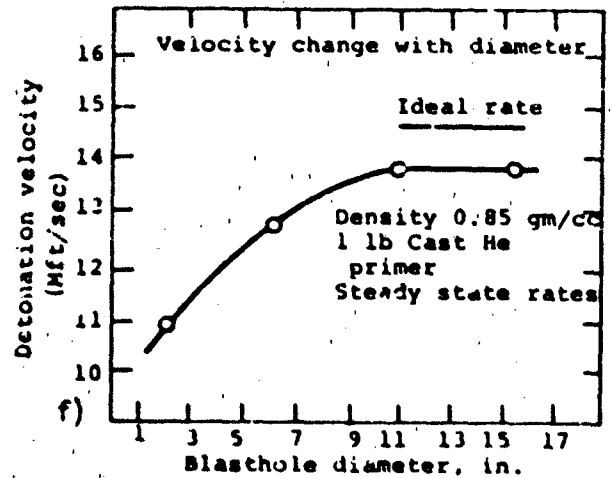
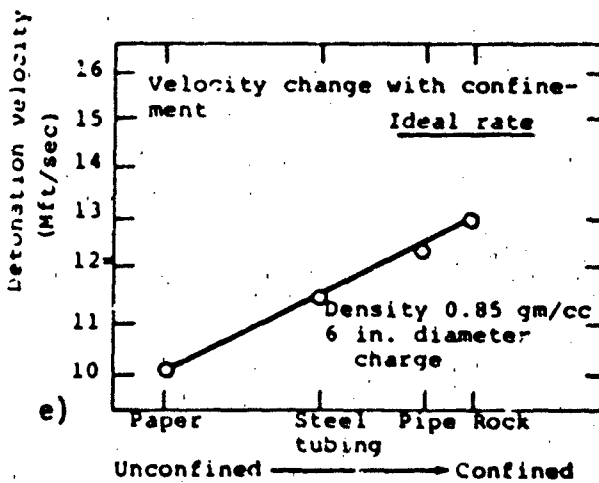
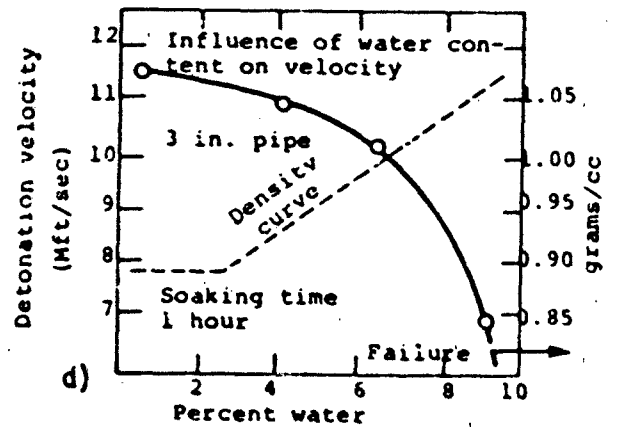
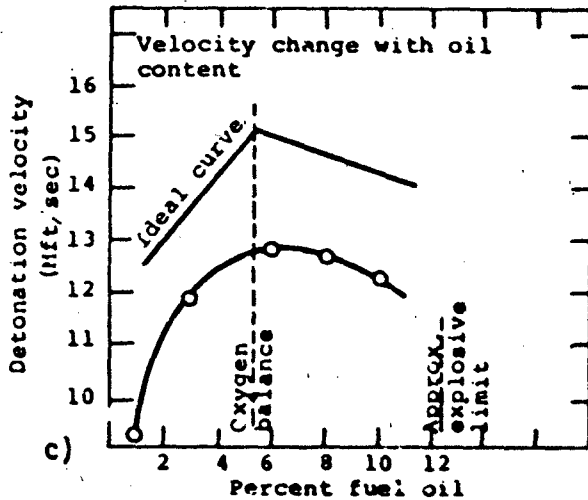
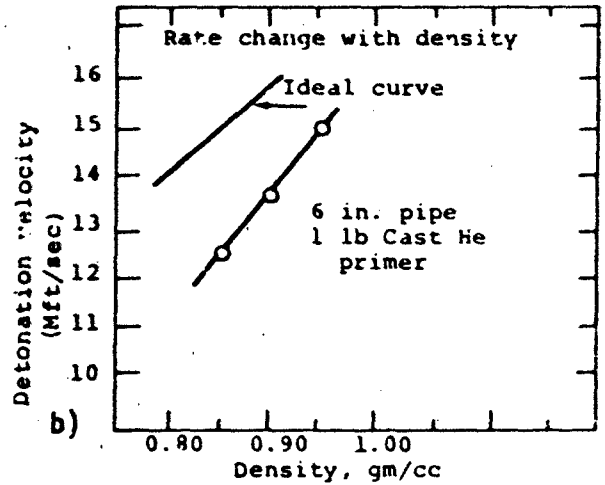
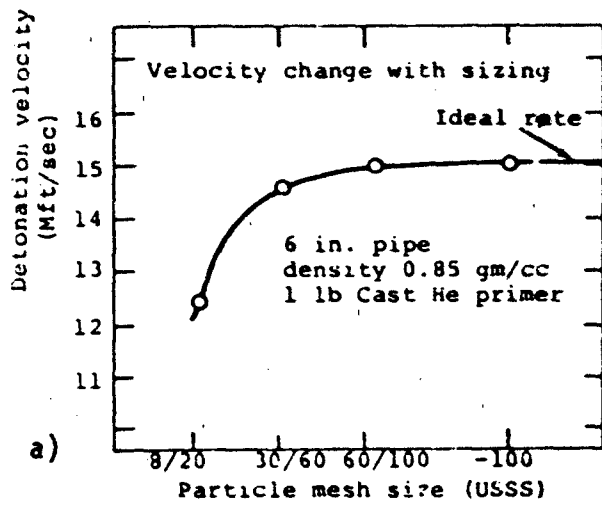


FIGURE 2-8. RELATIONSHIPS OF SEVERAL ANFO VARIABLES (Reference 15).

relationship between charge diameter and detonation velocity. In Reference 17, it is reported that the detonation velocity of ANFO at 0.88 g/cm^3 increases from about 11,500 ft/sec in 1.4 inch diameter bore holes to 18,000 ft/sec in 10.5 inch diameter charges. For an ANFO density of 0.8 g/cm^3 , others (Reference 18) have reported velocities of 10,660 ft/sec in 2 inch diameter cylinders to about 15,000 ft/sec in 11.5 inch diameter cylinders. All these results are not too disparate with the values shown in Figure 2-8f; they can be correlated qualitatively at least.

Besides the difficulty of making quantitative correlations when all variables in the different experiments are not held constant, another factor enters into comparing results, i.e., the methods used to determine detonation velocity. In the usual technique, the time between detonation wave arrival at a series of sensors is measured. With the spacing between the sensors known, the average velocity between sensors can be calculated; with many sensors arranged in a line, a history of detonation velocity is obtained. In few reports are the details of these measurements given; it may be (and in fact it is strongly suggested) that much of the published velocity data do not represent a steady state condition. The data may be average values over a length of the charge, or some final but not steady state value.

Details on attaining a steady state detonation are provided by Condon and Snodgrass (Reference 19). As in most explosives, a final steady state velocity is not reached and maintained instantly at the time of detonation; it takes time and therefore distance from the detonation source to get up to a velocity which will then be maintained throughout the rest of the passage of the detonation wave. For most explosives, this steady state is attained in short times and distances. Condon and Snodgrass have shown (Figure 2-9) that for ANFO it takes large distances, approximately 3 ft of travel of the detonation wave, to attain a steady value. And this is so regardless of whether the booster explosive used to initiate the ANFO initially under or over drives the ANFO. When the booster detonation velocity is the same as the steady state velocity of the ANFO, there is no run-up distance as shown in curve B of the figure.

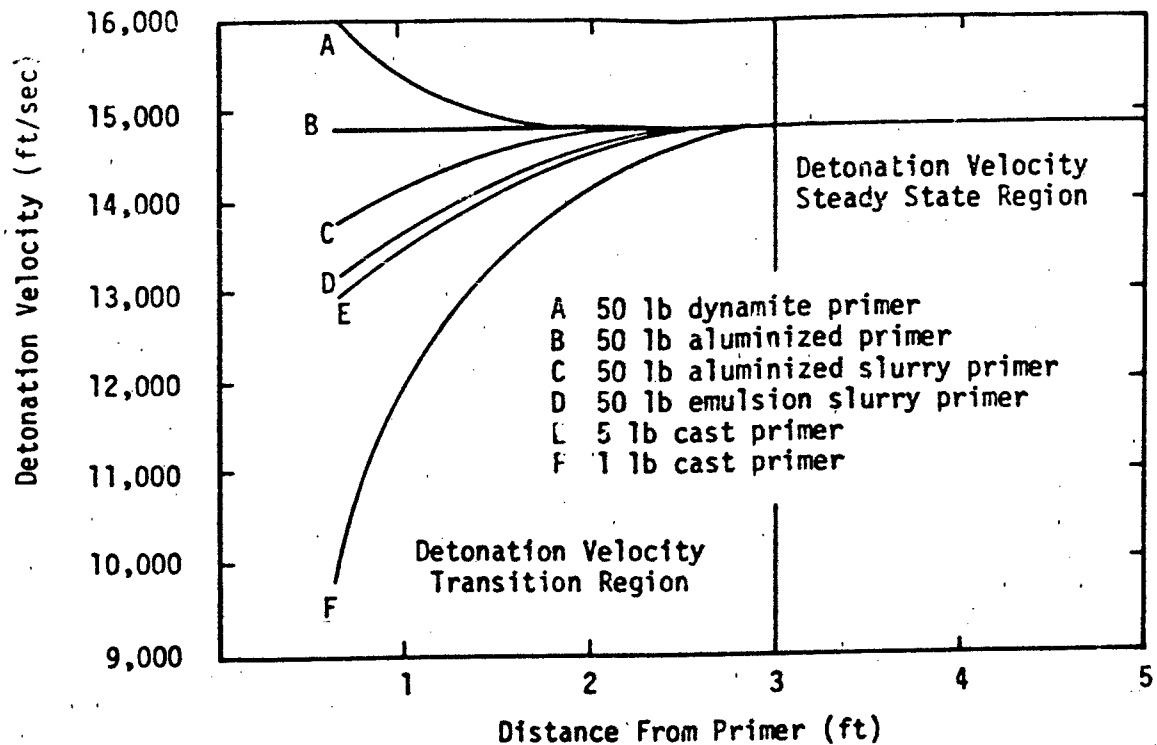


FIGURE 2-9. ANFO DETONATION VELOCITIES VS PRIMER TYPE.

Using the information presented in Figure 2-9, it is evident that the proximity of the sensors (detecting the arrival time of the detonation wave) to the booster, influences the velocity that may be reported. If all the sensors are at least 3 ft away from the booster, steady state values will be measured and there is no ambiguity in what to report as a detonation velocity. If all the sensors are within 3 ft of the booster, transient velocity values only will be attained. Now the question arises: what value to report, the average velocity or the final velocity? The average value would be lower than a steady state value and without a history of the transient phase, the experimenter would not know whether the final value had

reached the steady value. And it is apparent that if only two sensors are used to determine time over a single distance, and one of these sensors is close to the booster, an average velocity will be measured which will be less than the steady state value. The measuring details then, it is believed, account for some of the scatter in published detonation values. And this start-up distance has significance in analyzing the detonation velocities reported for the large ANFO charges used on DNA tests; this will be discussed shortly.

It should be noted that most of the figures and discussion in this and the preceding subsections regarding the relationships between the physical and chemical properties and the detonation/energy characteristics of ANFO are based on mining industry research with mostly heavily confined charges. There is no reason to suspect that those relationships do not apply to multi-ton ANFO charges as used in nuclear weapon effects simulation operations. Indeed, as will soon be evident in later subsections, the performance of the large simulation charges conform to the contained ANFO detonations.

2.7 LARGE SCALE ANFO DETONATIONS

As was discussed in earlier subsections, ANFO fuel oil content and bulk density have profound influences on detonation velocity, and velocity can be influenced by the techniques used to measure it. First, what are the FO contents and bulk densities of unconfined ANFO charges as used on DNA tests? Figure 2-10 lists and illustrates the large ANFO charges fired in the development and response test programs.

2.7.1 Measured FO Content

The Naval Surface Weapons Center has obtained rather extensive data on fuel oil content by monitoring via samples, the material used for almost all multi-ton detonations. On MISERS BLUFF, a DNA operation in Arizona in 1978, for example, "Samples were taken from each layer of each charge and analyzed for both fuel oil content and particle size distribution. Two samples were taken from the bulk ANFO placed on each layer. Each sample was analyzed separately for fuel oil content and the results averaged for each layer. The remains of each sample were then combined to perform the particle size distributions.





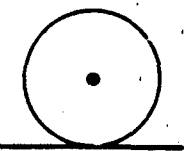
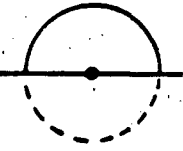
<u>Series</u> <u>Development Shots</u>	<u>Geometry</u>	<u>Cylinder</u>		<u>Nominal</u> <u>Wt (tons)</u>	<u>Remarks</u>
		<u>R (ft)</u>	<u>Ht (ft)</u>		
NSWC Phase I		1.3		0.13	Bulk
		1.7		0.25	Bulk
		2.1		0.5	Bulk
ANFO I		7.1		20	Bagged
ANFO II		7.0		20	Bulk
ANFO III		12.4		100	Bulk
ANFO IV		5.9		25	Bagged
ANFO V		5.9		25	Bagged

FIGURE 2-10. ANFO SHOTS FOR BLAST AND SHOCK.

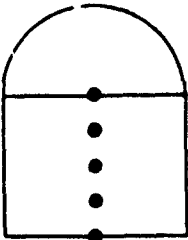
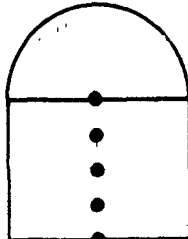
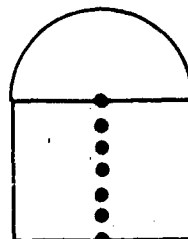
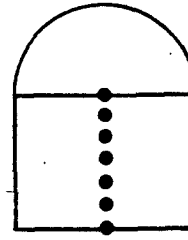
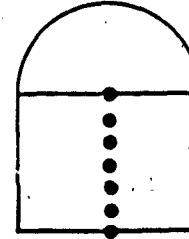
<u>Series</u> Development Shots	<u>Geometry</u>	<u>Cylinder</u>		<u>Nominal</u> Wt (tons)	<u>Remarks</u>
		R (ft)	Ht (ft)		
PRE-DICE THROW I					
Event 2		3.0	5.1	5.7	Bulk
Event 3					
Event 3		3.4	3.4	5.7	Bulk
Event 4					
Event 4		3.2	4.7	5.7	Bagged
PRE-DICE THROW II					
Event 2		8.74	13.11	120	Bagged
<u>Response Tests</u>					
DICE THROW		14.9	21.36	620	Bagged
MISERS BLUFF I & II		8.5	13.0	120	Bagged 7 Charges
DISTANCE RUNNER		8.5	13.0	120	Bagged 2 Charges
MILL RACE		14.9	21.9	600	Bagged

FIGURE 2-10. ANFO SHOTS FOR BLAST AND SHOCK (CONTINUED).



On MBII-1, every 25th bag was pulled from the conveyor, weighed, and returned. On MBII-2, the sampling frequency for bag weight was increased to every 20th bag" (Reference 16).

Table 2-6 presents stacking data for one of the nominal 120 ton MISERS BLUFF domed cylindrical charges, i.e., MISERS BLUFF II-22 (MBII-22); approximately 240 bags were measured for weight and about 75 bags were assayed for FO content and particle size distribution. Table 2-7 provides the same type of information on another MISERS BLUFF charge (MBII-26) designed to the same specifications as MBII-22. Obviously there are differences in the charges as constructed. For MBII-22, the average fuel oil of the sampled bags was 4.3 ± 1.3 percent, for MBII-26, the average FO content was 6.0 ± 1.2 percent near to the optimum. As disturbing as the low FO content for MBII-22 is because of its possible effect on blast output, equally of concern are the variations in FO content throughout both charges layer by layer; this apparent index of inhomogeneity could be a source of blast anomalies. Both these topics, i.e., low average FO, and fuel oil induced inhomogeneities will be discussed in Section 4. (It should be noted that the wide fuel variations in the seven MISERS BLUFF charges were unusual and not true for earlier large ANFO charges. Whereas the MBII charges had an average percent deviation of 21.9 percent, the pre-DICE THROW and DICE THROW charges had only 6.6 percent standard deviation (Reference 16).)

2.7.2 Calculated Bulk Density

Although not as evident as the FO variations shown in Tables 2-6 and 2-7, even a cursory inspection of those tables for average bag weights and total layer weight makes it apparent that there are bulk density variations within the charge. For instance, on MBII-22, layer 1 had bags weighing (as determined by a five bag sample) an average of 47.2 lbs while layer 17 had bags weighing an average of 54.6 lbs. Translated into bulk densities of layers 1 and 17, and considering each layer to have the same dimensions, i.e., radius 8.542 ft and height 0.383 ft or 4.6 inches, the bulk density for layer 1 is 0.88 g/cm^3 , for layer 17, 1.02 g/cm^3 . Again, this bag to bag and layer to layer variation leads to concern as to what these inhomogeneities

TABLE 2-6. STACKING DATA FOR MISERS BLUFF II-22

Layer Number	Layer Radius (ft)	Number of Whole Bags	Number of Bags Bulk	Total Number of Bags	Average Bag Weight (lb)	Total Layer Weight (tons)	Average Fuel Oil Content (%)
1	8.542	92	10	102	47.2	2.405	4.9
2					47.6	2.428	5.3
3					48.0	2.394	2.9
4					47.8	2.438	3.3
5					47.2	2.406	3.8
6					47.5	2.422	4.6
7					47.5	2.420	4.8
8					47.8	2.438	4.9
9					47.3	2.412	4.1
10					46.8	2.387	4.4
11					48.2	2.460	3.4
12					49.4	2.522	5.3
13					48.9	2.496	4.0
14					49.8	2.537	3.3
15					52.3	2.667	3.9
16					52.5	2.678	2.4
17					54.6	2.782	2.6
18					51.2	2.611	2.7
19					50.2	2.562	2.1
20					50.0	2.547	4.6
21					49.6	2.527	3.9
22					49.3	2.514	4.9
23					48.2	2.458	4.9
24					49.9	2.545	3.7
25					49.3	2.514	3.6
26					49.2	2.511	4.2
27					48.6	2.481	4.4
28					49.7	2.535	5.1
29					49.8	2.542	5.8
30					49.8	2.542	--
31					49.3	2.514	5.0
32					49.3	2.514	5.5
33					50.0	2.550	3.2
34					52.1	2.657	4.1
TOTAL FOR CYLINDER		3,128	340	3,468		85.388	

TABLE 2-6. STACKING DATA FOR MISERS BLUFF II-22 (Continued)

Layer Number	Layer Radius (ft)	Number of Whole Bags	Number of Bags Bulk	Total Number of Bags	Average Bag Weight (lb)	Total Layer Weight (tons)	Average Fuel Oil Content (%)
35	8.542	92	9	101	52.0	2.628	3.7
36	8.531	92	9	101	52.3	2.641	4.1
37	8.500	91	8	99	50.8	2.514	9.5
38	8.458	90	8	98	53.2	2.607	5.4
39	8.312	88	8	96	48.0	2.304	5.3
40	8.208	82	9	91	48.5	2.207	4.4
41	8.104	82	9	91	48.8	2.223	5.1
42	7.948	82	6	88	48.8	2.145	--
43	7.792	72	7	79	49.9	1.972	--
44	7.604	63	5	68	49.0	1.666	--
45	7.375	59	5	64	48.5	1.552	--
46	7.135	55	5	60	48.3	1.450	--
47	6.875	58	5	63	48.3	1.522	--
48	6.573	45	3	48	48.6	1.167	--
49	6.219	39	3	42	48.2	1.013	--
50	5.802	40	3	43	47.1	1.012	--
51	5.375	36	3	39	48.6	0.948	--
52	4.875	31	2	33	47.1	0.778	--
53	4.250	23	2	25	46.1	0.577	--
54	3.479	15	2	17	46.2	0.393	--
55	2.417	8	-	8	46.5	0.186	--
56	1.208	4	-	4	46.5	0.093	--
TOTAL FOR CAP		1,315	43	1,358		33.600	
TOTAL FOR CHARGE		4,443	383	4,826		118.988	

TABLE 2-7. STACKING DATA FOR MISERS BLUFF II-26

Layer Number	Layer Radius (ft)	Number of Whole Bags	Number of Bags Bulk	Total Number of Bags	Average Bag Weight (lb)	Total Layer Weight (tons)	Average Fuel Oil Content (%)
1	8.542	94	8	102	44.5	2.270	4.9
2					45.2	2.307	6.0
3					45.1	2.300	7.5
4					45.4	2.313	6.0
5					46.4	2.365	7.3
6					48.0	2.445	6.1
7					48.1	2.451	5.4
8					48.9	2.495	6.5
9					48.5	2.474	6.4
10					49.0	2.499	5.1
11					48.8	2.491	5.0
12					48.8	2.489	7.2
13					49.1	2.504	5.0
14					48.6	2.473	--
15					48.9	2.436	6.8
16					48.2	2.456	6.9
17					48.6	2.481	4.2
18					48.7	2.486	4.3
19					49.9	2.547	5.3
20					49.8	2.538	6.2
21					49.5	2.523	6.4
22					49.5	2.524	5.6
23					50.0	2.549	7.8
24					49.2	2.509	6.6
25					49.9	2.543	6.9
26					49.2	2.511	6.3
27					48.5	2.474	4.7
28					46.9	2.390	5.2
29					47.0	2.397	5.7
30					48.6	2.478	5.0
31					48.9	2.495	6.4
32					48.5	2.474	5.5
33					49.0	2.500	5.7
34					48.5	2.474	5.6
TOTAL FOR CYLINDER		3,196	272	3,468		83.726	

TABLE 2-7. STACKING DATA FOR MISERS BLUFF II-26 (Continued)

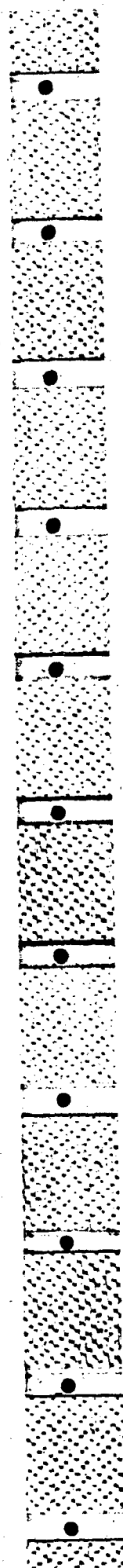
Layer Number	Layer Radius (ft)	Number of Whole Bags	Number of Bags Bulk	Total Number of Bags	Average Bag Weight (lb)	Total Layer Weight (tons)	Average Fuel Oil Content (%)
35	8.542	92	10	102	48.3	2.463	7.5
36	8.531	92	10	102	44.7	2.278	4.4
37	8.500	92	9	101	45.7	2.309	5.5
38	8.458	91	8	99	45.8	2.267	5.1
39	8.312	88	8	96	44.3	2.125	6.0
40	8.208	82	9	91	44.3	2.016	5.5
41	8.104	82	9	91	45.2	2.055	8.7
42	7.948	82	6	88	45.0	1.978	5.9
43	7.792	79	10	89	47.6	2.118	4.4
44	7.604	73	10	83	47.1	1.955	4.1
45	7.135	68	7	75	46.1	1.728	9.6
46	6.875	64	7	71	47.8	1.695	6.6
47	6.573	63	8	71	49.3	1.751	8.3
48	6.219	60	8	68	49.0	1.665	6.9
49	5.802	48	5	53	48.6	1.287	7.0
50	5.375	43	5	47	48.6	1.142	5.1
51	4.875	34	5	39	48.2	0.941	5.8
52	4.250	26	4	30	49.8	0.746	3.9
53	3.479	21	5	26	49.3	0.640	4.4
54	2.417	12	4	16	49.0	0.392	--
55	1.208	5	--	5	49.2	0.123	--
56	1.000	2	--	2	49.2	0.049	--
TOTAL FOR CAP		1,298	147	1,445		33.724	
TOTAL FOR CHARGE		4,494	419	4,913		117.450	

mean in terms of blast performance. But it also leads to questions as to what the bulk density of a completed charge is. For MBII-22, the bulk density for the charge is given in Reference 16 as 0.923 g/cm^3 . This seems high in view of the attempt to keep the density at 0.85-0.90 and brings into question the methods used to determine bulk density of a completed charge.

The bulk density is based on a calculation of the total charge weight and a calculation of the charge volume. For example, for the MBII-22 charge, the total weight, based on averaging five bags in most of the 56 layers used to construct the charge, is given as 119.208 tons. The volume is stated to be 4140 ft^3 . And, thus the bulk density is 57.59 lbs/ft^3 or 0.923 g/cm^3 . Actually, a slight correction can be applied to this calculation: the weight used to calculate the bulk density of the ANFO included non-ANFO parts of the charge such as the paper bag weights, booster weight, and miscellaneous material. The calculated pure ANFO weight was 117.966 tons. If this figure is used, the bulk density of the ANFO used in MBII-22 is calculated to be 0.913 g/cm^3 - still a high figure.

A sampling rate of five bags per 100 may not be adequate to ascertain the weight of a layer and then the whole charge. Perhaps, a better technique to determine total weight would be to revert to the system used on the earlier ANFO I, II, and III charges. For those charges the weights of ANFO were determined by weighing the trucks loaded with ANFO and then subtracting the weight of the empty truck (Reference 8). This method gives an accurate, measured weight not based on averaging samples. This method in conjunction with the sampling/calculating technique, would give a check on the validity of the sampling method. The sampling technique should still be used because it provides a qualitative picture of the density variations throughout the charge; these variations may be important information for correlating blast anomalies to density inhomogeneities.

Questions can be raised about the volume determinations also. Patently, it is difficult to determine the volume of a geometric solid with uneven scalloped surfaces and caps that aren't true hemispheres. It would take an extremely detailed surveying technique to get the true measure of volume; as much as one would like it, it probably is not feasible to do this.



As Table 2-5 shows, it isn't only the MBII-22 charge that has an apparently high density; all the charges using the sampling technique are higher than those of ANFO II and III where measured weights and easily calculated volumes were used to determine bulk density; these latter densities are nearer the desired values than the calculated densities of the bag constructed charges.

Before discussing the detonation velocities as measured on the large ANFO field test charges, there is another factor in bulk density determinations which arises. Given a specific density for a sample of ANFO before it is emplaced in a stack and assuming that that density is observed in all the pre-laid bags, is that density maintained after stacking? Specifically, does the in situ density of the ANFO at the bottom of the stack increase because of the hydrostatic loading provided by the layers above? Some rearrangement and break up of the ANFO prills can be expected leading to a denser packing. Consider for example, the MBII-26 stack. Rough back of the envelope calculations indicate a loading on the bottom layer of this 21 ft high stack to be about 1,000 lbs/ft². At the moment, there is no way to relate this loading to its affect on the bulk density. Assuming, however, that it does increase density, it can be expected that there is a smooth density gradient in the stack with the bottom layers being more dense than the topmost layers. Therefore, it can be expected, further, that detonation velocities would change from the bottom to the top of the charge. In situ density measurements would answer the question.

Another effect of this vertical loading, in conjunction with the lateral extent and mass of the ANFO in a large charge, is that what has been referred to as an "unconfined" charge because there is no massive, strong casing, in reality behaves to a large extent -- throughout much of its inner volume -- as a confined charge. As shown earlier (Figures 2.8e and f) confinement and diameter influence detonation velocity.

2.7.3 Detonation Velocity Measurements

Given that detonation velocity is a function of such parameters as fuel oil content, prill sizing, bulk density, confinement, diameter, and water content, and that it takes about 3 ft of detonation wave travel before reaching a steady state velocity, it is not surprising that detonation velocity measurements on large ANFO charges have led to a plethora of

results -- results which sometimes are difficult to fathom in terms of the variables. Table 2-8 presents the reported data on detonation velocities for most of the large ANFO shots fired to date; included in the table are charge characteristics pertinent to velocity. Figure 2-11 plots the velocities for these shots as a function of charge bulk density.

It is seen that the velocities range from a low of 13,944 ft/sec (4,250 m/s) to a high of 18,374 ft/sec (5,600 m/s) with the two largest charges (largest in weight and in height), DICE THROW and MILL RACE, having the highest velocities; the densities of the two charges are about the same, but there is a bit more difference in their FO percentages. The lowest detonation velocity occurred in one of the smaller charges, the nominal 20 ton ANFO II charge; this charge evidences also the lowest density, although its FO content is close to the optimum. The data in Figure 2-11 indicates an upward trend in detonation velocity as the density of the ANFO increases, as would be expected on the basis of Figure 2-8b, but there is large scatter in the data. The possible reasons for this scatter will be discussed on a shot to shot basis.

2.7.3.1 NSWC Phase I Shots (Reference 29)

Although not listed in Table 2-8 or plotted on Figure 2-11, some early small charge ANFO data are interesting from a historical standpoint and from a technical standpoint because they shed light on the learning process accompanying the ANFO simulation development. In 1968, NSWC fired 23 shots of unconfined ANFO in a hemispherical-like configuration (see Sections 1.2.2 and 1.2.3). Base radii of the charges ranged from 16 inches for the 250 lb charges to 25 inches for the 1000 lb charges. Heavy boosting was employed to assure ANFO detonation; cast pentolite cylinders weighing 8, 16, and 24 lbs were used for the 250, 500, and 1000 lb charges respectively. The start probes for velocity measurements were located 2 inches (5.08 cm) from the booster. For the 250 and 500 lb charges the stop probe was 6 inches (15.2 cm) from the start probe and for the 1000 lb charge, the spacing was 12 inches (30.5 cm). The measured velocities for the three 250 lb events were 3,908, 4,011, and 4,119 m/s, for the several 500 lb shots the velocities ranged from 4,011 to 4,354 m/s, and for the nine 1000 lb charges the range was from 4,119 m/s to 4,293 m/s.

TABLE 2-8. ANFO LARGE CHARGE SUMMARY

ANFO CHARGE	APPARENT DENSITY (g/cm ³)	CHARGE WEIGHT (tons)	CHARGE RADIUS (m)	CYLINDER HEIGHT (m)	CAP HEIGHT (m)	TOTAL CHARGE HEIGHT (m)	FUEL OIL (%)	RANGE REPORTED DETONATION VELOCITY (m/s)
ANFO I	0.88	19.96	2.17	0	2.17	2.17	5.85	4,570
ANFO II	0.84	18.68	2.13	0	2.13	2.13	5.90	4,250
ANFO III	0.86	100.32	3.78	0	7.38	7.38	5.95	4,600
ANFO IV	0.85	25.1	~1.8	--	--	3.6	6.2	4,390
ANFO V	0.85	23.9	~1.8	--	--	3.6	7.0	not measured
PDT-I EVENT 2	0.86	5.6	0.92	1.55	0.92	2.47	5.5*	4,871
PDT-I EVENT 3	0.88	5.8	1.04	1.04	1.04	2.08	5.5*	4,529
PDT-I EVENT 4	0.86	5.6	0.96	1.44	0.96	2.40	5.5*	4,602
PDT-II EVENT 2	0.88	122.45	2.66	4.00	2.66	6.66	6.0 ± 0.4	4,460-5,120
DICE THROW	0.91	628.0	4.53	6.51	4.33	10.84	6.1 ± 0.4	4,570-5,600
MB-II (1)	0.90	118.2	2.60	3.90	2.60	6.5	6.7 ± 1.3	4,429-4,969
MB-II (21)	0.91	117.5	2.60	3.97	2.15	6.12	5.6 ± 1.1	4,904
MB-II (22)	0.92	119.0	2.60	3.97	2.37	6.34	4.3 ± 1.3	4,804
MB-II (23)	0.89	117.9	2.60	3.97	2.66	6.63	6.0 ± 1.7	4,537
MB-II (24)	0.90	117.2	2.60	3.97	2.12	6.09	5.4 ± 0.7	4,904
MB-II (25)	0.91	117.9	2.60	3.97	2.23	6.20	5.3 ± 1.2	4,932
MB-II (26)	0.91	117.4	2.60	3.97	2.46	6.43	6.0 ± 1.2	4,895
MILL RACE	0.92	600.2	4.53	6.69	3.82	10.51	6.3 ± 0.4	5,246-5,576
DISTANT RUNNER II	0.87	120.8	2.62	4.0	2.58	6.58	6.3 ± 0.8	--
DISTANT RUNNER III	0.86	121.5	2.68	4.2	2.44	6.64	6.5 ± 0.3	--

*Procurement specification; not measured.

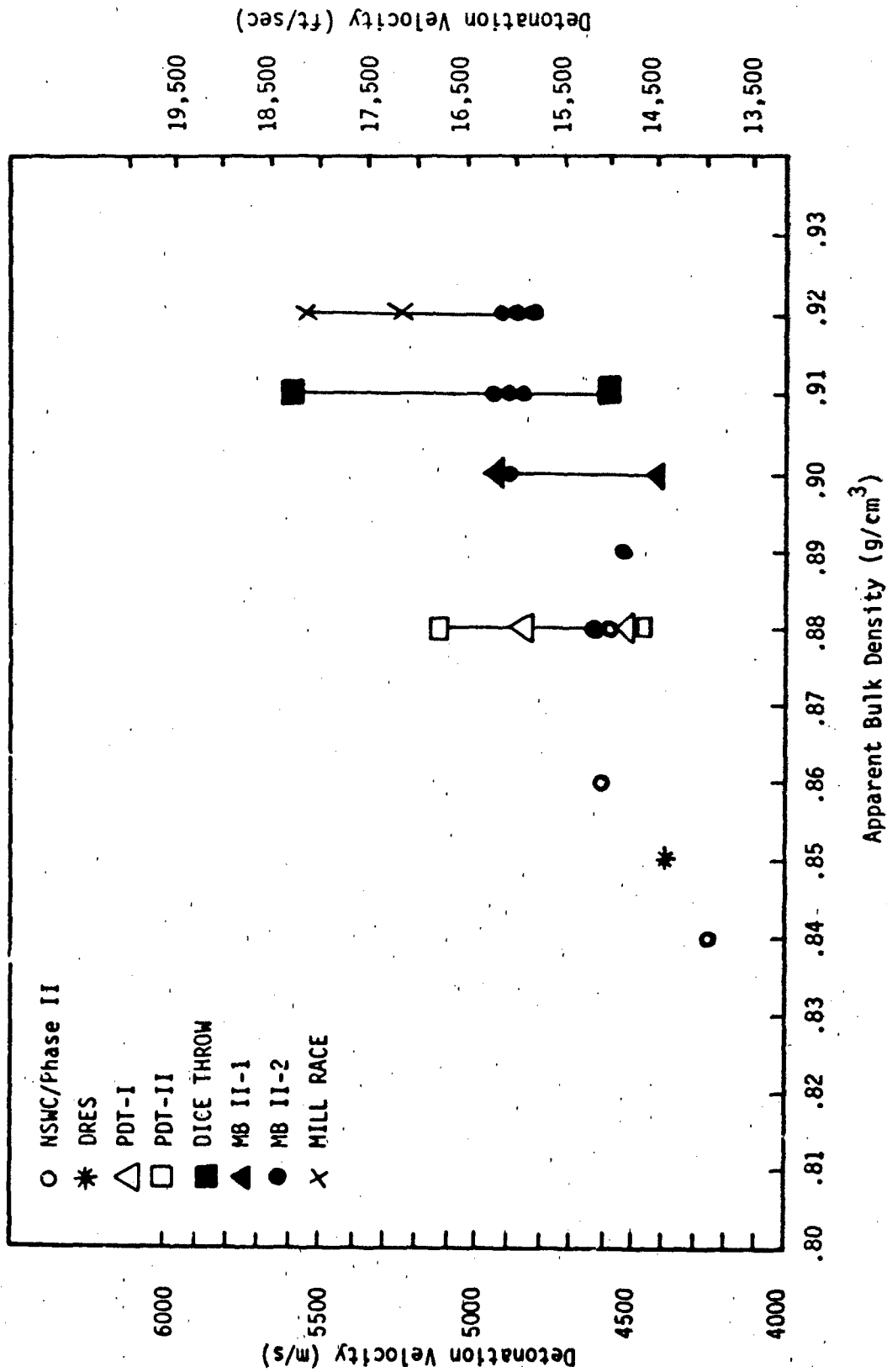


FIGURE 2-11. ANFO DETONATION VELOCITY VERSUS APPARENT BULK DENSITY.

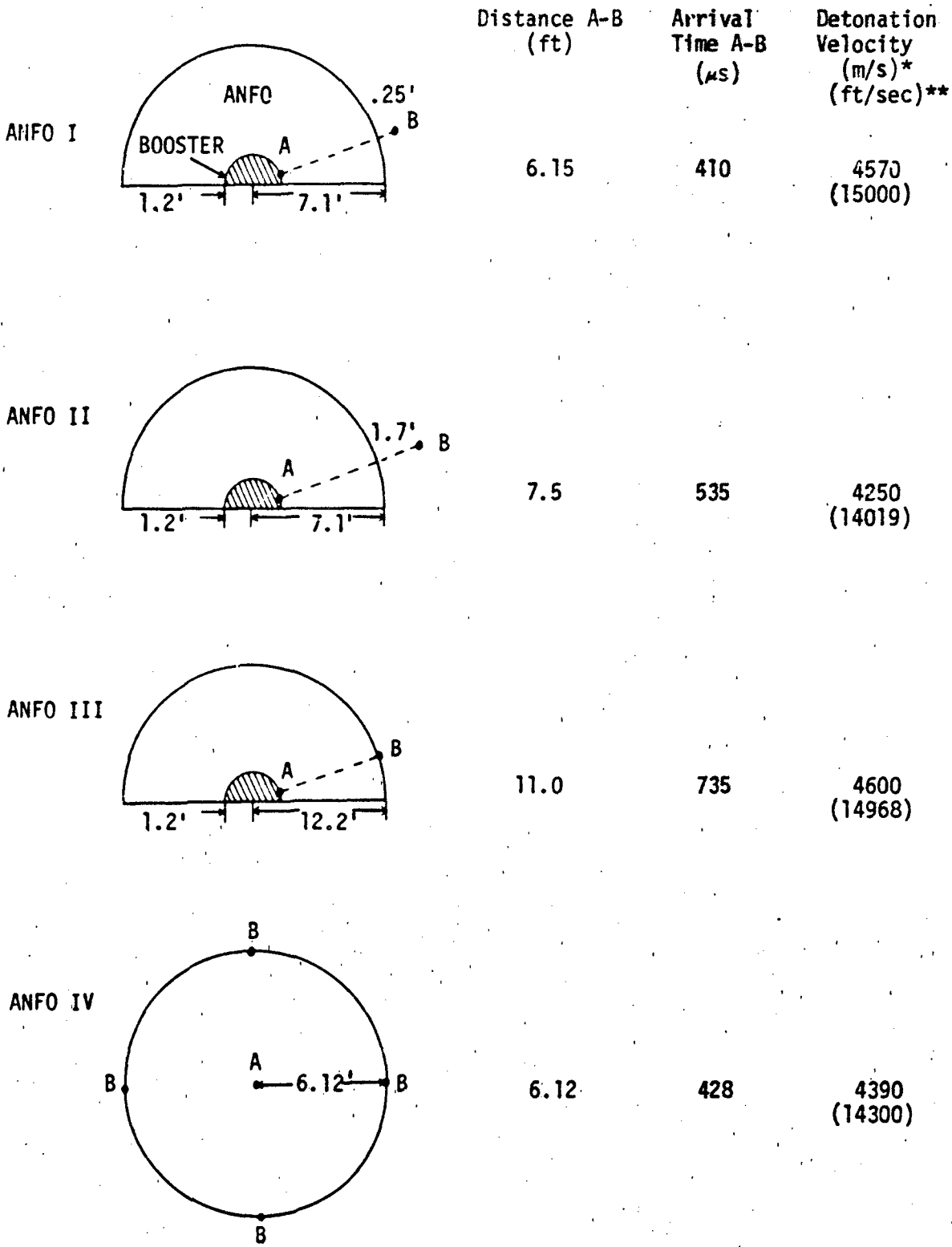
Although there is an increase in average velocity as the charge radii increase, it is apparent from the information presented in Figure 2-9, that these measurements do not represent steady state values but rather transient ones. On one hand, the detonation probes are much too close to the booster; on the other, the detonation wave has not had enough travel time or space even in the 25 inch radius charge to attain its steady state value.

These tests and measurements were done in 1968, the start of the ANFO simulation development program when information about ANFO characteristics was not widespread and questions about confined versus unconfined charges were unanswered (Reference 20). The discussions on the following shots regarding detonation velocity will indicate the rate at which the testing community is progressing on the learning curve.

2.7.3.2 ANFO I through V

The detonation velocity values reported for these events were "inferred from other observations" (Reference 21) and leave something to be desired, particularly for ANFO I (reported velocity 4,570 m/s) and ANFO II (reported velocity 4,250 m/s). On those shots, the inference of velocity comes from an ionization probe adjacent to the 1.2 ft radius pentolite booster and ABTOAD (Air Blast Time of Arrival Detector) gages some distance outside the charges (Figure 2-12). On ANFO I, the ABTOAD gage was about 0.25 ft from the charges; on ANFO II it was 1.7 ft away. The time interval between signals arriving at these sensors, about 410 μ s for ANFO I and 535 μ s for ANFO II, includes not only the transit time of the detonation wave through the charge, but the slower transit time of the blast wave outside the charge. Therefore the measurements are not those of detonation velocities and to infer so is wrong. The use of the ionization probe right at the booster compounds the error in that about three feet of the nominal charge radius of 7 ft represents a transient zone.

The reported values for ANFO III (4,600 m/s) and ANFO IV (4,390 m/s) may be more valid representations of steady state velocities than those of the other shots in this series. On ANFO III the same technique was used as on the earlier shots -- an ionization probe at the booster, an ABTOAD gage outside the charge -- except that now the ABTOAD gage was on the surface of the charge. So, indeed, the time difference between response of the two sensors



*Reported Values.
 **Calculated Values Based on Indicated Geometries (Not To Scale).

FIGURE 2-12. ANFO I-IV DETONATION VELOCITY GEOMETRIES.

is a measure of the transient time of the detonation wave alone (without a slower blast wave component as on ANFO I and II). Also, because the detonation wave had about 11 ft of travel through the ANFO, it could be expected that the velocity in the last 8 ft had attained a steady state value. Therefore, the averaging process involved in the two probe measuring systems would be influenced less by the initial three feet of travel with transient velocities than with a dimensionally smaller charge, e.g., ANFO IV.

This is evident in examining the ANFO IV detonation velocity measurement for which a velocity of only 4,390 m/s was reported. On ANFO IV, along with an ionization probe at the booster, four ionization gages were placed on the outside of the charge; the detonation wave travelled through about 6 ft of ANFO. So, a steady state value was probably realized in the last 3 ft of the charge, but the initial 3 ft of travel with its transient velocities influenced the average velocity measured. It appears reasonable to expect, therefore, that the large ANFO III charge had a higher average detonation velocity than ANFO IV because of the transient/steady state time difference for the two charges.

With the detonation velocities in question for ANFO I through IV (there were no measurements on ANFO V), there is little point in trying to relate bulk density and fuel oil content to velocity except to note that all the charges had about the same densities (0.85 g/cm^3), ANFO I, II, and III the same nominal FO content (5.9 percent) with ANFO IV having a 6.2 percent FO content.

2.7.3.3 Pre DICE THROW I, Events 2, 3, and 4

As Figure 2-10 indicates, the pre-DICE THROW I charges had the so called domed or capped cylindrical geometries. Each charge had a different L/D ratio but all had the same nominal weight, about 5.7 tons, and the same bulk density, 0.88 g/cm^3 . The charge for Event 3 had the largest radius, 1.04 m (or 3.4 ft) -- barely sufficient for the detonation wave to attain a steady state value.

Detonation velocities were obtained photometrically. The technique used was to measure the time intervals from booster initiation to the first explosion positive-going light radiation signals recorded by solarcell

sensors. This time was then divided into the nominal radii of the charges to obtain overall detonation velocities. Wisotski (Reference 22) reports velocities of 4871, 4529, and 4602 m/s, respectively.

It is apparent that these velocities do not represent steady state velocities of ANFO but rather they are averages of transient velocities over a 3 ft travel. The fact that the charge with the largest radius, Event 3, has a reported velocity lower than the smaller radii charges, may be attributable to errors in measurements or to the profile of the detonation waves. Events 2 and 3 used five boosters evenly spaced along the axis of the cylindrical portion of the charge; Event 4 used seven boosters. Mach interactions between the detonation waves of each booster could have caused jetting within the charges which evidenced itself as early break out of light (see Section 3.3). In the larger radius and squatter charge, Event 3, the detonation jets may have been contained within the charge to permit forming a smoother detonation front as the ANFO outer material was consumed in the explosion and therefore showed a later light break out.

With the apparent densities and the FO contents ostensibly the same for these three charges, no inference can be drawn about the relationships of those parameters to detonation velocity.

2.7.3.4 Pre-DICE THROW II, Event 2

This charge of 122.45 tons was similar in construction to the pre-DICE THROW I, Event 4 charge: L/D of 0.75/1 for the cylindrical portion of the charge, bagged ANFO, and seven axially positioned and equally spaced cylindrical boosters. Instrumentation coverage for detonation velocity, however, was greatly improved. DRI provided high speed photographic means and two photometric devices; the Lawrence Livermore National Laboratories (LLNL) used four rate sticks and an axially symmetric magnetic probe (ASMP) for detonation diagnostics (Reference 23).

Three 40.6 cm (16 inch) long rate sticks provided useful data; the fourth and longer (6 ft) stick malfunctioned. Each functioning stick had eight arrival time sensing pins spaced a nominal 54.7 mm (2.15 inches) apart. The rate sticks (S-1, S-2., S-3) were placed at various distances from the



mosters and at different heights within the charges (see Figure 1-33). The ASMP was placed about 5 ft off the ground and in intimate contact with the charge. The metal plate used in this device acquires the equivalent velocity of the explosive particles with which it is in contact; the recorded pulse width is proportional to detonation velocity.

The reported average velocities recorded by the rate sticks were 4,380 m/s for S-1, 5,120 m/s for S-2, and 4,880 m/s for S-3; the ASMP indicated a velocity of 4,460 m/s. Because the rate stick measurements provide a history of the detonation velocity, it is informative to plot the average velocity between pins as in Figure 2-13.

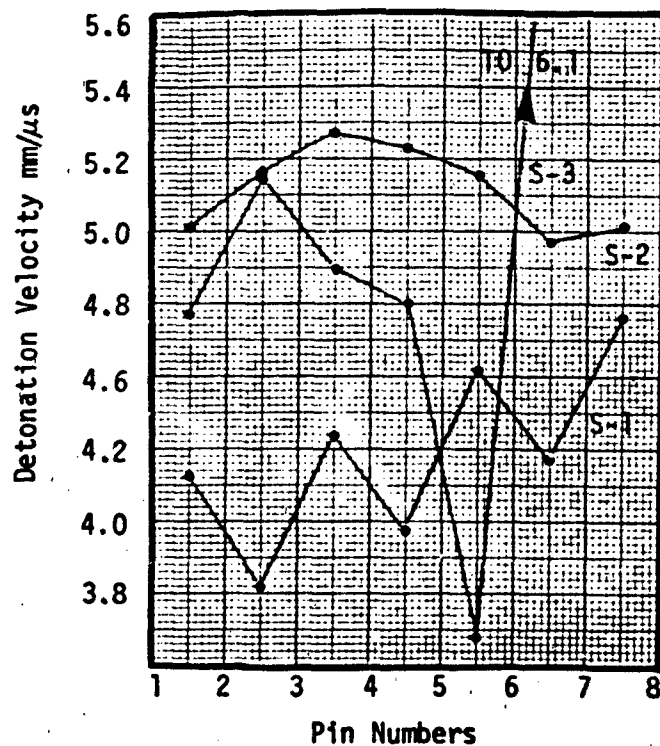
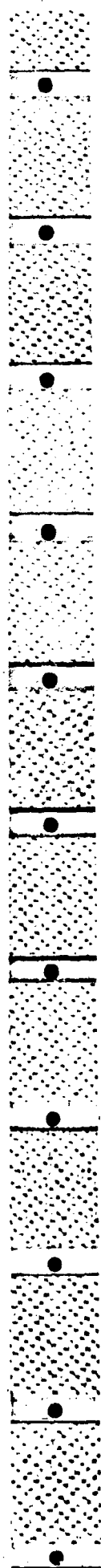


FIGURE 2-13. PRE-DICE THROW II, EVENT 2, DETONATION VELOCITY HISTORIES

Rate stick S-1, only a half foot from the booster evidences an oscillatory but increasing velocity as the detonation wave travels away from the booster. This increasing velocity is as could be expected on the basis of the 3 ft run-up distance required to attain a steady velocity. The record shows that the steady state had not been attained along the rate stick length; therefore, the reported average velocity has no real meaning in terms of a characteristic ANFO velocity.

Rate stick S-2, positioned 3.5 ft from and midway between boosters 5-6, is in an area where a steady state value can be expected. The plot shows considerably less oscillations than on S-1 and an average detonation velocity of 5,120 m/s (16,800 ft/sec). This velocity is considerably higher than that recorded on S-1 and it is indicative that a steady state value has been reached. It should be noted that this velocity falls between the ideal velocity, 4,633 m/s for 0.88 g/cm^3 ANFO shown in Figure 2-8b, and the calculated ideal, 5,428 m/s according to Kamlet's equation and plot (Figure 2-3). There is no clue in either the density or the FO content of the charge to explain the difference between the measured value and the two "ideal" determinations. However, a question can be raised about the measured value being a representative value for large ANFO charges. As discussed in Section 3.3, it may be that mach interactions between the fronts of the detonation waves coming off boosters 5 and 6, resulted in a jetting along rate stick S-2 which was positioned half way between these two boosters. This high velocity jet could have been the detonation wave that the rate stick witnessed; if this were so, the velocity measured would be higher than the "free field" velocity. Leaving conjecture aside, the velocity of 5,120 m/s (16,799 ft/sec) appears valid.

Rate stick S-3, positioned vertically about 6.5 ft distant from the top booster (and hence not subject to booster wave jetting) shows a wildly oscillating velocity pattern between sensors 5-6-7 (no measurement was obtained between 7-8). The average measured velocity was 4,940 m/s (16,208 ft/sec). If the arrival times between only the first three pairs of sensors are considered, the velocity average is 4,900 m/s (16,077 ft/sec). As with S-2, S-3 should be responding to a steady state detonation velocity because it



is completely away from the transient zone. The 4 percent difference in velocities measured by these two rate sticks may represent experimental scatter; this percentage is small compared to the 15 percent difference between "ideal" calculations. But they may be real differences, not scatter.

Consider that although the bulk density for the PDII-2 charge is calculated to be 0.88 g/cm^3 , it appears reasonable to posit that there is a gradation of ANFO densities through the height of the charge with the density higher at the bottom (because of hydrostatic loading, prill break up, and denser packing) than at the top. If this is so, the velocity at S-3 should be less than that measured by S-2 which is in a region where the density may be higher and, indeed, it is.

The ASMP device functioned well and provided a calculated velocity of $4,460 \text{ m/s}$ ($14,268 \text{ ft/sec}$). This velocity is less than that averaged by the S-2 and S-3 rate sticks which ostensibly measured steady state velocities also. It may be that there is no real disparity among these measurements. In attaching the ASMP to the charge, about 250 lbs of ANFO with a density of 0.84 g/cm^3 were used between the charge proper and the metallic plate; therefore, the particle velocity/detonation wave velocity of this coupling ANFO was what was measured, not the main charge. As Figures 2-3 and 2-8b indicate, for a density of 0.84 g/cm^3 the detonation velocity could be from 2 to 8 percent less than that for a density of 0.88 g/cm^3 . The ASMP velocity is about 13 percent less than that averaged by S-2, and 9 percent less than the S-3 average. With all the variables and the spread of results discussed in all the shots thus far, it is impossible to determine whether these percentage differences can be ascribed to normal experimental error/scatter, or whether they represent real differences.

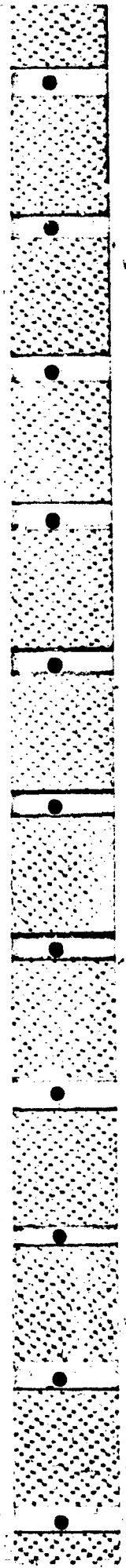
Wisotski (Reference 22) determined an overall velocity from photometric measurements of $4,746 \text{ m/s}$ ($15,571 \text{ ft/sec}$). As discussed earlier, a velocity determined by a two sensor system, i.e., a time of detonation and a time for light breakout, suffers by the averaging process, but the larger the dimensions of the charge, the more apt it is to represent a time steady state value. The 3 percent difference between Wisotski's value and the S-3 measurement is remarkably small; the two velocities can be considered to be consonant.

2.7.3.5 DICE THROW

DICE THROW was the first full scale test with an ANFO charge. It had the same geometry as the successful pre-DICE THROW II Event 2: a domed cylinder with an L/D = 0.75/1 for the cylindrical portion and seven points of initiation along the central axis of the cylinder. Figure 2-14 shows a cutaway view of the stack. The charge contained a nominal 620 tons of ANFO; the overall bulk density was calculated to be 0.91 g/cm^3 and the average FO content was 6.12 percent. As with many of the earlier large development charges, there was considerable variation in the layer to layer density and FO content of the emplaced ANFO. The supplied material had bulk densities as high as 0.92 g/cm^3 and FO content ranged from 4.96 to 6.83 percent.

The shot was fairly well instrumented for diagnostic purposes. DRI provided photographic coverage and photometric measurements and LLNL used a long rate stick and quartz gages within the charge. The rate stick with 15 shock sensitive crystal pins was 11.75 ft long and placed in the plane of and about 3 ft away from booster No. 3. The quartz sensors were used to measure detonation pressure; paired with each of these gages were trigger pins to record the time of arrival of the detonation wave from the booster. These sensors were placed 2.8 ft from booster No. 2, 6.3 ft from booster No. 4, and 9.8 ft from booster No. 6.

Wisotski (Reference 24) reported his photoelectrically measured and photographically interpreted velocity values opposite boosters Nos. 1 and 7 as 5,600 and 4,740 m/s respectively. Assuming simultaneity of these boosters (simultaneity measurements failed on this shot), these velocities appear valid in that the higher velocity was measured at the bottom of the stack where it could be expected that the bulk density of the ANFO was increased by hydrostatic loading. (The effect of this loading was evidenced at the completion of charge construction when it was noted that the lower portion of the stack had expanded about 6 inches in radius; see Section 3.2.1.) As discussed earlier, however, with this essentially two point time of arrival system, the DRI measurements give only an average velocity over about 14 ft of travel through the ANFO with the first 3 ft providing a transient, probably lower than steady state, component. So, the reported velocities are not quite steady state values but close to it.



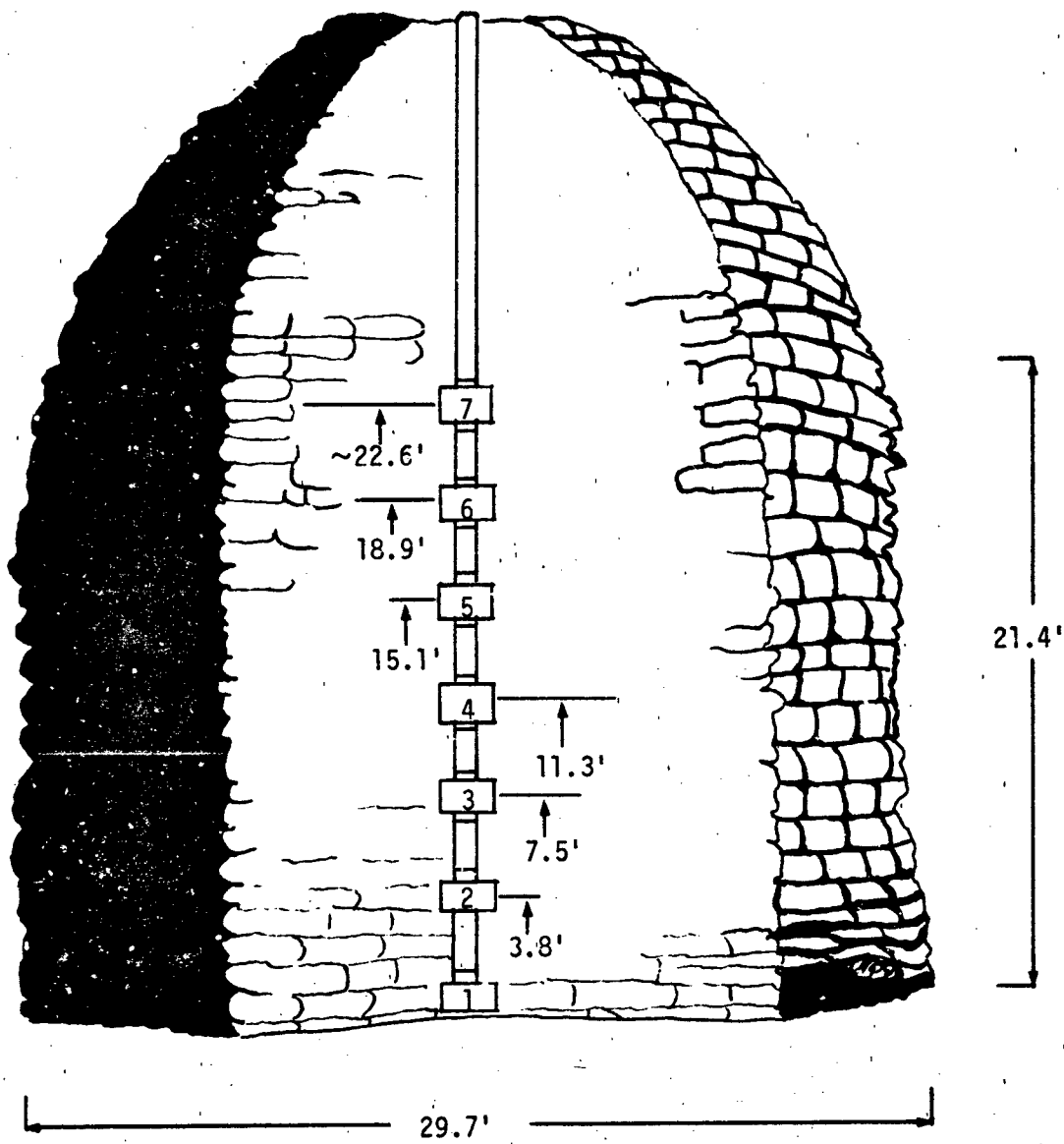
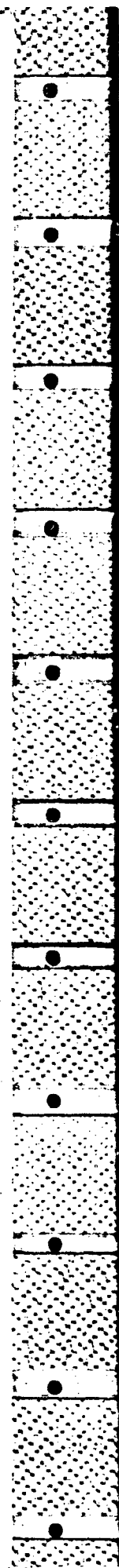


FIGURE 2-14. DICE THROW ANFO STACK (CUTAWAY).

A steady state value could be expected from the LLNL rate stick; this was sufficiently distant from the booster so that the transient phase of the detonation wave would not be recorded. The rate stick measured a value of 5,256 m/s (Reference 24). This velocity obtained 7.5 ft from the bottom of the charge is intermediate between the DRI values measured at the bottom and top of the charge and can be interpreted as further indication of a density profile through the charge top to bottom.

The data from the three trigger pin sensors corroborate to a large extent the existence of a density gradient. With the pin opposite booster No. 6, this two point system gave a velocity of 4,640 m/s, somewhat less than the top most DRI value which was averaged over a longer distance from the booster. The pin opposite booster No. 4, about halfway up the charge, provided a detonation velocity of 5,010 m/s; but this measurement included a transient velocity run up of about half the distance over which the average was obtained. The pin opposite booster No. 2 showed a velocity of only 4,570 m/s even though it was measured in a compacted, higher density ANFO; with this pin only 2.8 ft from the booster, it is apparent that it was averaging only a transient velocity, one that had not reached a steady state value.

Plotting the DICE THROW velocities reported by DRI and LLNL as a function of charge height, or its presumed corollary, charge density (Figure 2-15), it is evident that what earlier investigators have determined for confined charges, i.e., the higher the density, the higher the velocity, is true also for the DICE THROW charge. What was the detonation velocity for DICE THROW? As the figure shows, there is no single appropriate value because it is charge height or density dependent. Knowing that random density and FO inhomogeneities exist in the charge, there is not too much point in trying to refine or define the measurements to get a greater degree of accuracy. A center line between the DRI and LLNL data is a fair representation of the velocities for DICE THROW; the actual data are within less than 3 percent off this line.



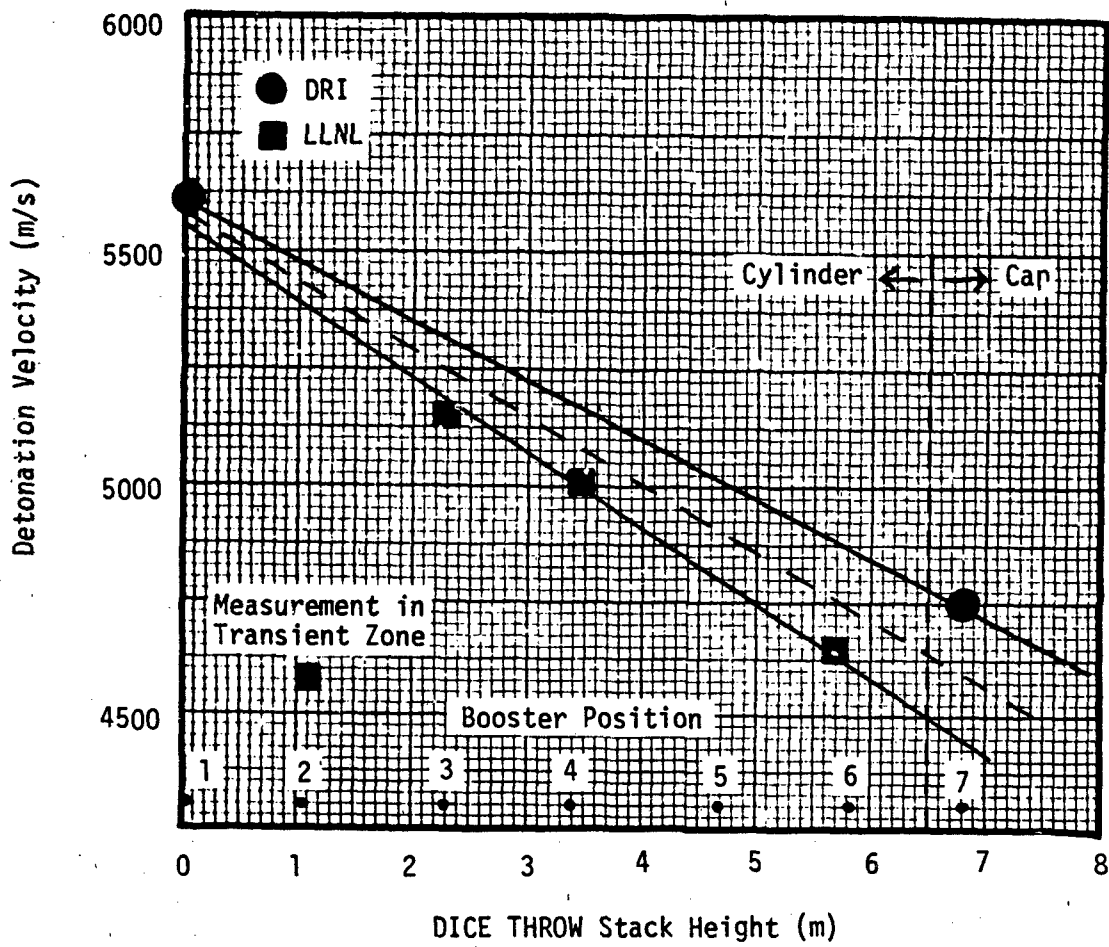


FIGURE 2-15. DICE THROW DETONATION VELOCITY.

2.7.3.6 Other Large Scale Operations

After DICE THROW, several test operations used the same charge geometry: MISERS BLUFF with seven 120 ton charges (six of them detonated simultaneously), MILL RACE another 600 ton shot, and DISTANT RUNNER with two 120 ton charges. On these tests detonation velocities were derived primarily by photographic means looking for time of light breakout from the charge and referring this to the time of detonation. Rate sticks within the charge were not used. Diagnostics for these charges were concerned more with the simultaneity of booster detonation. For this purpose, light pipes were inserted into the charge viewing directly the light from the boosters (see Section 3.3). These measurements are exceedingly useful and add another variable to the task of determining detonation velocity; boosters in any given charge did not detonate at the same time (Table 3-5); on MISERS BLUFF II-2, charge 3 had a spread of 72 μ sec between the first and last booster detonation times and MILL RACE had a spread of 90 μ sec. With the previously described layer to layer bulk density and fuel oil content variations in each of the charges, and now, with the evident non-simultaneity of the booster detonations, perhaps it will suffice to make a few general remarks on the reported velocities. Table 2-8 shows these velocities along with some of the important variables in charge characteristics.

The seven MISERS BLUFF charges had about the same bulk densities, ranging from 0.89 to 0.92 g/cm³, but the FO contents varied over a much larger range, from 4.3 to 6.7 percent. And yet the reported detonation velocities as determined by photographic means were all about 4,900 m/s, except for MBII 23 which had the lowest velocity even though the bulk density and fuel oil content were closer to specifications than the other charges. Note also that the earlier 120 ton pre-DICE THROW II Event 2 shot also reported a detonation velocity in the 4,900 m/s range. So, without diligent analysis, it appears that all these charges had similar detonation velocities. A similar statement can be made for the MILL RACE and DICE THROW shots; both had considerably higher velocities than the smaller charges and both were about the same.

However, as discussed earlier, single value detonation velocities for large domed cylindrical ANFO charges are not quite valid. It is expected and

it is evident on those shots where somewhat detailed analyses can be made of rate stick data that the detonation velocity is a function of the density gradient through the height of the charge.

2.7.3.7 Detonation Velocity Summary

There have been a wide range in experimentally determined and reported detonation velocities for large ANFO charges (but hardly wider than those evident in theoretical determinations). This range is attributable to many factors: the characteristics of ANFO, the methods of measurement, and the degree of detail in reporting.

There is no doubt that detonation velocity is a function of ANFO density; a 6 percent change in density leads to a 6 percent change in velocity (Figure 2-3). And there is no doubt that hydrostatic compaction of the lower layers of an ANFO charge produces a density gradient through the charge with the highest density at the bottom. Unfortunately, the density gradient has not been characterized quantitatively; nevertheless where adequately measured and analyzed, higher detonation velocities are reported for the bottom of cylindrical charges than at the top.

The photographic technique for measuring detonation velocities is crude and ambiguous. As stated by researchers from the Physical Sciences Laboratory of New Mexico State University in Reference 25, "Velocity data derived from breakout times should be considered with certain limitations in mind. Significantly, the breakout distribution was not uniform [in MILL RACE]. When observed at only a few discrete instants of time and along only part of the stack circumference, breakout times are not precise in themselves and initial breakout is not precisely assignable to [a] stack surface point."

Add to this the non-simultaneity of booster firings -- the reference point from which times are measured to calculate velocity -- and the task gets to be more difficult. And the determination is complicated further because the transient phase of the velocity is included in the overall measurement. Long rate sticks appear to be the best practical way to determine detonation velocity; with a sufficient number of sensors and a length extending along a complete radius of the charge, the long rate stick can give a detonation velocity history from transient to steady state phases. In fact, these sticks

may do more: the oscillations evidenced in the histories may give clues as to the degree of homogeneity of the charge along the rate stick path.

The detail (or lack of detail) in reporting detonation velocity results also adds to the scatter in reported values. Velocities should not be averaged when they may represent real differences due to bulk density variations. And the physical location of the measured velocities should be stated; as implied in the preceding, this would aid analysis.

It is clear that the large scale field test experimenting community is going through a learning process. Early on it recognized that ANFO was a non-ideal explosive and had characteristics different from military explosives such as TNT, but for want of something better, it employed old techniques and concepts. So important bits of information were not obtained. Now, more is known about ANFO and better and more complete definitive measurements can be made if necessary.

2.8 ENVIRONMENTAL FACTORS (Reference 26)

2.8.1 General

The principal effects on the environment from an explosion are those that result from airblast, noise, cratering and the ejecta surrounding the crater, missiles, ground shock, explosive detonation products, and a buoyant cloud which will carry dust and detonation products downwind. This section addresses only explosive detonation products since all other effects are primarily governed by the size of the explosion and the atmospheric conditions and not by the nature of the explosive material. However, since the hazard is different for underground explosions compared to those above ground, this section does address both regimes.

2.8.2 Detonation Products (Reference 7)

From the operative chemical reaction in the explosion of ANFO (equation 2.4.1) and TIGER code (see Section 2.5.2) calculations, the dominant combustion products are H_2O , N_2 , O_2 , and CO_2 , none of which are hazardous. Some amounts of H_2 , CH_4 , NH_3 , CO , NO , NO_2 , HCN , and N_2O are also produced; these can be hazardous or toxic.

Table 2-9 characterizes the composition of detonation products over a FO content range of 0 to 10 percent by weight.

TABLE 2-9. ANFO DETONATION PRODUCT COMPOSITION (moles/kg of ANFO)

WEIGHT PERCENT FO	0	1	2	3	4	5	6	7	8	9	10
<u>Products:</u>											
H ₂ O	25.0	25.4	25.9	26.3	26.8	27.2	27.4	26.9	26.2	25.5	24.7
N ₂	12.3	12.1	11.9	11.7	11.6	11.6	11.7	11.4	11.1	10.7	10.3
O ₂	6.06	4.82	3.59	2.40	1.29	0.340	0.002	1x10 ⁻⁴	2x10 ⁻⁵	6x10 ⁻⁶	2x10 ⁻⁶
CO ₂	--	0.715	1.43	2.14	2.85	3.53	3.53	2.97	2.65	2.48	2.39
H ₂	7x10 ⁻⁶	5x10 ⁻⁵	3x10 ⁻⁴	0.001	0.004	0.016	0.253	0.769	1.23	1.59	1.84
NH ₃	2x10 ⁻⁸	4x10 ⁻⁷	3x10 ⁻⁶	2x10 ⁻⁵	1x10 ⁻⁴	8x10 ⁻⁴	0.050	0.299	0.687	1.12	1.53
HCH	--	--	--	--	--	2x10 ⁻⁶	0.002	0.027	0.093	0.187	0.290
NO	0.279	0.492	0.701	0.848	0.855	0.578	0.053	0.011	0.004	0.002	0.001
NO ₂	0.047	0.049	0.046	0.036	0.022	0.007	5x10 ⁻⁵	2x10 ⁻⁶	4x10 ⁻⁷	1x10 ⁻⁷	4x10 ⁻⁸
N ₂ O	0.001	0.002	0.003	0.004	0.004	0.003	3x10 ⁻⁴	5x10 ⁻⁵	2x10 ⁻⁵	9x10 ⁻⁶	5x10 ⁻⁶
CO	--	2x10 ⁻⁵	3x10 ⁻⁴	0.002	0.008	0.046	0.761	2.00	2.96	3.68	4.23
CH ₄	--	--	--	--	--	--	2x10 ⁻⁵	0.003	0.024	0.094	0.239

The hazard associated with hydrogen (H₂) and methane (CH₄) is one of an explosive air mixture and is only significant in underground explosions where the product gases are confined to the cavity. Nitrous oxide (N₂O) has been a commonly used anesthesia and does not represent a hazard in either underground or above ground regimes. The toxicity of nitric oxide (NO) and nitrogen dioxide (NO₂) is 0.057 mg/l, ammonia (NH₃) is 0.076 mg/l, carbon monoxide (CO) is 0.120 mg/l, and hydrogen cyanide (HCN) is 0.011 mg/l (Reference 1). For a perspective, Table 2-10 contains data for the explosion of 120 tons of 94/6 ANFO (Reference 26).

TABLE 2-10. TOXIC PRODUCTS FROM A 120-TON ANFO EXPLOSION

Product	Molecular Wt. (g/mole)	Amount Produced	
		Moles	kg
HCN	27.03	109.0	2.9
NO	30.01	2887.4	86.7
NO ₂	46.01	2.7	0.1
NH ₃	17.03	2724.0	46.4
CO	28.01	41459.3	1161.3

2.8.3 Environmental Hazards

For the underground explosion the hazard of toxic gases is significant and deserves proper consideration because of confinement. For example, considering only the nitrogen oxides, NO + NO₂, with a toxicity of 0.057 mg/l, an underground explosion of 12 tons requires a cavity volume of better than 10.5×10^6 liters in order not to exceed a toxic level.

For the aboveground explosion of six 120-ton charges (MISERS BLUFF Phase II), the toxic products were carried downwind along with dust in the explosion cloud. The maximum downwind concentration calculated for this event

was for each species: CO, 5 mg/l; NO + NO₂, 4.58 mg/l; NH₃, 0.2 mg/l; and HCN, 0.015 mg/l. All are above toxic levels but will gradually diminish with dispersion due to absence of confinement.

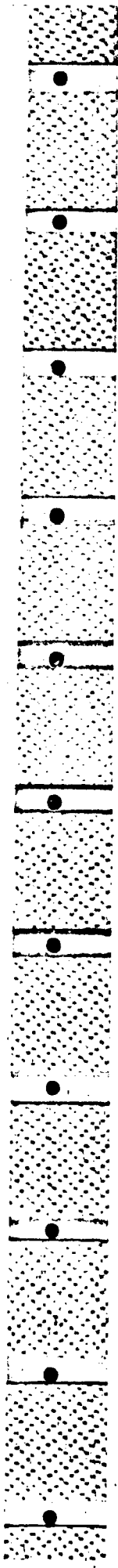
Environmental monitoring during the MISERS BLUFF Phase II event showed no significant alternation to the chemical content of the soil and water in the test bed area.

REFERENCES

1. Handbook of Chemistry of Physics, 46th Ed., Chemical Rubber Co., Cleveland, OH (1965).
2. Inorganic Chemistry, T. Moeller, John Wiley and Sons, New York, NY (1961).
3. The Science of High Explosives, M.A. Cook, Krieger Publishing Co., Huntington, NY (1971, reprint).
4. "Everything You Always Wanted to Know About Ammonium Nitrate But Were Afraid to Ask." Atlas Powder Company, Dallas, TX.
5. Blasters Handbook, E.I. du Pont de Nemours and Co., Wilmington, DE (1977).
6. Chemistry and Technology of Explosives, T. Urbanski, Polish Scientific Publishers, Warsaw, Poland (1965).
7. "Toxic Fumes from Explosives: Ammonium Nitrate - Fuel Oil Mixtures," U.S. Department of the Interior Report of Investigations, 7867 (1974).
8. "AN/FO Charge Preparation for Large Scale Tests," L.D. Sadwin and M.M. Swisdak, Jr., United States Naval Ordnance Laboratory, White Oak, MD, NOLTR 70-205 (1970).
9. "The New Look of Blasting," Gulf Oil Corporation Department, Kansas City, MO (1967).
10. "Determination of Equation-of-State Parameters for Four Types of Explosive," L. Penn, F. Helm, M. Finger, and E. Lee, Lawrence Livermore Laboratory, CA, UCRL-51892, (1975).
11. "Chemistry of Detonations, Part I: A Simple Method for Calculating Detonation Properties of C-H-N-O Explosives," M.J. Kamlet and S.J. Jacobs, J. Chem. Phys., 48:1 (1968).
12. "Chemistry of Detonations, Part II: Buffered Equilibria," M.J. Kamlet and J.E. Ablard, J. Chem. Phys., 48:1 (1968).
13. "Chemistry of Detonations, Part III: Evaluation of the Simplified Calculational Method for Chapman-Jouguet Detonation Pressures on the Basis of Available Experimental Information," M.J. Kamlet and C. Dickenson, J. Chem. Phys., 48:1 (1968).
14. "Chemistry of Detonations, Part IV: Evaluation of a Simple Predictional Method for Detonation Velocities of C-H-N-O Explosives," M.J. Kamlet and H. Hurwitz, J. Chem. Phys., 48:8 (1968).
15. "Monsanto Blasting Products ANFO Manual, Its Explosive Properties and Field Performance Characteristics," Monsanto Co., St. Louis, MO (1979).

REFERENCES (Continued)

16. "Proceedings of the MISERS BLUFF Phase II Results Symposium 27-29 March 1979," Volume I, Field Command, Defense Nuclear Agency, POR 7013-1 (1979).
17. "Swedish Methods of Mechanized Blasthole Charging," Proceedings of 104th AIME Meeting, P.A. Persson, (1975).
18. "Characterization of Commercial Composite Explosives," M. Finger, F. Helm, E. Lee, R. Boat, H. Cheung, J. Walton, B. Hayes, and L. Penn, Lawrence Livermore Laboratory, CA, UCRL-78244, (1976).
19. "Effects of Primer Type and Borehole Diameter on ANFO Detonation Velocities," J.L. Condon and J.J. Snodgrass, Mining Congress Journal, pp. 46-52 (June 1974).
20. "A History of the Use of ANFO for Nuclear Weapons Blast and Shock Simulation," J. Petes, 5th International Symposium for Military Applications of Blast Simulation, Stockholm, Sweden (1977).
21. "Performance of Multiton AN/FO Detonations, A Summary Report," L.D. Sadwin and M.M. Swisdak, Jr., United States Naval Ordnance Laboratory, White Oak, MD, NOLTR 73-105 (1973).
22. "MIDDLE NORTH SERIES PRE-DICE THROW I AND II EVENTS," University of Denver Research Institute, POR 6917 (1976).
23. "MIDDLE NORTH SERIES PRE-DICE THROW II EVENTS," Preliminary Results Report, Director, Defense Nuclear Agency, POR-6904 (1976).
24. "Proceedings of the DICE THROW Symposium 21-23 June 1977, Volume 1," GE TEMPO, Santa Barbara, CA, DNA 4377P-1 (1977).
25. "Proceedings of the MILL RACE Preliminary Results Symposium, 16-18 March 1982, Volume 1," Field Command, Defense Nuclear Agency, POR 7013-1 (1982).
26. "Environmental Impact Assessment for Phase II of the MISERS BLUFF Field Test," K.E. Gould and E.L. Harner, General Electric TEMPO (now Kaman Tempo), Santa Barbara, CA, DASIAC ES77-1 (1977).
27. "Numerical Modeling of Detonations," C.L. Mader, University of California Press, Berkeley, CA (1979).
28. "High Explosive Characterization for the DICE THROW Event," F. Helm, M. Finger, B. Hayes, E. Lee, H. Cheung, and J. Walton, Lawrence Livermore Laboratory, CA, UCRL-52042 (1976).
29. "Airblast Characteristics of ANFO, Phase I," L.D. Sadwin and J.F. Pittman, US Naval Ordnance Laboratory, White Oak, MD, NOLTR 69-82 (1969).
30. Thermodynamics, G.N. Lewis and M. Randall revised by K.S. Pitzer and L. Brewer, McGraw-Hill, Inc., New York, NY (1961).



APPENDIX 2-A

STEADY-STATE DETONATION*

by Dr. Robert Miller

Consider a large mass of solid explosive with density, ρ_0 , at a pressure of $P_0 Z$ (usually ambient atmospheric pressure). The specific volume of this mass is V_0 ($V_0 = 1/\rho_0$). Now initiate an explosion with a detonator system. The energy of the initiation must be sufficient to overcome the activation energy associated with the chemical reaction that describes decomposition of the explosive material. This chemical reaction proceeds quite rapidly and generates a shock front which propagates through the unreacted material with velocity, D , and causes compression of the material to a lower specific volume, V_1 , at a higher pressure, P_1 . The products of the chemical reaction are usually gaseous substances which undergo a rapid expansion at velocity, W .

After a finite period of time following initiation, the chemical reaction reaches a steady-state condition. This initial time period is generally referred to as the rise time. At steady-state conditions, the chemical reaction attains a unique set of parameters.

Figure A-1 is a one-dimensional representation of the steady-state condition. This figure shows a reaction zone with a finite length, l , in which the chemical reaction is taking place. At the front of the reaction zone is the shock front or detonation wave moving with velocity, D , through the unreacted explosive. Let us represent the quantity of solid explosive in the reaction zone in terms of mass fraction. Accordingly, at the front of the reaction zone the mass fraction is unity (all unreacted explosive and no reaction products); at the rear of the reaction zone the mass fraction is zero. The steady state condition is when the velocities of the front and rear of the reaction zone are equal.

*References 3, 6, 27, and 30.

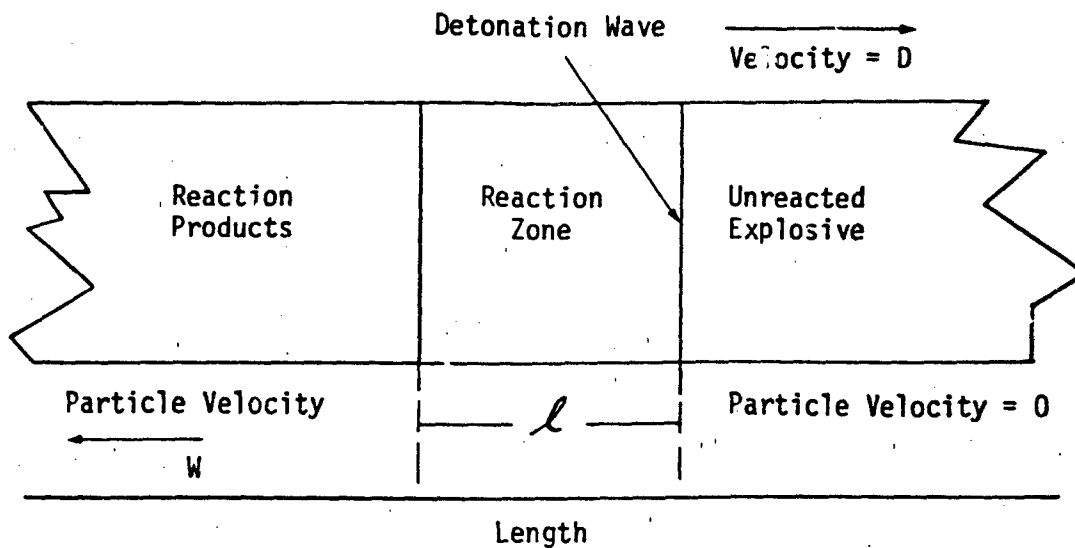
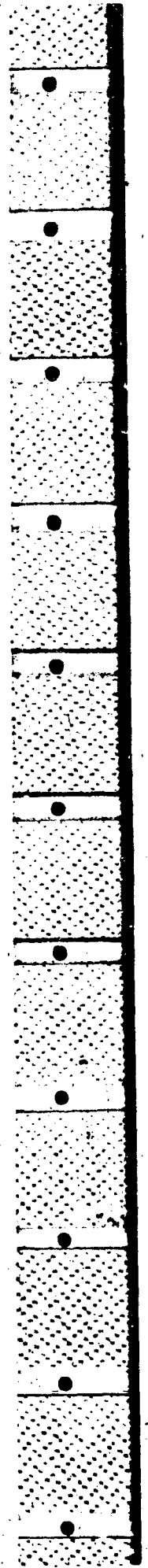


FIGURE A-1. SCHEMATIC REPRESENTATION OF ONE-DIMENSIONAL DETONATION.

Figure A-2 illustrates typical steady-state reaction zone profiles. These are not for ANFO but should assist in clarifying the preceding paragraph. The lower profile shows how mass fraction varies in the reaction zone which has a dimension of 580A. The center profile illustrates temperature variance being highest where the reaction is complete and dropping sharply to about ambient temperature at the front of the reaction zone. The upper profile shows detonation pressure which is essentially ambient pressure, P_0 , ahead of the reaction zone and is a maximum (P_1) at the detonation front.



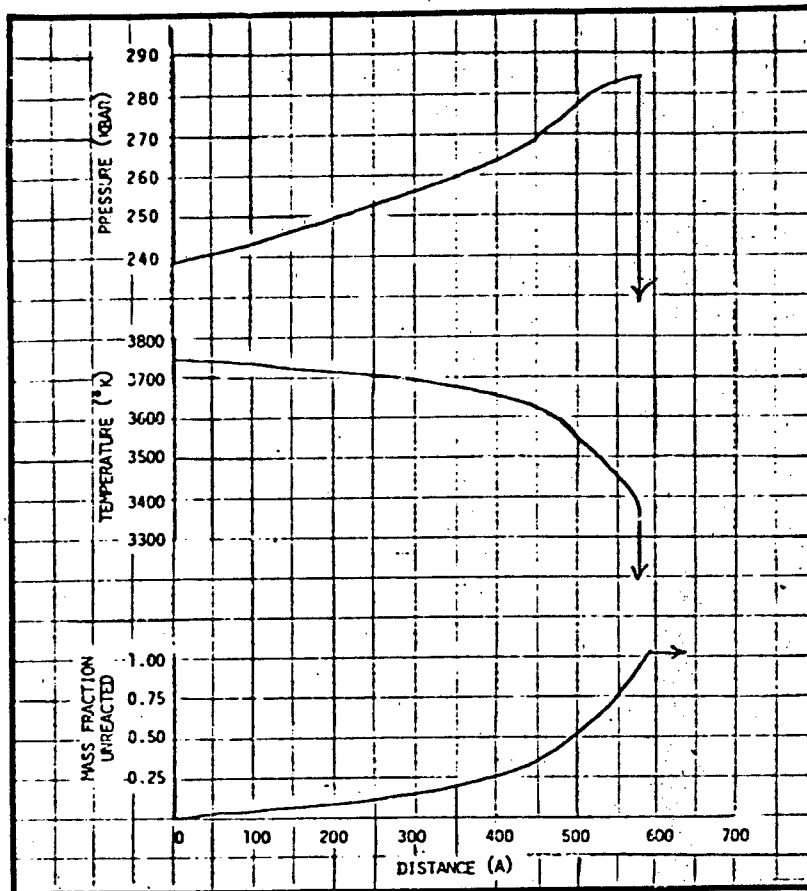


FIGURE A-2. STEADY-STATE REACTION ZONE PROFILES.

The gaseous products expand adiabatically at constant entropy to pressure, P , and specific volume, V . Applying the laws of conservation of mass, momentum and energy across the shock front for the steady-state condition gives the well-known Hugniot equation:

$$E - E_0 = \frac{1}{2} (P + P_0)(V_0 - V) \quad (A-1)$$

where:

E_0 = specific energy of solid explosive at P_0, V_0
 E = specific energy of reaction products at P, V

Figure A-3 illustrates Hugoniot curves describing the chemical reaction in pressure-volume plane. The point (P_0, V_0) represents the unreacted explosive ahead of the reaction zone. At the rear of the reaction zone are the reaction products (P_2, V_2) which expanded isentropically from the compressed explosive at P_1, V_1 . These points are colinear under steady-state conditions since the velocities of the front and rear of the reaction zone are equal and define the Rayleigh line for a steady-state condition.

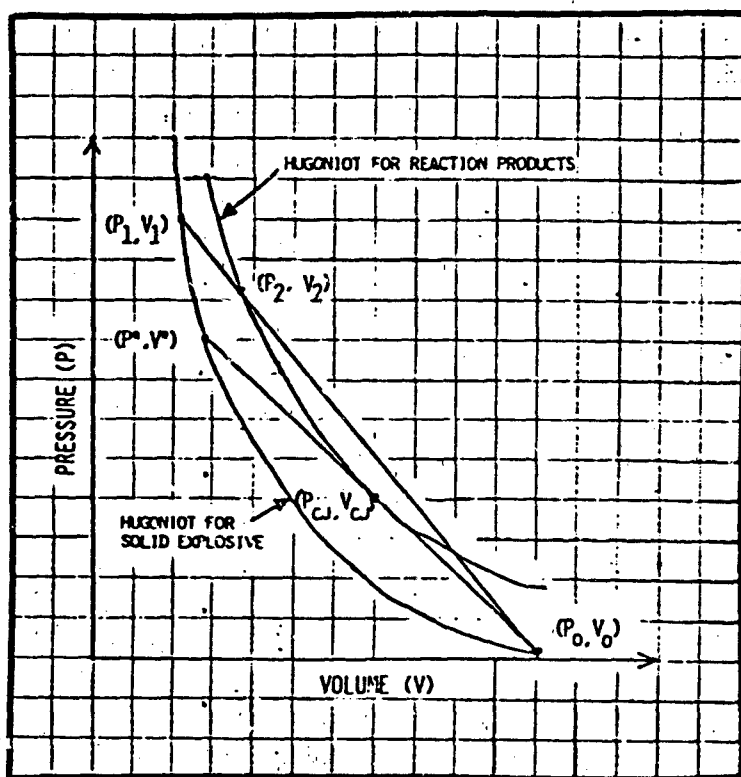


FIGURE A-3. REPRESENTATION OF EXPLOSIVE DETONATION IN THE PRESSURE-VOLUME PLANE.

Still referring to Figure A-3, we differentiate equation (A-1) to describe the energy change along the Hugoniot for the products:

$$\left(dE = \frac{1}{2} (V_0 - V) dP - (P + P_0) dV \right) \quad (A-2)$$

Substituting the first law of thermodynamics, $dE = TdS - PdV$; gives:

$$T \left(\frac{dS}{dV} \right) = \frac{(V_0 - V)}{2} \left[\left(\frac{dP}{dV} \right) - \left(\frac{P - P_0}{V - V_0} \right) \right] \quad (A-3)$$

Noting that $(P - P_0)/(V - V_0)$ is the slope of the straight line for an adiabat, then another straight line through P_0, V_0 which is tangent to the Hugoniot of the reaction products corresponds to the Chapman-Jouget (CJ) point where entropy(s) is a minimum.

By convention the negative of the logarithmic slope of an adiabat is defined as:

$$\gamma = - \left(\frac{\partial \ln P}{\partial \ln V} \right)_S = - \frac{V}{P} \left(\frac{\partial P}{\partial V} \right)_S \quad (A-4)$$

which we substitute into equation (A-3) at constant entropy:

$$\gamma = - \frac{V}{P} \left(\frac{P - P_0}{V - V_0} \right) \quad (A-5)$$

Since P_0 is negligible compared to P , the following well-known CJ relations can be derived:

$$\gamma_{CJ} = \frac{V_{CJ}}{V_0 - V_{CJ}} \quad (A-6)$$

$$P_{CJ} = 2 \frac{\rho_0 D_{CJ}^2}{\gamma_{CJ} + 1} \quad (A-7)$$

$$D_{CJ}^2 = \frac{P_{CJ} (\gamma_{CJ} + 1)}{\rho_0} \quad (A-8)$$

Calculation of the Hugoniot curve from equation (A-1) requires knowledge of the equation of state for the reaction products. The usual procedure is to apply some empirical equation of state in which the values for parameters are chosen to achieve the best possible agreement with experimental data. Detonation velocity is an especially important parameter.

Gaseous equations of state (EOS) have the general form:

$$\frac{PV}{\sum n_i RT} = \phi(T, V, n_i) \quad (A-9)$$

where P is pressure, V is volume, R is the Universal Gas Constant, T is temperature, n_i is the number of moles of the i th product, and ϕ is a compressibility factor. For products behaving as ideal gasses, ϕ is unity and:

$$PV = \sum n_i RT \quad (A-10)$$

But for explosive reactions, no gaseous product behaves as an ideal gas; the compressibility is not a constant but varies with T and V.

The Becker-Kistiakowsky-Wilson (BKW) EOS is given by the following:

$$PV/RT = 1 + X e^{\beta X}$$

where:

$$X = \frac{\eta \sum n_i k_i}{V(T + \theta)^\alpha} \quad (A-11)$$

and where α , β , η and θ are constant parameters determined by fitting the EOS to experimentally obtained velocity and pressure data. The k_i 's are the covolumes for the various gaseous products.

The virial EOS is yet another formulation for gaseous materials which considers interactions between the molecules of various gaseous products formed. For the virial EOS:

$$1 + \frac{B(T, n_i)}{V} + \frac{C(T, n_i)}{V^2} = PV/RT \quad (A-12)$$

In this formulation $B(T, n_i)$ and $C(T, n_i)$ are the second and third virial coefficients accounting for bimolecular and termolecular interactions, respectively:

$$B(T, n_i) = \sum_i \sum_j B_{ij}(T) n_i n_j$$

$$C(T, n_i) = \sum_i \sum_j \sum_k B_{ijk}(T) n_i n_j n_k$$

Another EOS is worthy of mention because of its past application to ANFO. This is the Jones-Wilson-Lee (JWL) equation of state which takes the form:

$$P = A \left(1 - \frac{\omega}{R_1 V} \right) e^{-R_1 V} + B \left(1 - \frac{\omega}{R_2 V} \right) e^{-R_2 V} + \frac{\omega E}{V} \quad (A-13)$$

In the JWL EOS, A , B , R_1 , R_2 , and ω are constants determined empirically; V is the relative volume - the ratio of the volume of gaseous products to the volume of unreacted explosive.

There are other forms for an EOS and it is not the purpose of this history to select the best. For C-H-N-O explosives, however, perhaps the BKW EOS has been the most widely used, historically.

SECTION 3
CHARGE DESIGN AND CONSTRUCTION

3.1 INTRODUCTION

The objective of this section is to present a comprehensive description of the design and construction of ANFO charges as used to date. The features and factors that influenced the design will be covered as well as the operational and safety considerations that influenced the construction. Many of these items have been mentioned or discussed in the first two sections of this report; some will be repeated here for continuity but frequent reference will be made to these earlier sections to avoid excessive repetition.

This section may be considered to be the field engineers "User's Guide" because it covers the subject matter from ANFO procurement to charge design to construction to the final arming and firing of the charge. As with any "guide," however, it is useful to know the bases for the guidelines so that new situations can be faced and handled with confidence; these bases are provided in detail in Sections 1 and 2.

3.1.1 ANFO Procurement

There are many manufacturers throughout the United States and overseas who prepare explosive grade AN and ANFO; Table 2-2 lists some of them. Both AN and ANFO are available in bulk form and in 50 lb water resisting bags. Depending on the size and geometry of the charge, either bagged or bulk ANFO may be preferable.

The specifications for 600 tons of bulk ANFO to be used on DIRECT COURSE in 1983 are typical of what is desired. The following items are cited from the procurement document:

"2. The ANFO shall have THE FOLLOWING SPECIFICATIONS:

<u>COMPOSITION</u>	<u>WEIGHT (%)</u>
"Explosive" Grade Prilled Ammonium Nitrate	94.0
No. 2 Diesel Fuel Oil	6.00

Tolerance: No. 2 Diesel Fuel Oil -0.25 to +0.75

(i.e., the percentage of No. 2 Diesel Fuel Oil may vary between 5.75% and 6.75%.)

BULK DENSITY: 0.77 g/cc Minimum. 0.84 g/cc Maximum.

GRANULATION:

<u>SCREEN SIZE</u>	<u>SAMPLE WEIGHT PASSING THRU THE SCREEN (% OF TOTAL)</u>
#6	100%
#14	no greater than 20%
#20	no greater than 2%

3. GENERAL:

The ANFO will contain phase-stabilizing ingredient(s), anti-caking agent(s), and oil soluble colored dye. Mixing of the Diesel fuel oil and explosive grade ammonium nitrate shall be no sooner than 72 hours prior to delivery to the DIRECT COURSE test site, White Sands Missile Range, New Mexico.

4. ANFO PACKAGING:

The ANFO shall be provided in bulk form and must not have been exposed to excess moisture between mixing and delivery.

5. ANFO QUALITY ASSURANCE:

The contractor shall sample each lot. The sampling frequency shall be at least every 10,000 lbs. A fuel oil analysis (i.e., determination of the fuel oil percentage) and a particle size analysis shall be performed using the following screen sizes: #6, #14, and #20. A certified copy of the results of both the fuel oil and particle size analysis shall be provided with each shipment in the format attached. At Government's option, observation and checking of the ANFO mix to assure compliance with specification may be performed at the manufacturer's plant, and at point of delivery. If any of the samples are not within the tolerances given above, upon delivery the lot/shipment will not be accepted."

Examining the specifications item by item, explosive grade prilled AN is called for because this type prill has the proper physical characteristics for oil absorption; agricultural grade prills are too hard and retain oil only as

a coating thus forming a non-homogeneous ANFO prill. About 6 percent by weight diesel oil is specified; this is the amount required for a maximum output ANFO performance. However, considering that there may be some loss of oil because of evaporation, it may be advisable to specify 7 (+ .25, -1.0) percent oil. A 93/7 ANFO still has close to the maximum output; with evaporation towards a 6 percent figure, the ANFO will attain its full potential. The bulk density and granulation specifications are appropriate goals for good detonability and energy output; they will tend to assure a total charge density of approximately 0.90 g/cm^3 . For charges in the 100 ton and larger range, compaction of the ANFO in the lower portions of the charge raises the average total charge density from the emplacement density.

The phase stabilizing ingredients and anti-caking agents are necessary to inhibit excessive prill volume changes and possible break up that may occur when the ANFO is exposed to wide temperature variations, and to inhibit moisture absorption. These additives, such as Barnette Clay or Petro-AG, enhance the free running of the prills to facilitate handling; they should be less than 2.5 percent of the prill weight, otherwise they will adversely affect oil absorption into the prill.

It is important that the ANFO be freshly prepared because of the oil evaporation problem. Getting freshly mixed ANFO is no problem however, because many plants have hundreds of tons per day capacities and with the plants distributed throughout the country, transit time from plant to test site can be a matter of only hours or a day. The longest time interval from manufacture to detonation will occur usually in building and firing the charge. Depending on many factors, e.g., size of charge, availability of personnel and equipment, and weather conditions, this time may be measured in weeks. The blasting industry seldom is faced with these long delays; they mix the AN and FO on site or use the mixed material immediately upon arrival from the plant. The important point is: minimize the time between ANFO preparation and charge firing. If the AN and FO are to be mixed on site, as has been done on some of the earlier development shots, there are no particular rules or concerns about deterioration with time so long as the AN and FO remain unmixed.

The ANFO packaging (and AN packaging when on site mixing is to be done) must be such as to preclude exposure to rain in order to prevent dissolution or caking of the prills. The 50 lb bags are usually of multi-wall, non-oil absorbing paper construction with valve type closures. For bulk transport in train hoppers or truck trailers adequate protection against the elements must be provided. With the strong hygroscopicity of ANFO, it bears emphasis that in storage and during construction of the charge, the AN and ANFO should be shielded from rain.

Serious attempts should be made to provide adherence to the ANFO specifications. As a review of Table 2-5 indicates, this has not been done successfully on some of the test shots; much variation in fuel oil content, particularly, is evident. This variation is found not only from charge to charge, but within a given charge. Although the full significance of these intra-charge variations is not known, they do constitute inhomogeneities and therefore could lead to detonation wave and blast wave perturbations or anomalies.

Table 3-1 outlines one of the procedures and the equipment used by Swisdak (NSWC) to ascertain the FO content; this technique can be used at the mixing plant and at the test site. Since the sampling technique provides only spot check information, it is important to monitor the FO content of ANFO on a continuous basis during the mixing process. This is done visually. At the correct percentage of FO, 6-7 percent, the ANFO has a pink color resulting from the addition of a red dye such as DuPont Oil Red B Liquid to the diesel oil. Color variations in the ANFO indicate FO percentage variations; when these occur, the mixing process should be checked and adjusted to provide the proper color and hence, the specified FO content.

To assure compliance with the specifications, the DIRECT COURSE Contracting Officer is using a certification sheet such as shown in Table 3-2; this is a recommended technique.

3.1.2 ANFO Safety

ANFO has important characteristics which make it one of the safest products available for nuclear blast simulations. There are a number of excellent publications which define the hazards of ammonium nitrate and ANFO.

TABLE 3-1 TEST METHOD USED TO DETERMINE AMOUNT OF NO. 2
DIESEL FUEL IN AN/FO MIXTURE

EQUIPMENT:

- 1 - Balance Scale
- 3 - Beakers
- 3 - Sintar Crucibles

METHOD:

1. Weigh beaker and record weight. Add 20 grams of AN/FO mixture and record weight.
 2. Pour Petroleum Ether over AN/FO mixture in beaker and decant--do this three times.
 3. Pour material in Sintar Crucible and allow to dry for 1 1/2 hours.
 4. Pour material into beaker and weigh--record weight.
 5. Deduct weight of beaker and record.
 6. If using 6 percent fuel oil, the weight removed should be 1.20 grams for 20.00 grams of AN/FO.
-

TABLE 3-2 CERTIFICATION OF FUEL OIL AND PARTICLE SIZE ANALYSIS

Date: _____ Shipment No. _____ Lot No. _____

Each 10,000 lbs of this shipment was tested for the percentage (by weight) of No. 2 Fuel oil in the ANFO mix and for particle size distribution.

% Fuel Oil	% of Total Sample Retained on Screen Size		
	#6	#14	#20

1st 10,000 lbs
 2nd 10,000 lbs
 3rd 10,000 lbs
 4th 10,000 lbs
 5th 10,000 lbs
 etc.

I certify that the foregoing findings are true and correct.

SIGNED

These publications contain recommendations for safe preparation, storage, transportation and use. Three such publications are listed below.

- (1) National Fire Protection Association, Manufacture, Storage, Transportation and Use of Explosives and Blasting Agents, NFPA No. 495, 1973.
- (2) Bureau of Mines Information Circular, Safety Recommendations for Ammonium Nitrate Based Blasting Agents, IC 8746, 1977.
- (3) Institute Makers of Explosives, Suggested Code of Regulations for the Manufacture, Transportation, Storage, Sale, Possession and Use of Explosive Materials, Publications, No. 3, 1974.

Test plans published by Field Command DNA for HE events contain a long list of general safety publications including Army TBs, DARCOM regulations and DOT regulations. Although a detailed treatment of all aspects of safety is beyond the scope of this document, some information is appropriate for inclusion herein.

Ammonium nitrate is classified as an oxidizer by the Department of Transportation provided it has less than 0.2 percent carbon content. It may be transported in accordance with DOT Specifications concerning marking as an oxidizer. Although it is not an explosive, under the right stimulus it can react violently and even detonate (see Sections 1.2.i and 2.2).

ANFO is classified as a blasting agent, not as an explosive. Paragraph 73.114 of the DOT Specifications defines blasting agents. Generally, they must pass several tests including blasting cap sensitivity, differential thermal analysis, thermal stability, electrostatic sensitivity, impact sensitivity, and a fire test. The tests are designed to insure that the candidate blasting agent is so insensitive that there is very little probability of accidental initiation to explosion. ANFO is inactive with most elements and compounds. However, it is reactive with pyritic ores at temperatures over 240°F. This combination can create temperatures in excess of 1500°F. ANFO has a certain dust explosion hazard in confined areas; electrical equipment should conform to explosive safety requirements. Fumes from recently manufactured ANFO are not a concern; however, post-detonation gases in confined underground locations must be considered. In open, aboveground areas post-detonation gases are not an operational concern except for environmental impact assessments. Caked ammonium nitrate or ANFO should never be broken up using other explosives. ANFO's sensitivity is a function of its fuel oil content. A 2 percent fuel oil content is the most sensitive combination. Above 8 percent fuel oil ANFO becomes very insensitive.

Remember: although ANFO is classified as a blasting agent, not as an explosive, the line between the two is very fine. For safety reasons, ANFO must be accorded all the respect and care normally given to high explosives.

3.1.3 Bagged versus Bulk ANFO

Bagged ANFO has been used in more large charge applications than bulk ANFO to date for a variety of reasons having to do with cost, blast performance, and certain test objective considerations. Charges built with bagged ANFO may be less expensive than those using bulk ANFO. The price for bulk ANFO is less than that for bagged, but in addition to the ANFO costs, several other factors have to be considered in determining total charge costs. For bag built charges, the cost of stacking and the cost of a temporary protective structure used during stacking has to be included; for a charge using bulk ANFO, the cost of the container has to be added. Depending upon the size of the charge, there may be a crossover in the cost of bulk built versus bag built charges because of the difference in labor costs; the bagged charges require intensive labor, the bulk charges can utilize mechanized loading procedures. Thus, for very large charges, the labor costs for bagged construction may outstrip the container costs for bulk charges.

Another consideration in determining whether bagged or bulk ANFO should be used in charge construction is the blast performance of the charge. Bagged charges provide cleaner airblast waves with fewer anomalies -- jetting and protuberances in the wave front -- than bulk ANFO charges which are contained within some case. For operational and safety reasons, thick, massive cases should be avoided because of the frequent hazard to test equipment and personnel, but even the relatively light fiberglass cases used on several operations have resulted in blast anomalies.

During the development phase of ANFO for nuclear blast simulation, NSWC (Reference 1) conducted tests to determine the response of fiberglass when in intimate contact with an explosive. A 1.5 inch diameter, 0.16 inch thick sample of fiberglass was butted against a 1.5 inch diameter, 7 inch long stick of pentolite; high speed photographs were taken of the explosion. Interpretation of the records led to the conclusion that the fiberglass completely burned in about 2 inches of its travel under the explosion forces. This conclusion was reinforced by the fact that no pieces of the material were found after the test. On ANFO Events II and III, where the fiberglass containers had wall thicknesses of 0.19 and 0.25 inches respectively, it is assumed that the cases were similarly consumed by the explosion; no fiberglass

pieces were found. It may be that the anomalies observed in these two tests and on the subsequent pre DIRECT COURSE shot, were induced by the overlapping joints required to construct the case. It is concluded, therefore, that in light of the current experience and design of cases, where feasible, bagged construction is preferable.

Test objective considerations, aside from the aforementioned anomaly free blast wave requirement, can favor bagged construction over bulk cased charges. For example, to simulate nuclear weapon induced ground shock, the pre MINE THROW charge was ellipsoid in shape; bags of ANFO lined a pre-excavated ellipsoidal shaped cavity in the ground (see Section 1.3.3). This shape would have been difficult and expensive to attain with a cased charge.

Cased charges, however, have their uses and merits. For unusual shapes and for very large charges with large L/D ratios, it may be necessary to containerize the ANFO; the container would afford structural stability and strength to the completed charge not attainable by simply stacking bags. Cased charges also provide better rain and moisture protection to the contained ANFO than the bag material, provided, of course, that the loading port is covered during inclement weather. Another advantage of containers is that ANFO loading can be more mechanized requiring less fatiguing, back breaking labor than is needed for bagged construction.

All in all, the use of bagged or bulk ANFO should be determined by the test requirements.

1.1.4 Handling ANFO

Explosive grade AN prills and ANFO are friable; care must be taken in handling to prevent excessive prill breakup because too many small size prill fragments tend to increase the bulk density of the material and thereby change the detonation characteristics. In the 50 lb packaging, the package itself provides some protection against breakage during handling. In building a bagged charge, the amount of tramping on the layers should be limited to that necessary for bag emplacement. Conveyor belts are convenient labor saving devices for moving the bags from the truck in which the ANFO is delivered to the test site to the charge site; the conveyor also helps in keeping traffic off the emplaced bags.

Handling of the bulk ANFO (or the AN prills if on site mixing is to be used) can be accomplished by means of augers, i.e., screw or spiral conveyors, grab type buckets, or pneumatic transport systems. Augering is usually a slower process than bucket or pneumatic transport of material unless several augers are used. For moving ANFO, the auger screw helix is about 3 inches in diameter and is housed in a rigid rubber tube. This construction precludes detonation run-up through the auger should the ANFO be initiated to detonation accidentally. Screw conveyors can move ANFO to about a 200 ft distance provided the inclination of the auger is no more than 35°; at 35° the reduction in capacity is 78 percent compared to that at a horizontal position.

Buckets of large capacity, e.g., from 3/4 to 12 yds³, are ideal for moving large quantities of ANFO during charge construction. Prill break up is minimal and a uniform loading density can be attained if the prills are rained into a charge container from moderate heights.

Pneumatic loading is another method for moving large quantities of ANFO at relatively high speeds. Depending on the loading rate which is determined by the air pressure driving the system, greater prill break up may occur leading to higher bulk densities with the pneumatic system than with the other methods discussed. Also, there is a height limit to which prills can be raised without the use of a booster pump which will tend to exacerbate prill break-up. There is one other concern with pneumatic loading: a static electric charge can build up during pneumatic placement which, of course, can be an explosive hazard. And the faster the ANFO stream velocity, the larger may be the static charge. This charge build up may be a serious concern particularly when AN and ANFO are being pneumatically emplaced in a low humidity environment such as at White Sands, New Mexico and when detonators are emplaced in the charge during its construction, e.g., DICE THROW. The Bureau of Mines publication RI-7139, "Electrification of Ammonium Nitrate in Pneumatic Loading," covers this subject and offers recommendations on ways to minimize the hazard.

Several of the handling techniques can be used on a given operation, as was done for example, on the pre-DIRECT COURSE 20 ton height-of-burst event in October 1982 at WSMR. The bulk ANFO was produced at the manufacturer's plant and trucked to WSMR. The ANFO was then pneumatically blown into a large hopper for temporary storage. From the bottom of the hopper, it was moved by conveyor

elt to a cement bucket which was hoisted by crane to the top of the tower supporting the fiberglass spherical charge container. The ANFO then was dumped into a smaller loading hopper, which had a flexible hose down into the sphere. The ANFO was directed throughout the interior of the sphere by a man inside the sphere controlling the hose. Plans for loading the bulk ANFO into the 600-ton main event for DIRECT COURSE are to repeat the pre-DIRECT COURSE procedures.

2 CHARGE DESIGN

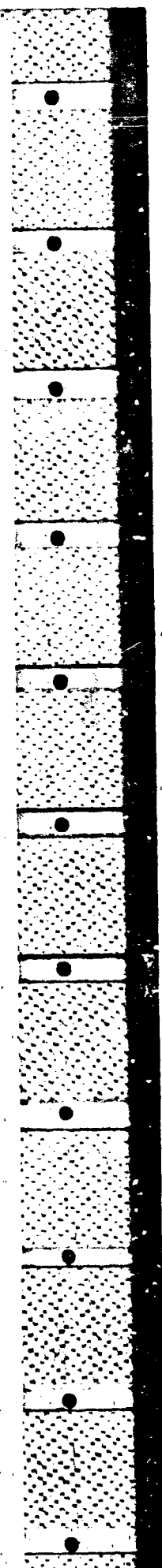
Bagged ANFO because of its pliability, and bulk ANFO because of its pourability, offer a variety of geometries in which a charge can be formed. This flexibility in design has been demonstrated in the development and nuclear weapons simulation test programs. Bagged ANFO has been used in the following charge shapes (on the parenthetically set off shots): hemisphere (ANFO I), sphere (ANFO IV), ellipsoid (pre MINE THROW), and domed cylinder (DICE THROW). Bulk ANFO has been used in hemispherical (ANFO II) and spherical (pre-DIRECT COURSE) shapes and in planar arrays of bore holes (DIHEST).

ANFO charges for airblast simulation with above ground unconfined shots should have a minimum weight of at least 1,000 lbs and a minimum dimension of from 2.5 to 3.0 ft so that full blast output can be attained. Lesser weights and sizes will produce results that are not amenable to scaling to larger charges. Where the ANFO is loaded into bore holes or cavities in the ground, lesser sizes can be used; the confinement provided by the ground material serves to assure full shock output.

2.1 Bagged Design and Construction

Bagged charges have been built to the desired geometries by stacking the bags layer upon layer. There are three basic features in this charge design that should be observed: 1) avoid air pockets within the charge; 2) provide a smooth outer contour to the completed charge; and 3) have structural integrity to the stack so that it is self standing.

It will be recalled (Section 1.1.7) that blast anomalies were ascribed to homogeneities in block built TNT charges. This led to the search for a new explosive for simulation work with the result that ANFO was developed. The rectangular bags of ANFO, even though pliable, cannot be laid and stacked without having air spaces between adjacent bags. These spaces have to be



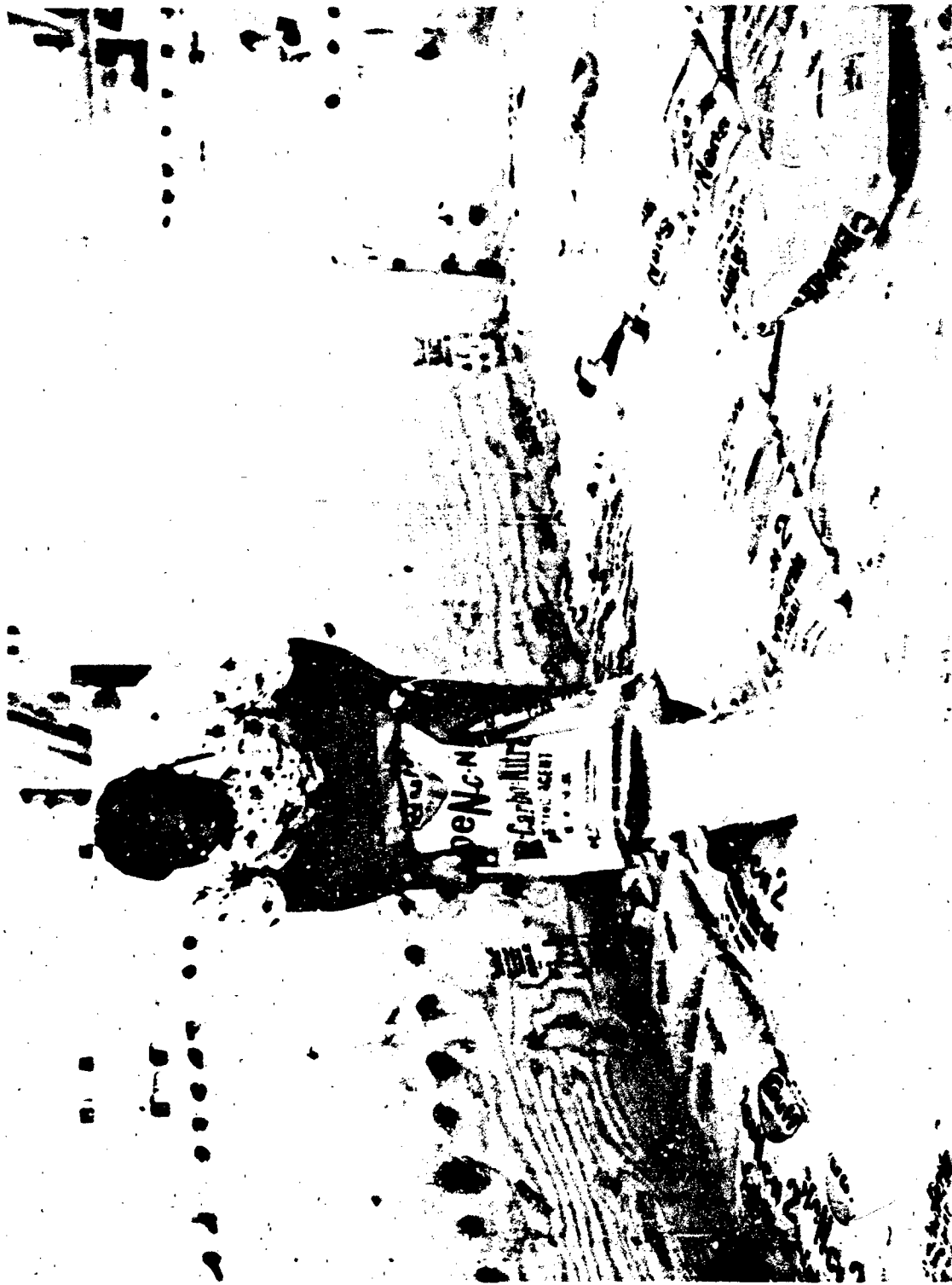


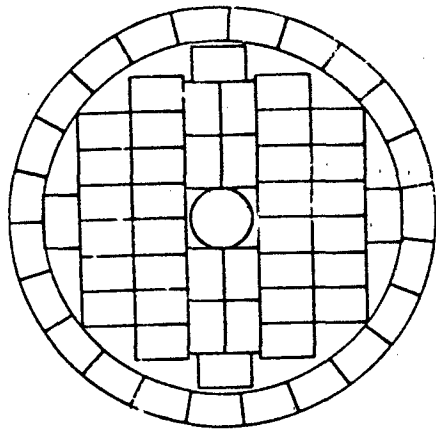
FIGURE 3-1. FILLING VOIDS WITH BULK ANFO (DICE THROW).

carefully filled with loose, bulk ANFO (as demonstrated in Figure 3-1) so that homogeneity is achieved in the charge material. (The inhomogeneity introduced by the bag material itself has not been addressed; apparently it has no significant influence on charge performance.) Another source of air pockets may be found in improperly or incompletely filled bags; an ice pick puncture of the bags will eliminate this entrapped air.

Again, recalling TNT block built experience, another possible source of blast anomalies is thought to be the many reentrant corners at the surface of the charge. The bag layout design should call for the outer bags to be butted one against the other so that a smooth contour is attained (Figure 1-32). This is difficult to do with 50 lb bags for charges less than about 5 ft in radius, but for larger charges the bags are sufficiently pliable so that the desired smooth contour can be attained (Figure 1-18). For smaller charges, the ANFO can be packaged in smaller bags; on pre-DICE THROW I-4, a 6-ton charge with a radius of 3.2 ft, 15 lb bags of ANFO were used (Figure 1-30).

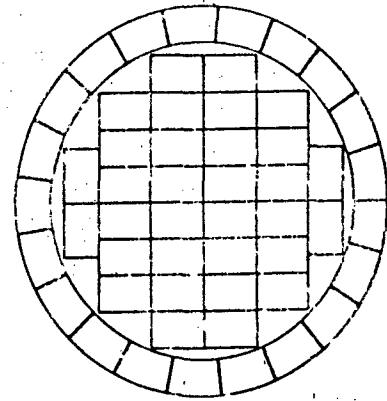
Structural integrity of the bagged built charge is necessary for operation best requirement and safety reasons. The structure must be stable during construction withstanding the traffic of the bag laying crew and the forces of wind and rain. For hemispherical charges and for relatively small domed cylindrical charges, the bag layer design shown in Figure 3-2 has proven adequate. For domed cylindrical charges of 120 tons and larger, however, a different design has been found necessary (see Section 1.4.5). Two procedures have been followed to achieve structural strength. In one, the outer two bags around the circumference of each layer were glued to prevent slipping. The glue used was Plycrinyl Acetate Emulsion Adhesive (Gulf Lot #B-3252). In the other, interlocking strength to the stack was provided by the layer design shown in Figure 1-34. As each layer was added the design remained unchanged except that the bag line was changed 45°. This new design sacrificed the smooth exterior desired but test results indicated that no anomalies could be ascribed to this rough surface.

In constructing the bagged charges, it is useful to use a template or removable form to guide and check the shape. On DICE THROW, circular plywood forms were used around the exterior of the stack to insure that the stack was circular and vertical (Figure 3-3). However, even a form does not guarantee



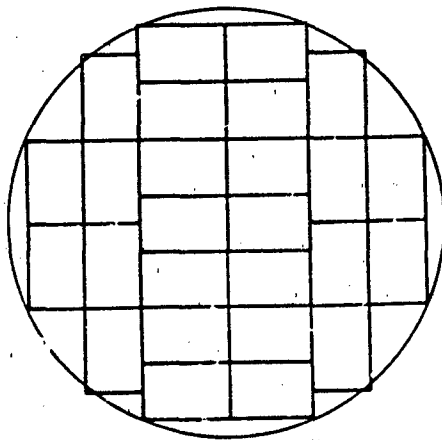
Layer 1 & Layer 2, R = 7.11"

63 Full Bags
 17 Bags Bulk
80 Total Bags



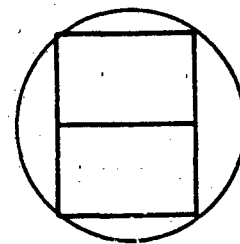
Layer 7, R = 6.40'

53 Full Bags
 12 Bags Bulk
65 Total Bags



Layer 12, R = 4.50'

26 Full Bags
 6 Bags Bulk
32 Total Bags



Layer 15, R = 1.51'

2 Full Bags
 2 Bags Bulk
4 Total Bags

FIGURE 3-2. STACKING PLAN FOR ANFO I.

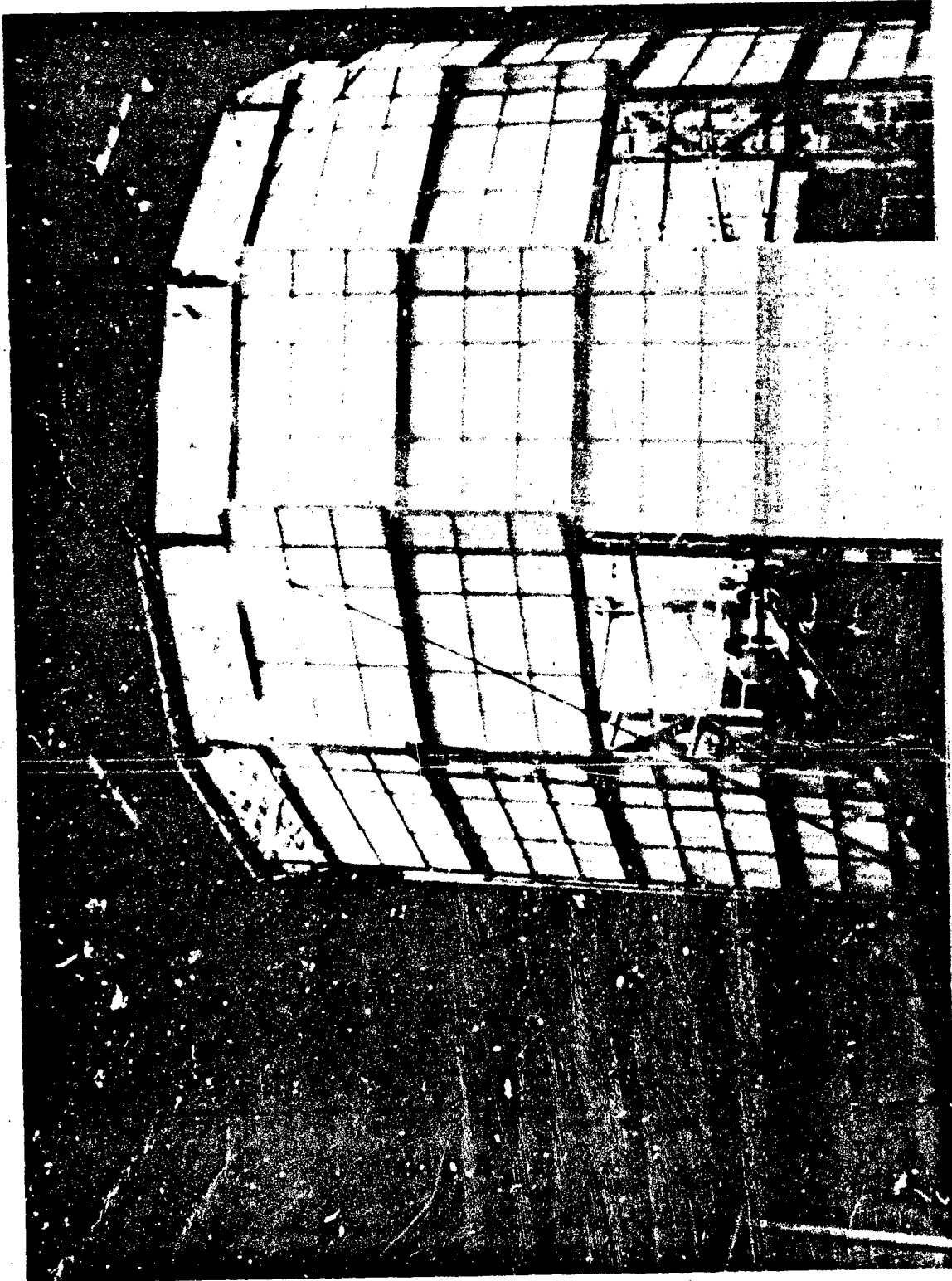


FIGURE 3-3. PLYWOOD FORM AND PROTECTIVE HOUSING FOR DICE THROW.

the attainment of the desired shape. On DICE THROW it was found upon removing the form from around the completed charge that the lower portion of the charge had expanded; at the base those bags that were originally spaced six inches from the form were now in contact with it. The hydrostatic load on the lower portions of the charge caused this expansion. Needless to say, this change in the cylindrical geometry of the charge to a frustrum of a cone complicated volume determinations. As a matter of fact, in order to keep the total charge weight at a nominal 620 tons, the dome of the charge was reduced in height by about 0.7 ft; thus, the desired hemispherical cap was no longer truly hemispherical.

Spherical bagged charges are constructed essentially in the same way as hemispherical and cylindrical stacks -- layered bags with loose ANFO filling the interstices between bags, layers rotated 45° one to the other, and gluing the outer bags. The bottom half of the charge is shaped by the hemispherical cavity formed in a supporting styrofoam base (Figure 1-25) or in the ground depending on the height-of-burst required on the test. The top half of the charge is constructed exactly in the same manner as a hemispherical charge.

Surveying techniques should be used to ascertain all completed stack dimensions. And as discussed earlier, it is necessary to protect the bagged ANFO and the loose ANFO filling the interstices between bags against rain at all times. Well secured canvas tarpaulin or heavy construction-type plastic covers can provide this protection.

Hemispherical, spherical or squat domed cylindrical charges of any size may not present any structural strength problems in the charge itself if the gluing and layer rotation procedures are followed; however, detailed analyses should be made to insure a viable structure. For large charges with large L/D ratios, bag stacking plans may have to be revised or abandoned as not feasible; cased charges with bulk ANFO may be the solution.

3.2.2 Cased Bulk Design and Construction

Cased charges have the immediately obvious advantage that the charge shape and volume can be controlled to a better extent than those for free standing bagged charges. This is not completely true, however, because in the endeavor to keep the case material as light as possible (to avoid blast anomalies and a

fragmentation hazard), large cases may tend to change dimensions especially when loaded with large quantities of ANFO. Structural design features such as ribbing or thickened sections, can take care of this distortion to a certain extent.

For small cylindrical charges, the charge container can be formed with construction type heavy cardboard or thin masonite sheets. For larger charges, fiberglass has been used successfully. On ANFO II and III, 20 and 100 ton charges, 3/16 and 1/4 inch thick fiberglass was used. Eleven gores, fabricated with compound spherical curvature, were used for the ANFO II case, 22 similar gores for the 100 ton charge. The gores were overlapped about 3 inches and held together by nylon bolts and an epoxy resin adhesive (HYSOL C-A571). It is advisable to use steel bolts initially in the construction of the case; when the adhesive sets, these bolts should be replaced with the nylon ones. At the test site, precautions have to be taken not to contaminate the epoxy with dust or other foreign matter lest the adhesive does not bond properly.

In designing the ANFO II and III containers, NSWC used a conservative design (Reference 1). Paraphrasing from this reference, the hoop stress at the base of the container was considered to be the controlling factor in establishing the container strength. It was assumed that the ANFO would behave like a liquid and that the container was analogous to a pressurized sphere. The hoop stress was calculated using the following formula:

$$S_{\text{hoop}} = \frac{PR}{2t} \quad (3.1)$$

where S_{hoop} = hoop stress (psi)
 P = hydrostatic pressure (psi)
 R = container radius (inches)
 t = container thickness (inches)

The hydrostatic pressure was calculated using the equation:

$$P = \gamma H \quad (3.2)$$

where γ = ANFO density (lbs/inch³)
 H = maximum height of ANFO (inches)

Using these two equations, the hoop stress for the container of ANFO II was calculated to be 563 psi and for ANFO III 1,320 psi. These stresses are far lower than the 25,900 psi tensile strength measured on a 3/16 inch thick sample of the fiberglass used in the case construction. For a joint with a 3 inch overlap of gore sections (as was used for these containers) the shear stresses corresponding to the calculated hoop stresses were 36 and 110 psi. Tensile tests on the HYSOL C-A571 adhesive bonded lap gave a shear strength of 568 psi for bonding after 48 hours at 71°F and 50 percent R.H. Thus the lap joint adhesive system provided a safety factor of about 15 for the ANFO II container and 5 for the ANFO III container. The nylon bolts were added as a further safety factor.

For surface shots, the cylindrical or hemispherical container should be fabricated on level ground with sheets of one inch thick plywood as a base to which the fiberglass container can be securely fastened. A plastic sheet should cover the wooden base to prevent absorption of the oil from the ANFO. An opening of appropriate size has to be left at the top of the hemisphere to facilitate ANFO loading; the openings had approximate radii of 3 ft for ANFO II and 4.5 ft for ANFO III. The top of the charge is formed by grading the loose ANFO into the hemispherical shape.

Spherical charges have been designed in a number of ways. The lower half of the charge can be contained in a hemispherically shaped cavity in the ground as on ANFO V, or in a styrofoam form as on ANFO IV. Styrofoam construction has been used with 500 ton TNT spherical charges, e.g., DIAL PACK, so there is no reason to doubt the feasibility of this type of construction for 600-ton or larger ANFO charges. Either bagged or bulk ANFO could be used to fill the form; the top hemisphere for large charges could be built with unconfined, bagged ANFO in a manner similar to that used for hemispherical charges (see Section 3.2.1).

In contrast to this half container construction for a spherical charge, a full spherical case can be built. This was done by Mesa Fiberglass, Inc., Colorado for the 20-ton pre-DIRECT COURSE shot in October 1982. The nominal 12 ft diameter sphere was made up of 24 gore sections (Figure 3-4). To provide dimensional stability and structural rigidity to the sphere, the

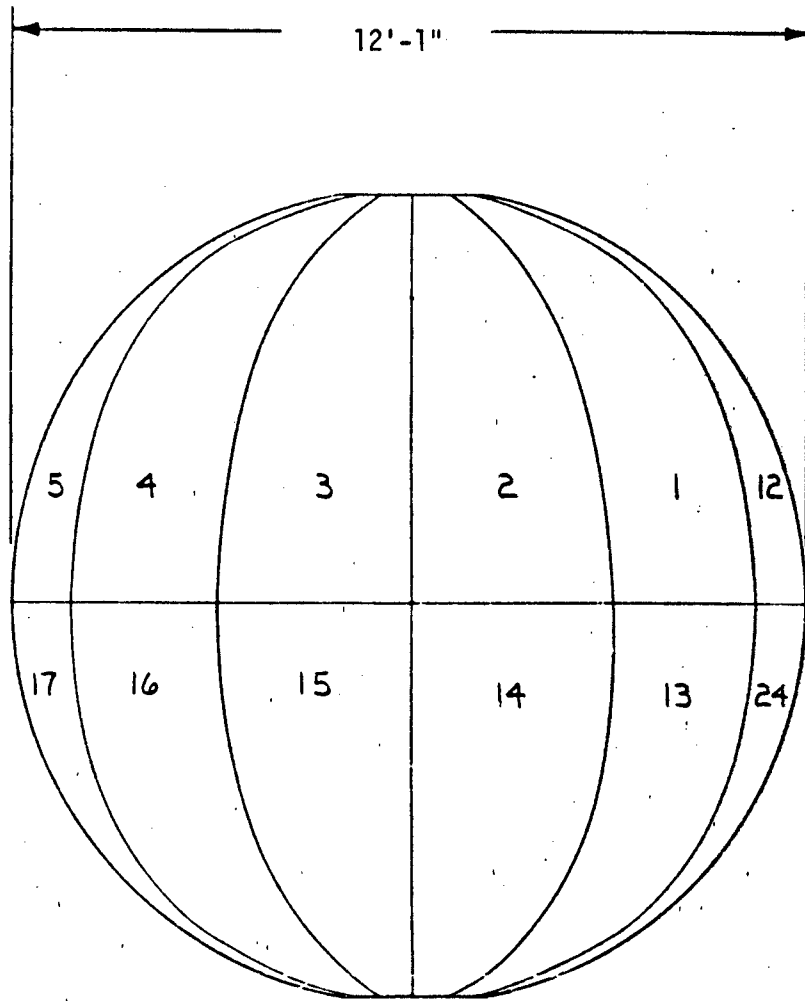


FIGURE 3-4. PRE-DIRECT COURSE SPHERE DESIGN.

sphere had a 2 inch thick wall made up of 1 1/2 inches of balsawood sandwiched between two layers of 1/4 inch thick molded fiberglass. The sections were butted together and held by fiberglass bolts through the 2 inch thick fiberglass seams.

This design was a compromise between the mechanical requirement for a strong container and the hydrodynamic precept for a minimal containment vessel to lessen the chance of producing airblast anomalies. Adding to the necessity for compromise and complicating the design was the requirement that this charge be detonated at a height of burst of approximately 57 ft. A tower and suspension system was designed to support the charge. As Figure 3-5 shows, the charge was suspended from the top of a steel tower in a polyester web net with a tower section going through the sphere. Recognizing the hazards of steel fragments and the disturbance to the detonation process introduced by the axial intrusion of the charge, the portion of the tower going through the charge was made of fiberglass in the hope that this would alleviate the worst conditions. Figure 3-6 provides details of the suspension system and ANFO loading arrangements into the sphere. Prior to the shot, everything above 75 ft, was removed from the structure.

The pre-DIRECT COURSE charge was fired successfully but at close-in distances, the blast was plagued with anomalies and perturbations particularly evident as originating at the 24 joints of the case. For DIRECT COURSE, scheduled for 1983, a design similar to that of the pre-DIRECT COURSE event will be used, but with modifications in construction to improve close-in blast performance. According to R.A. Flory, "the number of joints will be reduced from 24 to 16. The effect of this reduction when combined with the sphere size increase reduces the high density joint area from 25% (at the hemisphere) on Pre-DIRECT COURSE to less than 8% on DIRECT COURSE. Additionally, density of the joint when compared with the panel sections will also be reduced. In Pre-DIRECT COURSE, joints had an areal density of 16 pounds/foot² compared to 5.4 pounds/foot² in the panel sections or a 3 to 1 ratio. On DIRECT COURSE the joints will have an areal density of 18 pounds/foot² and the panels 11 pounds/foot² or a 1.5 to 1 ratio.... As a final note on the container, the ratio of container material mass to explosive charge mass may be the most

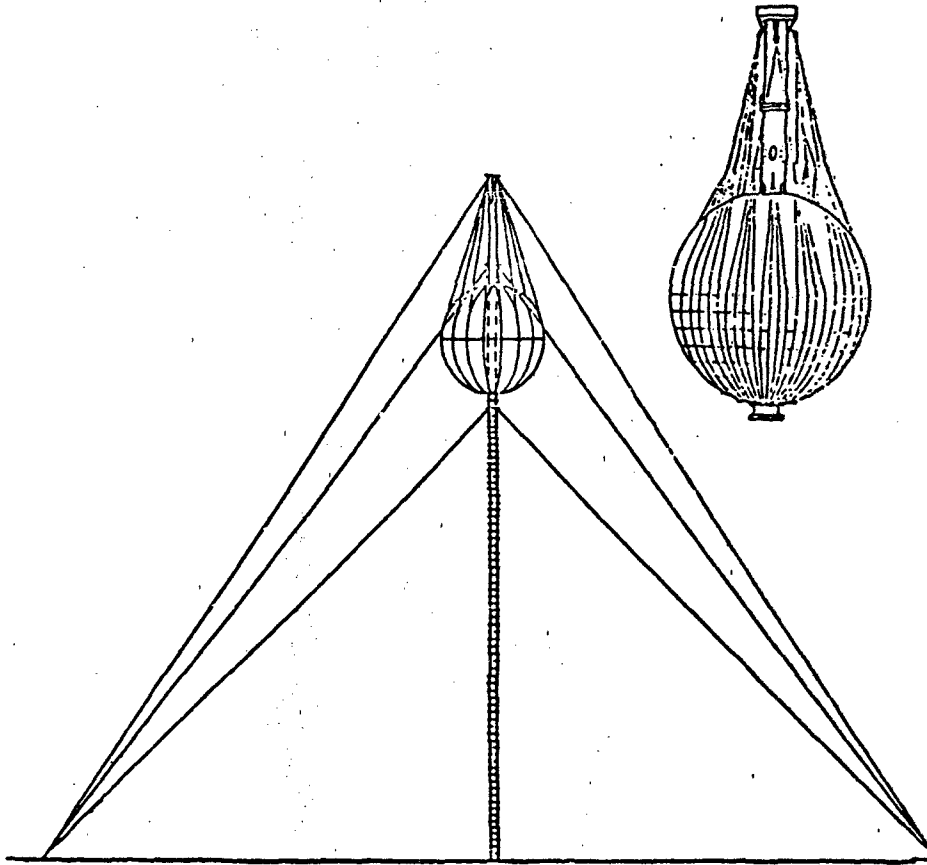


FIGURE 3-5. OVERALL TOWER DESIGN, PRE-DIRECT COURSE.

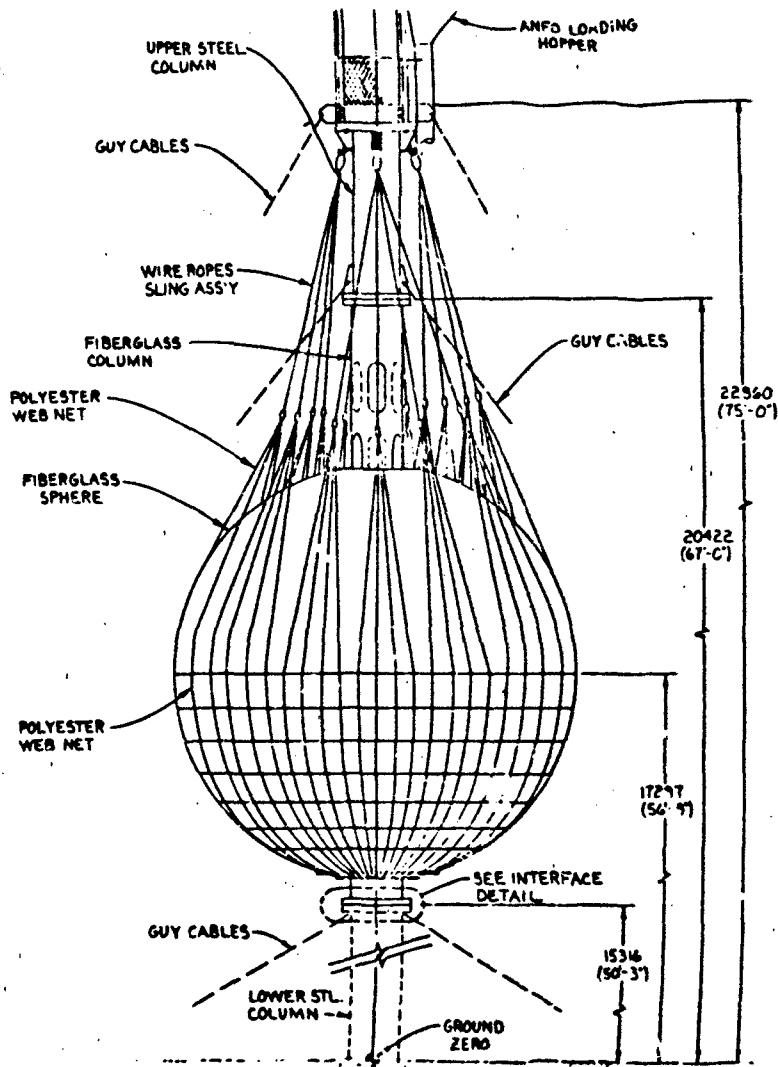


FIGURE 3-6. CHARGE SUSPENSION DETAILS, PRE-DIRECT COURSE.

meaningful. In pre-DIRECT COURSE the ratio was 2 tons of container for 23.02 tons of explosive or 8.7%. As presently planned the DIRECT COURSE container will weigh 20 tons compared with 600 tons of explosives for a ratio of 3.3%." (Reference 2)

Considering a shaped cavity in the ground as a container, ellipsoidal charges have been constructed and fired, e.g., in the pre-MINE THROW series (see Section 1.3.3). A cavity was excavated and lined with the required thickness of bagged ANFO (Figure 3-7); the size of the cavity was determined by the shock pressure desired at the charge/earth interface, and the thickness of the ANFO by the impulse required. Earth tamping was found necessary to attain the required impulse and multi-point initiation was used to produce a smooth detonation front at the interface. Ten pound bags with loose ANFO filling the spaces between bags further assured the generation of a proper detonation front.

As indicated earlier, cylindrical charges with large L/D ratios probably would require silo-like containers to provide structural stability. Guywires could be used to attain this stability. Very large and tall charges even with modest L/D ratios, may require a case. For example, a 6,000 ton domed cylinder with an L/D of 0.75 will be roughly 80 ft high. In bagged construction, the lower bags may burst under the hydrostatic load imposed by the stack; even if they did not, stable stacking would be questionable. So, depending on charge size, dimensions, test requirements, and economic considerations, containerized charges have their place in field test operations.

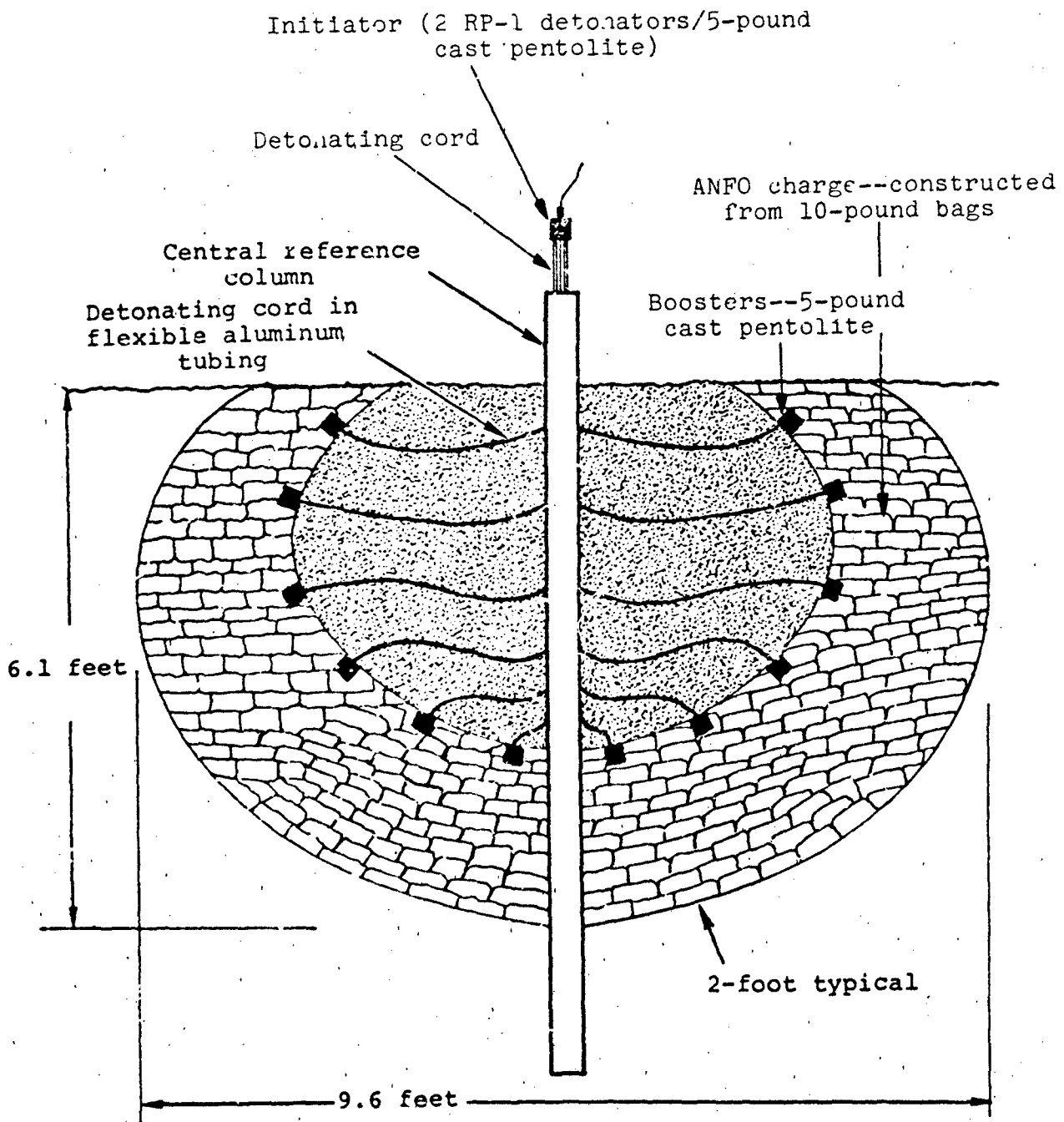


FIGURE 3-7. CONCEPTUAL DESIGN OF PRE-MINE THROW CHARGE.

3.2.3 Construction Times

Table 3-3 provides information on the number of manhours required to construct several of the larger tonnage ANFO charges. A marked decrease in time is shown for the bulk loading rate of ANFO III compared to ANFO II. This improvement is attributable to the experience gained in loading ANFO II. For this charge, the AN was transported in a 7 ton capacity mixer truck from a hopper car at a Suffield railroad siding about 35 miles from the test site. The FO was introduced to the AN in the mixer truck and the mixture augered into the fiberglass shell. For ANFO III, 22 ton loads of AN were delivered at a time directly to the ground zero site, mixed with the FO, and then augered into the shell (see Figure 1-17). This procedure reduced delays caused by transit times and made for an efficient loading operation. It took 5 men a total of 40 manhours to construct the case for ANFO II, and a crew of 8 working 64 manhours for the ANFO III case.

ANFO bagged stacking shows a similar history of more efficient operations as experience is gained; the MILL RACE 600-ton domed cylindrical charge was prepared in about 60 percent of the time it took to construct the first similar charge, DICE THROW. Construction times for peripheral structures such as forms and protective housings are not included in the time compilations. However, delays brought on by inclement weather and loading equipment malfunctions are reflected in the given manhours. The relatively fast loading rates shown for the DISTANT RUNNER charge construction results in part from good weather and minimal equipment problems. It is estimated that a crew of 12-15 men can stack, under perfect conditions, 60-70 tons of bagged ANFO in a 10 hour shift.

Whether bagged or bulk charge construction is used, the time between manufacture of the ANFO and the detonation of the charge should be kept to a minimum. Transit time between the mixing plant and the test site is usually small; the larger time span is taken up by the construction of the charge. Round the clock operations when and where feasible, should be employed and as much mechanized equipment should be used as is practicable. No definitive

TABLE 3-3 CHARGE CONSTRUCTION TIMES

Event	ANFO (tons)	No. Men	Manhours	Manhours/ton
<u>Bulk Construction</u>				
ANFO Event II	18.68	5	45	2.41
ANFO Event III	100.32	5	78	0.78
<u>Bagged Construction</u>				
ANFO Event I	19.96	9	54	2.71
ANFO Event IV	25.1	--	--	--
ANFO Event V	23.9	--	--	--
Pre-DICE THROW II-2	122.45	--	297	2.43
DICE THROW	628	19	2052	3.27
MISERS BLUFF	118	--	--	3.27*
MILL RACE	600.19	10	1200	2.0
DISTANT RUNNER II	119.35	6	210	1.76
DISTANT RUNNER III	120.08	6	180	1.5

*Estimated by CERF

information is available on how long ANFO will remain a viable and safe explosive. As noted earlier, there is a propensity for ANFO to lose oil in hot, dry climates; this oil loss leads to less energetic but more sensitive ANFO. Until more data are available, it is suggested that no more than 2-3 months time should elapse between ANFO mixing and charge detonation. (This time estimate is based on experience with some large bombs containing AN slurries which remained operational for many months but became unsafe after years of storage.) It is further recommended that periodic assays be made of the first emplaced ANFO for FO content if long construction times or firing delays are encountered.

3.3 DETONATION SCHEMES

Explosives and blasting agents require a detonation scheme for practical, operational reasons; the detonation scheme usually consisting of a firing circuit, an initiator (fuze), and a high explosive booster charge, provides safe control over when the charge is detonated. Although ANFO can be detonated by as few as two commercial #6 blasting caps (depending on particle mesh size), to assure proper, reliable detonation of the specified 94/6 AN/FO ratio at the 0.85 g/cm³ density, high explosive boosters are used. The function of the booster, upon detonation, is to raise the pressure and temperature of the surrounding ANFO in a short time to a sufficient level so that numerous hot spots are generated by adiabatic heating to cause the detonation of the ANFO.

In the early phases of ANFO development for simulation purposes, large TNT/pentolite boosters were used (Table 3-4). For instance, on the 20 and 100 ton shots ANFO I, II, and III, the boosters weighed 250 lbs. As experience was gained and more was learned about the properties of ANFO in unconfined charges, the booster size was decreased significantly; on the 600-ton DICE THROW charge, the individual booster (a pentolite and octol combination) weighed only 31 lbs. The booster size probably can be reduced further but only experience will demonstrate this. Because there is no particular penalty for using a nominal 30 lb booster, this size can be employed for ANFO charges of any size in the hemispherical, spherical, and domed cylindrical configurations with the assurance that it will drive the ANFO to proper and sustained detonation.

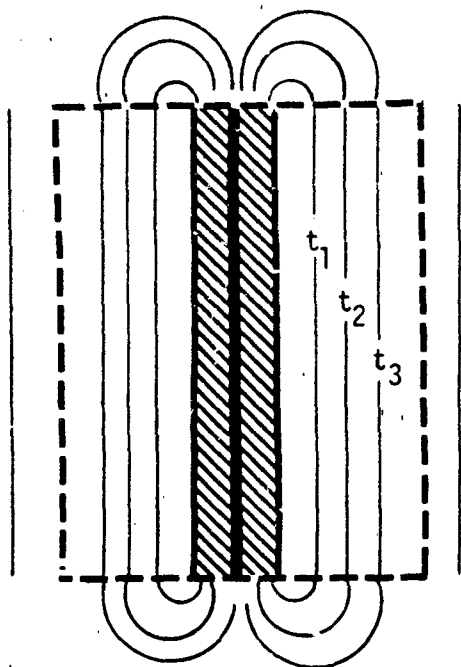
For best performance of the boosters with the detonation wave geometries as they exit the boosters, conforming to and symmetrical with the geometry of the charge, the booster shapes should be the same as that of the charge. For hemispherical charges the booster should be hemispherical, for spherical charges, spherical. For large cylinders with or without caps or domes, it is impractical for the booster to meet this criterion.

TABLE 3-4 BOOSTERS USED ON SELECTED LARGE ANFO CHARGES

Event	ANFO Weight (tons)	Booster Explosive Weight (lbs)
ANFO I	20	TNT/Pentolite 250
II	20	TNT/Pentolite 250
III	100	TNT/Pentolite 250
IV	25	TNT/Tetrytol 120
V	25	TNT/Tetrytol 120
Pre-DICE THROW II-2	120	Pentolite/Octol 31*
DICE THROW	600	Pentolite/Octol 31*
Pre-DIRECT COURSE	20	Octol 50

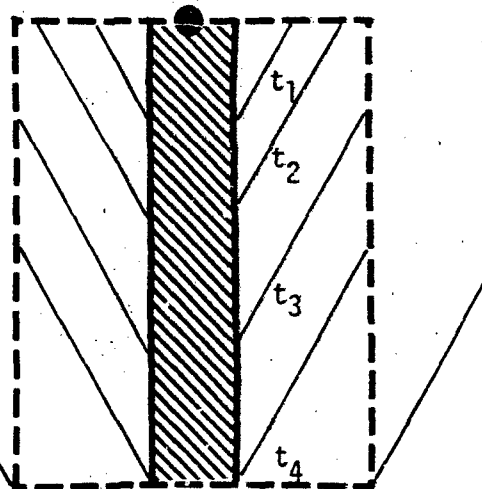
*Seven cylindrical boosters, each weighing 31 lbs, were spaced along the axis of the charge.

Ideally, a cylindrical booster along the full length of the axis of the charge would be required with the additional condition that this booster detonate simultaneously along its full length. This would generate a cylindrical detonation wave to propagate into the main ANFO charge (Figure 3-8) and as a result, a cylindrical airblast wave would be generated. If this booster charge were to be end or centrally initiated, a skewed detonation front would pass into the ANFO with the result that the ANFO generated airblast wave would be skewed also, i.e., not perpendicular to the ground. As a working compromise, several small booster charges equally spaced along the axis of the charge can be employed for detonating the main ANFO charge. The detonation wave progresses with time from each of the boosters as illustrated in Figure 3-8 for two boosters. Note that at the center line between the boosters, the detonation waves meet and interact to form a high velocity mach wave. With proper design, this protruding mach wave will be dissipated within the main charge so that a cylindrical wave engulfs the major volume of the ANFO charge thus resulting in an appropriate airblast wave. An adequate design is the one used on DICE THROW and the later domed cylindrical charges where seven boosters were used.

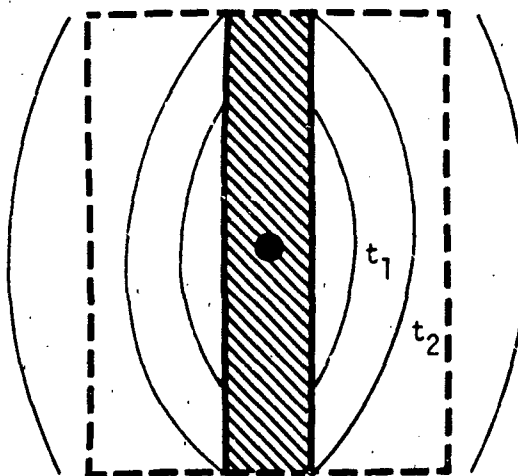


Ideal Booster

Airblast

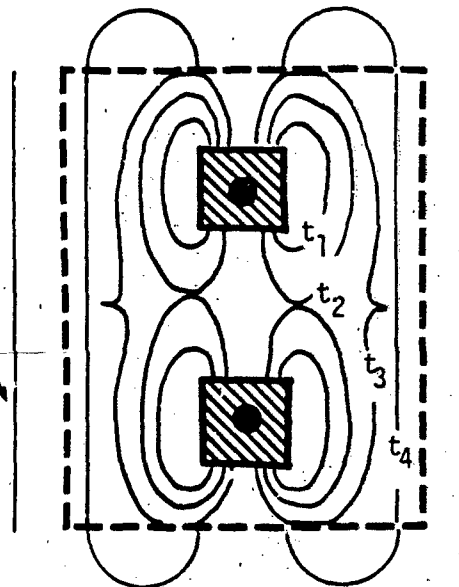


End Detonated Booster



Centrally Detonated Booster

Airblast



Multi-Point Booster

FIGURE 3-8. DETONATION DESIGNS FOR CYLINDRICAL CHARGES.

In order to achieve the desired detonation front characteristics, simultaneous detonation of all the boosters is required; non-simultaneity leads to a perturbed front and the possible production of blast anomalies. LLNL designed, built, and provided two firing sets for use on DICE THROW. The firing system, shown in Figure 3-9, consisted of four main elements: a high voltage controller with trigger generator, a 6,000 ft transmission line using RG 213 cable duplexed for charging and firing, a capacitor discharge unit (CDU), and firing lines and harness to initiate the seven quick acting (1.1 μ s) RP-1 detonators in a series string. A duplicate back-up system functioned 1.5 μ s after the primary system. Indications are that simultaneous detonation of all the detonators occurred on DICE THROW. However, some of the later shots, e.g., MISERS BLUFF and MILL RACE, were not so successful; large differences in booster activation times are reported. Table 3-5 summarizes the results; in the table all times are referred to the first booster to detonate which is listed as 0 μ s.

TABLE 3-5 BOOSTER DETONATION TIMES

Booster Number	Detonation Times (μ s)						
	1	2	3	4	5	6	7
MISERS BLUFF II-1	--	3.6	4.2	3.6	7.2	3.6	0.0
MISERS BLUFF II-2							
Charge 1	6.9	0.9	0.0	0.0	2.7	2.6	50
2	0.0	13	4.9	16	45	23	--
3	1.0	0.0	3.3	5.7	6.5	6.9	72
6	3.4	0.0	1.6	2.9	3.7	0.0	1.3
MILL RACE	30	0	40	90	90	90	90

For these later tests a new technique was developed by DRI (Reference 3) for determining booster detonation. At each of the seven booster locations, a light pipe (Figure 3-10) was embedded in the stack with one end of the pipe butted against the booster. High speed cameras provided light streak records by directly viewing booster light through the light pipe. One camera viewed all lightpipe outputs on a common film so relative times could be determined easily.

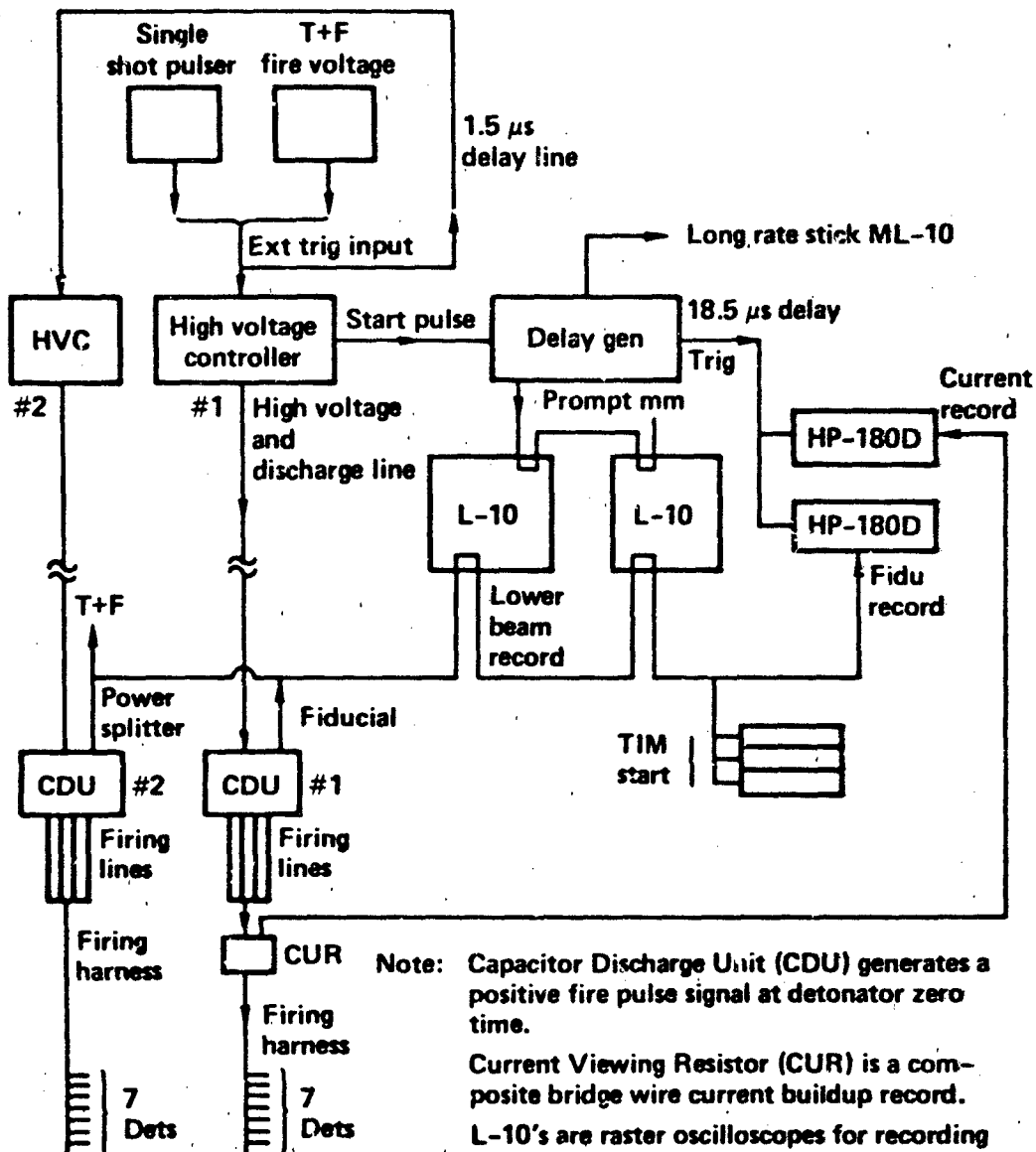


FIGURE 3-9. FIRING SYSTEM, LAWRENCE LIVERMORE LABORATORY EXPLOSIVES DIAGNOSTICS.

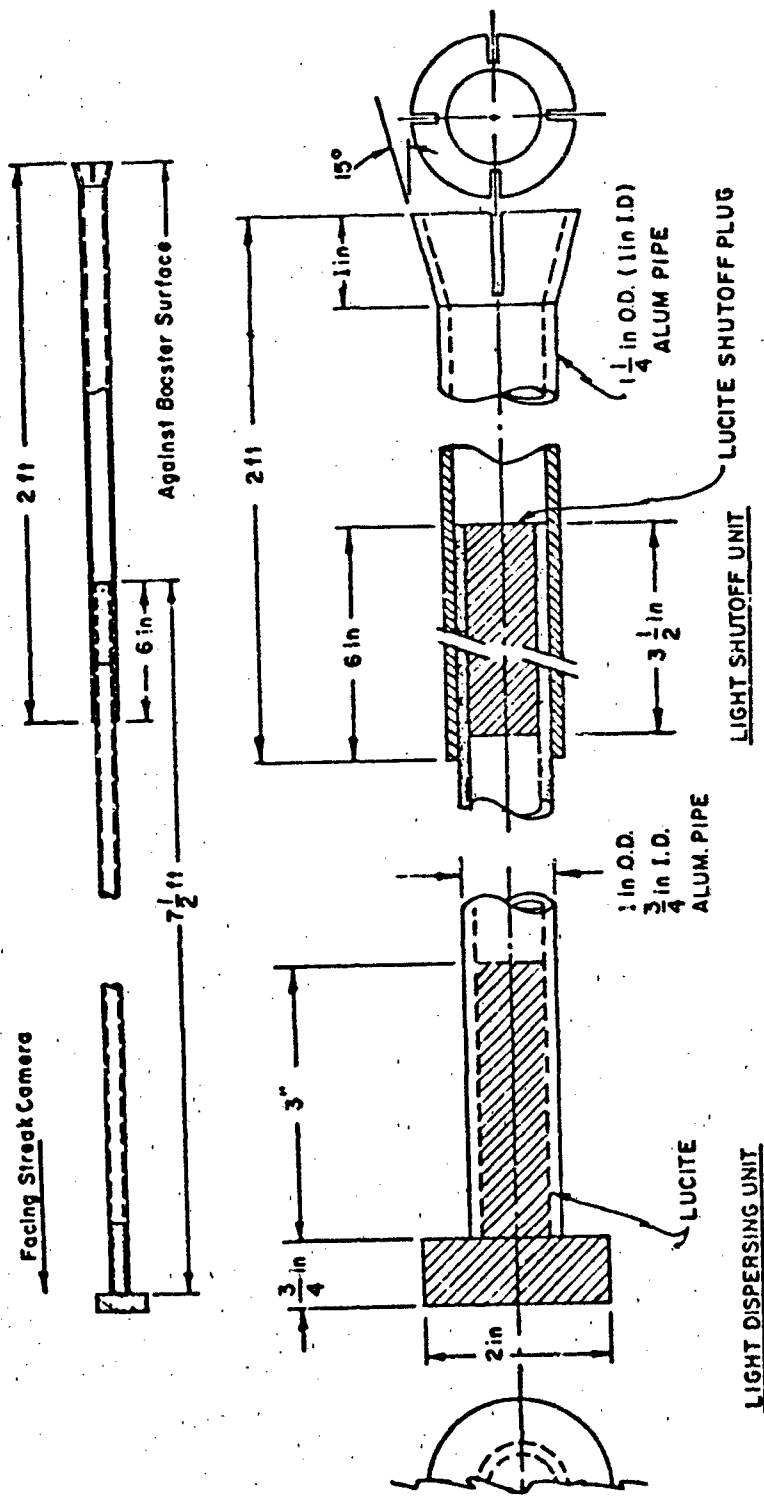


FIGURE 3-10. BOOSTER DIAGNOSTIC LIGHT PIPE SYSTEM (MISERS BLUFF II-1 and 2).

The reported simultaneity of the DICE THROW boosters may have been subject to the less sophisticated measurement system used on that event, or, in fact, it may be real. But a 90 μ s difference, as recorded for MILL RACE, is troublesome; it can lead to a skewed detonation wave through the ANFO with a resulting skewed airblast wave or anomaly. Taking the extreme time difference of 90 μ s, this amounts to a detonation wave from the late booster lagging that of the first booster by about 45 cm (assuming a nominal velocity of 5000 m/sec.). Obviously increased efforts are indicated to obtain reasonable simultaneity. Perhaps these efforts are paying off: DISTANT RUNNER II showed a spread of 25 μ s among booster detonation times; DISTANT RUNNER III, 34 μ s. (Reference 4).

The boosters, as indicated in Table 3-4, are comprised of two explosives. The outer explosive, i.e., the one in contact with the ANFO, is of lesser sensitivity and is more energetic than the inner one (the primer), i.e., the one in contact with the initiator or fuze. This is done for operational and safety reasons. On large ANFO charges it is necessary to emplace the booster as the main charge construction is underway. This exposes the booster to traffic and construction hazards; the less the sensitivity of the exposed explosive, the less the hazard.

The explosive train to detonate the charge proceeds from the most sensitive to the least sensitive explosive, from an initiator detonator to a primer explosive surrounded by the main booster charge to the ANFO, from the smallest charge to the largest. For example, for ANFO I, II and III, the primer explosive, 50/50 pentolite, weighed 16 lbs and the main TNT booster 234 lbs; on DICE THROW, the pentolite primer weighed 2 lbs, the main octol booster 29 lbs.

Figure 3-11 illustrates the explosive train for ANFO I, II, and III; Figures 1-36 and 1-37, that for the pre-DICE THROW II, Event 2 and subsequent domed cylinder shots. The detonation scheme for the early ANFO events was simple: a length of explosive primacord was threaded through the booster (the primacord was shallow buried under the charge) linking the booster with an electric detonator several feet from the main ANFO charge. Upon receiving an appropriate firing signal, the detonator initiated the primacord which in turn set off the pentolite, the pentolite the TNT, and the TNT the ANFO. In this

system there is a difference between the times when the firing signal arrives at the detonator and when the main charge explodes; this time can be measured with suitable instrumentation and it can be fairly well predicted and controlled by knowing the length of primacord used and its rate of detonation.

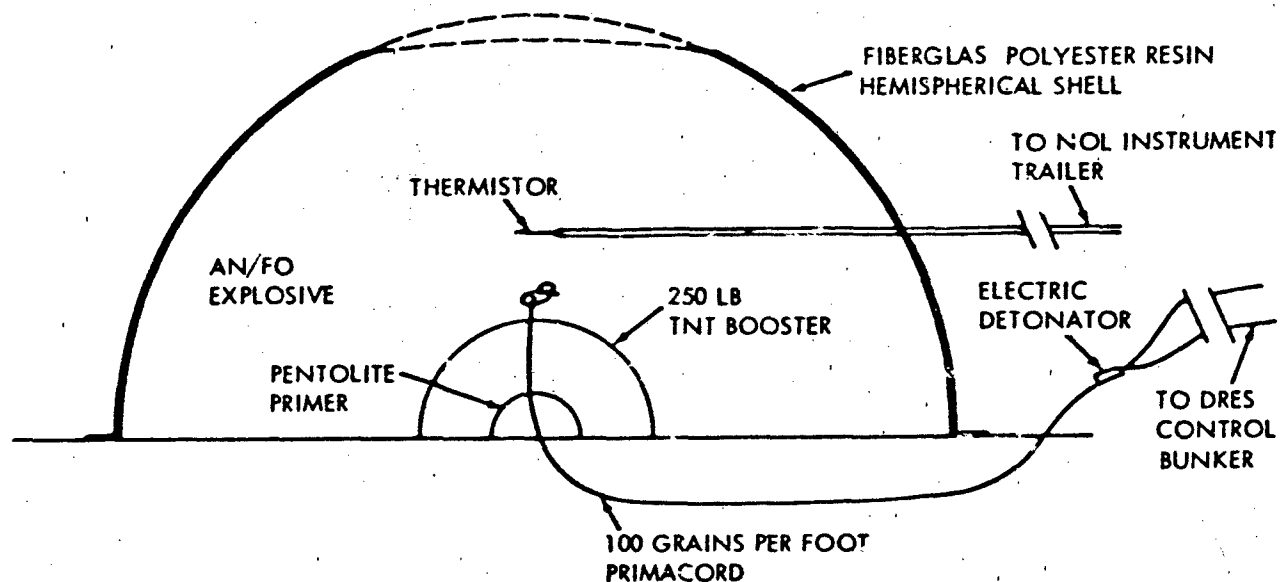


FIGURE 3-11. ANFO II AND III, SCHEMATIC DIAGRAM.

The detonation scheme for the DICE THROW and the subsequent domed cylindrical charges was more complicated because of the requirements for multiple point boosting as described earlier in this Section 3.3. The recommended detonator-primer-main booster-main charge explosive train was observed for safety reasons, but an additional safety feature was added to the design. The detonator-primer combination was not emplaced into the charge to arm it until shortly before firing; thus only the least sensitive explosives, the octol booster and the ANFO main charge, were exposed to the minimal -- but ever present -- hazards of charge construction. Details of the arming

procedures are discussed in Section 1.4.5. Figures 3-12, 3-13, and 3-14 illustrate the emplacement of the octol boosters during charge construction and the evident traffic around them; Figure 3-15 shows a cross-section of the boosting system.

3.3.1 Booster Safety

Unlike ANFO, the boosters such as TNT, octol and pentolite, used to detonate the ANFO are classified as high explosives; their storage and handling are more stringent than for ANFO and these are dictated by the DoD Explosives Safety Manual, DoD 5154.4S. The quantity of explosives establishes the separation distance necessary between booster storage locations and other facilities such as public highways, inhabited buildings and work areas. Storage facilities should protect the explosives from the elements and from pilferage. The storage facility should be clean, dry and well ventilated. Standard explosives-magazine construction is preferred. If other buildings are used they should be one-story, without basement and of non-combustible material. Proper warning signs should be posted on the building. Smoking or open flames should not be permitted near the facility.

Boosters must be transported in accordance with Part 173-SHIPPER'S-GENERAL REQUIREMENTS FOR SHIPMENTS AND PACKAGINGS of DOT Regulations and DoD 5154.4S. Vehicles must be in safe operating condition and driven by competent drivers who are familiar with Federal, State and local regulations. No smoking or open flames should be permitted in or near a loaded vehicle. Each vehicle should have two fire extinguishers of the CO₂ or dry chemical type. Explosives placards must be on all four sides of the vehicle whenever loaded. Vehicle fires should be fought only in the incipient stages. If the explosives become engulfed in flames, the area should be evacuated. (It is noted that similar regulations apply to ANFO; again repeating a now familiar refrain, when and where possible, ANFO should be treated as an explosive. This is particularly true because in normal field test operations, the charge construction crews are not necessarily experienced ordnance handlers.)



FIGURE 3-12. SEGMENT OF OCTOL BOOSTER READY FOR EMPLACEMENT, DICE THROW.



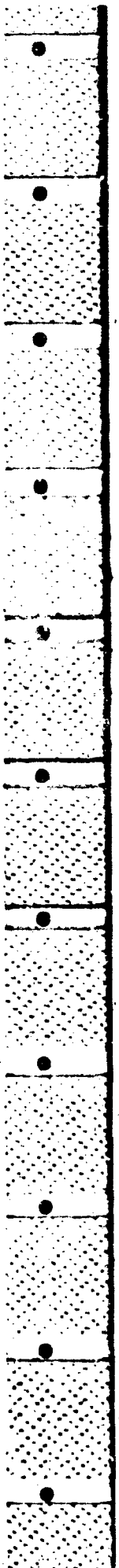
FIGURE 3-13. OCTOL BOOSTER EMPLACEMENT BEING COMPLETED, DICE THROW.



FIGURE 3-14. SECURING BOOSTER TO PVC PIPE WITH TAPE, DICE THROW.



FIGURE 3-15. CROSS SECTION OF BOOSTER SYSTEM, DICE THROW.



The practicalities of field operations sometimes preclude adherence to the regulations; magazines with the required security requirements may not be available. On some operations, the booster charges have had to be stored in vans or small bunkers. As many of the applicable regulations should be observed as possible, paying particular attention to distances from the ANFO storage and stacking sites and other operational sites, to the common sense ban on smoking and open fires in the area, proper posting of the booster housing structure, and keeping the area clean and uncluttered. For each operation, the explosive storage and handling safety procedures should be spelled out in detail.

3.4 SUMMARY

The relative insensitivity to detonation of ANFO when properly prepared makes it a practical source for simulating nuclear weapons blast and shock. It has been effectively used in a variety of charge shapes and in single quantities up to 620 tons but for scaleable results it should not be used in less than 1-2,000 lb sizes for airblast purposes. The flexibility in charge shaping results from the pliability of the 50 lb bags in which ANFO is usually packaged and from its pourability when bulk ANFO is used. Self standing charges using bagged ANFO have been constructed as well as charges in which a thin shell is employed to hold bulk ANFO; operational and test requirements determine the preferability of the type of charge construction to be chosen.

In both charge constructions, homogeneity of the charge material is a requirement to minimize blast anomalies. This requirement can be met by adherence to proper specifications for the ANFO itself and by the methods used to construct the charge. The principal specifications call for a 94/6 or 93/7 AN/FO ratio by weight and a bulk density of about 0.85 g/cm^3 with a specified prill size distribution. In construction, care has to be taken to avoid prill breakup lest the density increase beyond the desired limits and thereby preclude the desired detonation and blast characteristics of the charge. Auger, bucket, and pneumatic methods can be employed for handling bulk ANFO, the chosen method depending on operational conditions.

An explosive train consisting of a detonator and a primer and main booster high explosive charge is required to detonate the ANFO. The booster charge need not exceed about 30 lbs to attain reliable detonation of the ANFO charge. For best results the booster geometry should conform to and be symmetrical with the main charge geometry.

Even though ANFO is not classified as an explosive but rather as a blasting agent, obviously it explodes under proper stimulation. Prudence dictates that all safety rules and regulations observed in the handling, storage, and use of high explosives, should be applied to ANFO where possible. However, whereas high explosives can be stored for long periods of time under proper conditions, the length of time that ANFO can be stored has not been studied; it is recommended, therefore, that no more than 2-3 months should elapse from the time of preparing the AN and FO mixture to the time the ANFO is fired.

References

1. "ANFO Charge Preparation for Large Scale Tests," L.D. Sadwin and M.M. Swisdak, Jr., United States Naval Ordnance Laboratory, White Oak, MD, NOLTR 70-205(1970).
2. Eighth International Symposium on Military Applications of Blast Simulators, Spiez, Switzerland, 20-24 June 1983. Proceedings I.
3. "Proceedings of the MISERS BLUFF Phase II Results Symposium 27-29 March 1979," Volume I, Field Command, Defense Nuclear Agency, POR 7013-1(1979).
4. "Proceedings of the DISTANT RUNNER Symposium, 27-28 April 1982", Field Command, Defense Nuclear Agency, POR 7063 (1982).

SECTION 4 EXPLOSION EFFECTS

4.1 INTRODUCTION

More than a dozen large ANFO charges have been fired since 1969 for development and simulation testing purposes (Figure 2-10). The effects data obtained on the tests provide a reliable basis for making predictions of these effects on future testing operations. To facilitate the prediction process, in this Section, most of the data have been reduced to standard sea level conditions, i.e., barometric pressure = 14.7 psi and ambient temperature = 59°F, for 1 lb of ANFO. Basically three geometries of charge have been used on the tests, therefore reduced curves are presented for hemispheres, spheres, and domed cylinders with L/D = 0.75/1. These reduced data can be scaled up to any ANFO yield of interest provided that three caveats are observed: one, that the ANFO charge be larger than about 1,000 lbs and that its minimum dimensions be greater than about three feet; two, that the ANFO not be confined in a heavy casing; and three, that a detonation scheme similar to the ones used in the tests be used.

The original, as-read measurements taken by the various agencies, are presented also so that a feel can be obtained for the scatter in data. It should be noted that although there is scatter, it usually is less than that observed on TNT SHOTS (see Figure 1-43). As with TNT scatter, the possible sources of ANFO scatter may be many and seldom uniquely identifiable. This scatter can result from instrumentation inadequacies, record reading procedures, and environmental disturbances and variations that lead to real phenomenological differences. This later is particularly evident in crater measurements where the geology at ground zero and environs is seldom uniform or known in detail and seldom is the same at different specific test sites.

In Section 1 of this report, it is evident that a criterion ANFO had to meet before acceptance for simulation work was how it compared to TNT in its hydrodynamic properties. Several curves were used to show these comparisons. Indeed, it is on the basis of these curves that the TNT equivalence of ANFO was determined to be about 0.82 over a pressure range extending down from about 1,000 psi. In this Section 4 on results, ANFO data will be presented

almost exclusively because as a user's guide for ANFO, it is almost -- but not quite -- immaterial what the effects of TNT shots are. However, some TNT data will be presented to highlight differences and similarities in effects between ANFO and TNT.

4.2 AIRBLAST RESULTS

Although single shot simulation work with TNT and ANFO charges over the past twenty-five years has been concerned with airblast, ground shock, and cratering, most of the emphasis has been on airblast and the response of targets to this effect. Comparisons of airblast data from these shots for determining the behavior and reproducibility of the explosion source is more amenable to correlations than for craters or ground shock because of the relative homogeneity of the air medium of propagation as opposed to the known and unknown variables in the ground structure. Observing the caveat that only charges of similar geometry should be compared for this objective, i.e., comparing explosive sources, the airblast results for hemispherical, spherical, and cylindrical charges (with L/D = 0.75/1) are treated individually in this section. Both as-read and reported data and reduced values are presented in tabular forms; only reduced data are plotted.

The airblast data were cube root and Sachs scaled to standard sea level conditions of pressure and temperature following the precepts given in Reference 1. The following are the equations used:

$$\text{For Pressure} \quad P' = P_1 \left(\frac{P_{01}}{P_{02}} \right) \quad (4-1)$$

$$\text{For Distance} \quad R' = \frac{R_1}{w^{1/3} \left(\frac{P_{01}}{P_{02}} \right)^{1/3}} \quad (4-2)$$

For Times TOA' or τ' =
$$\frac{TOA_1 \text{ or } \tau_1}{w^{1/3} \left(\frac{P_{01}}{P_{02}}\right)^{2/3} \left(\frac{T_{01}}{T_{02}}\right)^{1/2}} \quad (4-3)$$

For Impulse I' =
$$\frac{I_1}{w^{1/3} \left(\frac{P_{02}}{P_{01}}\right)^{2/3} \left(\frac{T_{01}}{T_{02}}\right)^{1/2}} \quad (4-4)$$

where P_1 = measured pressure
 R_1 = measured distance
 TOA_1 = measured arrival time
 τ_1 = measured positive phase duration
 I_1 = measured impulse
 q_1 = measured dynamic pressure (similar to Eq. 4-1)
 Iq_1 = measured dynamic impulse (similar to Eq. 4-4)
 P_{01} = sea level barometric pressure (14.7 psi)
 P_{02} = barometric pressure at test site
 T_{01} = standard air temperature 519°R
 T_{02} = air temperature at test site, and,
 primed values are for the reduced parameters.

4.2.1 Hemispherical ANFO Charges

Three multiton hemispherical ANFO charges have been fired: ANFO I (20 tons, bagged), ANFO weight (20 tons, bulk), and ANFO III (100 tons, bulk). As reported in Reference 2, there is no significant difference in the airblast pressures generated by bagged or bulk ANFO, therefore all three shots can be compared on a common basis.

Table 4-1 presents the pressure data obtained on ANFO I by NGL, BRL, and DRES; Table 4-2 shows the data for ANFO II, and Table 4-3 the data for ANFO III.

TABLE 4-1. ANFO-1 AIRBLAST DATA
(20-Ton Hemispherical Charge, Bag Construction)

A. MOLA Data (Reference 2)

As Measured										Scaled to Standard Conditions					
R	TOA	P _m	r _m	I	TOA _{ss}	P _{ss}	R'	TOA'	P' _m	r' _m	I'	TOA' _{ss}	P' _{ss}		
ft	ms	psi	ms	psi-ms	ms	psi	ft/lb/l/3	ms/lb/l/3	psi	ms/lb ^{1/3} /3	psi ms/lb ^{1/3} /3	ms/lb ^{1/3} /3	psi		
80.1	12.5	381	9.22	831	--	--	2.28	0.366	328	0.269	26.2	--	--		
80.1	12.6	225	17.4	967	--	--	3.05	0.575	163	0.593	22.9	--	--		
107	19.7	154	20.0	700	--	--	4.16	0.985	56.7	0.869	13.6	--	--		
107	19.8	147	20.7	752	--	--	6.29	2.11	21.4	1.33	10.5	6.00	2.81		
146	33.8	53.2	18.6	334	--	--	9.02	3.92	10.4	1.84	7.11	8.58	1.18		
146	33.8	51.5	29.8	433	--	--	13.2	7.03	5.95	2.07	5.17	12.1	0.78		
221	72.2	19.1	45.5	330	205	2.50	21.9	14.1	2.60	2.58	3.21	20.3	0.78		
221	72.3	20.4	45.8	334	207	2.71	38.2	28.0	1.32	3.43	2.46	35.3	0.84		
317	135	9.97	63.0	222	289	1.83									
317	135	9.14	63.3	229	300	1.88									
464	241	5.98	67.7	173	414	1.00									
464	241	5.02	74.7	155	415	1.18									
772	486	2.34	84.4	106	703	0.69									
772	486	2.46	92.7	97.4	690	0.74									
1,340	959	1.28	117.5	94.2	1,210	0.61									
1,340	960	1.16	117.8	61.7	1,210	0.96									

Subscript ss - secondary shock

TABLE 4-1. ANFO I AIRBLAST DATA (Continued)

B. BRL Data (Reference 3)

As Measured				Scaled to Standard Conditions					
R	TOA	P _m	r _m	I	R'	TOA'	P' _m	r' _m	I'
ft	ms	psi	ms	psi-ms	ft/lb ^{1/3}	ms/lb ^{1/3}	psi	ms/lb ^{1/3}	psi-ms/lb ^{1/3}
15	1.75	866	3.7	1,357	.427	.051	--	--	--
20	2.2	1,125	5.3	1,020	.570	.064	1,217	.155	32.21
35	3.9	590	6.5	623	.997	.114	638	.190	19.67
51	6.4	291	7.0	446	1.452	.187	315	.204	14.09
80	12.4	186	10.6	496	2.28	.362	203	.309	15.66
110	20.2	88	25.5	472	3.13	.589	95	.744	14.91
148.5	34.6	50	30.3	396	4.23	1.01	54.2	.884	12.52

TABLE 4-1. ANFO I AIRBLAST DATA (Continued)

C. DRES Data Derived from ABTOAD Line (Reference 4)

As Measured				Scaled to Standard Conditions			
R ft	P _m psi	R ft	P _m psi	R' ft/lb ^{1/3}	P' _m psi	R' ft/lb ^{1/3}	P' _m psi
7.22	7,342	257.21	14.17	0.21	7,947	7.31	15.34
10.03	4,491	323.49	8.94	0.29	4,862	9.22	9.68
13.20	2,696	424.92	5.49	0.37	2,912	12.06	5.94
18.68	1,452	550.48	3.52	0.53	1,571	15.69	3.81
26.32	966.8	710.93	2.33	0.74	1,046	20.26	2.52
34.70	723.4	894.39	1.63	1.00	783.1	25.49	1.76
48.99	474.3	1,202.59	1.02	1.42	513.4	34.26	1.10
69.20	266.2	1,583.73	0.66	2.03	288.2	44.39	0.71
91.18	159.4	1,916.90	0.45	2.59	172.6	54.58	0.49
129.10	69.07	2,604.15	0.23	3.67	74.77	74.12	0.25
182.22	31.17	--	--	5.11	33.74	--	--

TABLE 4-2. ANFO III AIRBLAST DATA
(20-Ton Hemispherical Charge, Fiberglass Container, Bulk)

A. MOL Data (Reference 2)

As Measured										Scaled to Standard Conditions											
R	TOA	P _m	T _m	I	TOA _{ss}	P _{ss}	R'	TOA'	P' _m	T' _m	I'	TOA'	P' _{ss}	R'	TOA'	P' _m	T' _m	I'	TOA'	P' _{ss}	
ft	ms	psi	ms	psi-ms	ms	psi	ft/lb ^{1/3}	ms/lb ^{1/3}	psi	ms/lb ^{1/3}	psi	ms/lb ^{1/3}	psi	ft/lb ^{1/3}	ms/lb ^{1/3}	psi	ms/lb ^{1/3}	psi	ms/lb ^{1/3}	psi	
80.0	12.5	280	9.29	724	--	--	2.32	0.376	309	0.279	30.0	--	--	2.32	0.376	309	0.279	30.0	--	--	
80.0	12.6	290	17.8	1,120	--	--	3.16	0.615	108	0.813	19.6	--	--	3.16	0.615	108	0.813	19.6	--	--	
109	--	--	--	--	--	--	4.22	1.02	63.2	0.890	14.0	--	--	4.22	1.02	63.2	0.890	14.0	--	--	
109	20.5	99.9	27.1	603	--	--	6.42	2.14	21.6	1.39	9.83	--	--	6.42	2.14	21.6	1.39	9.83	--	--	
145	34.1	57.9	31.9	458	--	--	9.22	4.03	10.3	1.91	7.64	--	--	9.22	4.03	10.3	1.91	7.64	--	--	
145	34.1	58.8	27.5	404	--	--	13.5	7.24	5.38	2.34	5.50	--	--	13.5	7.24	5.38	2.34	5.50	--	--	
221	71.3	19.9	45.0	278	189	3.66	22.4	14.5	2.46	2.94	3.28	--	--	22.4	14.5	2.46	2.94	3.28	--	--	
221	71.4	19.9	48.1	327	195	3.56	39.0	28.7	1.08	3.48	1.62	--	--	39.0	28.7	1.08	3.48	1.62	--	--	
317	134	9.40	62.3	235	286	1.83															
317	134	9.68	65.2	235	288	1.55															
464	241	4.78	79.2	174	404	1.12															
464	241	5.14	77.0	164	413	1.19															
772	485	2.27	98.2	101	693	0.49															
772	--	--	--	--	--	--															
1,340	956	1.00	116	49.9	1,190	0.22															
1,340	--	--	--	--	--	--															

Subscript ss = secondary shock

TABLE 4-2. ANFO II AIRBLAST DATA (Continued)

B. 5RL Data (Reference 3)

As Measured				Scaled to Standard Conditions						
R	TOA	P _m	r _m	I	R'	TOA'	P' _m	r' _m	I'	
ft	ms	psi	ms	psi-ms	ft/lb ^{1/3}	ms/lb ^{1/3}	psi	ms/lb ^{1/3}	psi-ms/lb ^{1/3}	
15	2.0	879	4.0	1,580	.434	.060	--	--	--	
20	2.4	796	6.0	914	.579	.072	862	.179	29.6	
35	4.2	413	13.7	720	1.01	.125	447	.41*	23.32	
51	6.4	296	6.6	484	1.48	.191	321	.198	15.67	
80	12.4	189	13.2	559	2.32	.370	205	.395	18.11	
106	19.6	90	23.2	482	3.26	.586	97.5	.693	15.61	
144	33.2	52	29.1	391	4.41	.992	56.3	.870	12.66	

*Data Point Questioned and Not Plotted.

TABLE 4-2. ANFO II AIRBLAST DATA (Continued)

C. DRES Data Derived from ABTOAD Line (Reference 4)

As Measured		Scaled to Standard Conditions	
R ft	P _m psi	R' ft/lb ^{1/3}	P' _m psi
8.65	3,312	0.25	3,589
12.40	2,361	0.36	2,559
16.20	1,727	0.47	1,871
22.70	1,142	0.67	1,237
32.40	747.2	0.94	809.7
45.50	476.7	1.33	516.5
64.50	280.2	1.88	303.6
85.10	170.2	2.50	184.4
119.90	84.56	3.50	91.63
148.00	53.68	4.28	58.17
374.02	6.76	10.92	7.32
519.20	3.85	15.19	4.18
773.84	2.18	22.61	2.36
987.29	1.54	28.84	1.67
1,408.39	0.88	41.16	0.95
1,735.19	0.63	50.65	0.68
2,361.80	0.36	69.04	0.39

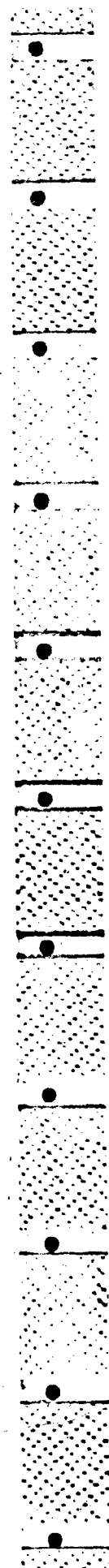


TABLE 4-3. ANFO III AIRBLAST DATA
(100-Ton Hemispherical Charge, Fiberglass Container, Bulk)

A. NOL Data (Reference 2)													
As Measured					Scaled to Standard Conditions								
R	TOA	P _m	r _m	I	TOA _{ss}	P _{ss}	R'	TOA'	P' _m	r' _m	I'	TOA' _{ss}	P' _{ss}
ft	ms	psi	ms	psi-ms	ms	psi	ft/lb ^{1/3}	ms/lb ^{1/3}	psi	ms/lb ^{1/3}	psi ms/lb ^{1/3}	ms/lb ^{1/3}	psi
136	20.4	326	9.86	842	--	--	2.26	0.341	284	0.165	18.4	--	--
136	20.4	197	-4	1,190 ^a	--	--	3.05	0.563	91.0	0.750	16.6	--	--
184	33.6	83.8	44.9	914	--	--	4.14	0.982	44.5	0.925	13.3	--	--
184	33.8	--	--	--	--	--	6.28	2.14	21.7	1.49	10.2	6.06	2.86
249	58.7	42.8	55.0	763	--	--	9.00	3.99	10.1	2.05	7.61	8.55	1.69
249	58.8	39.2	55.6	702	--	--	13.2	7.22	5.19	2.52	5.41	12.6	0.89
378	128	19.5	50.7	547	362	2.20	24.7	17.0	2.11	2.98	2.85	23.7	0.42
378	128	20.4	87.4	585	365	3.06	40.9	31.2	1.04	3.71	1.89	38.9	0.23
542	238	9.16	124	410	514	1.54							
542	239	9.34	122	428	509	1.58							
754	432	4.85	152	294	749	0.80							
754	432	4.70	149	301	763	0.84							
1,490	1,020	1.86	205	174	1,420	0.36							
1,490	1,020	2.02	152	139	1,420	0.41							
2,460	1,870	0.96	219	98.7	2,300	0.22							
2,460	1,870	0.96	225	110.0	2,350	0.20							

Subscript ss - secondary shock

^a Signal did not cross baseline; impulse was estimated

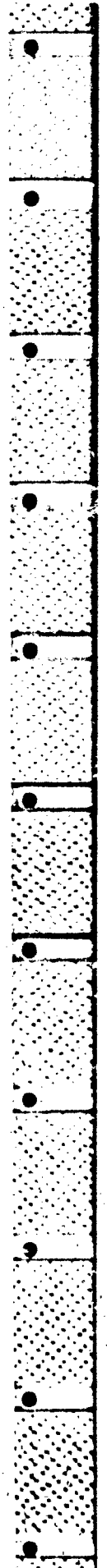


TABLE 4-3. ANFO III AIRBLAST DATA (Continued)

B. BRL Data (Reference 3)

As Measured				Scaled to Standard Conditions					
R	TOA	P _m	r _m	I	R'	TOA'	P' _m	r' _m	I'
ft	ms	psi	ms	psi-ms	ft/lb ^{1/3}	ms/lb ^{1/3}	psi	ms/lb ^{1/3}	psi-ms/lb ^{1/3}
25	3.0	1,260	--	--	.416	.0502	1,368	--	--
35	3.8	1,222	13.9	1,256	.58	.064	1,327	.233	22.83
60	6.4	752	10.2	850	.928	.011	817	.171	15.45
87	10.0	373	9.2	922	1.45	.167	405	.154	16.76
120	15.9	273	12.6	882	1.99	.266	236	.211	16.03
136	19.4	217	30.9	871	2.26	.325	236	.517	15.84
184	32.0	96.1	38.9	802	3.06	.536	104.4	.651	14.58
249	58.0	47.3	54.5	669	4.14	.971	51.4	.912	12.16
300	83.4	31.0	64.1	589	4.99	1.396	33.7	1.07	10.71

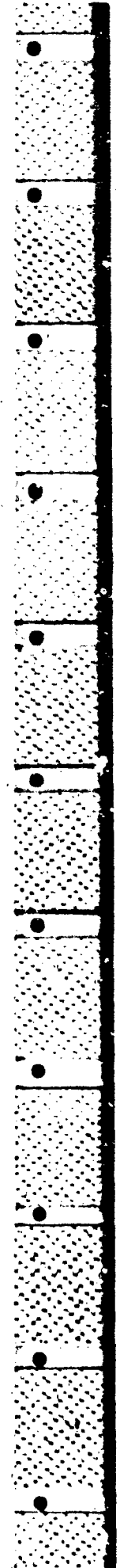


TABLE 4-3. ANFO III AIRBLAST DATA (Continued)

C. DRES Data Derived from ABTOAD Line (Reference 4)

As Measured		Scaled to Standard Conditions	
R ft	P _m psi	R' ft/lb ^{1/3}	P' _m psi
12.10	3,745	0.20	4,067
20.18	2,628	0.33	2,855
30.20	1,785	0.50	1,939
39.70	1,314	0.66	1,427
56.26	863.1	0.94	937.53
79.37	545.6	1.32	592.60
91.07	444.0	1.51	482.27
512.99	9.14	8.54	9.93
617.67	6.41	10.27	6.96
794.32	4.05	13.21	4.40
944.02	2.97	15.70	3.23
1,321.6	1.62	21.98	1.76
1,699.5	1.01	28.27	1.09
2,077.1	0.66	34.54	0.72

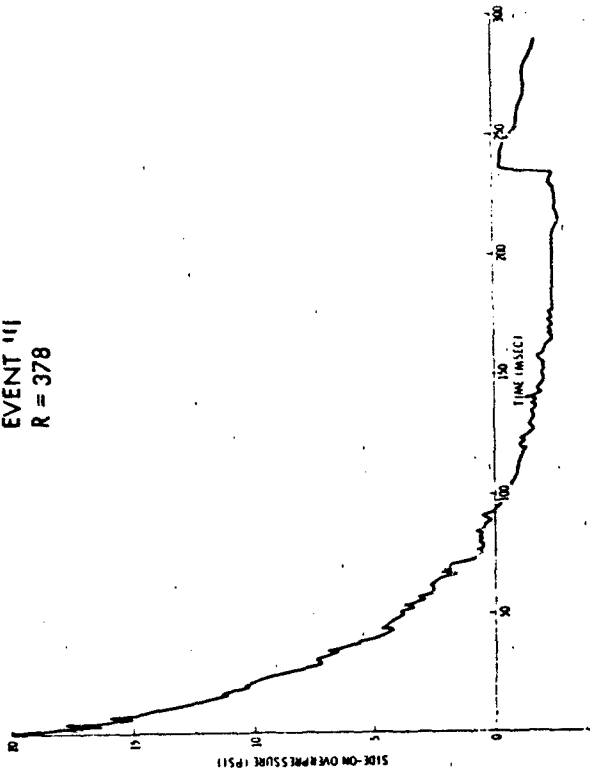
It is interesting to note that for these three shots, the authors (Reference 2) reported the presence of a secondary shock and measured its time of arrival (TOA_{SS}) and pressure (P_{SS}). This shock appeared in the negative phase of the airblast wave on all records with a peak overpressure below about 20 psi.

Figure 4-1 illustrates the typical appearance of the secondary shock on pressure-time records. The time of arrival and the pressure level of these shocks is scalable as is evident in Figures 4-2 and 4-3, and therefore predictable for other charge sizes with the hemispherical configuration. Secondary peaks are not novel to hemispherical charges or to ANFO; they have been reported for TNT spherical charges by Granstrom (Reference 5), Muirhead and Palmer (Reference 6) and others.

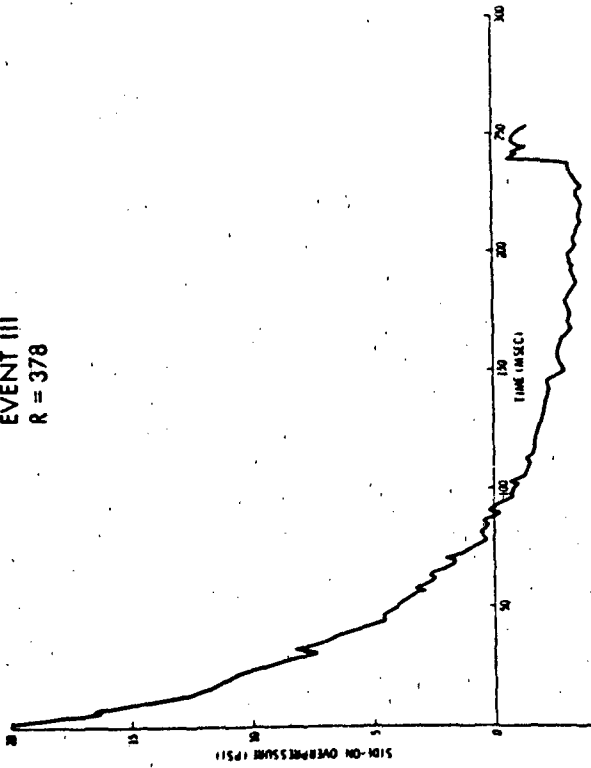
Information on secondary shocks seldom is reported; as will soon be evident, no such data have been reported for the post-ANFO I, II, and III shots. The reason for this omission is not evident. At the least, there should be interest in the hydrodynamics of the generation of this shock. What causes it? And, this shock may be of significance in target response analyses. Although it is relatively low in amplitude, the very presence of an input function which has a peak value anywhere from 15 to 50 percent of the primary shock may impose a damaging force. (It may be that for a 600-ton ANFO charge, where the secondary shock may appear as late as 900 ms after detonation time, the recording system is shut off before this time. Or, it simply may be that even though recorded, this second pulse is ignored. It should not be. In a similar vein, the duration, amplitude, and impulse of the negative phase of the airblast should not be ignored as it has been in the past. The negative phase, too, has hydrodynamic and target response implications.)

The scaled data for the ANFO I, II, and III shots are presented in Figure 4-4 for reduced maximum peak pressure (P'_m), in Figure 4-5 for reduced time of arrival (TOA'), in Figure 4-6 for reduced maximum positive pulse duration (τ'_m), and in Figure 4-7 for reduced impulse (I'). On all figures, the line is faired by eye through the data points. It is evident that indeed all the hemispherical charges had similar airblast characteristics. While there is scatter in the data, it is not excessive (and no more than that exhibited by the measurements of a single organization at a given distance, e.g., the difference between the two measurements reported by NOL in Table 4-1A

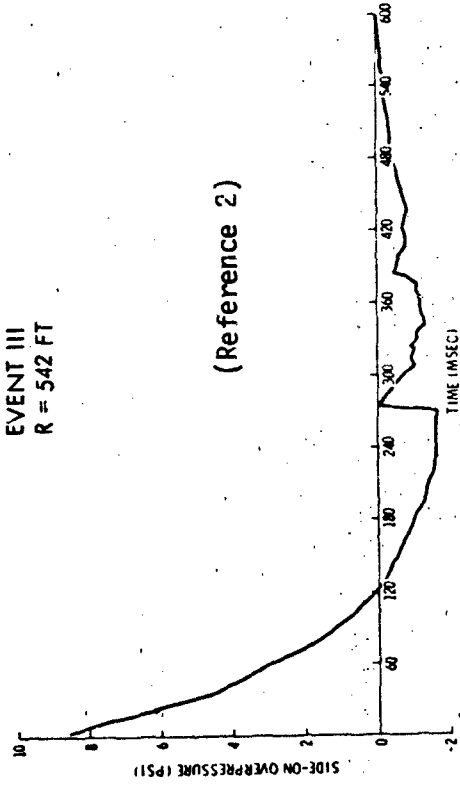
EVENT III
R = 378



EVENT III
R = 378



EVENT III
R = 542 FT



EVENT III
R = 542 FT

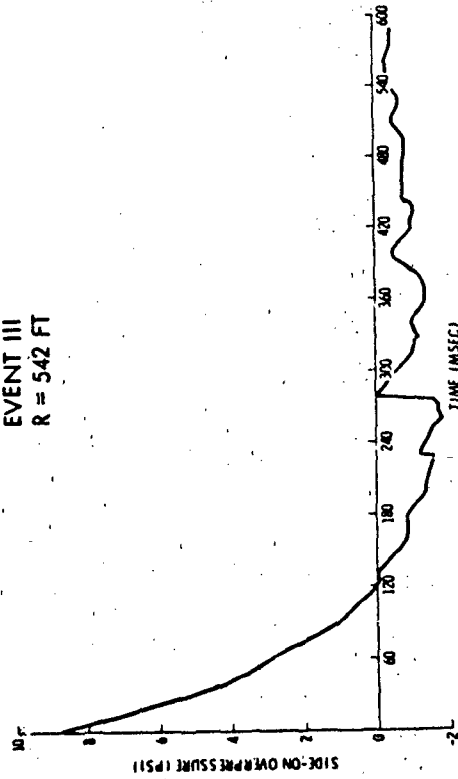


FIGURE 4-1. SECONDARY PRESSURE PULSES ON ANFO III.

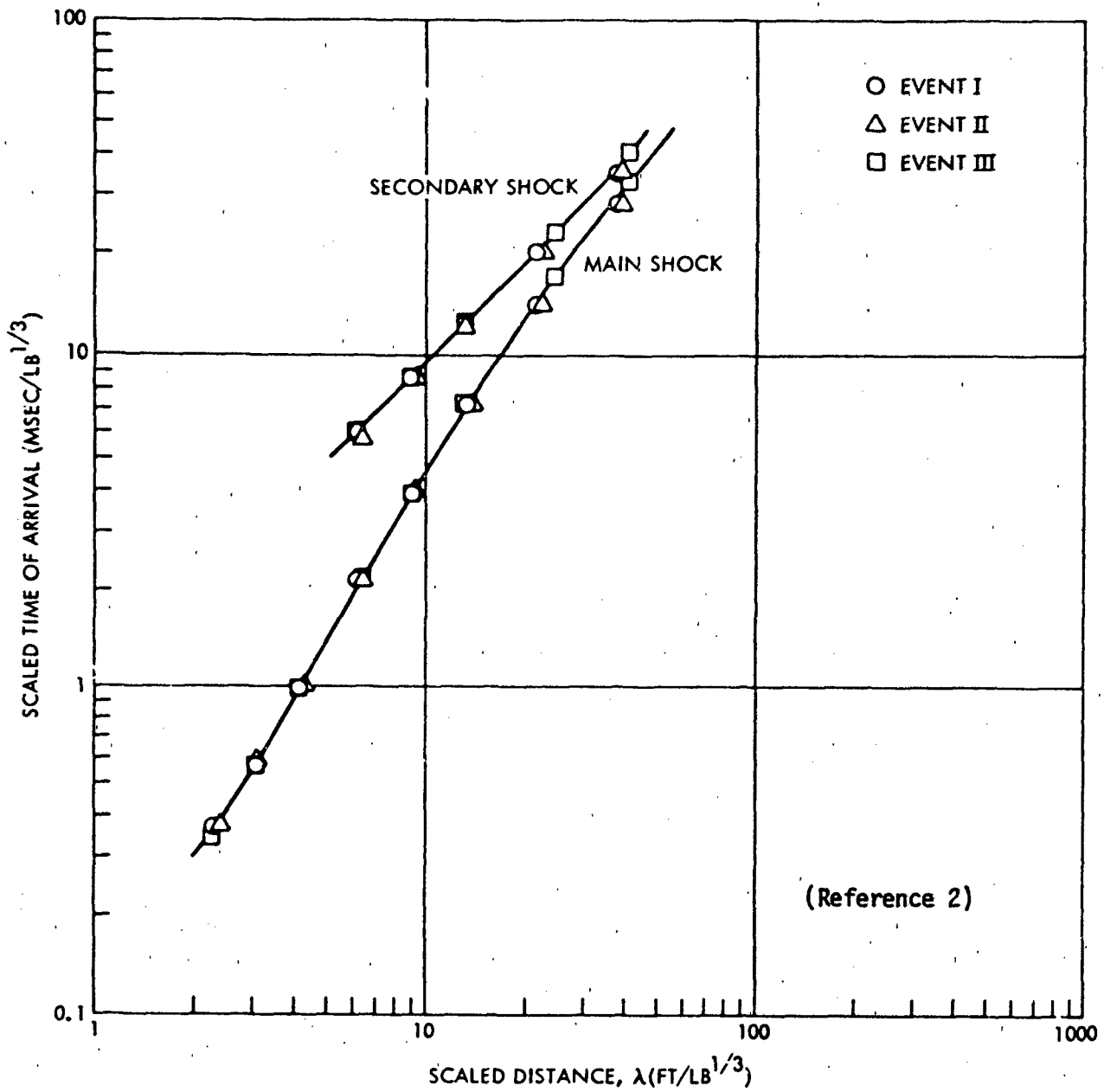


FIGURE 4-2. TIMES OF ARRIVAL VERSUS DISTANCE FOR ANFO AT DRES.
 (SCALED TO SEA LEVEL CONDITIONS.)

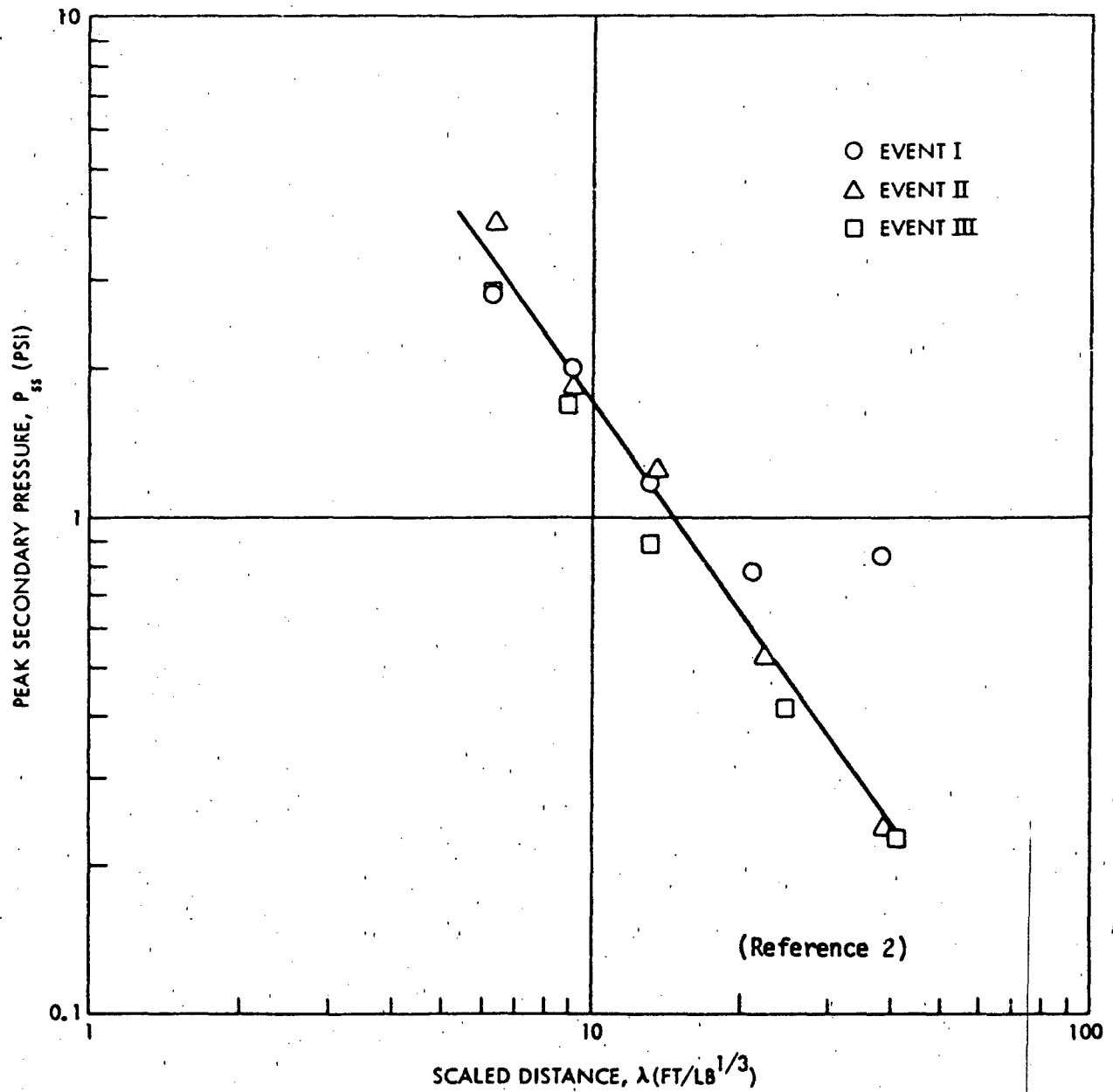


FIGURE 4-3. PEAK SECONDARY SHOCK PRESSURE VERSUS DISTANCE. ANFO TRIALS, DRES, AUGUST 1969. (SCALED TO SEA LEVEL CONDITIONS.)

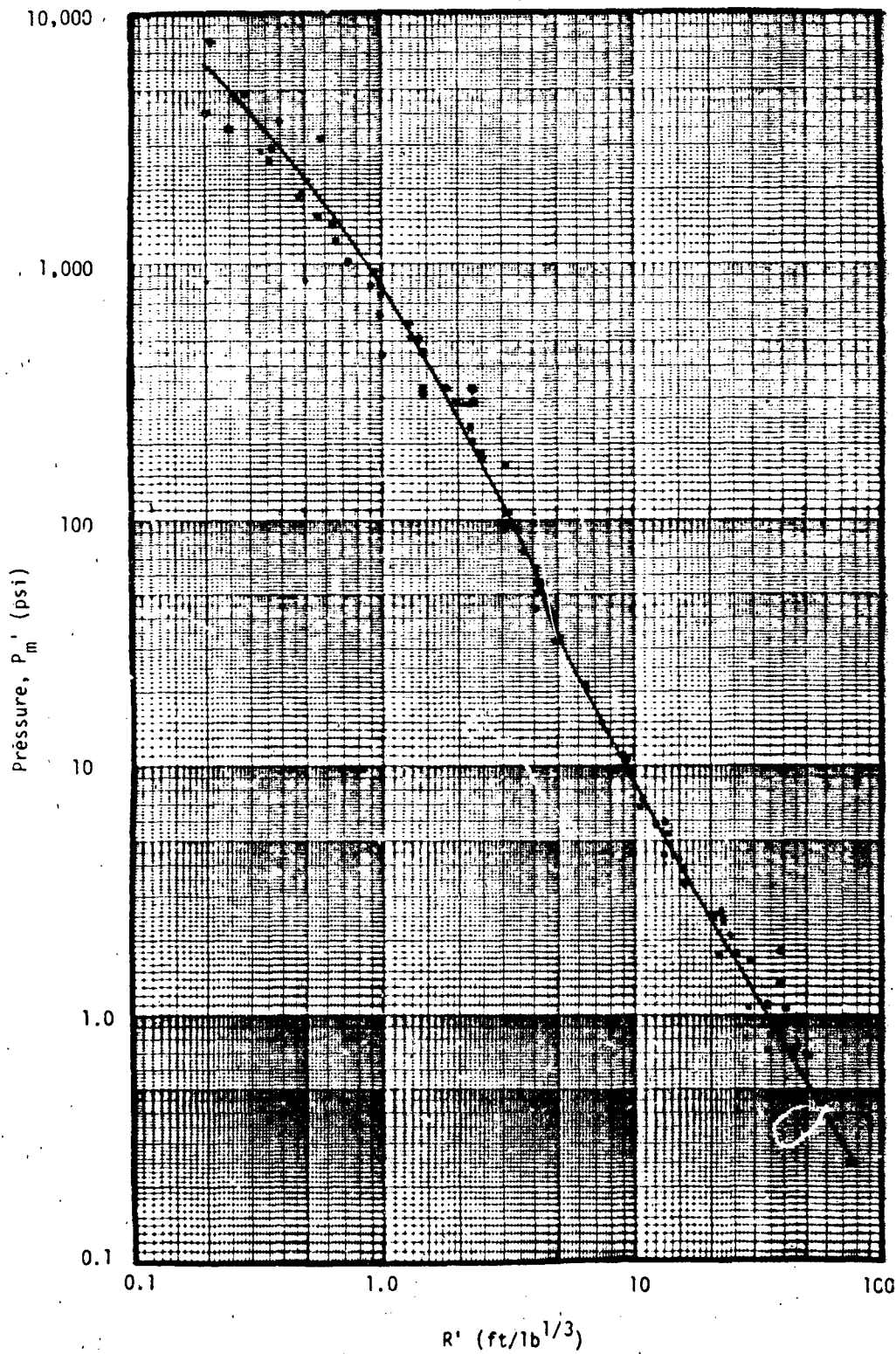


FIGURE 4-4. REDUCED PRESSURE - DISTANCE FOR ANFO I, II, AND III. SCALED TO SEA LEVEL CONDITIONS.

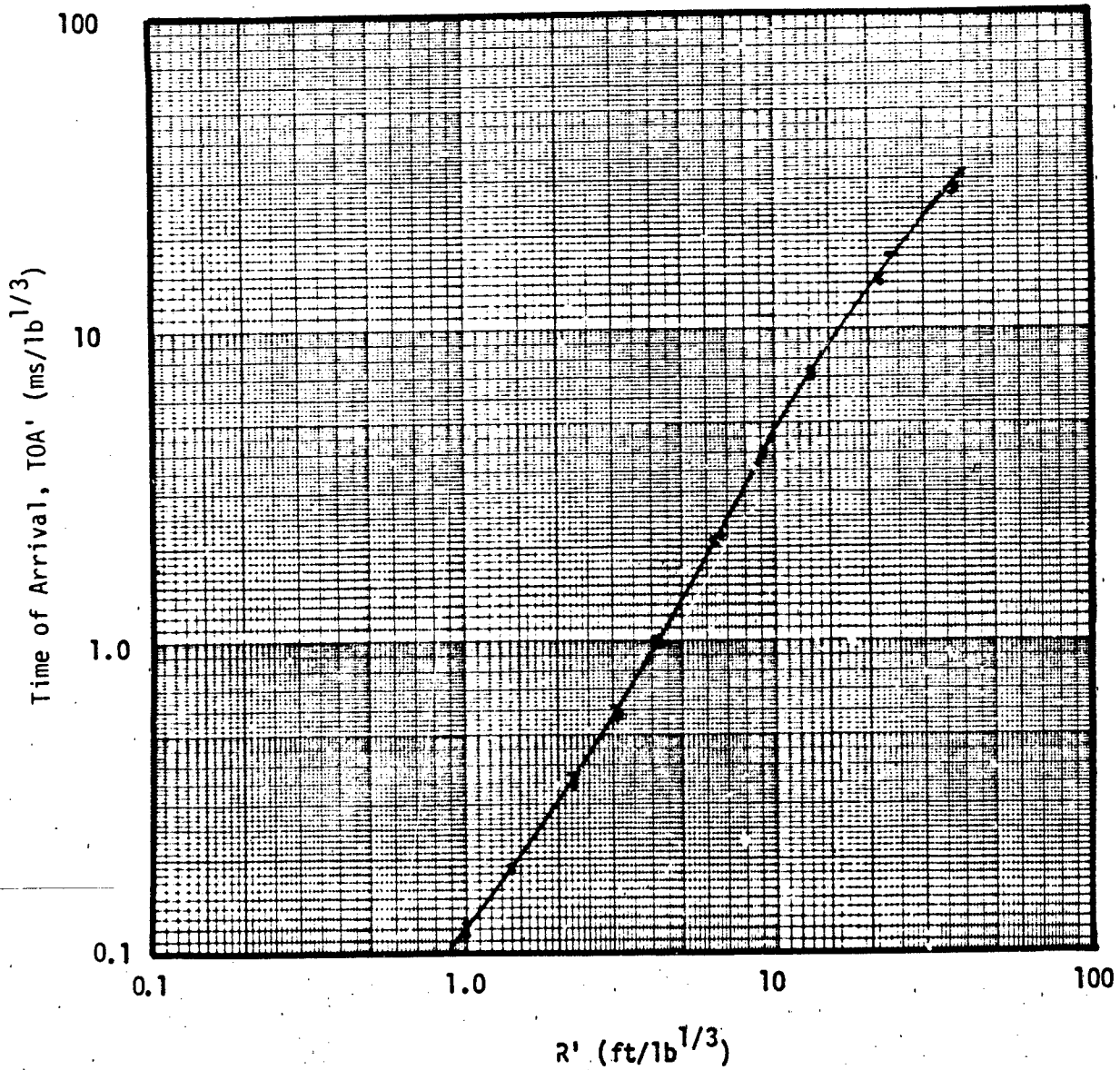


FIGURE 4-5. REDUCED TIME OF ARRIVAL (TOA') - DISTANCE FOR ANFO I, II, AND III. SCALED TO SEA LEVEL CONDITIONS.

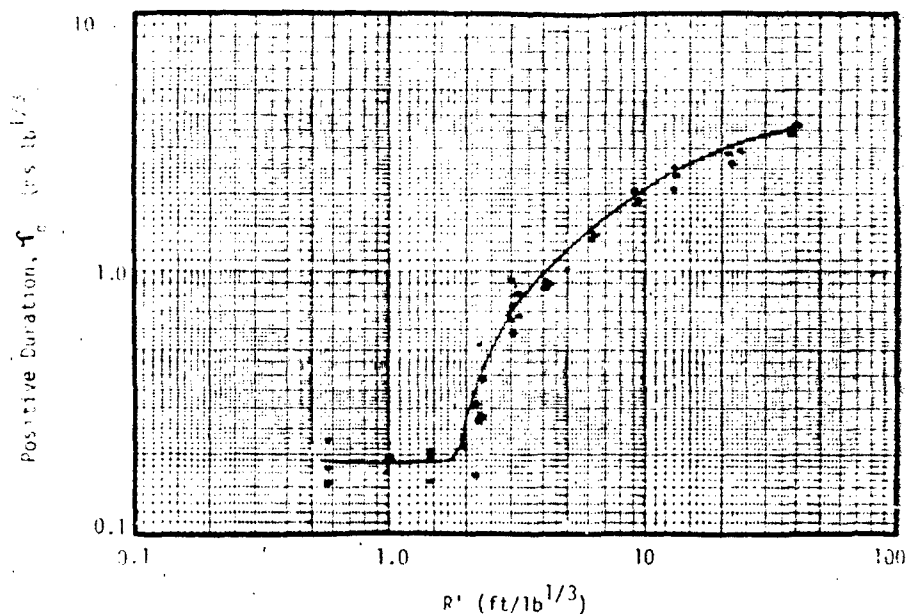


FIGURE 4-6. REDUCED POSITIVE PHASE DURATION (τ') - DISTANCE FOR ANFO I, II, AND III. SCALED TO SEA LEVEL CONDITIONS.

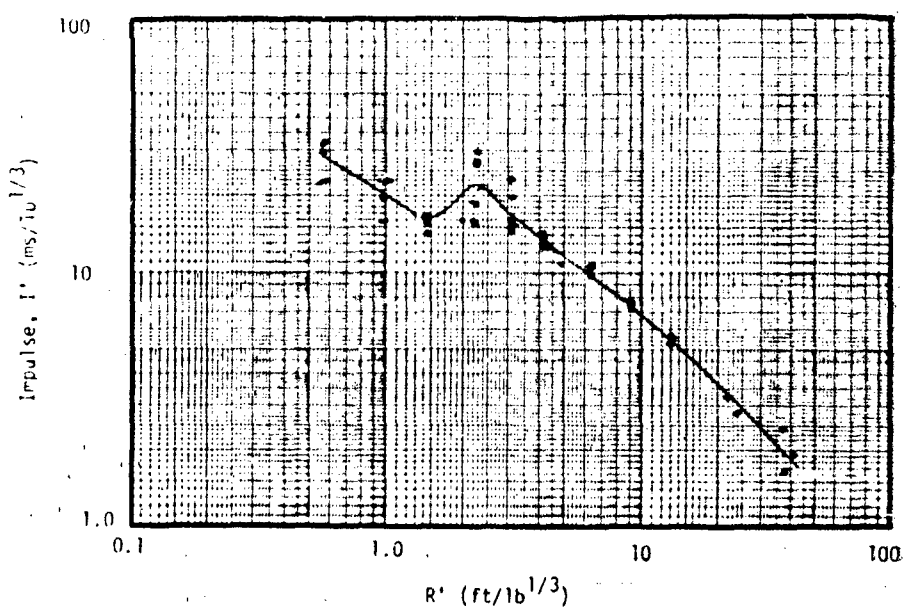


FIGURE 4-7. REDUCED IMPULSE (I') - DISTANCE FOR ANFO I, II, AND III. SCALED TO SEA LEVEL CONDITIONS.

at the 80.1 ft station). The data probably reflects the realities of large scale detonation effects in terms of the influence of environmental differences, instrumentation performance, and record interpretation procedures. The faired lines can be used with confidence for prediction purposes.

4.2.2 Spherical ANFO Charge, Tangent to Surface

There has been only one large scale tangent sphere shot, ANFO IV (25-tons). It was sparsely instrumented; all the available data are shown in Table 4-4. The reduced data are plotted in Figure 4-8. The coincidence of the BRL and DRES data lends confidence to the merits of using the faired curves for scaling purposes.

4.2.3 Spherical ANFO Charge, Half Buried

On ANFO V, a 25-ton spherical charge with its center at the ground surface, there were even fewer measurements of airblast than on ANFO IV. The BRL data obtained with self recording gages are shown in Table 4-5 and the reduced data plotted in Figure 4-9. Because the data are so sparse, the reduced curve for DISTANT PLAIN Event 3, a 20-ton TNT charge with the same geometry as ANFO V, has been added to the figure for comparison and guidance.

4.2.4 Domed Cylindrical ANFO Charges With L/D = 0.75/1

Observing the precept that when comparing explosive charges to determine their airblast characteristics on a common basis only charges of similar shape, test geometry, and detonation scheme should be so compared, the data for several large domed cylindrical charges with an L/D ratio of 0.75/1 (over the cylindrical portion of the charge) are presented. The charges so considered and the tables in which the data are presented are:

Table 4-6	Pre-DICE THROW I-4	6 tons
Table 4-7	Pre-DICE THROW II-2	120 tons
Table 4-8	MISERS BLUFF II-1	118 tons
Table 4-9	DICE THROW	628 tons
Table 4-10	MILL RACE	607 tons

(DISTANT RUNNER data became available too late for convenient inclusion in this report. A check of the data, however, indicates that they fall within the scatter of the plotted curves.)

TABLE 4-4. ANFO IV AIRBLAST DATA
(25-Ton Spherical Charge On Surface)

A. BRL Data (Reference 7)

		As Measured				Scaled to Standard Conditions								
R	TOA	P _m	r _m	I	R'	TOA'	P' _m	r' _m	I'	FT	ms	psi	ms	psi-ms
	ms				ft/lb ^{1/3}	ms/lb ^{1/3}	psi	ms/lb ^{1/3}	psi-ms/lb ^{1/3}					
45	4.1	610	7.5	771	1.19	0.11	655.5	0.20	21.82					
70	7.6	347	7.9	694	1.85	0.20	372.9	0.21	19.64					
125	19.8	121	31.5	836	3.31	0.52	130.0	0.83	23.66					
150	28.1	115	31.0	620	3.97	0.74	123.6	0.82	17.55					
150	--	80.0	34.7	453	3.97	--	86.0	0.91	12.82					
185	41.5	43.8	38.5	456	4.89	1.09	47.1	1.01	12.90					
250	76.8	22.6	52.4	347	6.61	2.02	24.3	1.38	9.82					
250	--	12.7	53.0	320	6.61	--	13.6	1.40	9.06					
340	136	10.0	74.4	241	8.99	3.58	10.7	1.96	6.82					
500	259	4.9	98.0	167	13.2	6.82	5.3	2.58	4.73					
1,400	1,030	.86	148	62.7	37.0	27.13	.9	3.90	1.77					

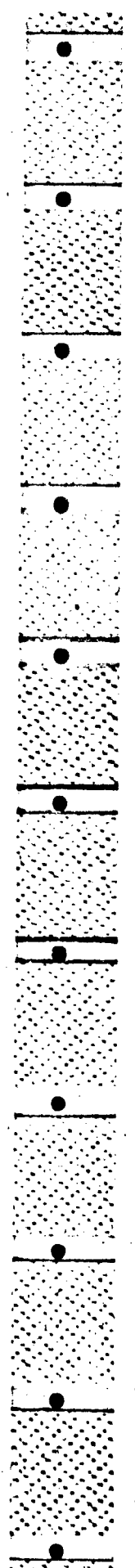
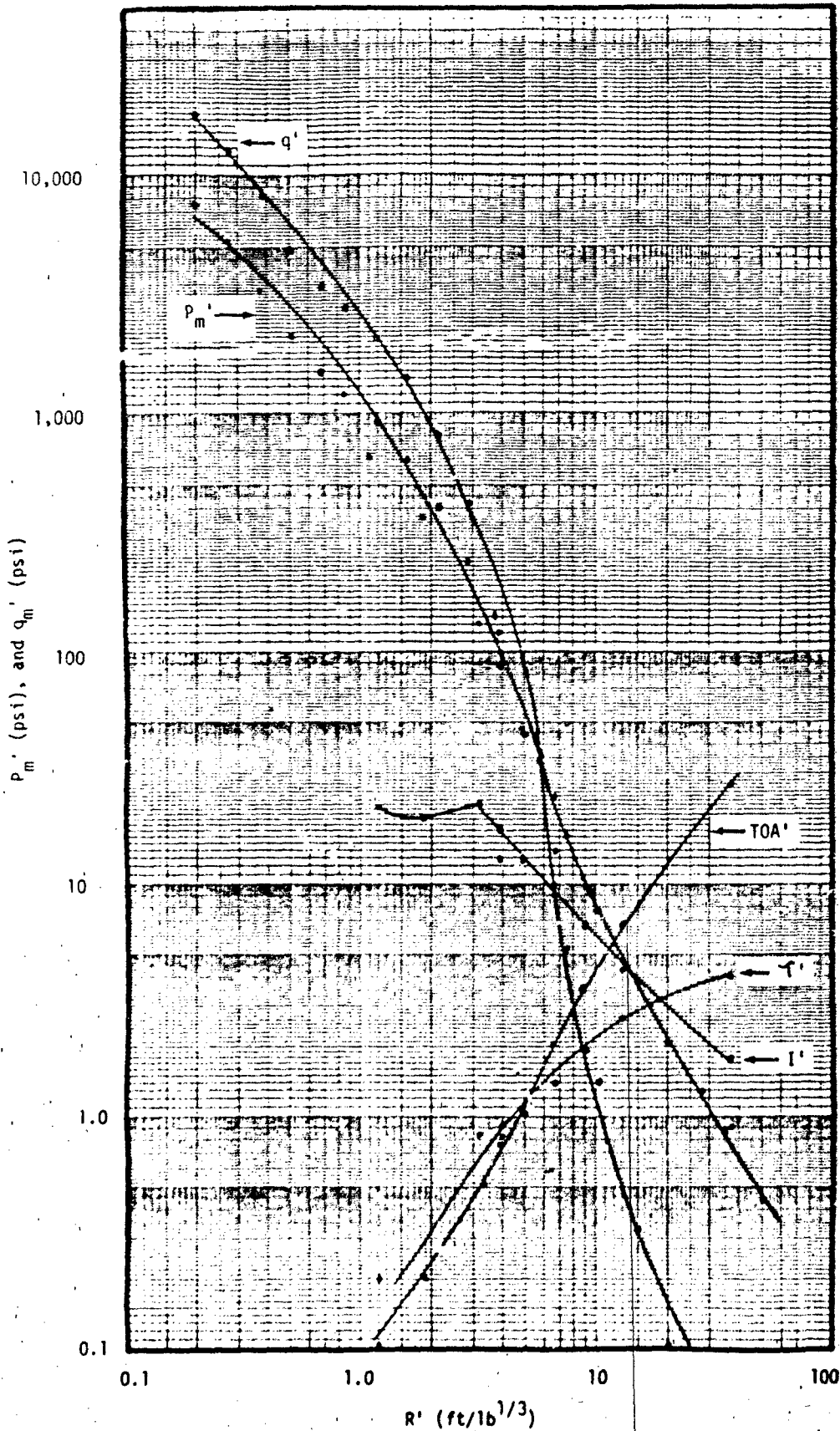


TABLE 4-4. ANFO IV AIRBLAST DATA (Continued)

B. DRES Data Derived from ABTOAD Line (Reference 8)

As Measured			Scaled to Standard Conditions		
R ft	P _m psi	q _m psi	R' ft/lb ^{1/3}	P' _m psi	q' _m psi
7.42	7,007	17,160	0.19	7,530	18,440
10.25	4,851	11,810	0.27	5,213	12,691
13.87	3,156	7,605	0.37	3,391	8,172
18.92	1,961	4,644	0.51	2,107	4,990
25.75	1,387	3,222	0.69	1,490	3,462
32.63	1,125	2,574	0.86	1,209	2,766
44.34	861.3	1,925	1.17	925.6	2,069
60.34	616.0	1,324	1.58	622.0	1,423
82.10	374.0	740.0	2.17	401.9	795.2
103.7	224.9	392.3	2.76	241.7	421.6
140.8	103.0	132.9	3.72	110.7	142.8
191.6	41.89	31.76	5.07	45.02	34.13
281.9	14.77	4.92	7.46	15.87	5.29
383.6	7.38	1.32	10.15	7.93	1.42
563.7	3.52	0.31	14.93	3.79	0.34
767.4	2.00	0.10	20.30	2.15	0.11
1,044	1.19	0.04	27.62	1.28	0.04
1,316	0.81	0.02	34.80	0.87	0.02
1,934	0.42	0.005	51.20	0.45	0.005



TOA' (ms/lb^{1/3}), I' (ms/lb^{1/3}), and I' (psi ms/lb^{2/3})

FIGURE 4-8. REDUCED AIRBLAST PARAMETERS FOR ANFO IV. SCALED TO SEA LEVEL CONDITIONS.

TABLE 4-5. ANFO V AIRBLAST DATA
(25-Ton Spherical Charge, Half Buried, Bagged)

A. BRL Data (Reference 7)

As Measured						Scaled to Standard Conditions					
R	TOA*	P _m	r _m	I	I'	R'	TOA'	P' _m	r' _m	I'	
FT	ms	psi	ms	psi-ms	psi-ms	ft/lb ^{1/3}	lb ^{1/3}	psi	ms/lb ^{1/3}	lb ^{1/3}	
105	--	116.	47.5	736		2.82	--	126.31	1.27	21.39	
180	--	35.2	43.7	352		4.83	--	38.3	1.17	10.23	
230	--	17.8	63.8	281		6.17	--	19.4	1.70	8.86	
310	--	11.8	62.2	207		8.31	--	12.8	1.66	6.02	
400	--	7.2	108.	253		10.73	--	7.8	2.88	7.35	
1,000	--	2.0	157.	107		26.82	--	2.2	4.19	3.11	

*Records obtained with self-recording gages; TOA not available.



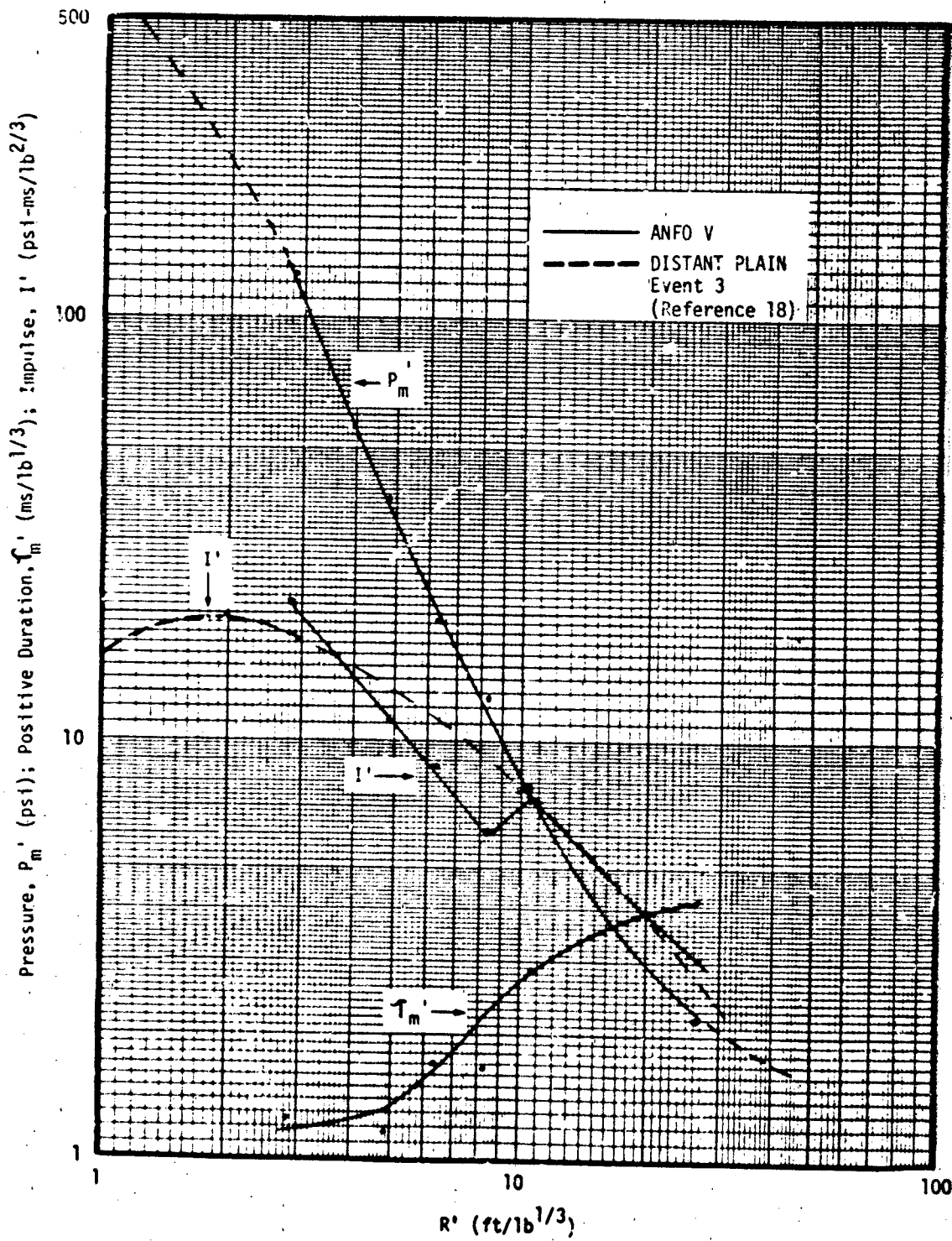


FIGURE 4-9. REDUCED AIRBLAST PARAMETERS FOR ANFO V. SCALED TO SEA LEVEL CONDITIONS.

TABLE 4-6. PRE-DICE THROW I-4 AIRBLAST DATA
 (6-Ton Domed Cylinder, L/D = 0.75/1)

(Reference 9)		As Measured		Scaled to Standard Conditions	
R	P _m	R'	P' _m	R'	P' _m
ft	psi	ft/lb ^{1/3}	psi	ft/lb ^{1/3}	psi
21	2,200.	0.89	2,623.		
80	90.	3.37	107.3		
145	16.5	6.11	19.67		
145	16.8	6.11	20.03		
230	8.5	9.70	10.13		
230	7.5	9.70	8.94		

TABLE 4-7. PRE-DICE THROW II-2, AIRBLAST DATA (Continued)

SCALED TO STANDARD CONDITIONS												
R' FT/lb ^{1/3}	TOA'			P' psi			τ' ms/lb ^{1/3}			I'		
	"A"	"B"	"C"	"A"	"B"	"C"	"A"	"B"	"C"	"A"	"B"	"C"
0.60	0.04	0.04	0.04	1,839.56	1,529.59	2,182.92	--	--	--	--	--	--
1.06	0.08	0.08	0.08	964.49	1,103.98	940.65	0.13	--	0.13	20.18	--	21.03
1.66	0.15	0.15	0.15	530.53	540.07	536.49	0.21	0.18	0.15	20.78	19.27	18.16
2.41	0.27	0.28	--	342.16	344.55	--	0.35	0.30	--	19.04	19.40	19.43
3.77	0.60	0.56	0.61	123.99	153.79	121.60	0.74	0.93	0.62	18.27	17.59	16.29
3.77	0.59	--	--	127.57	--	--	0.62	--	--	18.86	--	--
4.90	1.03	0.95	1.02	51.50	52.10	--	1.04	1.07	1.05	13.10	12.17	13.16
5.80	1.47	1.40	--	33.14	28.37	--	1.23	1.31	--	10.85	10.97	--
5.80	1.47	--	--	32.90	--	--	1.22	--	--	10.99	--	--
8.75	3.34	3.29	3.35	10.01	10.25	--	1.88	1.92	1.86	7.26	7.26	7.10
8.75	3.34	--	--	10.85	--	--	1.83	--	--	7.30	--	--
12.67	6.27	--	--	5.13	--	--	1.97	--	--	4.64	--	--
12.67	6.27	--	--	5.25	--	--	2.41	--	--	5.16	--	--
16.89	9.62	--	9.61	4.41	--	--	2.75	--	2.59	3.78	--	3.84
16.89	9.62	--	--	4.53	--	--	2.75	--	--	3.94	--	--
36.19	26.01	--	--	1.55	--	--	3.26	--	--	1.68	--	--

TABLE 4-7. PRE-DICE THROW II-2, AIRBLAST DATA (Continued)

SCALED TO STANDARD CONDITIONS														
R' FT/lb ^{1/3}	TOA'			P' ^m			τ' ^m			I'				
	ms/lb ^{1/3}	"A"	"B"	ms/lb ^{1/3}	"A"	"B"	psi	"A"	"B"	"C"	ms/lb ^{1/3}	"A"	"B"	"C"
0.60	0.04	0.04	0.04	1,839.56	1,529.59	2,182.92	--	--	--	--	--	--	--	--
1.06	0.08	0.08	0.08	964.49	1,103.98	940.65	0.13	--	0.13	--	20.18	--	--	21.03
1.66	0.15	0.15	0.15	530.53	540.07	536.49	0.21	0.18	0.15	--	20.78	19.27	--	18.16
2.41	0.27	0.28	--	342.16	344.55	--	0.35	0.30	--	--	19.04	19.40	--	19.43
3.77	0.60	0.56	0.61	123.99	153.79	121.60	0.74	0.93	0.62	--	18.27	17.59	--	16.29
3.77	0.59	--	--	127.57	--	--	0.62	--	--	--	18.86	--	--	--
4.90	1.03	0.95	1.02	51.50	52.10	--	1.04	1.07	1.05	--	13.10	12.17	--	13.16
5.80	1.47	1.40	--	33.14	28.37	--	1.23	1.31	--	--	10.85	10.97	--	--
5.80	1.47	--	--	32.90	--	--	1.22	--	--	--	10.99	--	--	--
8.75	3.34	3.29	3.35	10.01	10.25	--	1.88	1.92	1.86	--	7.26	7.26	--	7.10
8.75	3.34	--	--	10.85	--	--	1.83	--	--	--	7.30	--	--	--
12.67	6.27	--	--	5.13	--	--	1.97	--	--	--	4.64	--	--	--
12.67	6.27	--	--	5.25	--	--	2.41	--	--	--	5.16	--	--	--
16.89	9.62	--	9.61	4.41	--	--	2.75	--	2.59	--	3.78	--	--	3.84
16.89	9.62	--	--	4.53	--	--	2.75	--	--	--	3.94	--	--	--
36.19	26.01	--	--	1.55	--	--	3.26	--	--	--	1.68	--	--	--

TABLE 4-7. PRE-DICE THROW II-2, AIRBLAST DATA (Continued)

B. Systems, Science and Software (SSS) Data (Reference 10)

As Measured			Scaled to Standard Conditions			
R ft	TOA ms	P _m psi	R' ft/1b ^{1/3}	TOA' ms/1b ^{1/3}	P' _m psi	
17.5	0.97	--	0.26	0.01	--	
21.5	1.20	--	0.34	0.02	--	
26.0	1.47	--	0.39	0.02	--	
40.5	2.52	--	0.61	0.04	--	
59.8	4.22	1,230.	0.90	0.06	1,466.41	
26.4	1.48	1,910.	0.40	0.02	2,277.10	

TABLE 4-8. MISERS BLUFF II-1, AIRBLAST DATA
(118-Ton Domed Cylinder, L/D = 0.75/1)

BRL Data (Reference 12)

AS MEASURED						
R	TOA	P_m	τ_m	I	q	I_q
ft	ms	psi	ms	psi ms	psi	psi ms
294.3	56.6	69.33	73.6	992.7	59.5	477.2
315.	64.8	49.31	64.8	765.0	--	--
338.	75.0	42.64	62.3	697.6	--	--
374.	92.4	28.72	81.5	614.9	--	--
374.	95.7	29.59	89.6	674.4	--	--
395.	104.	21.61	82.4	563.5	10.7	192.2
493.	164.	12.05	109.	467.0	4.2	105.9
571.	217.	8.31	123.	410.4	3.7	85.7
623.	254.	7.14	130.	373.5	0.9	31.2
692.	304.	5.64	127.	319.8	--	--
866.	436.	3.74	144.	229.9	0.5	27.3
1,129.	643.	2.81	151.	198.7	--	--
1,273.	760.	2.12	182.	168.2	0.4	28.6
1,745.	1,150.	1.42	207.	136.0	--	2.0
2,346.	1,660.	0.96	171.	67.4	--	--
2,920.	--	1.1	333.	--	--	--
5,414.	4,415.	0.29	264.	41.0	--	--

TABLE 4-8. MISERS BLUFF II-1, AIRBLAST DATA (Continued)

SCALED TO STANDARD CONDITIONS							
R'	TOA'	P' _m	τ _m	I'	q'	I' _q	
ft	ms/lb ^{1/3}	psi	ms/lb ^{1/3}	psi-ms/lb ^{1/3}	psi	psi-ms/lb ^{1/3}	
4.72	0.95	71.02	1.23	16.98	60.95	8.16	
5.06	1.08	50.51	1.08	13.09	--	--	
5.43	1.25	43.68	1.04	11.93	--	--	
6.0	1.54	29.42	1.36	10.52	--	--	
6.0	1.60	30.31	1.50	11.54	--	--	
6.34	1.74	22.14	1.38	9.64	10.96	3.29	
7.91	2.74	12.34	1.82	8.0	4.30	1.81	
9.17	3.62	8.51	2.05	7.02	3.79	1.47	
10.0	4.24	7.31	2.17	6.39	0.92	0.53	
11.1	5.08	5.78	2.12	5.47	--	--	
13.9	7.28	3.83	2.40	3.93	0.51	0.47	
18.12	10.74	2.88	2.52	3.40	--	--	
20.44	12.69	2.17	3.04	3.0	0.41	0.49	
28.01	19.20	1.45	3.46	2.33	--	0.03	
37.66	27.72	0.98	2.86	1.15	--	--	
46.88	--	1.13	5.56	--	--	--	
86.92	73.72	0.30	4.41	0.70	--	--	

TABLE 4-9. DICE IHKUM AIRBLASI DATA
(628-Ton Domed Cylinder, L/D = 0.75/1)

A. BRL Data, Line 1 (Reference 11)

AS MEASURED

R ft	TOA ms	P _m psi	τ _m ms	I psi ms	q psi	I _q psi ms
32.4	1.67	2,895.	8.82	13,035.	--	--
37.4	1.98	2,595.	8.57	11,570.	--	--
37.4	2.00	3,995.	--	--	--	--
113.	8.20	1,235.	--	--	--	--
113.	8.23	--	--	--	--	--
206.	19.6	487.	21.1	1,935.	--	--
250.	26.9	327.	28.2	1,820.	--	--
281.	32.8	339.	--	--	--	--
300.	36.6	268.	--	--	--	--
332.	43.4	199.	27.8	1,895.	--	--
350.	47.7	182.	--	--	--	--
400.	61.0	159.	--	--	--	--
440.	89.9	65.6	67.8	1,435.	87.0	1,445.
450.	77.0	80.2	68.3	1,435.	117.	2,165.
500.	95.0	70.6	98.4	1,165.	--	--
525.	104.	59.2	74.3	1,210.	--	--
540.	110.	52.5	119.	1,260.	67.4	2,395.
640.	156.	31.2	122.	1,005.	21.3	532.

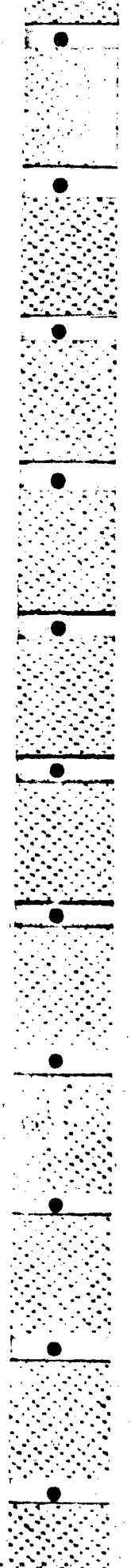
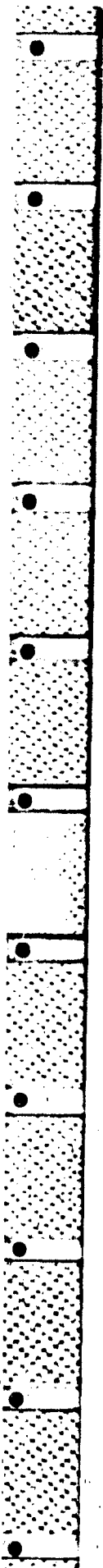


TABLE 4-9. DICE THROW AIRBLAST DATA (Continued)

AS MEASURED							
R	TOA	P _m	τ _m	I	q	I _q	
ft	ms	psi	ms	psi ms	psi	psi ms	
740.	210.	19.9	140.	820.	--	--	--
820.	257.	14.9	153.	704.	--	--	--
965.	352.	8.8	174.	587.	--	--	--
965.	352.	10.9	195.	741.	--	--	--
1,020.	390.	8.6	220.	678.	2.39	141.	--
1,140.	476.	6.7	235.	615.	--	--	--
1,230.	542.	6.1	240.	574.	1.17	81.9	--
1,370.	648.	5.8	249.	550.	--	--	--
1,730.	910.	4.0	290.	370.	.65	6.65	--
2,000.	1,125.	3.4	245.	312.	--	--	--
5,000.	3,690.	1.3	365.	105.	--	--	--
5,000.	3,690.	1.5	410.	154.	--	--	--
6,000.	4,510.	1.2	391.	114.	--	--	--



SCALED TO STANDARD CONDITIONS

R'	TOA'	P' _m	T' _m	I'	q'	I' _q
ft/lb ^{1/3}	ms/lb ^{1/3}	psi	ms/lb ^{1/3}	psl-ms/lb ^{1/3}	psf	psl-ms/lb ^{1/3}
0.28	0.01	3,451.42	0.08	135.13	--	--
0.33	0.02	3,093.76	0.07	119.94	--	--
0.33	0.02	4,762.84	--	--	--	--
1.00	0.07	1,472.37	--	--	--	--
1.00	0.07	--	--	--	--	--
1.81	0.17	580.60	0.18	20.06	--	--
2.19	0.23	389.85	0.25	18.87	--	--
2.47	0.29	404.16	--	--	--	--
2.63	0.32	319.51	--	--	--	--
2.91	0.38	237.25	0.24	19.64	--	--
3.07	0.41	216.98	--	--	--	--
3.51	0.53	189.56	--	--	--	--
3.86	0.78	78.21	0.59	14.88	103.72	14.98
3.95	0.67	95.61	0.59	14.88	139.49	22.44
4.39	0.83	84.17	0.86	12.08	--	--
4.61	0.90	70.58	0.65	12.54	--	--
4.74	0.96	62.59	1.03	13.06	80.35	24.83
5.62	1.36	37.20	1.06	10.42	25.39	5.51
6.50	1.83	23.72	1.22	8.50	--	--
7.20	2.23	17.76	1.33	7.30	--	--
8.47	3.06	10.49	1.51	6.09	--	--

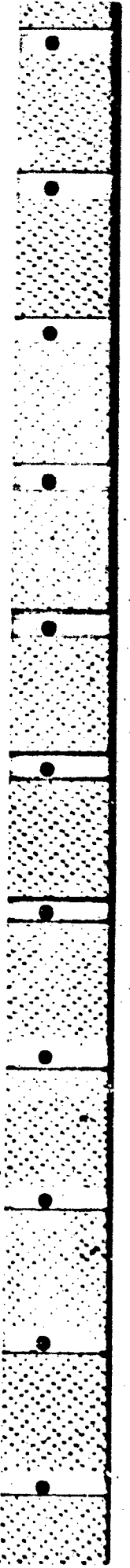


TABLE 4-9. DICE THROW AIRBLAST DATA (Continued)

SCALED TO STANDARD CONDITIONS							
R' ft/lb ^{1/3}	TOA' ms/lb ^{1/3}	P'_m psi	τ'_m ms/lb ^{1/3}	I' psf-ms/lb ^{1/3}	q' psf	I'_q psf-ms/lb ^{1/3}	
8.47	3.06	13.00	1.70	7.68	--	--	
8.95	3.39	10.25	1.91	7.03	2.85	1.46	
10.00	4.14	8.00	2.04	6.38	--	--	
10.80	4.71	7.27	2.09	5.95	1.39	0.85	
12.00	5.63	6.91	2.17	5.70	--	--	
15.19	7.91	4.77	2.52	3.84	.77	0.07	
17.56	9.78	4.05	2.13	3.23	--	--	
43.89	32.08	1.55	3.17	1.09	--	--	
43.89	32.08	1.79	3.56	1.60	--	--	
52.67	39.21	1.43	3.40	1.18	--	--	

B. BRL Data, Line 2 (Reference 11)

AS MEASURED							
R	TOA	P _m	τ _m	I	q	I _q	
ft	ms	psi	ms	psi ms	psi	psi ms	
32.4	1.72	2,970.	--	--	--	--	--
37.4	2.10	2,375.	--	--	--	--	--
113.	8.33	1,150.	30.	2,835.	--	--	--
206.	19.4	612.	14.0	1,820.	--	--	--
281.	32.4	322.	50.5	2,185.	--	--	--
300.	35.2	276.	68.1	2,155.	--	--	--
450.	74.8	93.5	62.3	1,430.	--	--	--
500.	84.4	90.1	104.	1,535.	48.3	844.	
540.	107.	49.6	97.3	1,145.	44.0	919.	
605.	118.	54.0	150.	1,060.	36.6	237.	
640.	143.	29.4	139.	1,030.	--	--	
740.	190.	11.0	177.	790.	--	--	
965.	354.	9.2	218.	739.	--	--	
3,000.	2,030.	2.0	386.	249.	--	--	
4,490.	3,330.	1.1	425.	133.	--	--	
5,000	3,780.	.8	385.	124.	--	--	
6,000	4,630.	.6	435.	127.	--	--	

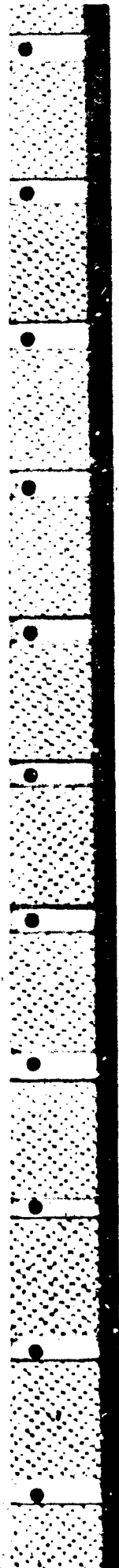


TABLE 4-9. DICE THROW AIRBLAST DATA (Continued)

SCALED TO STANDARD CONDITIONS							
R' ft/lb ^{1/3}	$\cdot TOA'$ ms/lb ^{1/3}	P'_m psf	τ'_m ms/lb ^{1/3}	I' psf-ms/lb ^{1/3}	q' psf	I'_q psf-ms/lb ^{1/3}	
0.28	0.02	3,540.83	--	--	--	--	
0.33	0.02	2,831.48	--	--	--	--	
0.99	0.07	1,371.03	0.26	29.39	--	--	
1.81	0.17	729.63	0.12	18.87	--	--	
2.47	0.28	383.89	0.44	22.65	--	--	
2.63	0.31	329.05	0.59	22.34	--	--	
3.95	0.65	111.47	0.54	14.82	--	--	
4.39	0.73	107.42	0.90	15.91	57.58	8.75	
4.74	0.93	59.13	0.85	11.87	52.46	9.53	
5.31	1.03	64.38	1.30	10.99	43.63	2.46	
5.62	1.24	35.05	1.21	10.68	--	--	
6.50	1.65	13.11	1.54	8.19	--	--	
8.47	3.08	10.97	1.90	7.66	--	--	
26.34	17.65	2.38	3.36	2.58	--	--	
39.42	28.95	1.31	3.70	1.38	--	--	
43.89	32.87	0.95	3.35	1.29	--	--	
52.67	40.26	.72	3.78	1.32	--	--	

C. BRL Data, Line 3 (Reference 11)

AS MEASURED

R	TOA	P _m	r _m	I	q	I _q
ft	ms	psf	ms	psf ms	psf	psf ms
37.4	1.92	1,710.	--	--	--	--
113.	8.06	946.	--	--	--	--
206.	19.4	472.	28.6	1,885	--	--
281.	32.3	223.	47.8	2,000	--	--
310.	38.0	200.	126.	2,030	--	--
332.	43.1	190.	102.	3,180	--	--
450.	75.9	98.6	70.1	1,515	--	--
540.	109.	57.0	93.4	738	--	--
470.	122.	43.5	119.	1,520	--	--
580.	126.	43.4	114.	1,160	31.6	365.
640.	155.	31.8	132.	1,060	20.2	463.
690.	176.	23.5	144.	905	--	--
680.	176.	31.3	148.	1,195	--	--
740.	208.	21.3	167.	855	8.44	80.6
820.	259.	12.7	198.	882	--	--
820.	258.	15.2	185.	995	--	--
850.	279.	12.5	190.	797	--	--
965.	358.	9.2	212.	711	3.48	124.

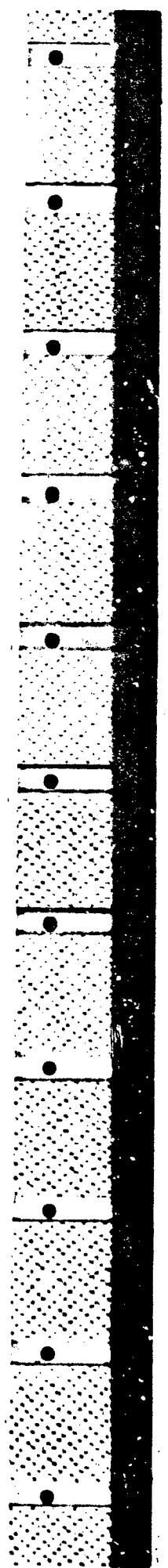


TABLE 4-9. DICE THROW AIRBLAST DATA (Continued)

AS MEASURED							
R	TOA	P _m	τ _m	I	q	I _q	
ft	ms	psi	ms	psi ms	psi	psi ms	
1,050.	419.	8.1	225.	767.	--	--	--
1,112.	465.	6.7	236.	646.	--	--	--
1,140.	485.	6.3	243.	632.	--	--	--
1,370.	661.	4.9	238.	487.	.56	56.3	
2,000.	1,170.	3.3	319.	482.	--	--	--
2,750.	1,805.	2.5	345.	276.	--	--	--
4,000.	2,895.	1.0	281.	183.	--	--	--
5,000.	3,775.	.9	319.	115.	--	--	--
6,000.	4,615.	.7	--	--	--	--	--
7,000	--	--	--	--	--	--	--

TABLE 4-9. DICE THROW AIRBLAST DATA (Continued)

SCALED TO STANDARD CONDITIONS							
R' ft/lb ^{1/3}	TOA' ms/lb ^{1/3}	P'_m psi	τ'_m ms/lb ^{1/3}	I' psi-ms/lb ^{1/3}	q' psi	I'_q psi-ms/lb ^{1/3}	
0.33	0.02	2,038.66	--	--	--	--	--
0.99	0.07	1,127.82	--	--	--	--	--
1.81	0.17	562.72	0.25	19.54	--	--	--
2.47	0.28	265.86	0.42	20.73	--	--	--
2.72	0.33	238.44	1.10	21.04	--	--	--
2.91	0.37	226.52	0.89	32.97	--	--	--
3.95	0.66	117.55	0.61	15.71	--	--	--
4.74	0.95	67.96	0.81	7.65	--	--	--
4.13	1.06	51.86	1.03	15.76	--	--	--
5.09	1.10	51.74	0.99	12.03	37.67	3.78	
5.62	1.35	37.91	1.15	12.03	24.08	4.80	
5.97	1.53	28.02	1.25	9.38	--	--	
5.97	1.53	37.32	1.29	12.39	--	--	
6.50	1.81	25.39	1.45	8.86	10.06	0.84	
7.20	2.25	15.14	1.72	9.14	--	--	
7.20	2.24	18.12	1.60	10.31	--	--	
7.46	2.43	14.90	1.65	8.26	--	--	
8.47	3.11	10.97	1.84	7.37	4.15	1.29	
9.22	3.64	9.67	2.00	7.95	--	--	
9.76	4.04	7.99	2.05	6.70	--	--	
10.01	4.22	7.51	2.11	6.55	--	--	

TABLE 4-9. DICE THROW AIRBLAST DATA (Continued)

SCALED TO STANDARD CONDITIONS							
R'	TOA'	P' _m	r' _m	I'	q'	I' _q	
ft/lb ^{1/3}	ms/lb ^{1/3}	psi	ms/lb ^{1/3}	psi-ms/lb ^{1/3}	psi	psi-ms/lb ^{1/3}	
12.03	5.75	5.84	2.07	5.05	.67	0.58	
17.56	10.17	3.93	2.77	5.00	--	--	
24.14	15.69	2.98	3.00	2.86	--	--	
35.11	25.17	1.19	2.44	1.90	--	--	
43.89	32.82	1.07	2.77	1.19	--	--	
52.67	40.13	.83	--	--	--	--	
61.45	--	--	--	--	--	--	

TABLE 4-10. MILL RACE AIRBLAST DATA
(600-Ton Domed Cylinder, L/D = 0.75/1)

BRL Data (Reference 15)

AS MEASURED

R ft	TOA ms	P _m psi	τ _m ms	I psi-ms
38.29	2.20	3,978.96	--	--
76.95	4.98	1,384.64	--	--
157.20	12.80	755.80	17.80	1,969.49
441.51	13.90	91.38	75.40	1,519.60
474.32	85.00	68.18	79.80	1,259.67
549.19	115.00	47.99	88.40	1,134.70
567.93	124.00	42.59	115.00	1,184.69
591.16	133.00	38.49	121.00	1,134.70
648.44	161.00	29.39	180.00	994.74
748.69	215.00	14.80	174.00	823.79
944.14	340.00	10.60	200.00	713.81
1,179.20	520.00	6.30	210.00	538.86
1,363.66	646.00	5.20	250.00	507.87
5,079.05	3,192.00	--	--	--
5,900.03	--	0.62	483.00	142.96
9,285.00	--	0.37	471.00	--
14,982.00	--	--	--	--
77.13	4.98	1,624.58	--	--

TABLE 4-10. MILL RACE AIRBLAST DATA (Continued)

BRL Data (Reference 15)

AS MEASURED

R ft	TOA ms	P _m psi	τ _m ms	I psi-ms
154.19	12.70	704.82	18.80	1,944.49
206.60	19.60	619.84	18.00	2,354.39
328.20	42.80	230.94	--	--
441.72	74.00	99.67	70.60	1,769.54
549.23	114.00	89.18	98.00	1,929.50
591.33	131.00	40.49	125.00	1,159.70
648.63	159.00	33.79	138.00	1,334.65
748.82	215.00	18.00	162.00	898.77
834.17	270.00	13.30	168.00	748.80
913.91	322.00	10.90	186.00	699.82
1,202.50	525.00	6.60	245.00	631.84
1,364.03	647.00	5.70	249.00	749.81
2,866.00	1,869.00	1.80	294.00	204.95
5,078.97	--	0.66	337.00	111.97
5,900.05	--	0.53	334.00	85.68
549.21	112.00	51.79	114.00	1,279.67
591.16	131.00	48.19	124.00	1,344.65
--	362.00	8.30	217.00	638.83
1,142.03	479.00	6.90	216.00	576.85
1,179.06	504.00	7.00	236.00	569.85
1,444.02	707.00	4.20	260.00	447.88

TABLE 4-10. MILL RACE AIRBLAST DATA (Continued)

BRL Data (Reference 15)

AS MEASURED

R ft	TOA ms	P _m psi	T _m ms	I psi-ms
1,854.09	1,033.00	2.80	386.00	476.88
2,090.11	1,348.00	2.80	--	--
32.84	1.45	5,693.52	--	--
55.82	3.40	1,624.58	--	--
78.76	5.76	1,319.66	--	--
98.39	6.86	1,224.68	--	--
131.14	9.70	1,007.49	13.7	1,829.52
206.73	19.60	501.87	20.7	1,794.53
275.63	31.50	293.92	37.1	1,989.48
328.13	42.30	217.94	--	--
98.4	6.56	1,399.64	17.2	2,804.27
131.20	10.30	912.76	--	--
206.75	19.90	478.88	22.7	1,844.52
275.51	31.80	259.93	37.8	1,849.52
328.14	48.60	262.93	--	--

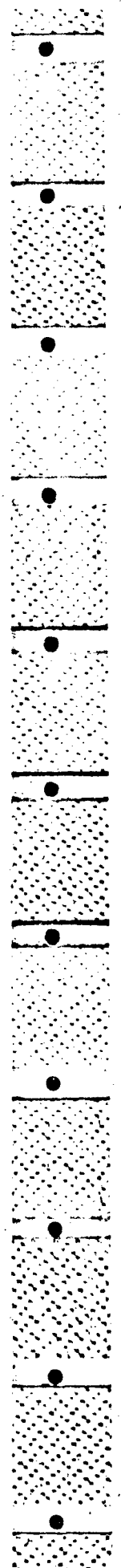


TABLE 4-10. MILL RACE AIRBLAST DATA
(600-Ton Domed Cylinder, L/D = 0.75/1)

BRL Data (Reference 15)

SCALED TO STANDARD CONDITIONS					
R'	TOA'	P' _m	τ' _m	I'	
ft	ms/lb ^{1/3}	psi	ms/lb ^{1/3}	psi-ms/l ^{1/3}	
0.34	0.02	4,709.50	--	--	--
0.69	0.05	1,638.86	--	--	--
1.40	0.12	894.56	0.16	21.09	
3.93	0.13	108.16	0.68	16.28	
4.22	0.77	80.70	0.72	13.49	
4.89	1.04	56.80	0.80	12.15	
5.06	1.12	50.41	1.04	12.69	
5.26	1.20	45.56	1.09	12.15	
5.77	1.46	34.79	1.63	10.65	
6.66	1.95	17.52	1.57	8.82	
8.40	3.08	12.55	1.81	7.65	
10.50	4.70	7.46	1.90	5.77	
12.14	5.84	6.15	2.26	5.44	
45.21	28.88	--	--	--	
52.52	--	0.73	4.37	1.53	
82.65	--	0.44	4.26	--	
133.36	--	--	--	--	
0.69	0.05	1,922.85	--	--	
1.37	0.11	834.23	0.17	20.83	
1.84	0.17	733.64	0.16	25.22	
2.92	0.39	273.34	--	--	

TABLE 4-10. MILL RACE AIRBLAST DATA (Continued)

BRL Data (Reference 15)

SCALED TO STANDARD CONDITIONS					
R'	TOA'	P'	r'	I'	
ft	ms/lb ^{1/3}	psf	ms/lb ^{1/3}	psf-ms/lb ^{1/3}	
3.93	0.67	117.97	0.64	18.95	
4.89	1.03	105.55	0.89	20.67	
5.26	1.19	47.92	1.13	12.42	
5.77	1.44	39.99	1.25	14.29	
6.67	1.95	21.30	1.47	9.63	
7.43	2.44	15.74	1.52	8.02	
8.14	2.91	12.90	1.68	7.50	
10.70	4.75	7.81	2.22	6.77	
12.14	5.85	6.75	2.25	8.03	
25.51	16.91	2.13	2.66	2.20	
45.21	--	0.78	3.05	1.20	
52.52	--	0.63	3.02	0.92	
4.89	1.01	61.30	1.03	13.71	
5.26	1.19	57.04	1.12	14.40	
--	3.28	9.82	1.96	6.84	
10.17	4.33	8.17	1.95	6.18	
10.50	4.56	8.29	2.14	6.10	
12.85	6.40	4.97	2.35	4.80	
16.50	9.35	3.31	3.49	5.11	
16.61	12.20	3.31	--	--	
0.29	0.01	6,738.85	--	--	

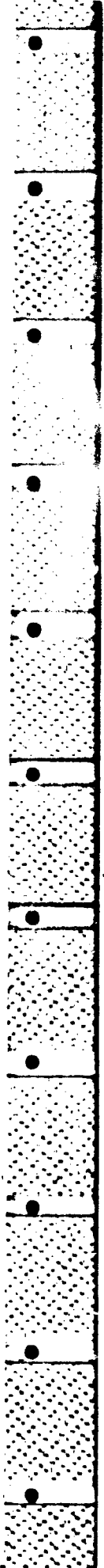


TABLE 4-10. MILL RACE AIRBLAST DATA (Continued)

BRL Data (Reference 15)

SCALED TO STANDARD CONDITIONS					
R' \dot{r}_t	TOA' $ms/lb^{1/3}$	P'_m psi	τ'_m $ms/lb^{1/3}$	I' $psi-ms/lb^{1/3}$	
0.50	0.03	1,922.85	--	--	--
0.70	0.05	1,561.95	--	--	--
0.88	0.06	1,449.53	--	--	--
1.17	0.09	1,192.47	0.12	19.59	
1.84	0.18	594.01	0.19	19.22	
2.45	0.29	347.88	0.34	21.31	
2.92	0.38	257.95	--	--	
0.88	0.06	1,656.61	0.16	30.03	
1.17	0.09	1,080.34	--	--	
1.84	0.18	566.80	0.21	19.76	
2.45	0.29	307.65	0.34	19.80	
2.92	0.44	311.20	--	--	

There appears to be some question as to whether the MISERS BLUFF II-1 charge detonated properly. Teel (Reference 12) questions the detonation of the charge because the peak pressures under about 50 psi fall below a predicted curve; the other blast parameters, however, meet predictions. Wisotski (Reference 13) deduces poor detonation from photographic evidence, and Swisdak (Reference 14) calculates the yield of MISERS BLUFF II-1 (on the basis of peak pressures) in megacalories/lb to be about 25 percent lower than the average of the other large MISERS BLUFF II cylindrical charges. Regardless of these doubts, the MISERS BLUFF II-1 reported data are presented, reduced, and plotted because as a single shot, the results are not disparate with single shot histories; the peak pressures fall within the normal scatter exhibited on any large shot.

For all the domed cylindrical charges considered, the airblast parameters as a function of distance, reduced and scaled to standard sea level conditions, are plotted in the following figures:

- Figure 4-10 Reduced Peak Pressure, P_m
- Figure 4-11 Reduced Time of Arrival, TOA
- Figure 4-12 Reduced Positive Phase Duration, τ_m
- Figure 4-13 Reduced Positive Impulse, I
- Figure 4-14 Reduced Dynamic Pressure, q
- Figure 4-15 Reduced Dynamic Pressure Impulse, I_q

As with the graphs for the hemispherical and spherical charges, so on Figures 4-10 through 4-15 for the domed cylindrical charges, lines are faired through the data points by eye. The points are plotted for all the data in Tables 4-6 through 4-10, which cover a range of shots with nominal yields from 6 to 620 tons -- a scale factor of almost 5. Obviously there is scatter in the plots, more for some parameters of the blast wave than for others. But there is no doubt that the data scale for the five charges considered.

Looking at the graphs individually, Figure 4-10 for pressure, shows the usual larger scatter at the higher and lower pressure levels than at the mid-range pressures. The lower pressure level scatter can be attributed to unrecorded variations in the local environment of the far out measuring stations; wind effects, particularly, can influence the strength of the blast

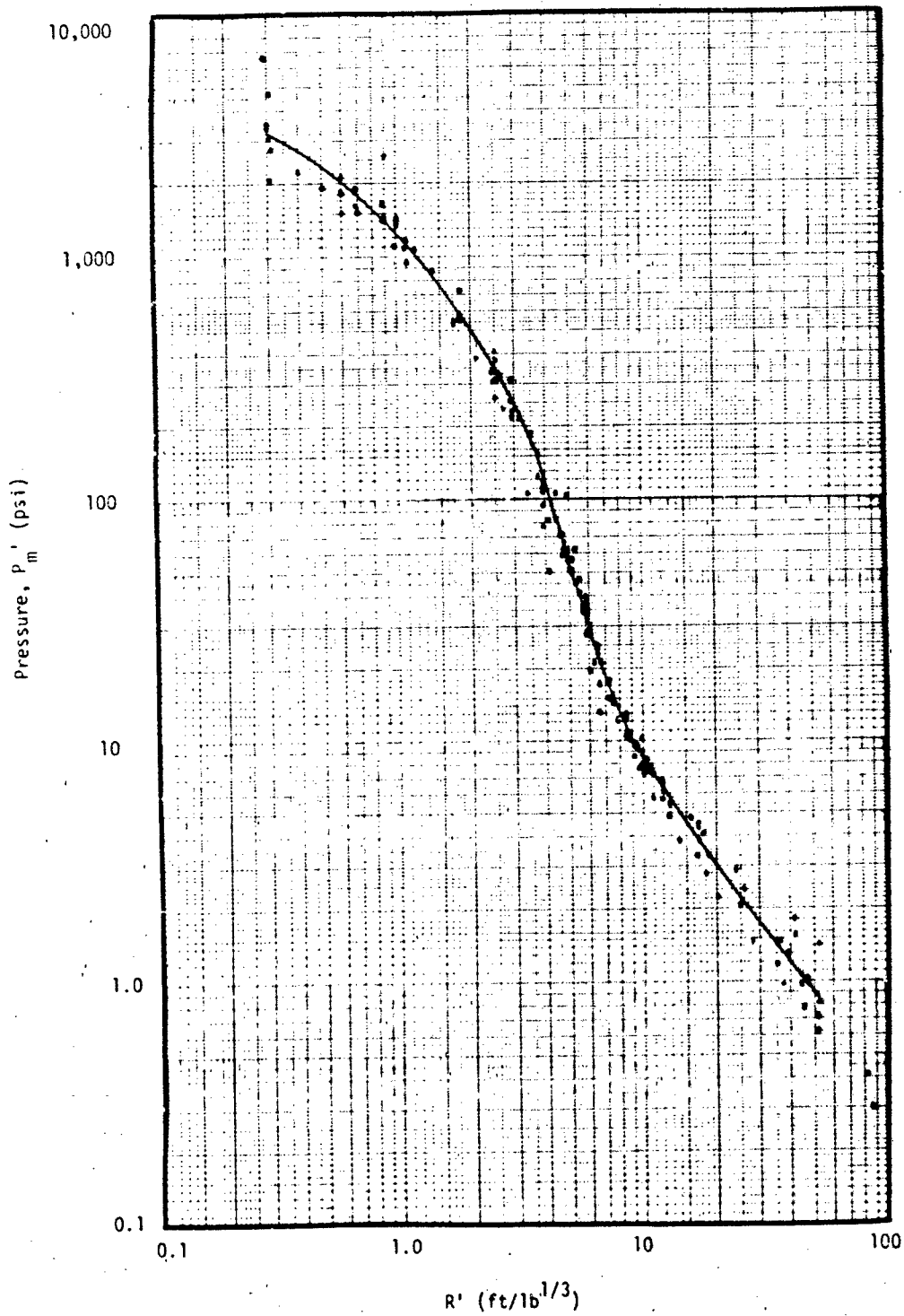


FIGURE 4-10: REDUCED PRESSURE FOR DOMED CYLINDERS ($L/D = 0.75/1$).

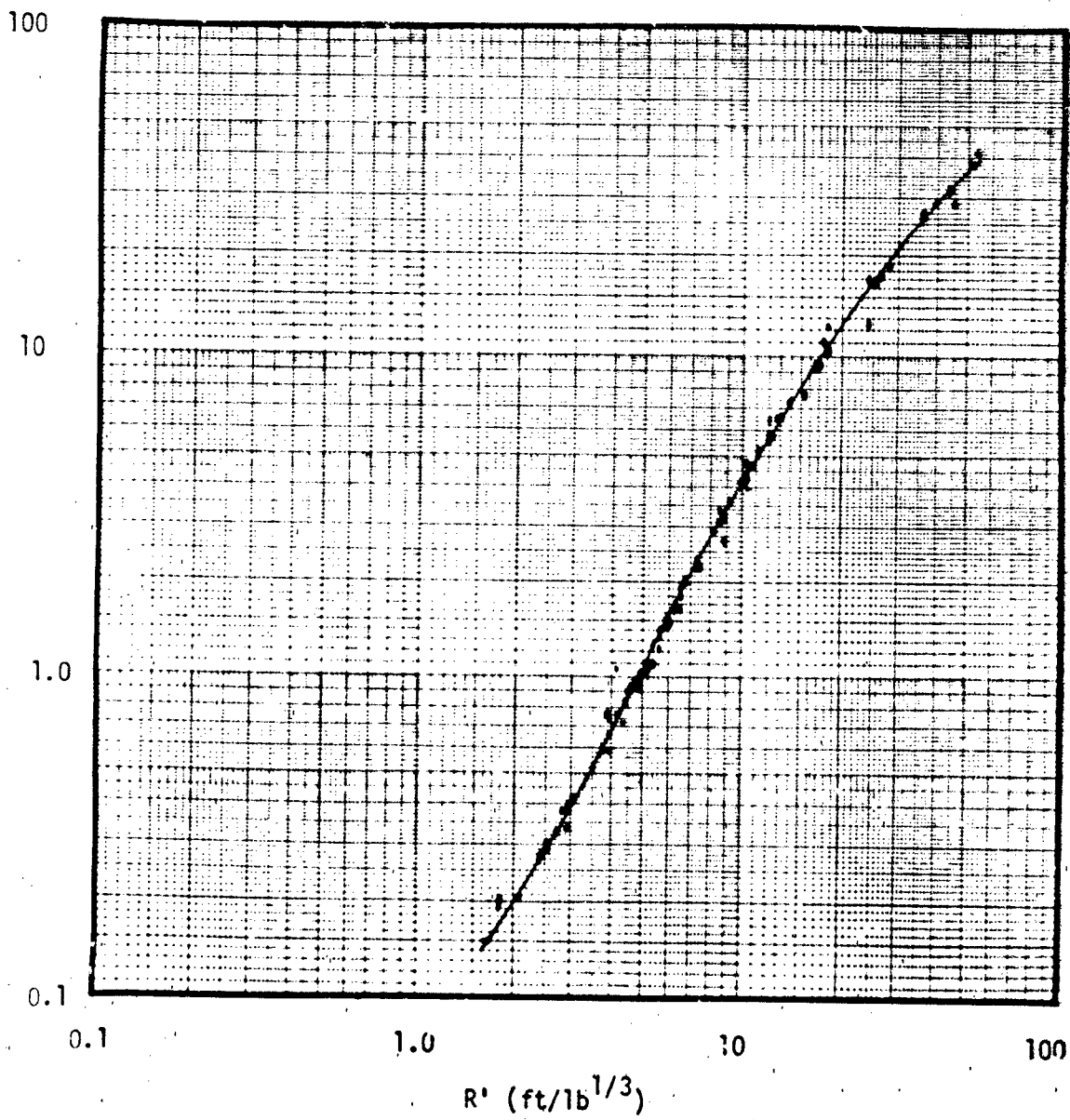
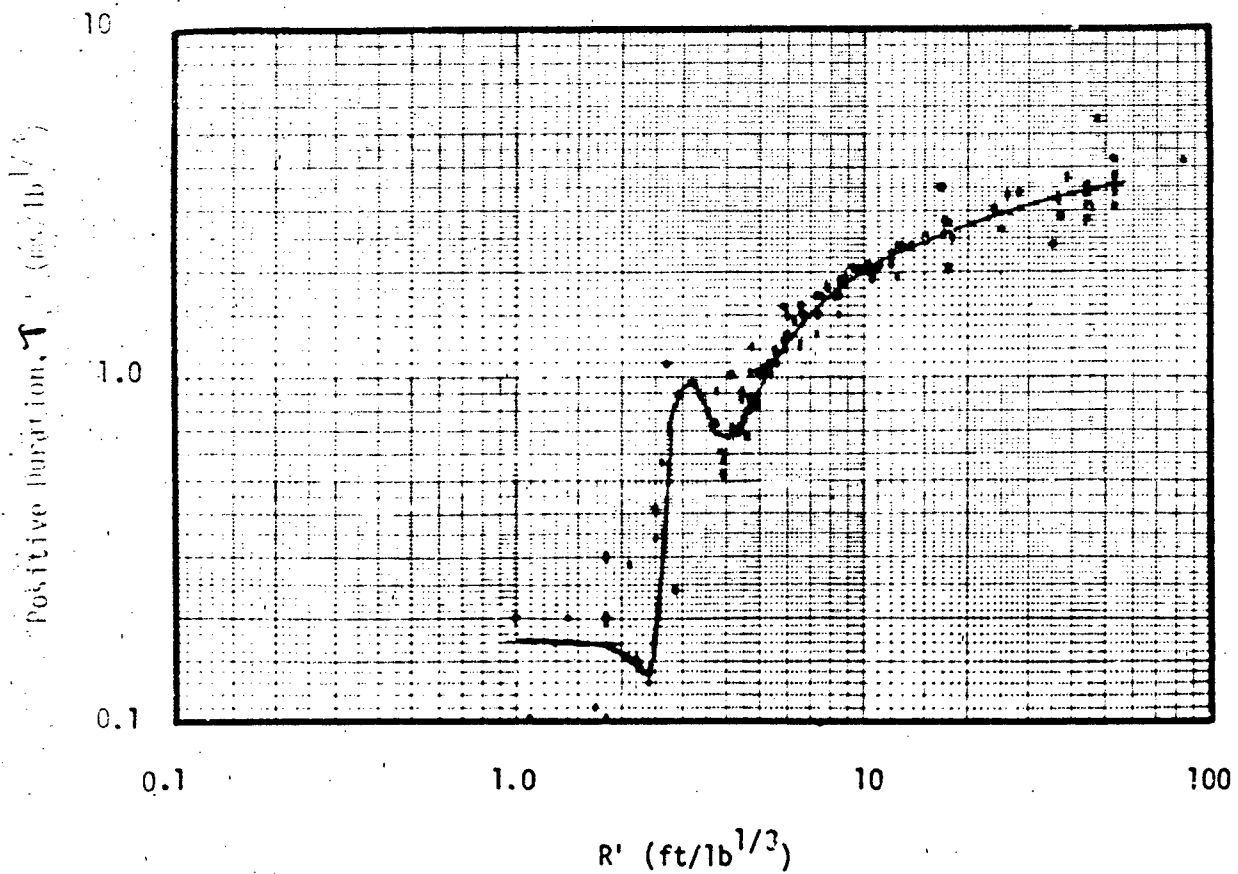
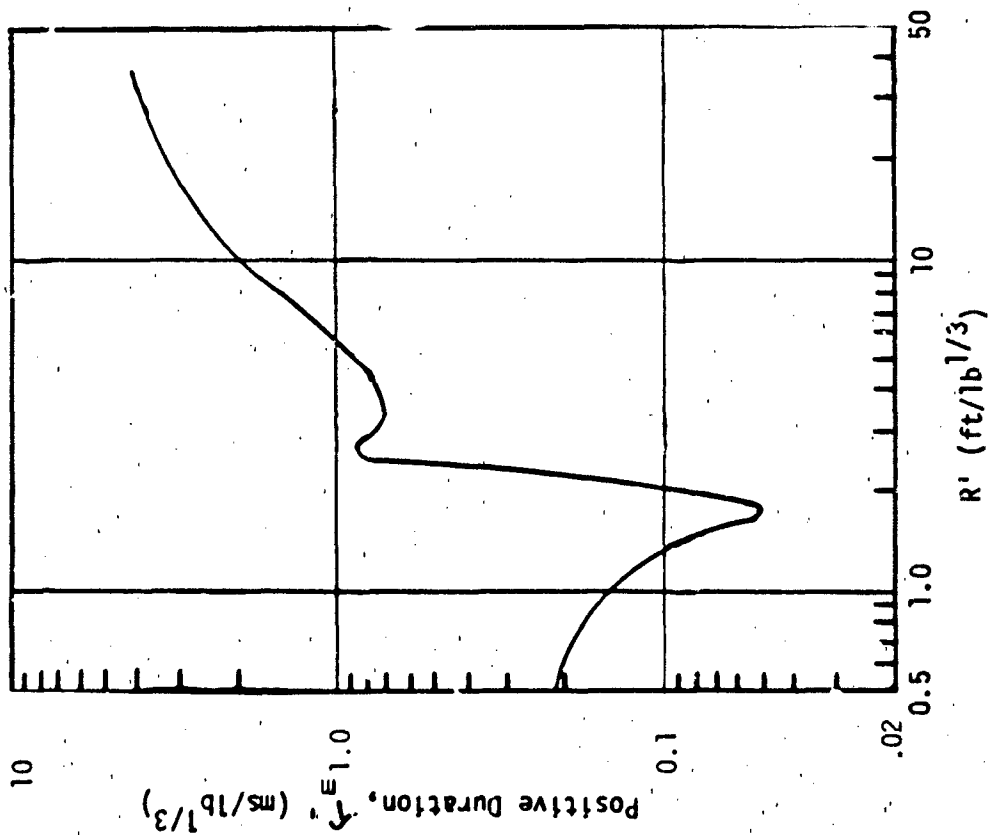


FIGURE 4-11. REDUCED TIME OF ARRIVAL FOR DOMED CYLINDERS ($L/D = 0.75/1$).

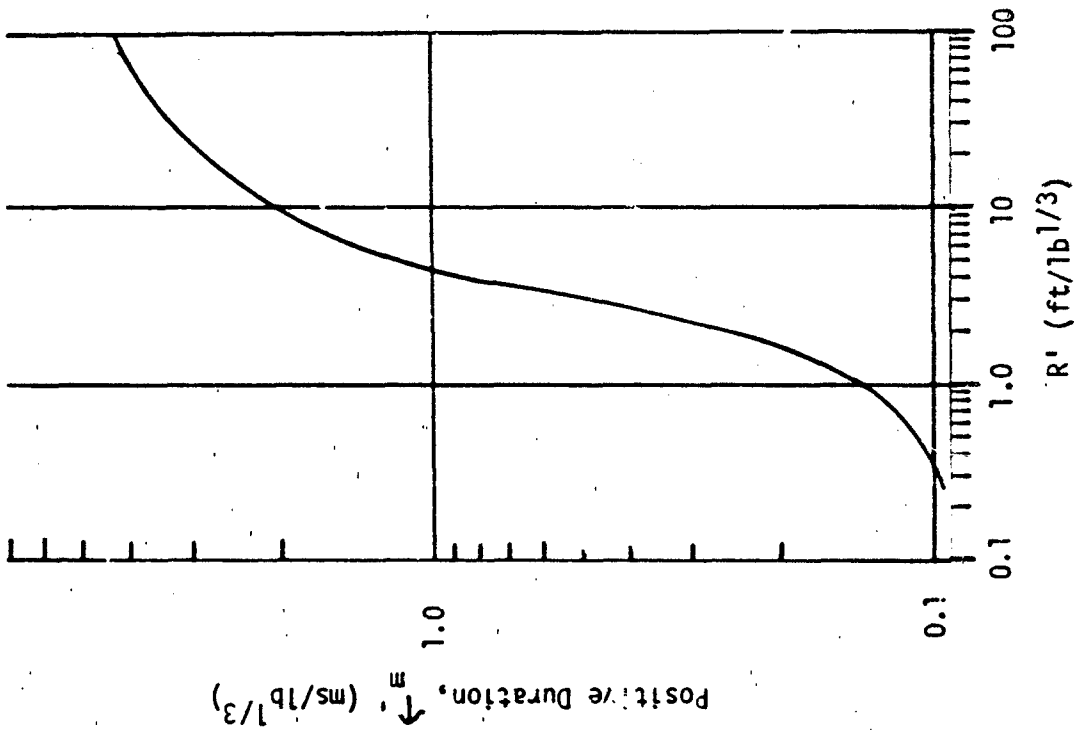


a) Compiled Data

FIGURE 4-12. REDUCED POSITIVE DURATION FOR DOMED CYLINDERS (L/D = 0.75/1).

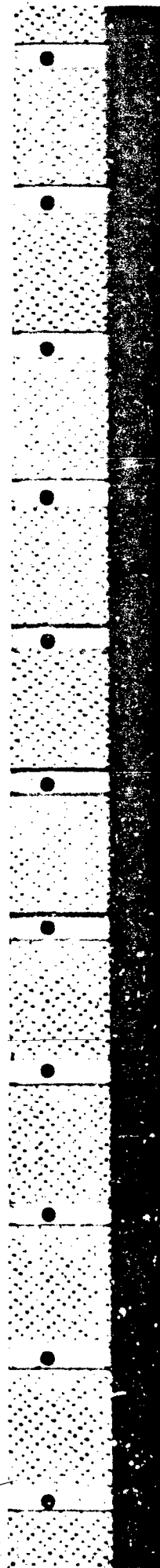


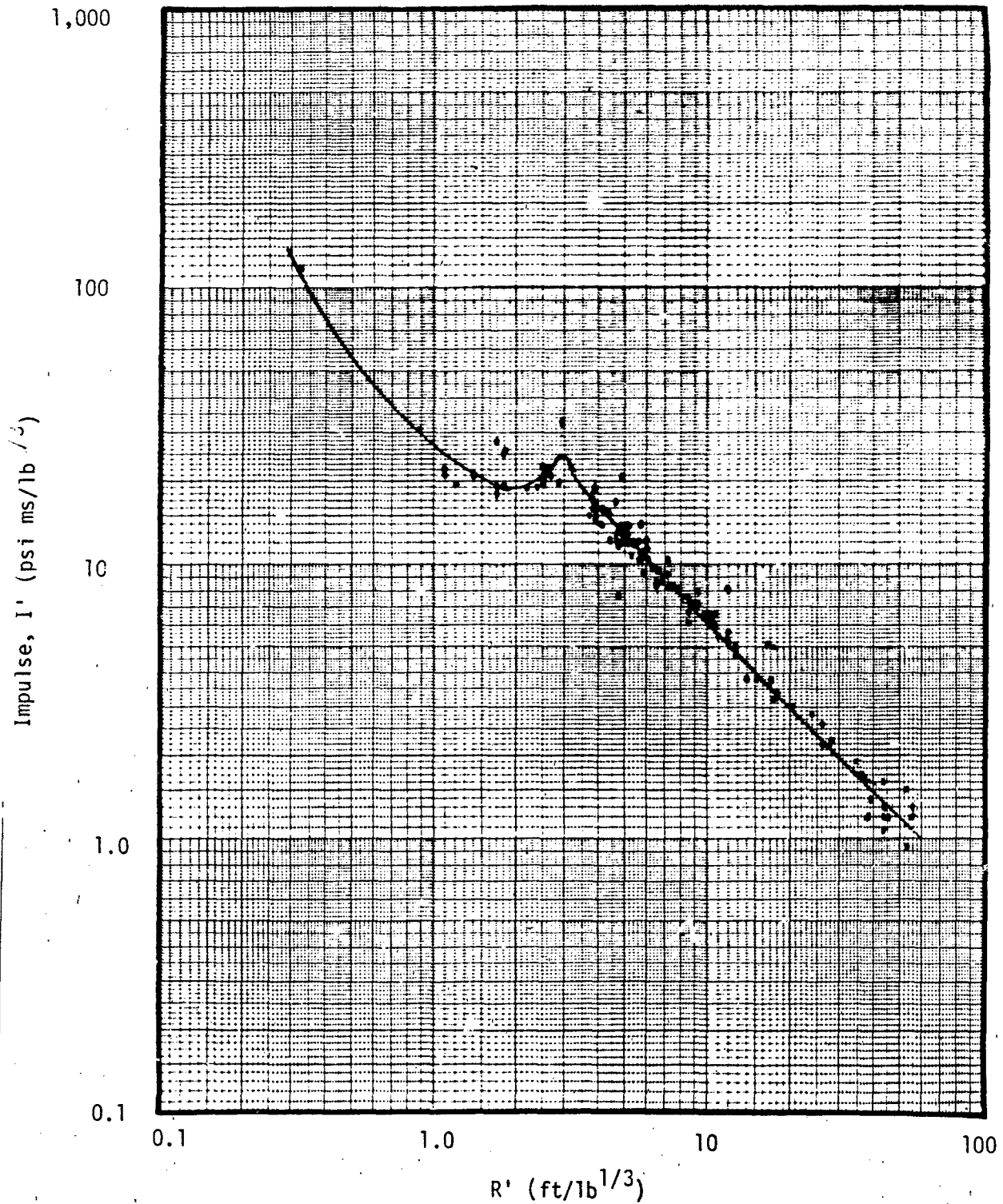
b) Predicted Curve for DICE THROW



c) Predicted Curve for MILL RACE

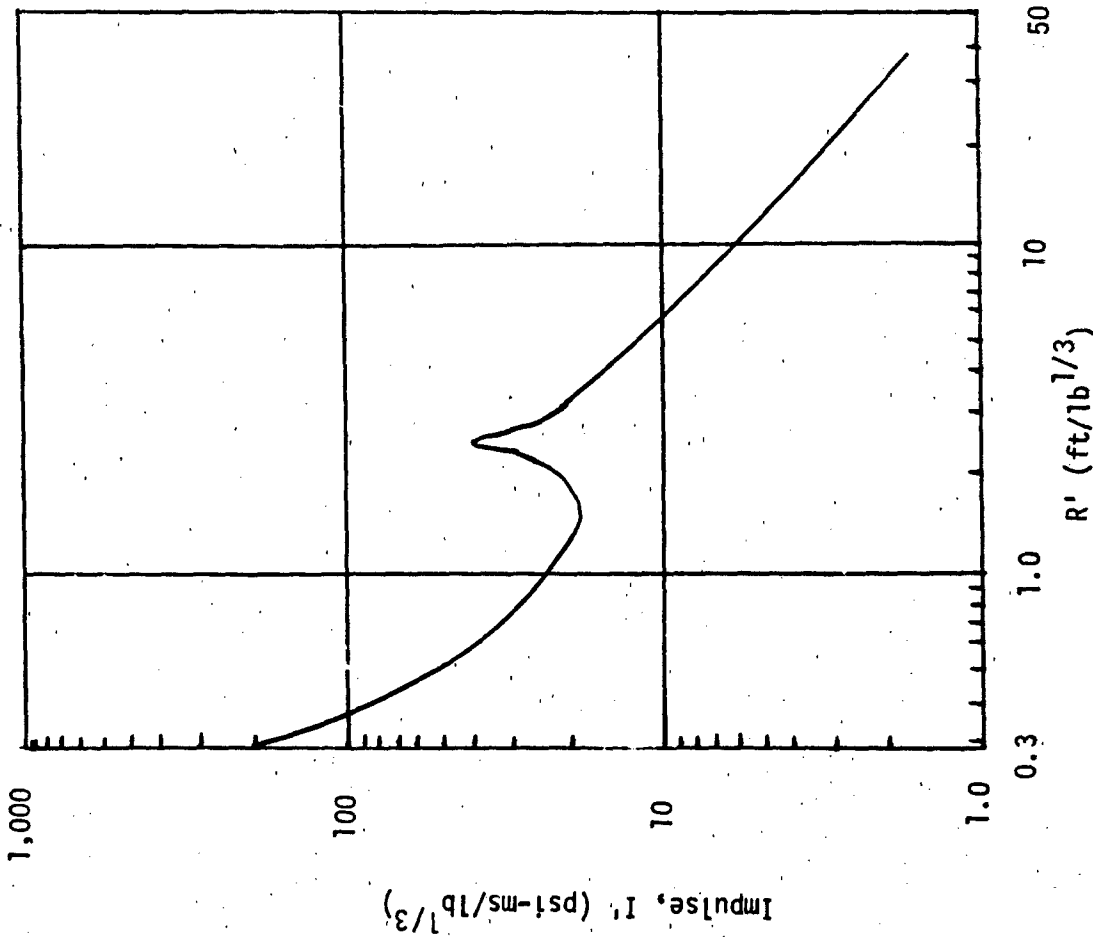
FIGURE 4-12. REDUCED POSITIVE DURATION FOR DOMED CYLINDERS (L/D = 0.75,1) (CONTINUED).



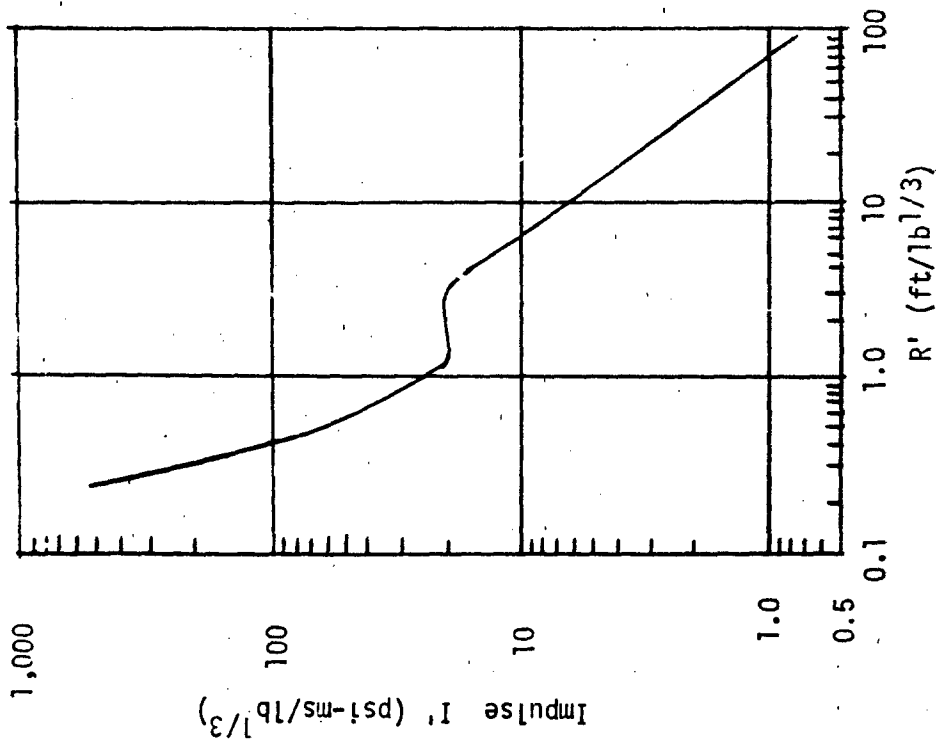


a) Compiled Data

FIGURE 4-13. REDUCED IMPULSE FOR DOMED CYLINDERS (L/D = 0.75/1).



b) Predicted Curve for DICE THROW



c) Predicted Curve for MILL RACE

FIGURE 4-13. REDUCED IMPULSE FOR DOMED CYLINDERS (L/D = 0.75/1) (CONTINUED).

1,000

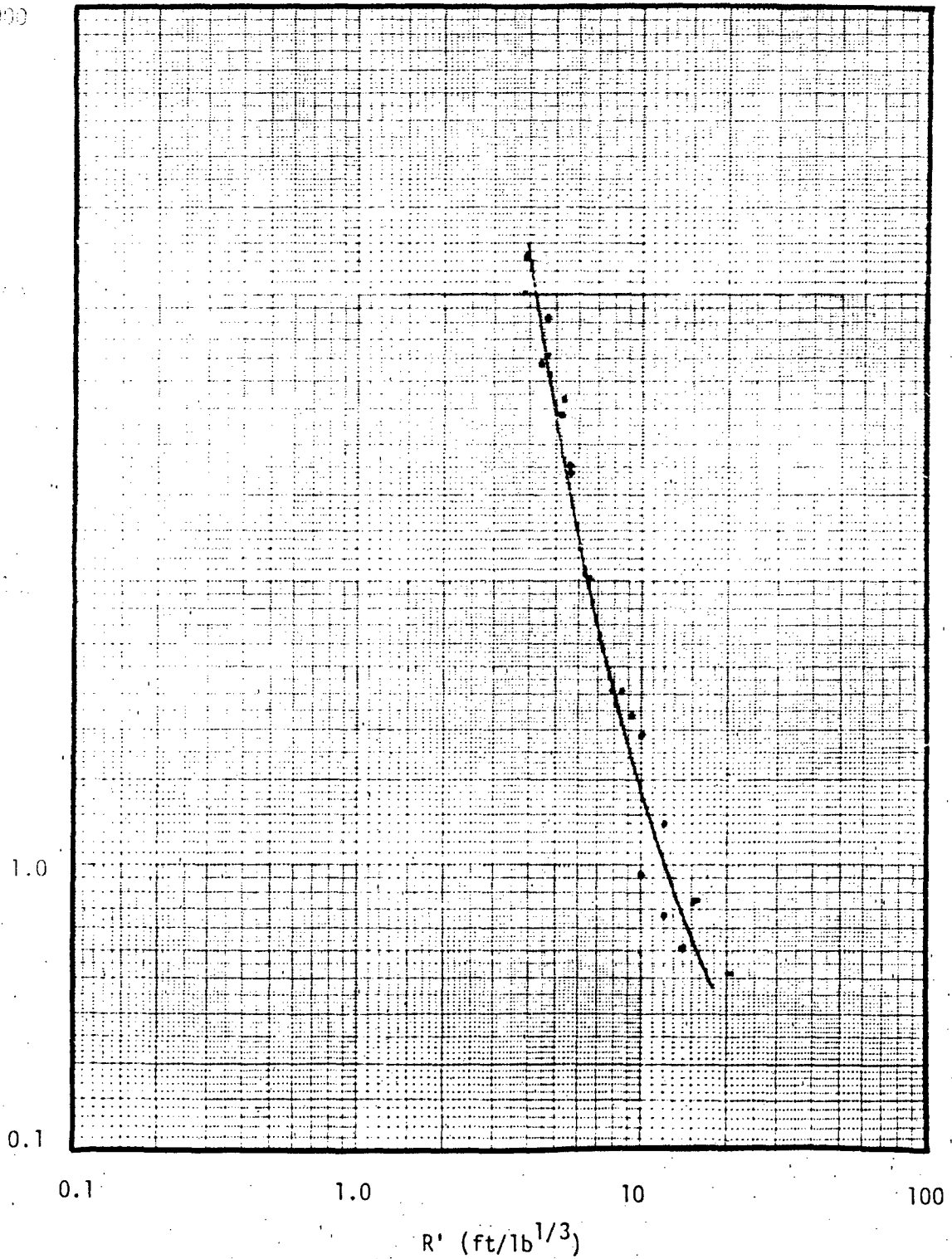


FIGURE 4-14. REDUCED DYNAMIC PRESSURE FOR DOMED CYLINDERS ($L/D = 0.75/1$).

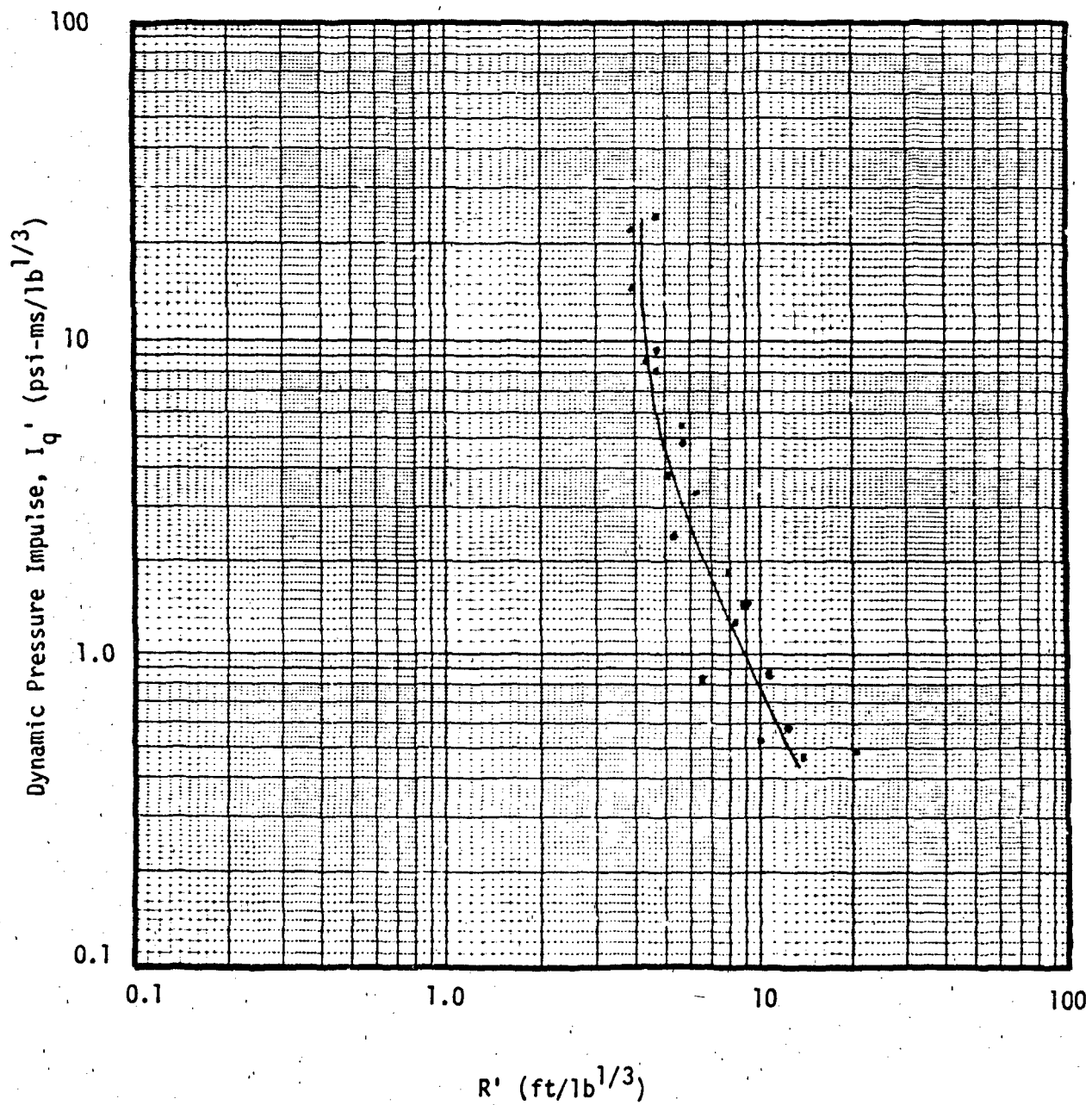


FIGURE 4-15. REDUCED DYNAMIC PRESSURE IMPULSE FOR DOMED CYLINDERS (L/D = 0.75/1).

at the low levels. At the highest pressures measured close-in to the charge, real pressure variations can occur because of irregularities in the initial blast front caused by many factors including high velocity jets of detonation products. Reduced time of arrival data as a function of distance, Figure 4-11, shows the least scatter of all the parameters; this arises primarily because there is little ambiguity in the records as to when the sharply rising blast wave arrives at the measuring station.

The positive phase duration, Figure 4-12a), shows considerably more scatter particularly at the close-in distances. As compared to the arrival time measurements, it is quite often difficult to determine when the positive phase ends, when the pressure wave reaches ambient levels initially; so scatter creeps in the plot. The faired curve shows two cusps, one at the scaled distance of about 4, the other at a scaled distance of about 1.5. The drawing of this curve was guided largely by the curve predicted for DICE THROW by AFWL and BRL on hydrocode and empirical data bases (Reference 11). Figure 4-12b) shows the DICE THROW predicted curve reduced to standard conditions to facilitate comparison with Figure 4-12a). Note, however, Figure 12c); this is the reduced prediction curve for the MILL RACE event, a charge with the same geometry and weight as the DICE THROW charge. The differences in these two curves are readily evident with no cusp predicted for MILL RACE. Which is the best prediction curve? On the basis of all the data available, the faired line in Figure 4-12a) can be used with the same degree of confidence -- maybe more -- than the hydrocode based curves in Figure 4-12b) and c).

The reduced impulse curve, Figure 4-13, also shows a cusp similar to the one predicted for DICE THROW (Figure 13a)). Again, there are marked differences between the DICE THROW (Figure 13b)) and MILL RACE (Figure 13c)) prediction curves. And, again, it is recommended that the Figure 4-13a) curve be used for prediction purposes.

The dynamic pressure and dynamic pressure impulse curves, Figures 4-14 and 4-15 respectively, show nothing of particular note; there is no disparity between them and the DICE THROW hydrocode predictions.

4.2.5 Airblast Summary

There is a large quantity of experimentally derived data points for various airblast parameters obtained on tests with hemispherical, spherical, and domed cylindrical charges. Through scaling procedures, these data permit the construction of effects curves which can be used with confidence to represent what has been measured and which can be used for prediction purposes. It can be fully expected that if all the important parameters of a test are modeled to the conditions under which the plotted data were obtained, the new data will fall within the scatter shown in Figures 4-10 through 4-15.

4.3 CRATER RESULTS

4.3.1 General

Data on the craters produced by several of the large ANFO shots are presented in this section. In contrast to the extensive use of scaling to compare the airblast parameters for ANFO shots, only a modest use of scaling is employed here to compare craters. This is so for several reasons. One, the reproducibility of craters under the best of replicate and modeled conditions produces 10 percent variations in crater dimensions (see Section 1.4.2); under field conditions, a scatter of 20-25 percent is common. If data are sparse, the large scatter clouds the validity of the scaling process. Two, ANFO crater data are indeed sparse making statistical approaches difficult. And three, there are several scaling procedures in vogue; some use the cube root of weight as a scaling factor (Reference 16), others use the 5/16 power of weight (Reference 17), and still others use more complicated formulas. Without exploring the merits of any of these methods, the cube root scaling procedure is employed in this section.

The size of an explosively generated crater depends on a) the energy released by the explosive, b) the shape of the charge, c) the position of the charge relative to the ground surface, d) the coupling of the charge to the ground, e) the ground material, and f) gravitational effects. On a large scale test the most difficult of these crater determining parameters to control, replicate, or even know, is the ground material. Soil or ground properties, e.g., material strength and moisture content, vary from site to site and even within a test site water table levels vary and lenses, stratification and other intrusions preclude a homogeneous ground medium.

This inhomogeneity leads to craters with irregular outlines although, in general, for surface burst charges, the craters are conical or bowl-like in shape. The irregularities lead to difficulties in measuring crater size and in reporting, simply in simple value terms, the crater dimensions. Figure 4-16 shows a typical crater profile. There are three craters of interest: the lip-to-lip crater, the apparent crater, and the true crater. In an elevation view, each of these craters would show irregular circular outlines. To report the apparent crater dimensions, for instance, several measurements are made of the diameter along different radial angles. Which diameter to report -- the largest diameter or the average diameter? In the reported data, it is not always clear as to what is reported; it is assumed here that it is the average. Similarly, with the depth of the crater: is it the maximum depth that is reported, or the depth directly under ground zero? There can be significant differences particularly if there is an upwelling in the center of the crater. And which crater, the true or apparent, is being measured? Unless otherwise indicated, it is assumed that it is the apparent crater that is measured because it is by far the easier to measure.

Another complication: the apparent crater size is influenced by the weather. As the figure indicates, the dimensions of the apparent crater are affected by the quantity of ground material falling back into the true crater (the true crater representing the material excavated by the explosion). The fallback is normally loose, unconsolidated material that responds to wind forces with increased fallback in the downwind direction. If the crater measurements are not made immediately after the shot, the apparent crater may change in size and shape because of slumping of the sides under its own weight or because of rain and wind erosion or the entrance of ground water into the cavity. So, it is not surprising that crater sizes show large variations one to another or on a scaled basis under the realities of field conditions.

4.3.2 Craters From Hemispherical Charges

During the development program for ANFO and test programs with TNT, several large charges were fired in the hemispherical configuration. A number of these charges were fired at the same test site so that comparisons could be made between ANFO and TNT craters and between charges of different weights. The

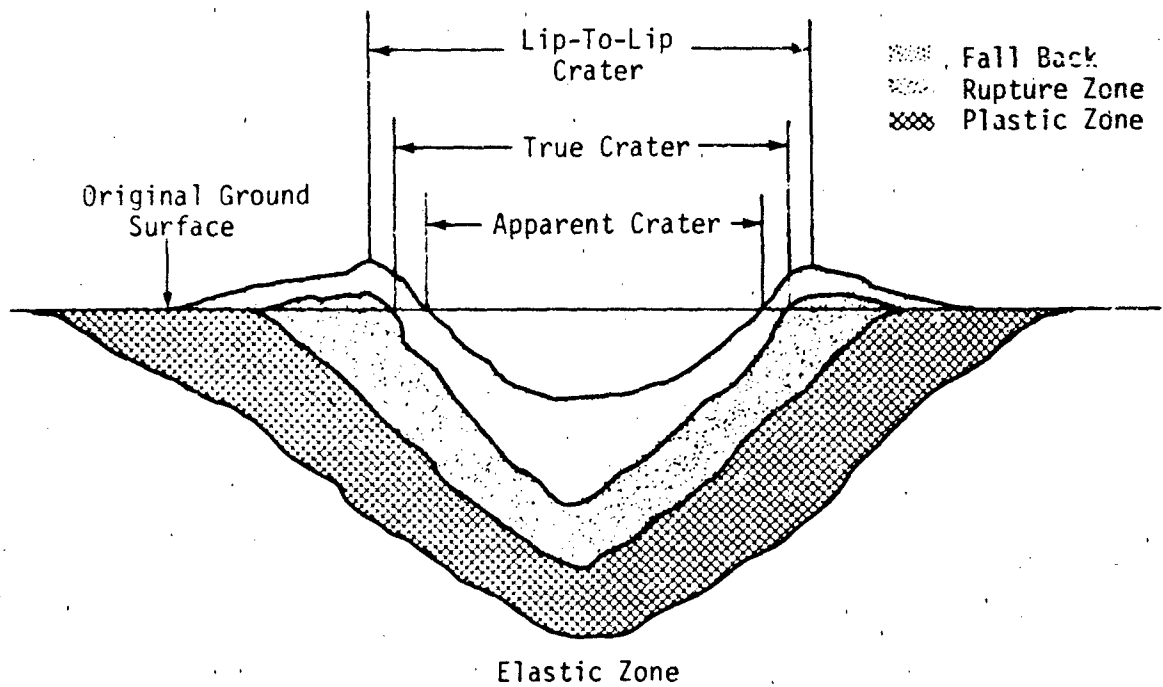


FIGURE 4-16. TYPICAL CRATER PROFILE.

reported crater dimensions are listed in Table 4-11. Mean crater profiles and dimensions for the 20 ton hemispherical events are shown in Figure 4-17 and in Figure 4-18 for the 100-ton events. The non-symmetries in the crater profiles and the differences in dimensions are evident in these figures. In Figure 4-17, there are evident differences between the two ANFO shots at the same location and differences between the ANFO charges and the TNT charge at this same site. The difference in ANFO crater depth may be attributable to some extent, to the groundwater that entered the ANFO I crater. There are differences of about the same magnitude between the two 20-ton TNT charges at the two different sites.

Notwithstanding the earlier comments about the scatter in crater dimensions, the average of the two 20 ton hemispherical ANFO events scale up very well to the 100 ton hemispherical ANFO shot fired at the same Watching Hill site.

$$\text{ANFO I and II - Average Diameter} = 67.85 \text{ ft} \times \frac{100}{20}^{1/3} = 115.35 \text{ ft}$$

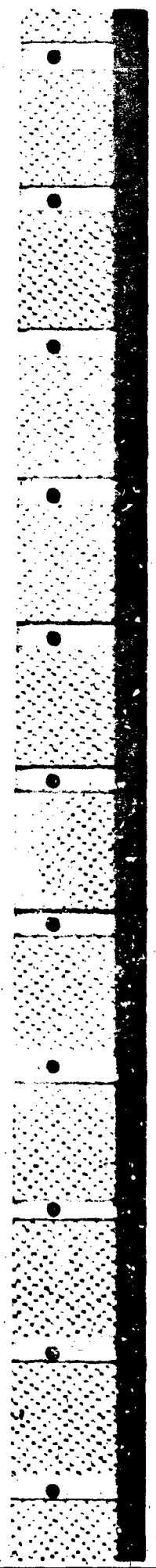
$$\text{ANFO III - Reported Diameter} = 115.8 \text{ ft}$$

$$\text{ANFO I and II - Average Depth} = 17.25 \text{ ft} \times \frac{100}{20}^{1/3} = 29.33 \text{ ft}$$

$$\text{ANFO III - Reported Depth} = 28.1 \text{ ft}$$

In contrast, the TNT craters do not scale as well. For instance, scaling up the 20-ton shot, DRES-FE535, data at Watching Hill to that of the 100-ton shot, DRES-FE538, also at Watching Hill, results in a calculated diameter of 127.16 ft and a depth of 24.65 ft; the reported dimensions for the 100-ton TNT shot were 153.9 ft and 19.9 ft for diameter and depth respectively. The average values of the crater dimensions of the two 20-ton TNT shots at the different sites do not scale up to 100 tons any better; the scaled values are 122.15 ft for diameter and 30.77 ft for depth. The differences between scaled and measured values, however, fall close to the 20-25 percent scatter usually found on tests.

SHOT	EXPLOSIVE	WEIGHT tons	SITE	APPARENT DIAMETER ft	LIP-TO-LIP DIAMETER ft	APPARENT DEPTH ft
<u>Hemispherical Charges</u>						
ANFO I	ANFO	20	Watching Hill	72.5	80.0	16.5
ANFO II	ANFO	20	Watching Hill	63.2	77.8	18.0
DRES-FE535	TNT	20	Watching Hill	74.8	87.2	14.5
DRES-FE556	TNT	20	Drowning Ford	68.9	91.9	21.7
ANFO III	ANFO	100	Watching Hill	115.8	154.0	28.1
DRES-FE538	TNT	100	Watching Hill	153.9	182.1	19.9
<u>Surface Tangent Spherical Charges</u>						
ANFO IV	ANFO	25	Watching Hill	49	--	9.5
DISTANT PLAIN 5a	TNT	20	Drowning Ford	59	--	10.5
<u>Half Buried Spherical Charges</u>						
ANFO V	ANFO	25	Drowning Ford	71	--	17.5
DISTANT PLAIN 3	TNT	20	Drowning Ford	73.5	--	15.5



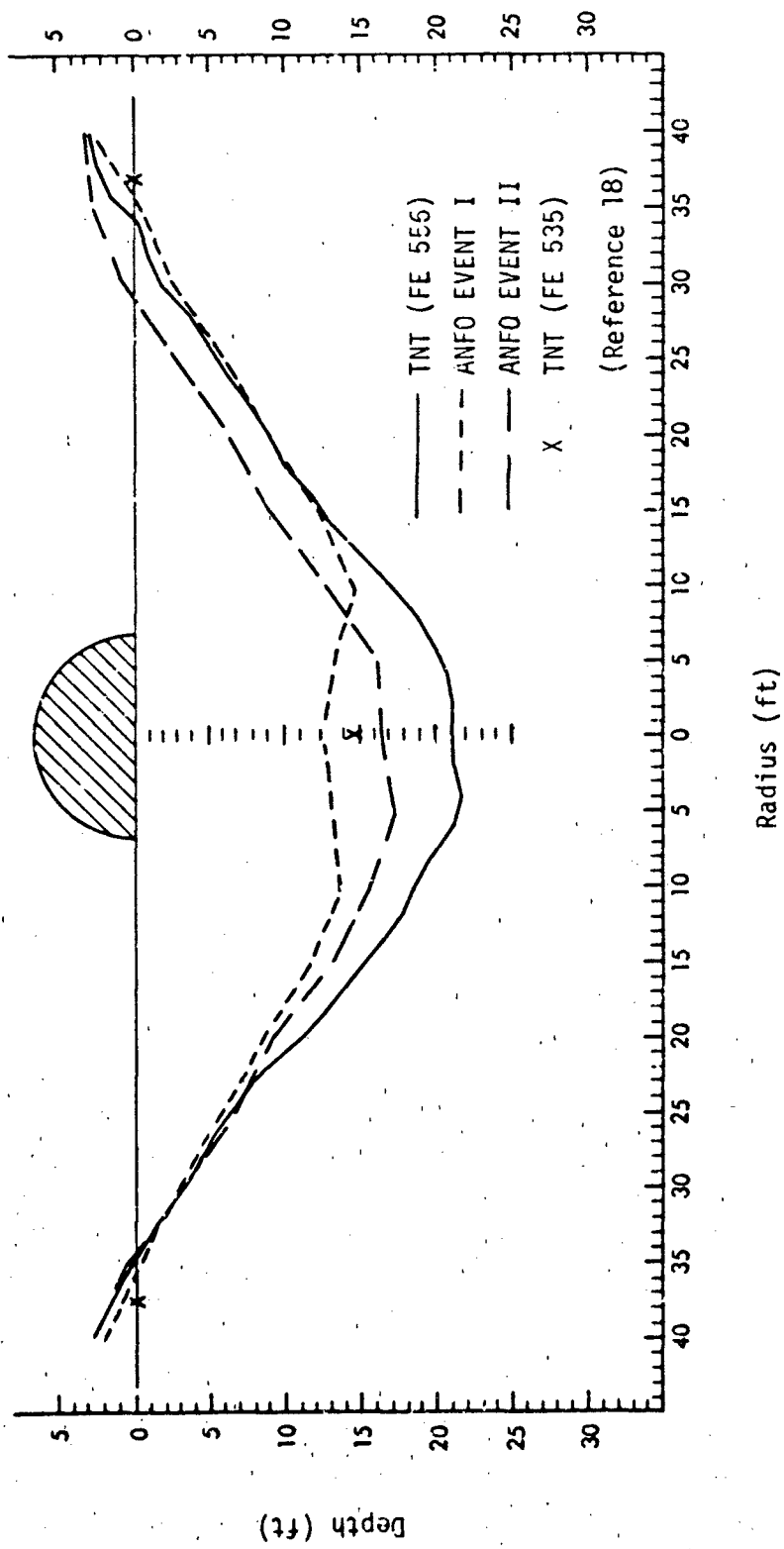
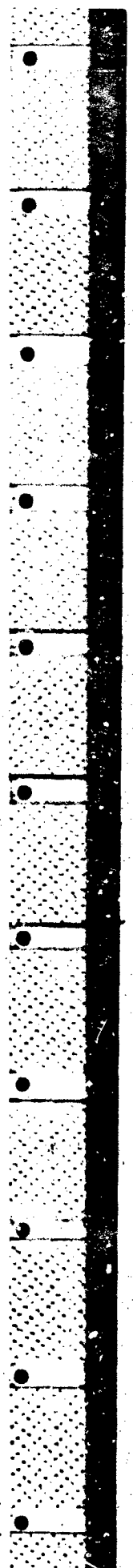


FIGURE 4-17: MEAN APPARENT CRATER PROFILES FOR 20 TON HEMISPHERICAL SHOTS.



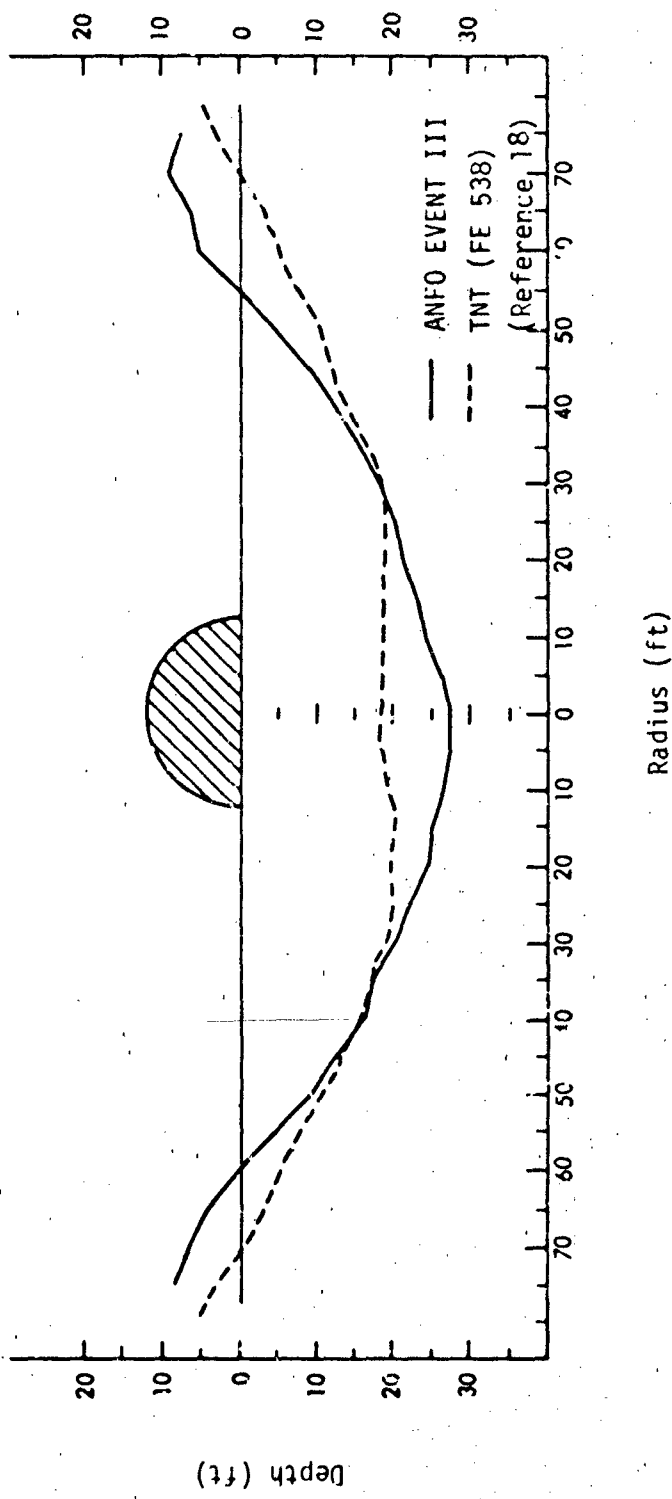
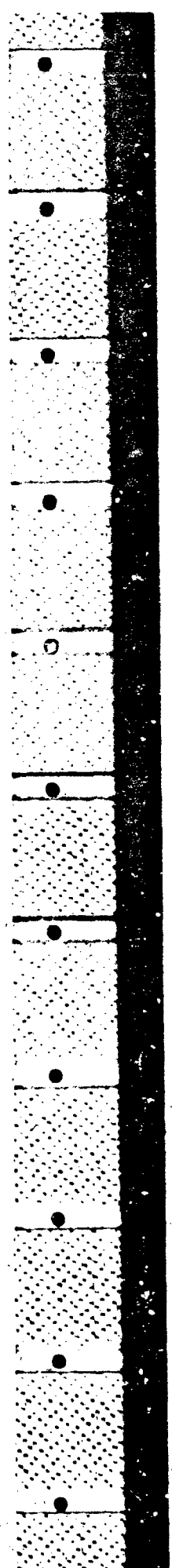


FIGURE 4-18. MEAN APPARENT CRATER PROFILES FOR 100 TON HEMISPHERICAL SHOTS.



4.3.3 Craters From Spherical Charges

Figures 4-19 and 4-20 show the mean crater profiles for tangent-to-the surface and half-buried spherical charges respectively; the dimensions of the craters are given in Table 4-11. The 25-ton ANFO charges have a TNT equivalence of about 20 tons so one-to-one comparisons between the cratering effects of the two explosive sources can be made. This comparison can be made more legitimately for the half-buried spherical charges because both were fired at the same test site, i.e., Drowning Ford; the crater shape and dimensions are remarkably similar. The tangent sphere charges were fired at different sites; this could account for the differences in crater dimensions for these shots.

4.3.4 Craters From Domed Cylindrical Charges (L/D = 0.75/1)

Table 4-12 lists the apparent crater dimensions generated by several large domed cylindrical charges with L/D = 0.75/1. The charges range in size from a nominal 6 tons to a nominal 620 tons, so it is possible to try to compare the craters on a scaled basis.

First, though, it is interesting to note that the nominal 620-ton DICE THROW and MILL RACE charges produced craters at the Giant Patriot site, WSMR, of about the same dimensions with the differences in diameter and depth averaging about 15 percent and in volume about 25 percent. This can be considered normal scatter particularly when it is considered that the MILL RACE event was held about 2 miles from the DICE THROW shot.

Scaling the crater of the 6-ton Pre-DICE THROW I-4 shot to that of the 120-ton Pre-DICE THROW II-2 shot at the same Queen 15 test site at WSMR, shows a large difference. Using cube root scaling, the PDT II-2 crater diameter and depth should be $\left(\frac{120}{6}\right)^{1/3} = 2.71$ times larger than the PDT I-4 crater dimensions, or 79.3 ft for diameter and 19 ft for depth. As the table shows, the measured values of the PDT II-2 crater and substantially different, 171.2 ft for diameter and 10.6 ft for depth. Surprisingly, the PDT I-4 crater dimensions scale up to the average of the DICE THROW and MILL RACE dimensions very well even though the 6-ton shot was at a different site than the 620-ton shots. The scaling factor is $\left(\frac{620}{6}\right)^{1/3} = 4.69$, giving scaled up values of 136 ft for diameter and 32.9 ft for depth. These contrast with the average measured values of 134 ft for diameter and 26.6 ft for depth.

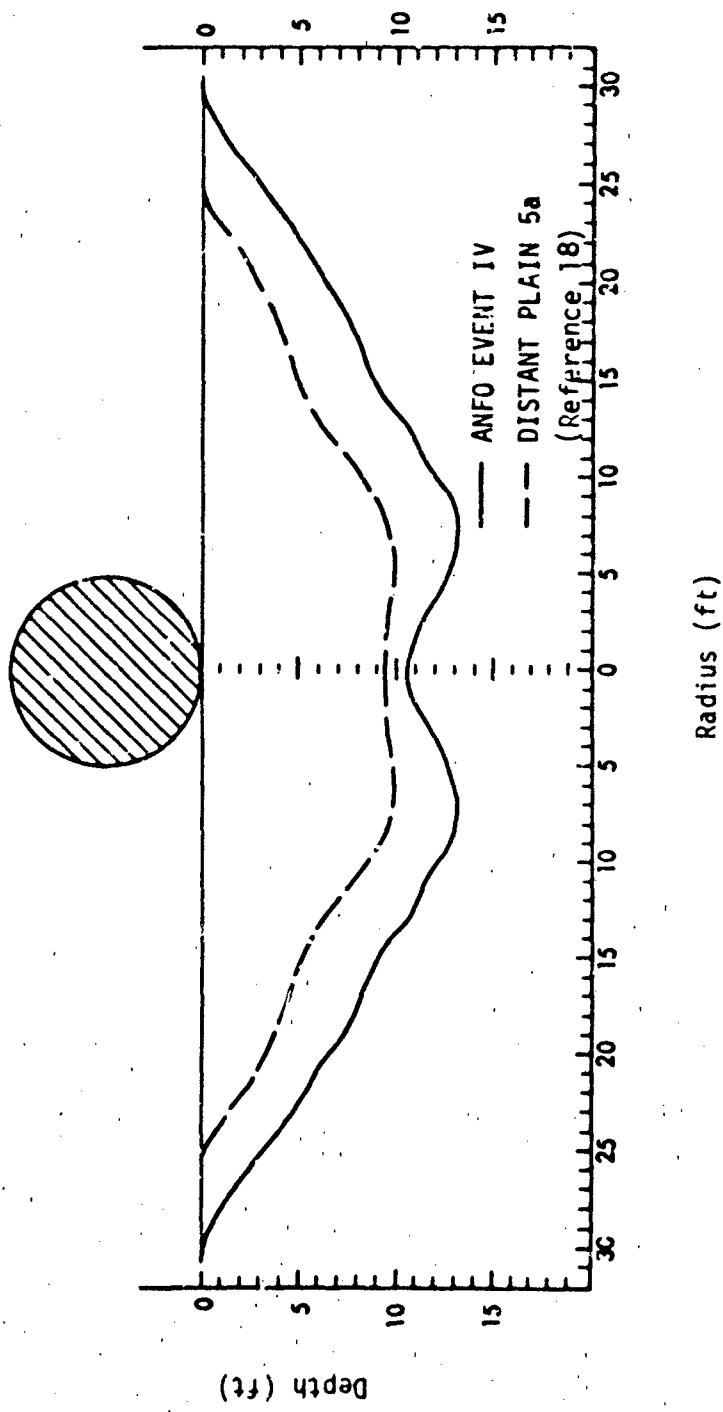
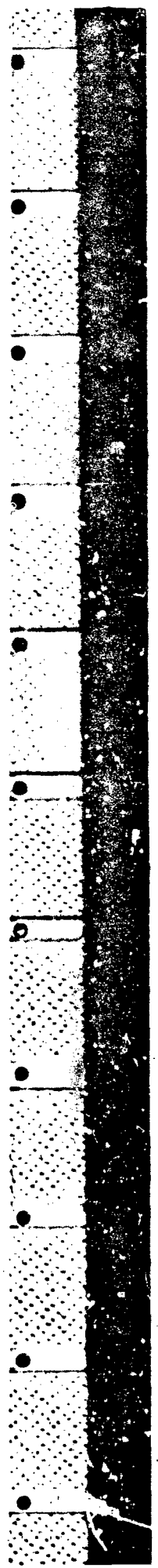


FIGURE 4-19. MEAN APPARENT CRATER PROFILES FOR 20 TON TNT EQUIVALENT SURFACE TANGENT SPHERICAL SHOTS.



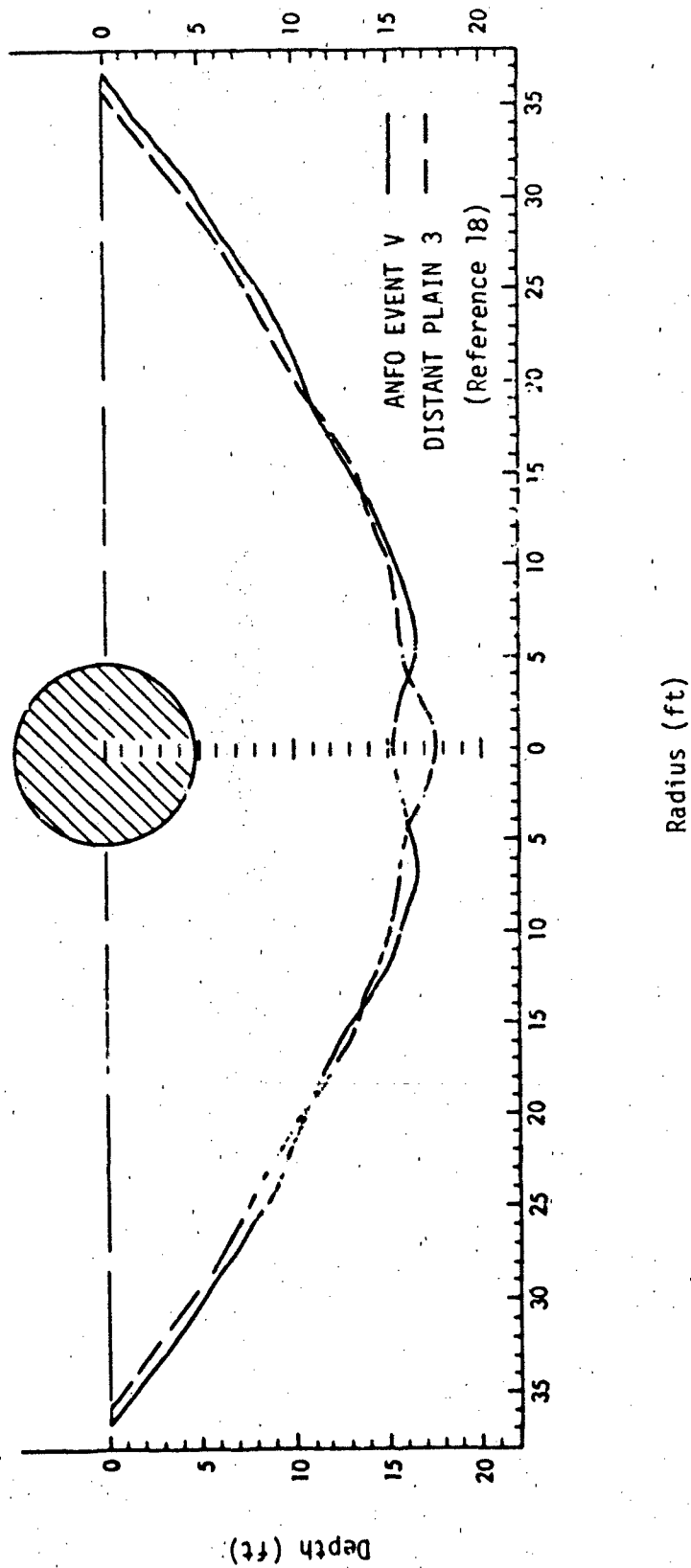


FIGURE 4-20. MEAN APPARENT CRATER PROFILES FOR 20 TON TNT EQUIVALENT HALF BURIED SPHERICAL SHOTS.

TABLE 4-12. CRATER DIMENSIONS FOR DOMED CYLINDRICAL ANFO CHARGES WITH L/D = 0.75/1

SHOT	WEIGHT tons	SITE	APPARENT CRATER			VOLUME ft ³
			DIAMETER ft	DEPTH ^c ft	DEPTH (max) ^d ft	
Pre-DICE THROW I-4	6	Queen 15 ^a	29.2	7.0		2,041
Pre-DICE THROW II-2	120	Queen 15	171.2	10.6		166,000
MISERS BLUFF II, Event 1	120	Planet Ranch ^b	97.4	10.9	14.9	54,400
MISERS BLUFF II, Event 2						
Charge 1	120	Planet Ranch	106.0	12.7	20.8	74,800
2	120	Planet Ranch	103.0	21.0 ^e	24.0 ^e	73,000 ^e
3	120	Planet Ranch	93.6	18.3	18.5	45,000
4	120	Planet Ranch	87.8	14.6	14.9	37,700
5	120	Planet Ranch	104.2	14.1	20.3	66,400
6	120	Planet Ranch	105.8	19.6	22.8	80,500
DICE THROW	620	Giant Patriot ^a	143.7	24.94		174,800
MILL RACE	620	Giant Patriot	124.2	28.3		138,000

^a Located at White Sand Missile Range, New Mexico

^b Located in Arizona

^c Depth measured from GZ

^d Maximum depth

^e Estimated values; bottom of crater filled with water

The validity of scaling crater dimensions is not questioned; however, when scaling of large charges on field operations to "check out" or "prove" the scaling procedure, a certain element of fortuity may be present because it is difficult to believe that all the rules for scaling are met. The charges may be the same shape and coupled to the ground in the same way and detonated exactly as desired but there is doubt that the ground material is alike at the test sites. The influence of specific site geology is illustrated in the MISERS BLUFF II Event 2 shots.

On this operation, 6 charges with nominal 120-ton weights were fired simultaneously. The charges were arrayed in a hexagonal pattern 100 meters (328 ft) on a side. It could be (and was) expected that the ground characteristics in the vicinity of each charge were similar and thus, similar craters would result. As shown in Table 4-12, there are wide variations in the crater dimensions for these six charges; diameters show a spread of about 15 percent, depth 40 percent, and volume 50 percent. The physical appearances of the craters were different. Craters 3 and 4 were simple bowl shaped with upraised rims and overturned flaps. The other four craters were complex with prominent to subdued benches along the walls at a depth of about 8 ft. Crater 2 contained a significant pool of water; crater 5 had a smaller pool. And craters 1, 5, and 6 had clearly defined central uplifts.

In analyzing the MISERS BLUFF II Event 2 craters, D.L. Orphal (Reference 19) grouped them into two classes. He noted that craters 3 and 4 were small (apparent volume = $41,350 \text{ ft}^3 \pm 12$ percent) while the other four craters were much larger (apparent volume = $73,675 \text{ ft}^3 \pm 8$ percent). Craters 3 and 4 had a smaller average diameter ($90.7 \text{ ft} \pm 11$ percent) and a shallower depth ($16.5 \text{ ft} \pm 11$ percent) compared to the average of the other four craters (apparent diameter $104.8 \text{ ft} \pm 4$ percent and maximum depth $22.0 \text{ ft} \pm 8$ percent). Orphal feels that local geology variations do not account for the observed crater differences. He suggests that differences in performance of the six charges and hence energy coupling to the ground was a more responsible factor.

Although this may be true, it is not evident in other data related to the performance of these charges. As shown in Table 2-8, there is little difference in charge weight, size, apparent density, and fuel oil content in

any of these six charges -- parameters that could influence the explosion effects. And while the detonation velocity of charge 3 is lower than that of the other five charges, the charge 4 detonation velocity is almost the highest. Recognizing that detonation velocity and pressure are related, it could be expected that the charge 4 crater would be larger than that of charge 3, yet is by far the smaller. So, the variations in site geology remain a plausible explanation for the differences in crater shapes and dimensions.

D.J. Roddy (USGS) suggests that the different crater shapes on MISERS BLUFF were caused by synergisms of stratigraphic variation effects, ground shock interactions, and charge performance effects. On other test events, Roddy and other investigators have concluded that indeed, variations in the ground material and structure result in differences between predictions and measured crater dimensions, and between craters produced ostensibly by the same explosive energy release. Ground shock interactions may result in differences in apparent crater dimensions through slumping of the fallback material. And, again, inadequate charge performance, e.g., poor detonation, could result in different size craters. The charge would have to be drastically underperforming, however, to have a marked effect on craters. To illustrate this, consider the MISERS BLUFF II Event I charge. As discussed in Section 4.2.4, this shot was believed to have released only 75 percent as much energy (in terms of airblast peak pressures) as expected. Yet, the detonation velocities reported ranged from 4,429 to 4,969 m/s with the velocities at the bottom of the stack being about 4,900 m/s. This supposedly low yield shot produced a crater with a volume considerably larger than the MISERS BLUFF II Event 2, charges 3 and 4 craters. In fact, charge 4 had the smallest crater of the seven MISERS BLUFF shots, although its detonation velocity was the same as that of the Event 1 charge. Using detonation velocity as the criterion of charge performance, charge 4 appeared to detonate properly. Therefore, ground variations seem to be a reasonable explanation for most of the crater size variations on MISERS BLUFF.

4.3.5 Crater Summary

The crater size produced by any explosive is determined by several factors: energy release, shape of charge, coupling of charge to the ground, and material and structure of the ground. All other things being equal, the larger the energy release of the explosive, the larger the crater; this is evident in Tables 4-11 and 4-12. Within limits, scaling of charges with different yields can be done successfully so long as all other parameters of the test configuration are the same.

The effect of charge shape and coupling to the ground is shown in Table 4-13 for hemispherical, spherical and domed cylindrical charges.

TABLE 4-13. CRATER DIMENSIONS FOR CHARGES WITH ENERGY RELEASE OF 20 TONS TNT EQUIVALENT

CHARGE SHAPE	APPARENT CRATER	
	DIAMETER ft	DEPTH ft
Hemisphere	69.9	17.8
Surface Tangent Sphere	54.0	10.0
Half-Buried Sphere	72.3	16.5
Domed Cylinder, L/D = 0.75/1	43.6*	10.4*

*Scaled from Pre-DICE THROW I-4 crater dimensions

Hemispherical charges with a larger explosive/ground interface than a domed cylindrical charge with L/D = 0.75/1 has a larger crater than the cylindrical charge. Similarly, the half buried spherical charge with a large explosive/ground contact surface has a larger crater than a tangent spherical charge. For any of the large charges, however, ground material and strength variations are relatively unknown and uncontrolled and therefore lead to difficulties in making predictions with an accuracy greater than about 20-25 percent. Accumulated data and hydrodynamic code calculations have to be relied upon as guides in planning new operations; no great surprise should be evidenced if results do not agree with predictions.

4.4 ANOMALIES

Throughout this report there has been evidenced a concern about blast wave and fireball anomalies or non-symmetries, jets, and protuberances generated by ANFO detonations. It will be recalled that one of the main reasons for investigating the use of ANFO as an explosion source for nuclear weapon blast simulation was because it had the promise of alleviating the anomaly problems associated with the previously used block built TNT explosive source. The promise was partially realized; anomaly production in terms of number and severity on ANFO shots was less than those observed on large TNT shots. But what are the roots of these anomalies with ANFO? Can they be attributed to the ANFO material itself or to the charge design and construction details? Or is some new factor entering the picture, multipoint detonation, for instance? If the causes for anomalies on ANFO shots could be determined, then, perhaps they could be eliminated. (Only anomalies attributable to explosive material and charge construction are considered here. Those anomalies arising from terrain features, such as roads and cable trenches running radially into ground zero and patches of vegetation are not charge or explosive type oriented; it is believed that they can be eliminated by proper test field layout.)

Some anomalies produced by the TNT charges were attributed to the non-homogeneity of the charge such as the variations in crystal structure within each 32 lb block and the non-regular interfaces and airgaps between adjacent blocks. It was postulated that these non-uniformities precluded the propagation of a uniform, steady detonation wave through the charge resulting in incomplete detonation, i.e., deflagration, of some blocks and ahead running or lagging detonation spikes within the charge. And these detonation aberrations manifest themselves as fireball and airblast anomalies.

Another suspected reason for some of the anomalies was the presence of myriad reentrant corners on the periphery of the block built charge; these possibly could produce mach interactions of the blast waves exiting from the surface of the charge and these interactions, in turn, produced jets in the airblast field. A third reason advanced for anomalies with block built TNT charges was the observation that depending on the block stacking pattern, there appeared to be large flat areas on what were designed to be spherical

surfaces; these could be generators of non-spherical shock waves leading to protuberances in the shock front.

Despite much study, analysis, and interpretation (References 20 and 21) and regardless of the plausibility of the conjectured causes of anomalies, none of the above characteristics of the TNT material or the block built charge was ever linked directly to the many anomalies observed. In fact, it was concluded that anomalies may be characteristic of most, if not all, condensed explosives detonated in air. They had been observed on all charges both large and small even down to carefully pressed and machined one gram sizes. Taylor instabilities, the thousand to one density mismatch between the explosive and the surrounding air, magnify the effects of any imperfections or inhomogeneities in the charge. Ever hopeful, however, it was reasoned that by eliminating, or at best reducing some of the imperfections in TNT charges, the characteristics of ANFO would lend themselves to reducing the propensity of charges to produce seriously disrupting anomalies.

4.4.1 ANFO Homogeneity

ANFO charges were thought to be homogeneous - homogeneous in the sense that some small volume such as, for example, a cubic inch, would be the same in all its important characteristics as any other unit volume of the material. Within this micro-volume - less than a millionth of the volume of a 20-ton charge - inhomogeneities would be present because of prill size distribution and fuel oil absorption variations. With adequate quality control, however, these physical characteristics of the material could be maintained at specified levels. With prill type, prill size distribution, and oil content specified, the bulk density of ANFO would be determined within narrow limits. On theoretical and experimental bases, these features of ANFO were considered to be important and necessary to control. It was known that as the particle size decreases, the detonation velocity increases; as the bulk density increases so does the detonation velocity; and that the detonation velocity reaches a peak at about 5.6 percent oil content (Figures 2-8a), b), and c) respectively). If the micro-volume characteristics were held to specifications, then the whole charge would be within specifications and so, on a macro scale, a homogeneous charge would result.

This ideal homogeneity was not attained. The several nominal 120-ton charges of MISERS BLUFF II-2 show this dramatically. Tables 2-6 and 2-7 present the stacking data for two of the charges. On MISERS BLUFF II-22, the layer by layer fuel oil content varied from a low of 2.1 percent to a high of 9.5 percent; on charge 6, i.e., MBII-26, the variation was from 3.9 to 9.6 percent. The average FO content for MBII-22 was 4.3 ± 1.3 percent, that for MBII-26 was 6.0 ± 1.2 percent. The average deviation for all the MISERS BLUFF charges was 21.9 percent. This was unusually high; on DICE THROW and MILL RACE, nominal 620-ton shots, the deviation was only 6.6 percent with FO percentages ranging from 5.0 to 7.0 for DICE THROW and from 5.3 to 7.8 for MILL RACE. The DICE THROW average FO content was 6.1 ± 0.4 percent, for MILL RACE 6.3 ± 0.4 percent. It is evident that viewed as a total charge, homogeneity so far as FO is concerned, is not attained on any of the shots and in some cases it is considerably less homogeneous than on others.

Although there is no information available in reports on the layer to layer prill size distribution for a given charge, information available on the total prill size distribution for several charges, such as shown in Figure 2-6, suggests that there are differences within any given charge. With prill size distribution and FO inhomogeneities, it is not too outlandish to conjecture that there are bulk density inhomogeneities within the charges. Certainly, as Table 2-8 shows, there are apparent average bulk density differences between charges.

Another inhomogeneity could occur in the charge if all the spaces between bags were not filled with loose ANFO; air pockets would be present. Similarly, air could be entrapped within bags that are not completely filled. (Indeed, on ANFO IV, the 25-ton tangent sphere charge, it was noted that air was entrapped in some bags and an attempt was made to release this air by puncturing the bags.) Although entrapped air is a concern, there is no evidence or record that in any of the bag constructed charges there was air entrapped.

In summary, the ANFO charge is not as homogeneous as was originally expected and hoped. Throughout the charge there are fuel oil, prill size distribution, and density variations and possibly pockets of entrapped air.

These inhomogeneities appear to be randomly distributed within the charge with no large concentrations at any particular place. Because of the random nature of these imperfections and their apparent large numbers, it is not possible to attribute the observed ANFO anomalies, which are few in number, to the inhomogeneities.

As discussed in Section 2.7.3.7, there is evident a smooth bulk density gradient from top to bottom of the charge because of hydrostatic compaction of the lower layers of ANFO. Observed anomalies cannot be correlated with this "inhomogeneity." In fact, the conjectured smoothness of this gradient, even conceptually, would not lead to anomalies such as jets, spikes, and discontinuities; it would result only in a symmetrically expanding blast wave with the front in its early passage, not quite perpendicular to the ground.

Although the inhomogeneities in the ANFO charges cannot be correlated with the presence of anomalies, quality control of the ANFO should be maintained lest major concentrations of inhomogeneities occur in large charges. As an extreme example, consider a DICE THROW-like charge with the random distribution of inhomogeneities found in these charges. Now, replace a 15 layer (approximately 6 ft high) quadrant of the charge centered on the fifth booster (about 8.5 ft above the ground) with out-of-specifications ANFO such as 2.5 percent fuel oil, prill size distribution skewed towards larger particles resulting in low bulk density. All these features are conducive to a low detonation velocity. It could be expected that this gross and concentrated 30 ton inhomogeneity would result in an anomaly - probably an initial lagging blast front in line with the quadrant and possibly a later spike or jet as the blast fronts from the surrounding ANFO coalesce in a mach interference. (It is interesting to conjecture that the presence of this 30 ton low yield quadrant would hardly be perceived in total charge blast output except along the postulated path of the anomaly. This thought is in line with the earlier discussion in Section 1.2.3 that blast pressure measurements taken in the field are not particularly sensitive to 10-15 percent differences in yield of any explosion on a single shot basis.)

4.4.2 Reentrant Corners

Responding to the postulate that reentrant corners on the surface of explosive charges, such as are present on block built TNT charges, lead to anomalies, in the design of the early large ANFO charges determined efforts were made to eliminate such corners. On ANFO II and III, the 20-ton and 100-ton hemispherical charges, light fiberglass cases were used to contain the loose bulk ANFO. Somewhat surprisingly, even though the charges were devoid of reentrant corners (and there was little likelihood of air pockets within the charge) anomalies occurred on these shots. They were attributed to the discontinuous change in thickness of the case material at the overlapping joints of the gores which made up the case. A second source for the appearance of anomalies was attributed to possible incomplete early combustion of the fiberglass. It was noted, however, that the anomalies were less severe than those evidenced on similar sized and shaped TNT charges. Anomalies were present on the Pre DIRECT COURSE event in which the loose ANFO was again encased in a fiberglass-wood sandwiched container. Again, these perturbations were attributable to the case construction with thickened sections at the joints.

ANFO I, a 20 ton hemispherical charge, was constructed of bagged ANFO with the bags placed so that reentrant corners were essentially eliminated or muted except in the top four layers of the charge (Figure 3-2). On this event no anomalies attributable to the explosive material or the charge construction was observed except that an early time fireball perturbation occurred at the top of the charge; this was believed to be due to the departure from hemispherical geometry in this region of the charge. So, on the basis of these results and interpretations, credence was provided to the thought that reentrant corners or discontinuities on the surface of the charge can lead to anomalies.

The results of ANFO V, however, brings in question this conclusion. This shot, a 25 ton spherical charge with its center of gravity at ground level, was built of bagged ANFO. The bags were loosely stacked one against the other with many gaps and reentrant-like corners at the surface of the charge. And yet, no anomalies were observed. To confound the issue, not only was the surface pock marked with reentrant corners, but also, the geometry of the

charge was lopsided, not quite symmetrical or spherical and this did not seem to introduce anomalies. Since this was a lightly instrumented event, it may be that insufficient observations were made to definitively ascertain the presence of anomalies.

Event 4 of the Pre DICE THROW I series was a better instrumented shot. This charge was a 5.6 ton domed cylinder built with bagged ANFO. Because 50 lb. bags of ANFO, the usual construction "block", precluded stacking to obtain a smooth outer contour on this relatively small charge, the ANFO was repackaged in 15 lb. bags which could be and were butted closely together resulting in a relatively smooth charge surface. No significant anomalies were noted.

On subsequent bagged ANFO shots in the domed cylinder geometry, i.e., Pre DICE THROW II-2, DICE THROW, MISERS BLUFF, and MILL RACE, the charges were constructed, for structural strength reasons (see Section 3.2.1) in such fashion as to form a reentrant cornered surface similar to ANFO V. Several anomalies were present on all these shots but there is no evidence to link the surface roughness to anomalies.

While reentrant corners do not present an ideal smooth charge surface (such as can be attained with small charges and in hydrodynamic code models), it may be that a uniformly indented surface should no longer be suspected as a source of anomalies for large multi-ton bagged ANFO (or block built TNT) charges. While it is probable that interferences occur among the blast fronts coming off the irregular surfaces of the charge, there are so many in number that they can be expected to coalesce thus forming a smooth blast front in short time and short distance from the charge. Certainly, there are only a few--two to five--significant anomalies observed on shots, not the thousands that the surface irregularities would produce.

4.4.3 Multi-Point Detonation

In the design of the domed cylindrical charges, a new element enters the picture which could influence anomaly production, namely, the use of multi-initiation points along the axis of the charge. If these initiation points are not detonated simultaneously, or near simultaneously, it may be expected that detonation wave, fireball, and airblast perturbations would occur. These

anomalies would be centered in the horizontal plane on the late or early activated booster or would come off at some angle if mach interactions took place between the shock waves emanating from neighboring boosters with disparate times of detonation.

Three events with similar geometries and detonation schemes can be examined in an attempt to correlate simultaneity of booster detonations and the presence of anomalies - Pre DICE THROW II-2, DICE THROW, and MILL RACE. In PDII-2, one anomaly was observed; this was a vertical jet at the top center of the charge. Early-time high speed photographs (Reference 10) showed a smoothly expanding fireball with no perturbations except the spike at the top. This could be interpreted as indicating simultaneity of booster detonations; no direct measurements are reported on booster activation times. The vertical jet may be attributable to the central PVC column running the length of the charge, housing the boosters. This could act like a shock tube directing and concentrating detonation wave energy through the column resulting in rapid exit of the shock wave at the apex of the charge and manifesting itself as a jet. A similar, though not as pronounced, jet was observed on an early photographic frame of the DICE THROW detonation (Reference 11) which had a detonation system like that of PDII-2.

On DICE THROW, aircraft and ground station photographic records indicated that there were three major jets with their tips approximately 34.4 ft above the ground. As the jets expanded radially, they were non-luminous and became translucent. (Translucency, indicating little solid material in the jet, is a characteristic of most ANFO anomalies.) Since the top-most booster, number 7, on DICE THROW was only 22.6 ft above the ground, these jets cannot be correlated with early or late detonation of this booster alone. However, there is evidence based on fireball photography by Wisotski (Reference 11) that all boosters did not detonate simultaneously. Light breakout occurred at the bottom and top of the charge first with the main body of the charge becoming radiant at a slightly later time. At a still later time a narrow band symmetrical bulge developed around the charge which Wisotski ascribes to the late detonation of boosters number 6 and 7. This interpretation can be questioned: with light breakout occurring at the apex of the charge early on,

it is difficult to reconcile this apparent fact with the inferred conclusion that booster number 7 was late. But if booster number 6 were late, its shock wave interacting with the shock wave from number 7 could be skewed and angled upwards so that the bulge in the fireball and the subsequent jets rose to the observed 34.4 ft height. This reasoning, however, breaks down in that although the bulge essentially girds the charge, only three jets are observed rather than a continuous spray of jets. So, for DICE THROW, the origin of the jets is unknown: they cannot be linked to booster detonation times or as indicated earlier, to fuel oil variations, prill size distributions, density variations, or reentrant corners.

MILL RACE presents similar inconsistencies between various features of the explosion and postulated causes for anomalies. Through measurement with light pipes (Figure 3-10) directly viewing booster detonations, it was estimated that there was a 90 μ sec difference in activation times (Reference 22). Personnel from the Data Reduction Section, Physical Science Laboratory, New Mexico State University in this reference provide a profile of the first breakout of light from the fireball along the surface of the charge plotted against the height of the charge (Figure 4-21). Added to this figure are the estimated detonation times of the boosters and the fuel oil content of the ANFO layers in line with the boosters. It is noted that light breakout occurs first at the apex of the charge as was noted for Pre DICE THROW II-2 and DICE THROW. This lends substance to the premise that the PVC column containing the boosters, channels the detonation wave through the ANFO at a high speed leading to early manifestation of light at the apex of the charge. But surprisingly, no jet emanating from the apex is reported. And equally surprisingly, even though the boosters detonated at different times "The fireball produced by MILL RACE appeared to be relatively uniform for the entire time that it existed... Pictures of the fireball taken from different directions are very similar, and that indicated that it was relatively symmetric. The film records do not show any clearly identifiable anomalies (p 106, Reference 21)." On a cautionary note, the NMSU authors conclude their detailed and careful study of the MILL RACE blast diagnostics: "On the basis of film records, the conclusion that anomalies were completely absent cannot be made. However, any which were produced were inconspicuous, and probably were minor."

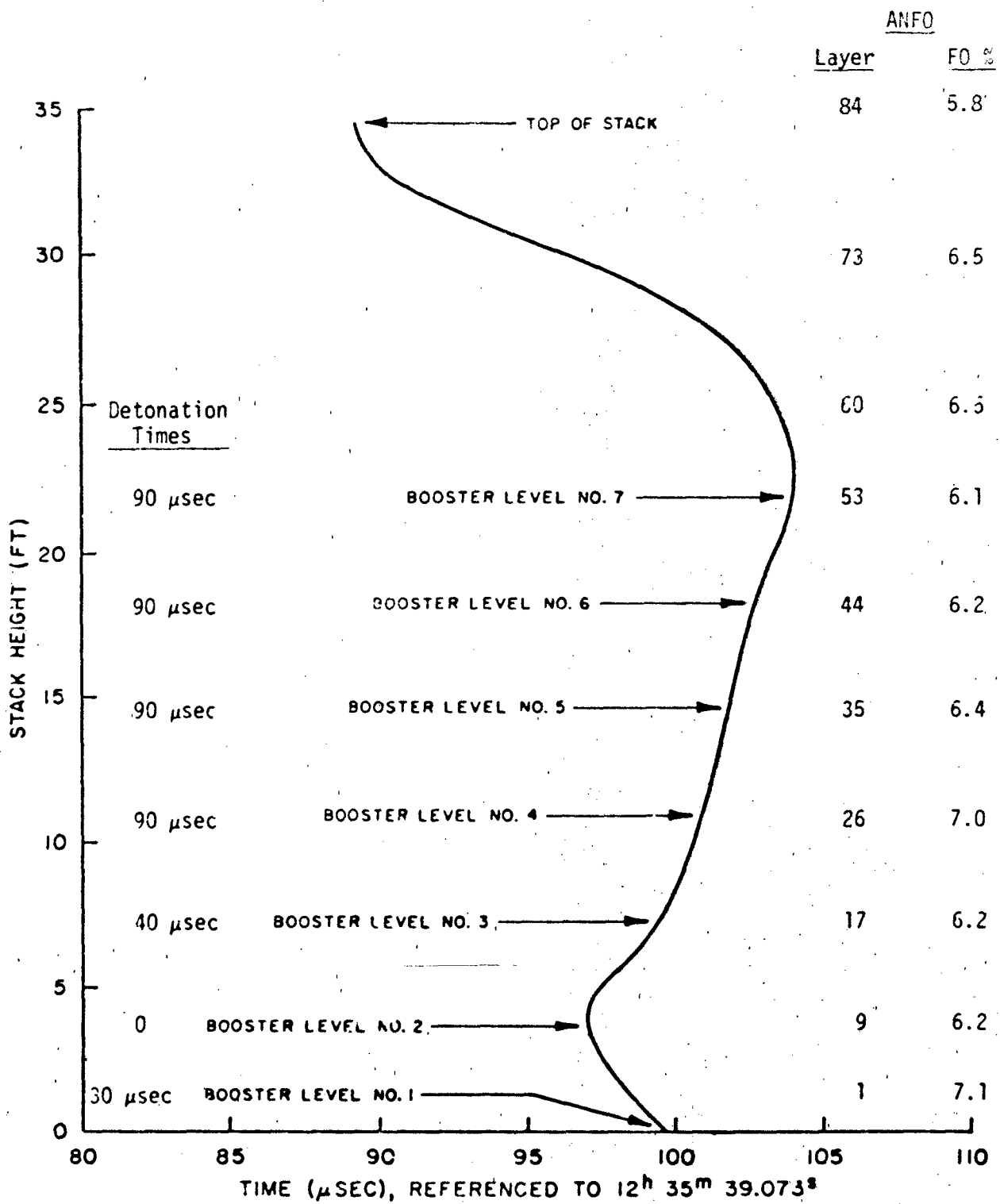


FIGURE 4-21. MILL RACE SURFACE BREAKOUT PROFILE ALONG RADIAL 178°. (Derived From E-1783 Streak Camera Film - Times are Approximate, With Probable Accuracy $\pm 30 \mu\text{sec.}$)

The fuel oil variations shown in Figure 4-21 for the layers of ANFO centered on the boosters are not very large and as indicated earlier, these variations distributed in a random pattern appear to be acceptable, that is, not conducive to anomaly production. Figure 4-21 presents some other interesting information. Note that although the top four boosters all detonated at the same time, light breakout at the surface of the charge occurred earlier at the lower booster, number 4, than at the uppermost one, number 7. This profile can be further indication of the bulk density gradient in the ANFO charge as a function of height; the lower layers are more compressed, have higher densities and detonation velocities, and hence, earlier light breakouts than the ANFO layers on top. The relatively late breakout at the most dense portion, at the very bottom of the charge, probably results from the late detonation of booster number 1.

Another interesting feature of the profile plot is that there is only about a 7-8 μ sec difference in the arrival of the detonation wave along the surface of the cylindrical portion of the charge. This means that at the early very high airblast pressures starting at the surface of the charge, the lower portion of the blast front is only about 0.25 ft ahead of the upper portion of the wave, i.e., the front is not quite perpendicular to the ground. This slant would not be discernible in photographs or in pressure measurements. Hence, the density gradient in the ANFO due to hydrostatic compression has but little influence on the practical ideality of the airblast front and should be of little concern.

4.4.4 Anomaly Summary

As with block built TNT charges, so with ANFO charges whether bag constructed or encased in light containers, there are many postulations as to the reasons for anomalies but no conclusive and self-consistent proofs that are attributable to charge material, charge construction features, or detonation performance. Inhomogeneities within the charge material do exist in numerous and randomly located small volumes but perhaps the unit volume previously considered is too small. On a larger unit volume basis, for example several cubic yards, the charge may appear to be homogeneous. Similarly, the pock-markings on the surface of bag built charges are so numerous and small that, again, viewed in perspective of the large charge

surface, the surface can be considered to be relatively smooth. And even though all boosters do not detonate at the same time, with the non-simultaneity evidenced on shots so far, perhaps, for large charges, "similtaneity" can be defined as detonations occurring within a 90-100 μ sec time span.

Perhaps, as stated earlier, anomalies are a fact of life of explosions; they have been present on TNT shots and ANFO shots. All evidence supports the conclusion that the anomalies produced by ANFO charges are fewer in number and less in severity than those developed by large TNT shots; on some shots, e.g., MILL RACE, no significant anomalies were observed and on DISTANT RUNNER none were mentioned. It is recognized that a comparison between anomalies from ANFO shots and TNT shots and between the several ANFO shots is somewhat qualitative and depends to large extent on the instrumentation coverage employed on the shots. Since the root cause for the anomalies has not been determined, it appears impractical to apply scaling procedures, which are quantitative, to the comparisons. Further, without a definitive finding for anomaly production, it appears judicious to accept the conjectures and postulations as to the origin of anomalies because they have some degree of plausibility. Therefore, it is suggested that the present specifications for ANFO material, charge construction, and detonation schemes should not be relaxed.

There should not be undue concern if specifications are not met precisely; the specifications have not been attained on any of the ANFO shots and, yet, no malfunction of the charge or excessive generation of anomalies has occurred or can be ascribed to a departure from specifications. For the intended purpose -- the production of nuclear weapon proportioned blast and shock for testing military targets -- ANFO, today, is the best, most inexpensive, safest, and easiest explosive to use.

REFERENCES

1. Sachs, R.G., "The Dependence of Blast on Ambient Pressure and Temperature," BRL 466, May 1944.
2. Sadwin, L.D., and Swisdak, M.M., Jr., "Blast Characteristics of 20 and 100 Ton Hemispherical ANFO Charges, NOL Data Report" NOLTR 70-32, March 1970.
3. Giglio-Tos, L., and Reisler, R.E., "Air Blast Studies of Large Ammonium Nitrate/Fuel Oil Explosions," BRL-MR-2057, Aug. 1970.
4. Anderson, J.H.B., and Patterson, A.M., "Ammonium Nitrate/Fuel Oil Trials Carried Out at DRES, Part I," DRES TN-268, January 1970.
5. Granstrom, S.A., "Loading Characteristics of Air Blasts from Detonating Charges," Transactions of the Royal Institute of Technology, Stockholm, Sweden, 1956.
6. Muirhead, J.C., and Palmer, W.O., "Canadian Participation in DISTANT PLAIN, Air Blast Pressure Gauge Measurements," Suffield Technical Note No. 177, 13 July 1967.
7. Private Communication - Teel, G. (BRL) letter 3 July 1972 to Sadwin, L.D. (NOL).
8. Anderson, J.H.B., "Observations on the Blast Phenomenology of Unconfined Charges of Ammonium Nitrate/Fuel Oil Explosive (ANFO IV and ANFO V - October 1971)," DRES STN-319, June 1972.
9. Edwards, T.Y., "ANFO Charge Development Program, Program Summary," DNA Field Command, June 1977.
10. Edwards, T.Y., and Perry, G.L.E., "Middle North Series, Pre-DICE THROW II Events, Preliminary Results Report," POR 6904, Defense Nuclear Agency, 1976.
11. "Proceedings of the DICE THROW Symposium 21-23 June 1977," DNA 4377P-1, July 1977.
12. Teel, G.D., and Peterson, R., "MISERS BLUFF Series, MISERS BLUFF II-1 Event, Free Field Airblast Definition," Ballistics Research Laboratory, POR-7019 (WT 7019) November 1979.
13. Wisotski, J., "MISERS BLUFF Series - MISERS BLUFF I and II Technical Photography," POR 6983, October 1980.

REFERENCES (Continued)

14. Private Communications from M.M. Swisdak, Jr., (NSWC) to J. Petes, February 1983 (Information to be presented at the Seventh International Military Applications of Blast Simulators in June 1983).
15. Private Communications from G. Teel, BRL to J. Petes, Kaman Tempo, via M.M. Swisdak, Jr., NSWC.
16. Sauer, F.M., Clark, G.B., and Anderson, D.C., "Nuclear Geoplosics, Part Four, Empirical Analysis of Ground Motion," DASA 1285 (IV), May 1964.
17. Dillon, L.A., "The Influence of Soil and Rock Properties on the Dimensions of Explosion Produced Craters," AFWL-TR-71-144, February 1972.
18. Sadwin, L.D., and Swisdak, M.M., Jr., "Performance of Multiton ANFO Detonations, A Summary Report," NOLTR 73-105, July 1973.
19. "Proceedings of the MISERS BLUFF Phase II Results Symposium, 27-29 March 1979, Volume I," Field Command, Defense Nuclear Agency, POR 7013-1 (1979).
20. Patterson, A.M., Kingery, C.N., Rowe, R.D., Petes, J., Dewey, J.M., "Fireball and Shock Wave Anomalies," DASIAC Special Report No. 105, Panel N-2 Report N2-TR 1-70, 1970.
21. Schoutens, J.E., "Review of Large HE Charge Early-Time Detonation Anomalies," GE-TEMPO, DASIAC, DASIAC SR 182, 31 December 1979.
22. "Proceedings of the MILL RACE Preliminary Results Symposium 16-18 March 1982," POR 7073-1, 23 July 1982.

SECTION 5
FUTURE APPLICATIONS OF ANFO

5.1 "WHAT IS PAST IS PROLOGUE"

The first four sections of this report have discussed the properties and characteristics which led to several ANFO charge designs for simulating nuclear weapons proportioned airblast and ground shock. This information can serve as a guide to what other uses can be made of ANFO charges for large scale testing. For example, ANFO can be used at sea to test the response of ships and their on-board equipment; it can be used in shapes to provide enhanced directed blast effects. ANFO can be used to a greater extent than in the past on underground tests to study the hydrodynamic characteristics of ground shock and the response of underground structures. And ANFO can be used in thousands of tons quantities to better simulate the long blast durations of nuclear weapons.

In the past, ANFO charge design has been dominated by axially symmetrical shapes. This has been so for at least three reasons: one, this geometry provides the largest uniform test bed area appropriate for target response and phenomenology studies; two, these symmetrical charges are more amenable to hydrodynamic calculations and prediction techniques than odd shaped charges; and, three, historically, symmetrical charges have been used on most tests, large and small. Looking to the future, as new test requirements and objectives are developed, new geometries for ANFO may help meet these objectives.

The following discussions present concepts and suggestions on new uses for ANFO. Some of these are based on small scale tests done with conventional military explosives; others have no direct experimental basis. The suggestions, therefore, are starting points; *small scale tests, computations, and analysis are required to establish the merits and feasibility of the suggestions.*

5.1.1 "Conventional" Charge Shapes

Before discussing new uses and shapes for ANFO charges, it is interesting to compare the blast fields generated by hemispherical, spherical, and domed cylindrical charges as they have been used to date for surface bursts. Figure 5-1 shows the pressure-distance and the positive duration-distance relationships for all charges reduced to a 1-lb ANFO base. It is seen that for the cylindrical charge, the pressure range from about 100 to 1,000 psi extends to a significantly farther distance than for the other charge geometries with the tangent sphere next and the half buried sphere having the least range. The positive phase durations, τ' , fall in the opposite order with the half buried sphere having a longer duration than the cylindrical charge at the same scaled distance.

On tests where it is important to have a large, symmetrical area covered by high pressures, it is apparent that the domed cylindrical charge best meets this objective (at the sacrifice of positive duration). This area coverage can be increased farther, it appears, if instead of using an $L/D = 0.75/1$ cylinder, a larger L/D charge is built.

Work by Reisler, et al, BRL (Reference 1), experimentally explored the pressure fields around small pentolite cylindrical charges with several L/D ratios. Figure 5-2 shows the results in terms of pressure ratios between these charges and a pentolite tangent sphere charge. For the cylinders tested, it is apparent that the pressure field generated by a cylinder with an $L/D = 3/1$, is significantly higher than that from a sphere -- about 68 percent higher at a scaled distance of $4.5 \text{ ft/lb}^{1/3}$. And this $3/1$ cylinder provides a 15 to 20 percent higher pressure than a $1/1$ (and by extrapolation, a $.75/1$) cylinder over a scaled range from 4.5 to $23 \text{ ft/lb}^{1/3}$. Roughly translating this into a DICE THROW-like situation, a 620-ton ANFO charge with an $L/D = 3/1$ would result in a 100 psi blast wave occurring at a range about 5 percent greater than that experienced on DICE THROW. (The translation is rough because in Reisler's experiments the cylindrical charge was single point detonated at the top while on DICE THROW the charge was multipoint detonated along the longitudinal axis of the charge. Nevertheless, qualitatively, the larger L/D charge will give a higher pressure over the measured distance range than the DICE THROW charge.

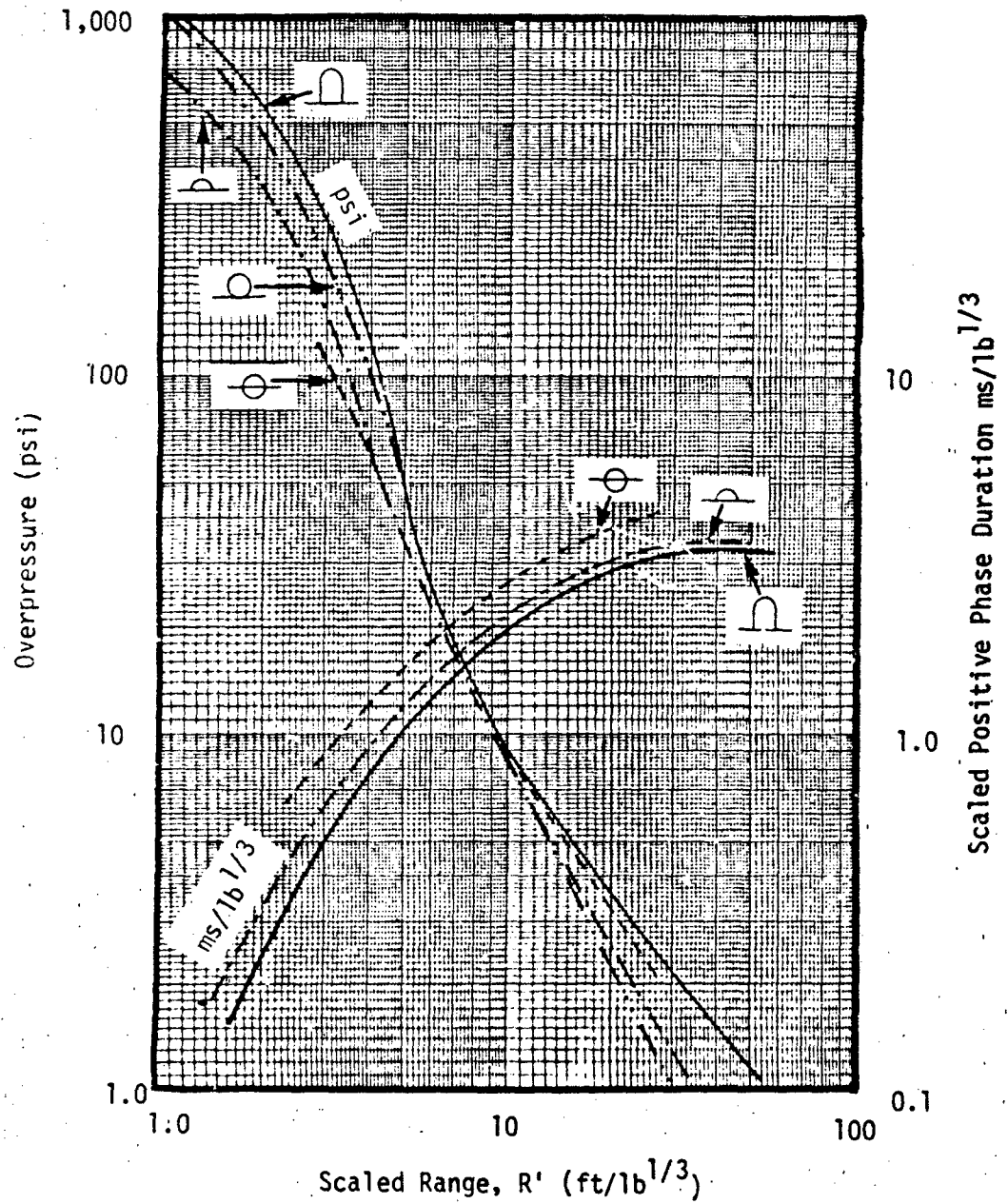


FIGURE 5-1. PRESSURE AND POSITIVE DURATION FROM SURFACE BURST ANFO CHARGES (SCALED TO STANDARD CONDITIONS).

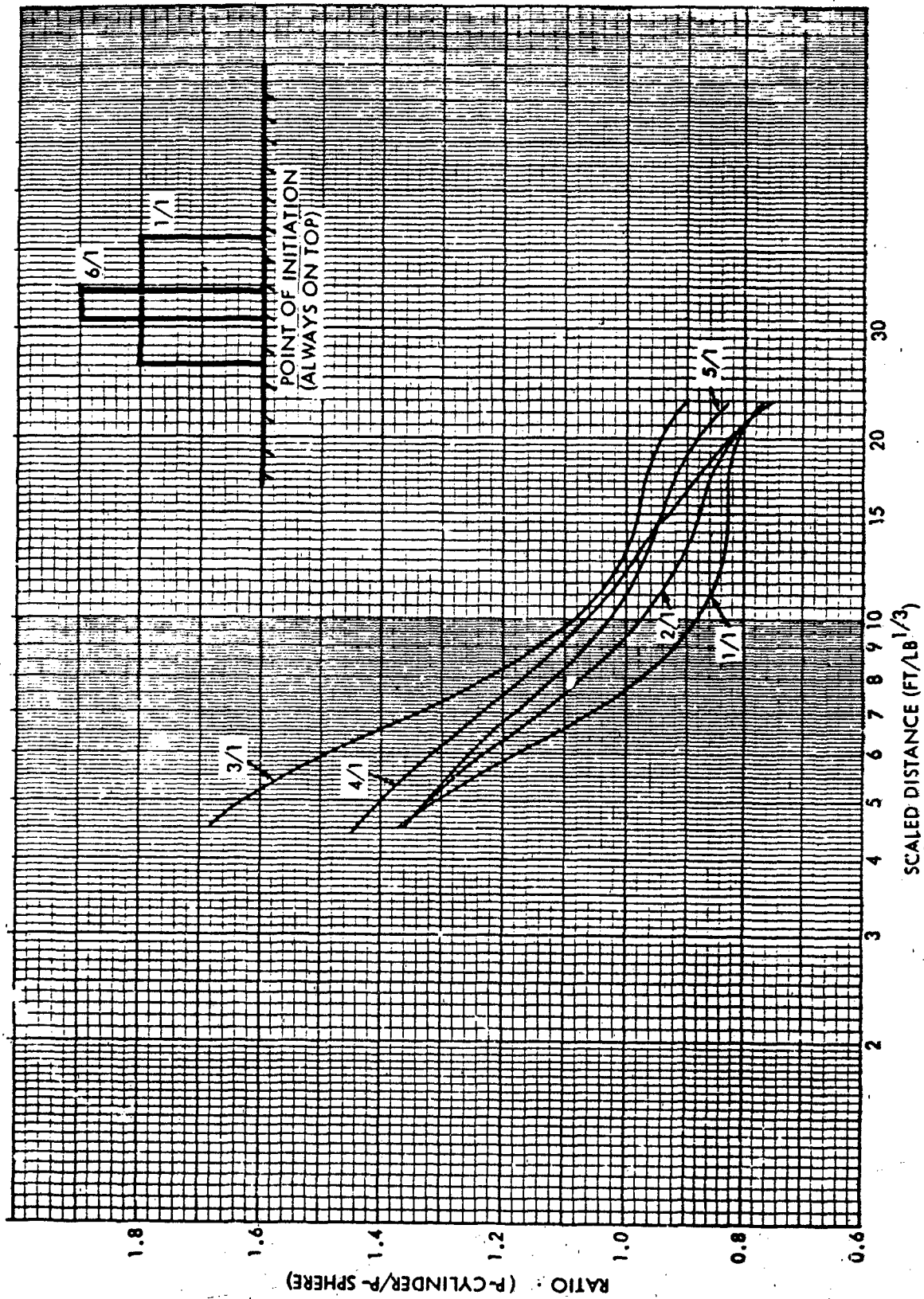


FIGURE 5-2. CYLINDRICAL CHARGE L/D EFFECTS ON PRESSURE.

Now, as discussed in Section 1.2.3, a 5 percent difference in range or pressure may not be discernible in measurements on a single shot. However, for design purposes, it is best to keep in mind that different L/D cylinders will give different pressure-distance results.

So, if airblast effects are of primary concern on a test, perhaps an L/D larger than that used on DICE THROW can satisfy the requirements. Ground shock and crater effects will be minimized with this taller charge; this may or may not be a detriment.

5.2 BLAST DIRECTING

The airblast off a hemispherical, spherical, or vertical capped cylindrical charge, to all practical purposes, expands in a smooth circular pattern on the ground plane; great pains are taken in charge design and preparation to achieve this uniform and omnidirectional front. There may be times, however, when a non-uniform, non-circular blast front contour better meets test and operational requirements. This non-uniform field, of course, must be predictable. Various charge geometries can indeed provide reliably lobed or directed blast fields with some areas of the test bed receiving an enhanced blast compared to some other areas at the same distance. Because bagged ANFO is stackable in many shapes and bulk ANFO is pourable into cases of almost any shape, it seems that ANFO has unique advantages in building blast directing charges.

What are the reasons for considering blast directing techniques? They are involved mostly with cost, the cost of the explosive material and the cost for constructing the charge. If only a small number of targets are to be exposed on a test and a small directed charge can provide a blast environment similar in magnitude to that obtained from a larger, omnidirectional blast generating charge, the cost savings are apparent.

Over the years, several blast directing charge configurations have been investigated with military high explosives and detonable gases. The findings of these studies are applicable to ANFO directed blast charges.

Early on it was determined that the blast off the face of a cubic charge is considerably higher at a given distance than that from a spherical charge of the same weight. Capitalizing on this knowledge, investigators at the

General American Research Division, GATX, devised several experimental designs suitable for blast directing (Reference 2). In one, the charge was shaped like a slice out of a semi-cylinder as illustrated in Figure 5-3. In the other, several charges were arranged in a vertical planar array (Figure 5-4). In both configurations, only a small portion of the blast field has enhanced pressures suitable for target testing purposes; rarefaction effects from the sides and edges of the charge configuration limit the extent of the field. However, where the size of the field is adequate, these charges have their merits and they can be constructed easily with bagged or cased bulk ANFO.

5.2.1 Horizontal Cylindrical Charges

Blast directivity can be obtained from cylindrical charges, too, provided the charge is positioned on the ground horizontally rather than in the familiar vertical position. Guerke and Scheklinski-Glueck mapped the pressure field around such geometries (Reference 3). They used RDX charges of three weights, 0.016, 0.128, and 1.024 kg with L/D's for each weight of 1/1 and 5/1. All charges were detonated at one end and measurements were made at several azimuthal angles as shown in Figure 5-5.

The pressure results, scaled to 1 kg, are given in Figures 5-6 and 5-7 for cylinders with L/D's = 1/1 and 5/1 respectively, and for impulse in Figures 5-8 and 5-9 for the same two cylindrical configurations. As a basis of comparison, Guerke et al have superimposed on their figures the pressures and impulses from surface burst hemispherical charges. Even a cursory look at the figures shows that there are pronounced high pressure lobes in the field. For example, at around the 90° line there are high pressure and impulse lobes for both cylinders. For the 1/1 cylinder, the peak pressure is about five times larger than that from a hemispherical charge and the impulse about twice as large. For the 5/1 cylinder, a similar comparison shows peak pressure ten times higher and impulse twice as high.

Guerke et al found that for the range of charge weights used in their tests, for a given L/D the results are amenable to cube root scaling. If the scaling can be extended up to large ANFO charges, the horizontal cylindrical geometry could serve as a directed blast source.

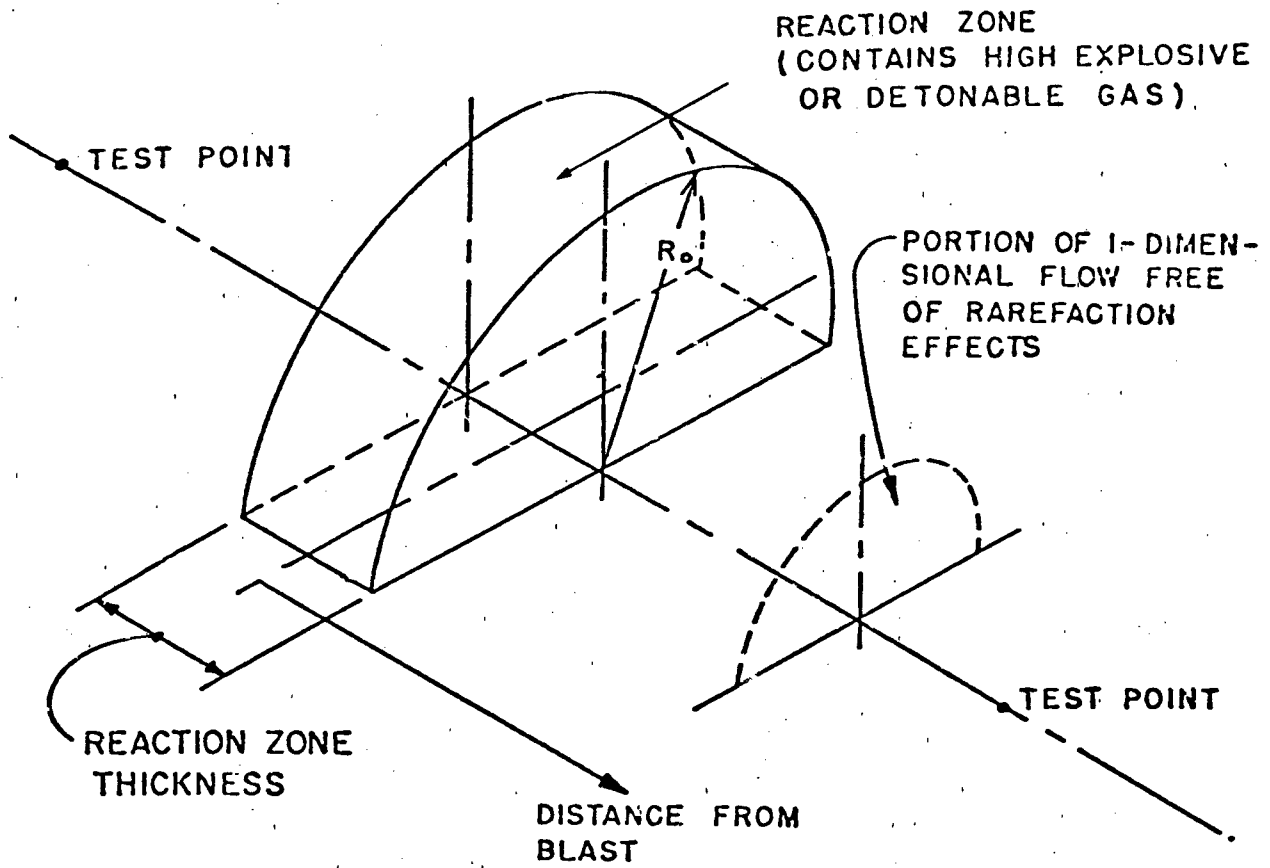


FIGURE 5-3. BLAST DIRECTING SCHEME.

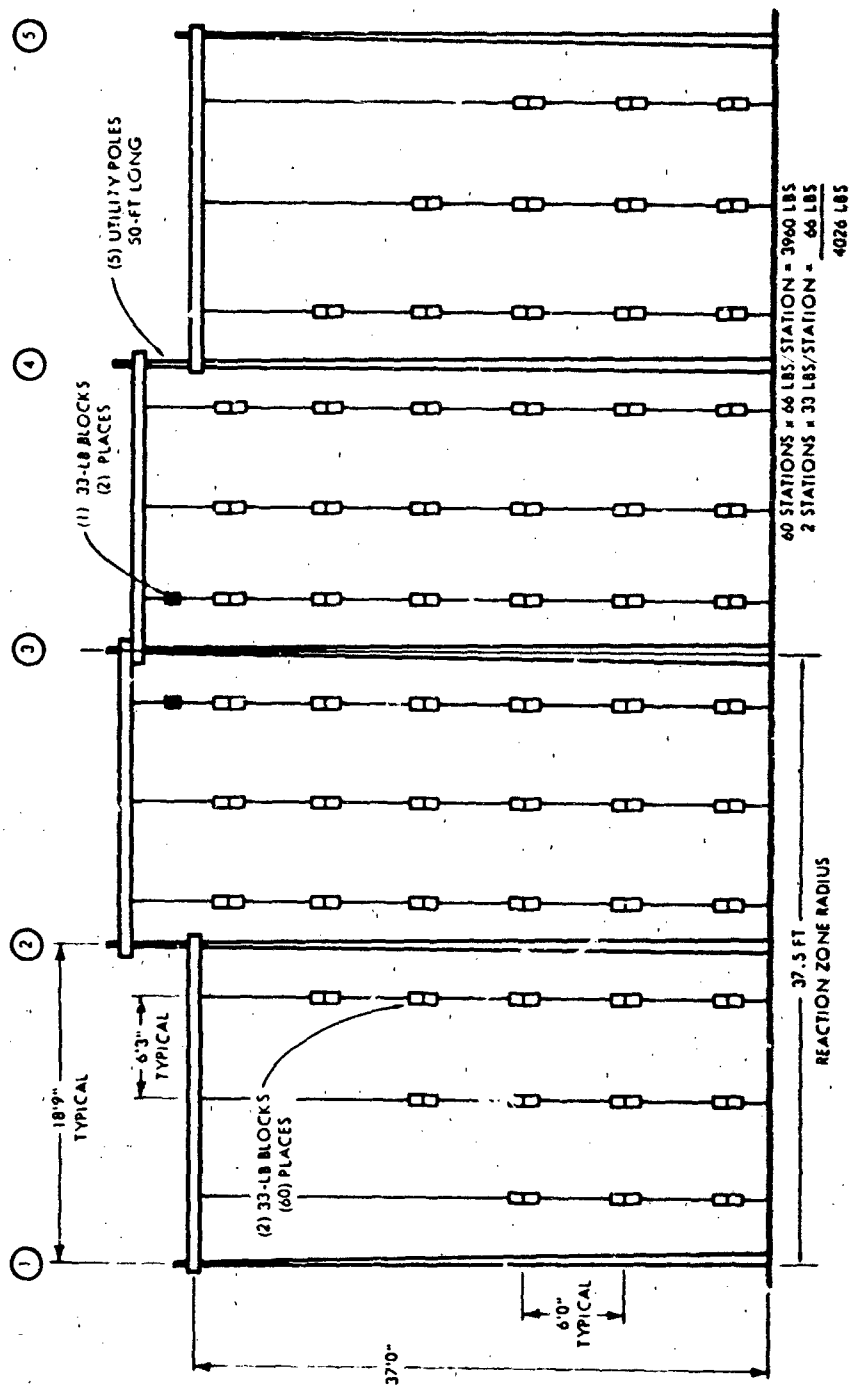


FIGURE 5-4. TWO-TON BLAST-DIRECTING SYSTEM FOR DIAL PACK.



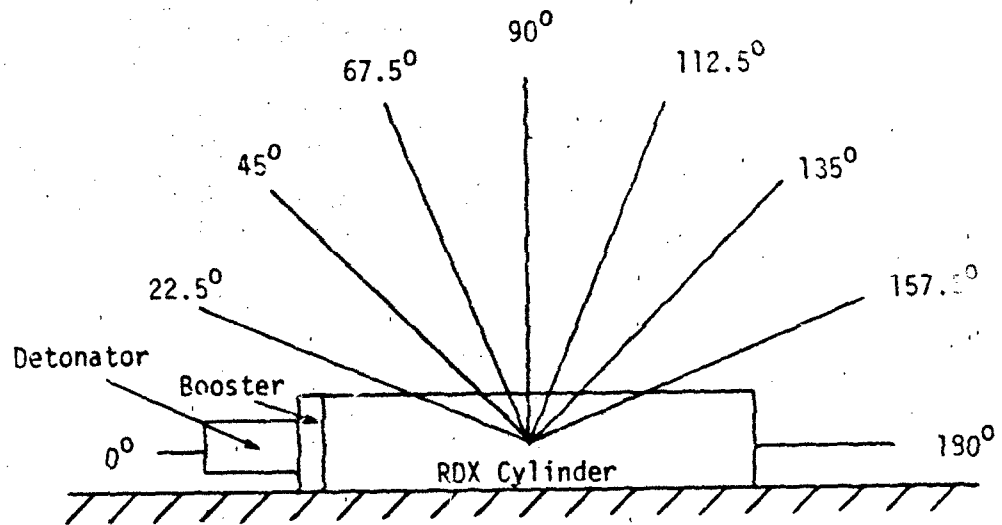
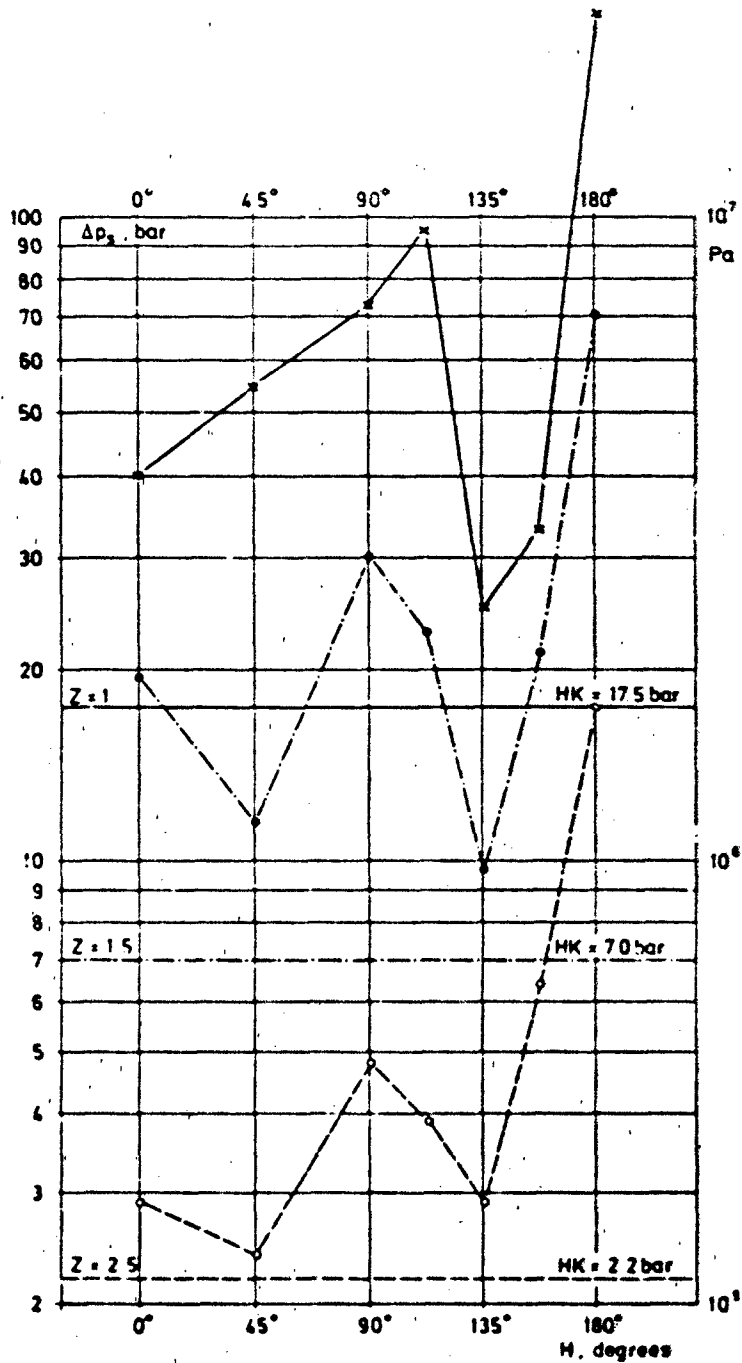


FIGURE 5-5. PLAN VIEW OF AZIMUTHAL BLAST LINES.



Primary shock front side-on overpressure as a function of azimuth angle H and scaled distance $Z = R/Q^{1/3}$ in $m/kg^{1/3}$ for cylindrical charges with L/D ratio of 1. Horizontal lines indicate shock front overpressure of semispherical charges of identical mass at the same scaled distance (Reference 3).

FIGURE 5-6. PRESSURE VS AZIMUTHAL ANGLE FOR $L/D = 1$ CYLINDRICAL CHARGES.

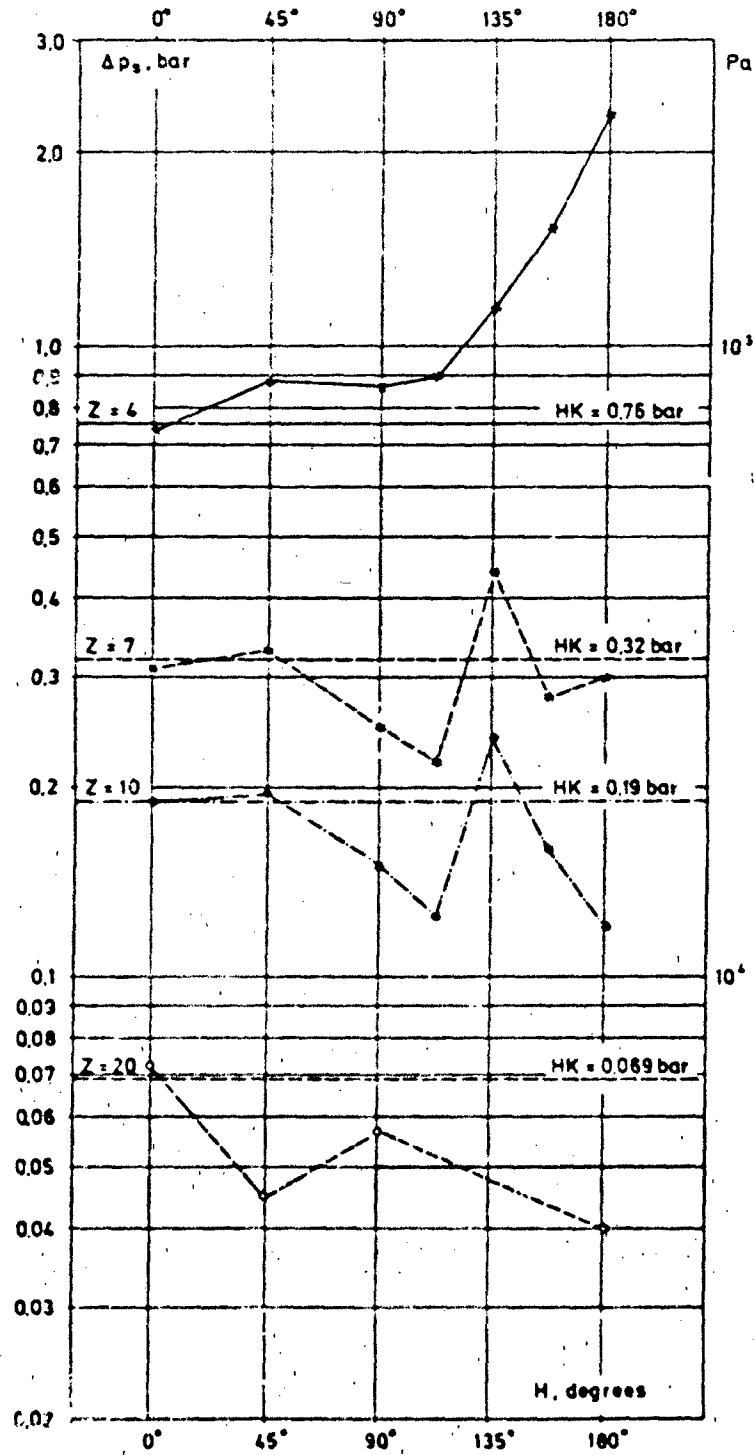
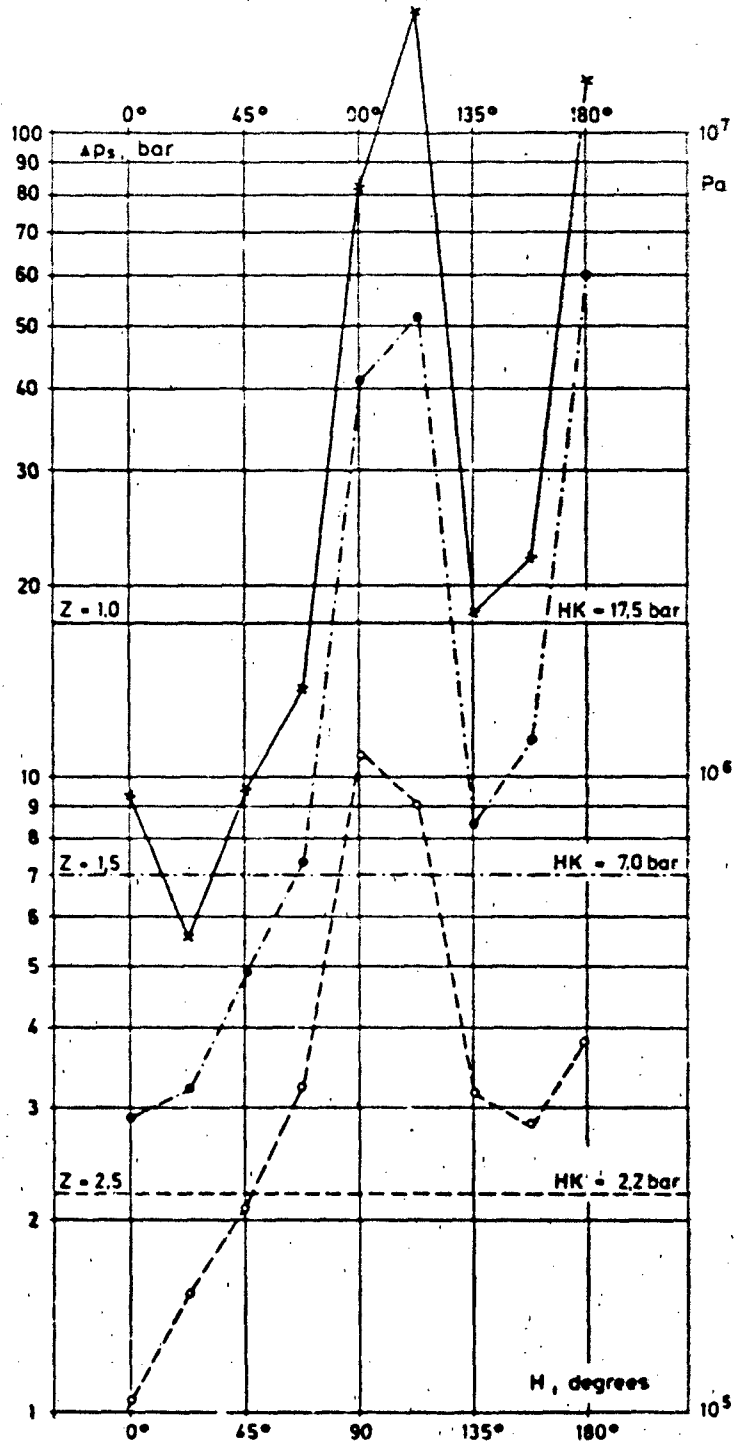


FIGURE 5-6. PRESSURE VS AZIMUTHAL ANGLE FOR $L/D = 1$ CYLINDRICAL CHARGES (CONTINUED).



Primary shock front side-on overpressure as a function of azimuth angle H and scaled distance $Z = R/Q^{1/3}$ for cylindrical charges with L/D ratio of 5. Horizontal lines indicate shock front overpressure of semispherical charges of identical mass at the same scaled distance (Reference 3).

FIGURE 5-7. PRESSURE VS AZIMUTHAL ANGLE FOR $L/D = 5$ CYLINDRICAL CHARGES.

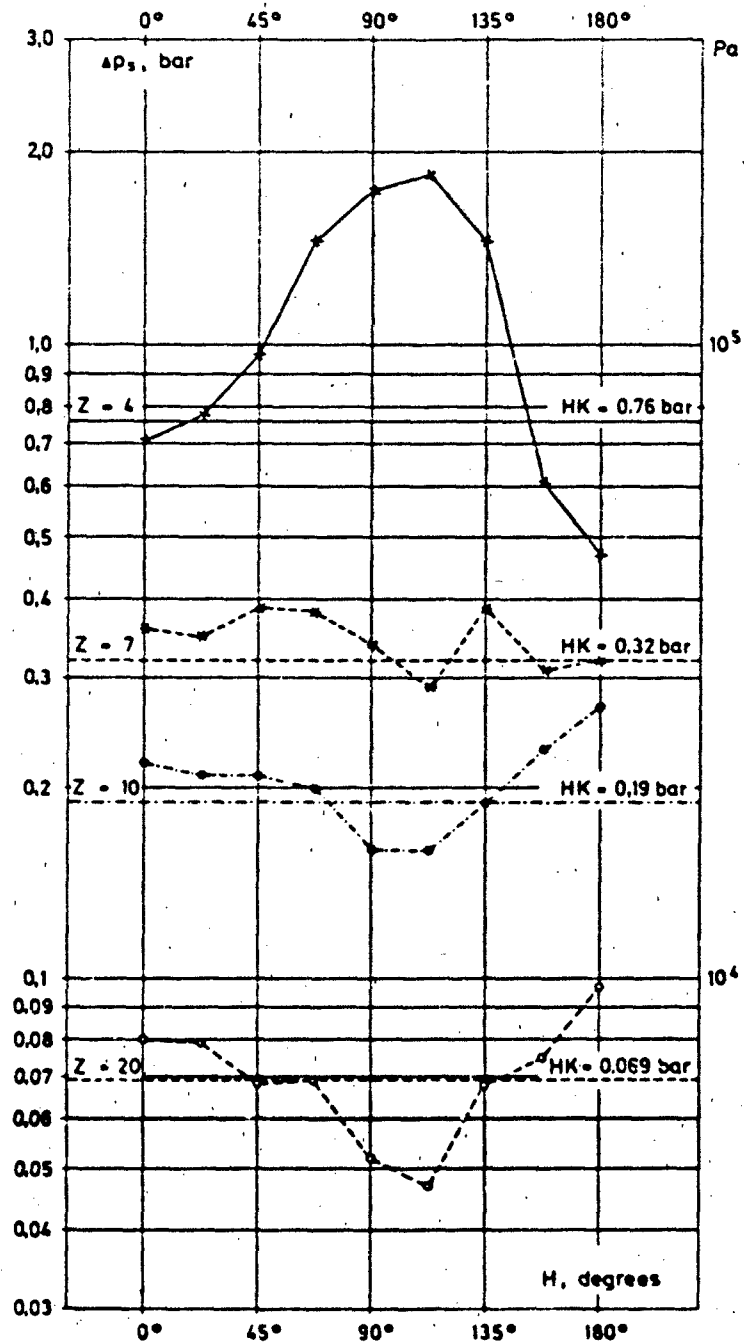
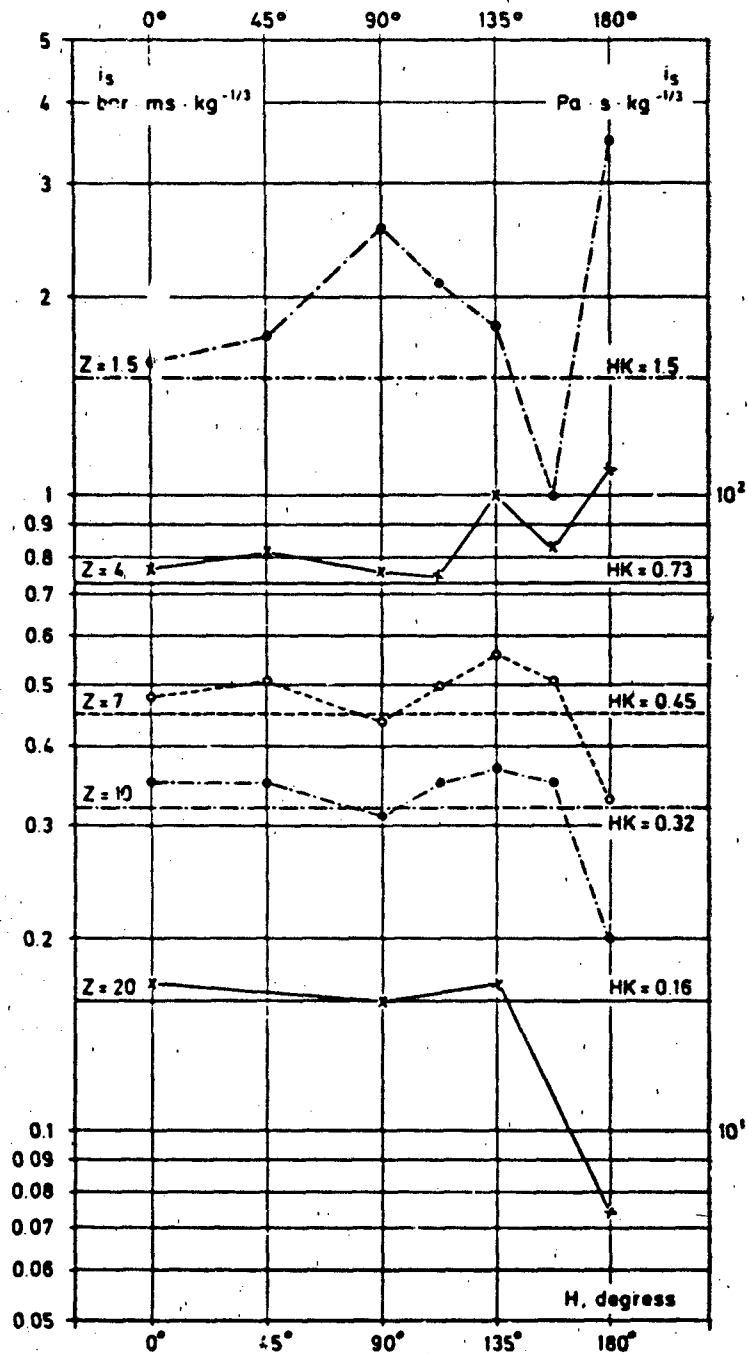
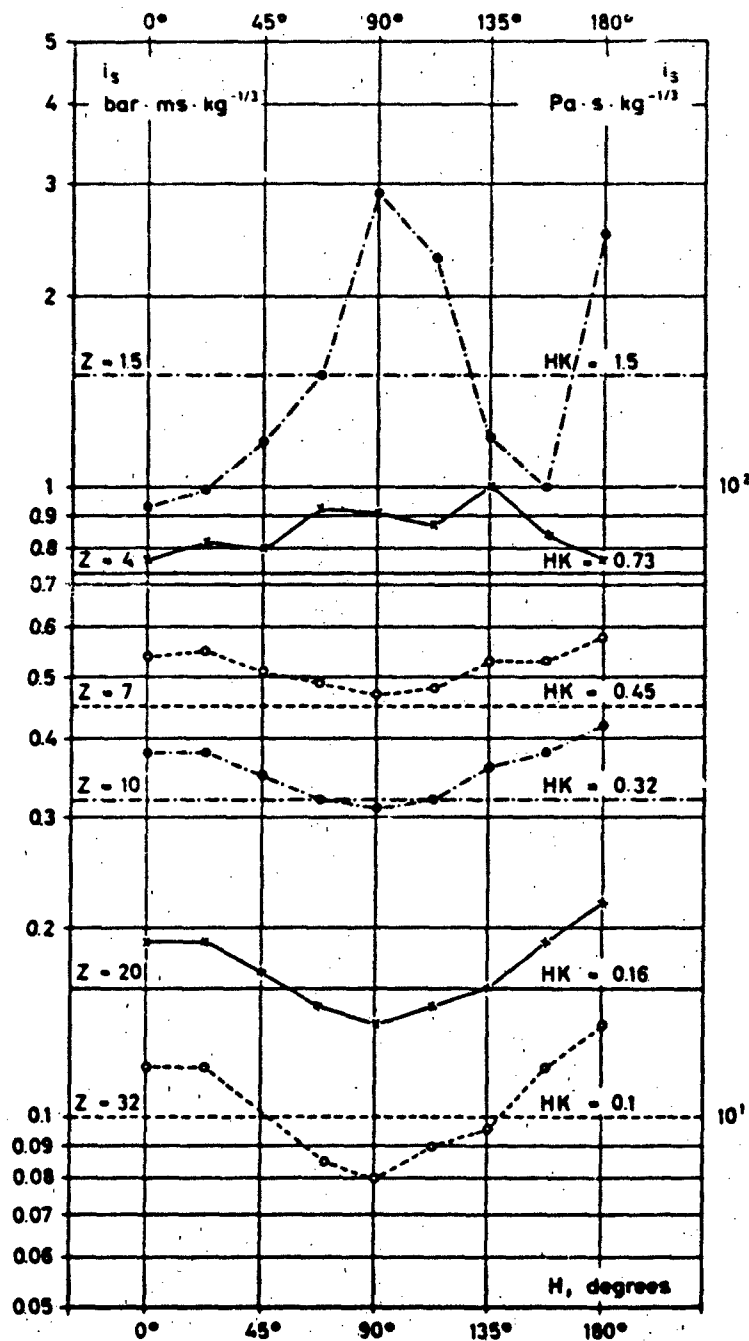


FIGURE 5-7. PRESSURE VS AZIMUTHAL ANGLE FOR L/D = 5 CYLINDRICAL CHARGES (CONTINUED).



Side-on overpressure impulse as a function of azimuthal angle H and scaled distance Z in $m/kg^{1/3}$ for cylindrical charges with L/D ratio of 1. Horizontal lines indicate impulses of semispherical charges of identical mass at the same scaled distance (Reference 3).

FIGURE 5-8. IMPULSE VS AZIMUTHAL ANGLE FOR $L/D = 1$ CYLINDRICAL CHARGES.



Side-on overpressure - impulse as a function of azimuth angle H and scaled distance Z in $m/kg^{1/3}$ for cylindrical charges with L/D ratio of 5. Horizontal lines indicate impulses of semispherical charges of identical mass at the same scaled distance (Reference 3).

FIGURE 5-9. IMPULSE VS AZIMUTHAL ANGLE FOR L/D = 5 CYLINDRICAL CHARGES.

An extension of this concept is to build the charge as a semi-cylinder with its longitudinal axis on the ground surface. Qualitatively, this shape should give a lobed blast field similar to that of the cylinder, but its chief advantage would be that it would be easier to build than a cylindrical charge.

Other charge shapes can be designed for blast directing or focusing; some of these shapes have been explored already with conventional explosives. The results can be applied to ANFO. Only the fertile imagination of explosive and test scientists and engineers and the requirements of a test operation limit the charge shapes that may be investigated.

5.3 OTHER CHARGE CONSTRUCTIONS

A variation of the hemispherical design is one which would use bulk ANFO poured onto the ground so as to assume its natural slumping shape. This charge construction may be suitable for large charges calling for thousands of tons of ANFO. The advantage of this design is cost: bulk ANFO is cheaper than bagged ANFO and no container is required.

The natural slump angle of prilled ANFO is 33° . As can be seen in Figure 5-10, a fairly good hemispherical shape can be obtained provided the

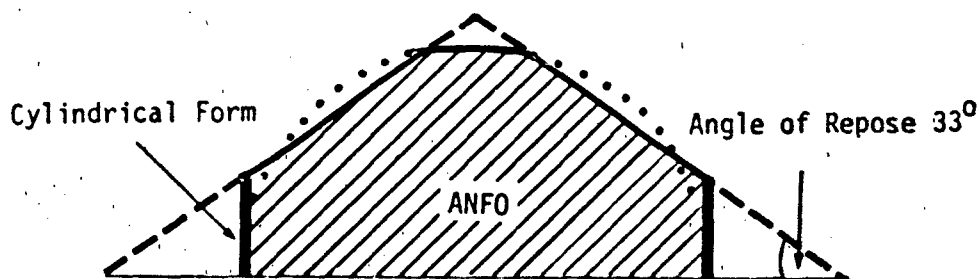


FIGURE 5-10. NATURAL SLUMPING SHAPED CHARGE.

top of the charge is rounded off as indicated. An even better hemispherical shape results if a short cylindrical form is used to contain the lower portion of the charge.

In light of what has been said about the properties of ANFO -- its hygroscopicity and its tendency to cake in moist atmospheres -- a whole series of tests and studies would be required to establish the feasibility of this charge construction design. Can the poured ANFO be protected against the elements with a suitable structure or tarpaulin-like cover? If the ANFO should cake, would it detonate reliably and with predictable detonation and blast characteristics? There is little doubt that caked ANFO can be detonated under adequate stimulation; recall the tragic experience at Oppau with even less sensitive AN (see Section 1.2.1). Should a completed charge cake on the outside, would this provide protection from farther caking and oil evaporation on the inside of the charge? These and other questions would have to be answered before natural slumping construction for charges can be employed in the field.

Perhaps some of the problems posed can be avoided if a light structure is built to house the bulk ANFO. Many state and municipal highway maintenance departments use a large but lightly constructed beehive shaped building for storing salt and sand. Although the salt and sand fill the structure from wall to wall, the shape of the building and the natural slump angle of the salt and sand preclude a large stress being exerted on the walls of the structure. This type of structure may be adaptable for protecting and shaping a large ANFO charge.

5.4 ANFO USES AT SEA

It is somewhat ironic that although one of the main reasons for the development of ANFO was its intended use at sea to subject surface ships to nuclear weapons proportioned blast, this application has not come to pass. The concept, however, appears to have merit.

It is envisioned that a floating platform -- a seagoing barge, for instance -- can be loaded heaping full with hundreds of tons of bulk or bagged ANFO at some port facility. The barge is then towed to the test site at sea; during the test it can be anchored or towed. At the time of the explosion, the target ships are arrayed around the barge in preassigned positions; some target ships could be anchored, others could be underway. A small armada could be deployed for simultaneous testing (Figure 5-11).

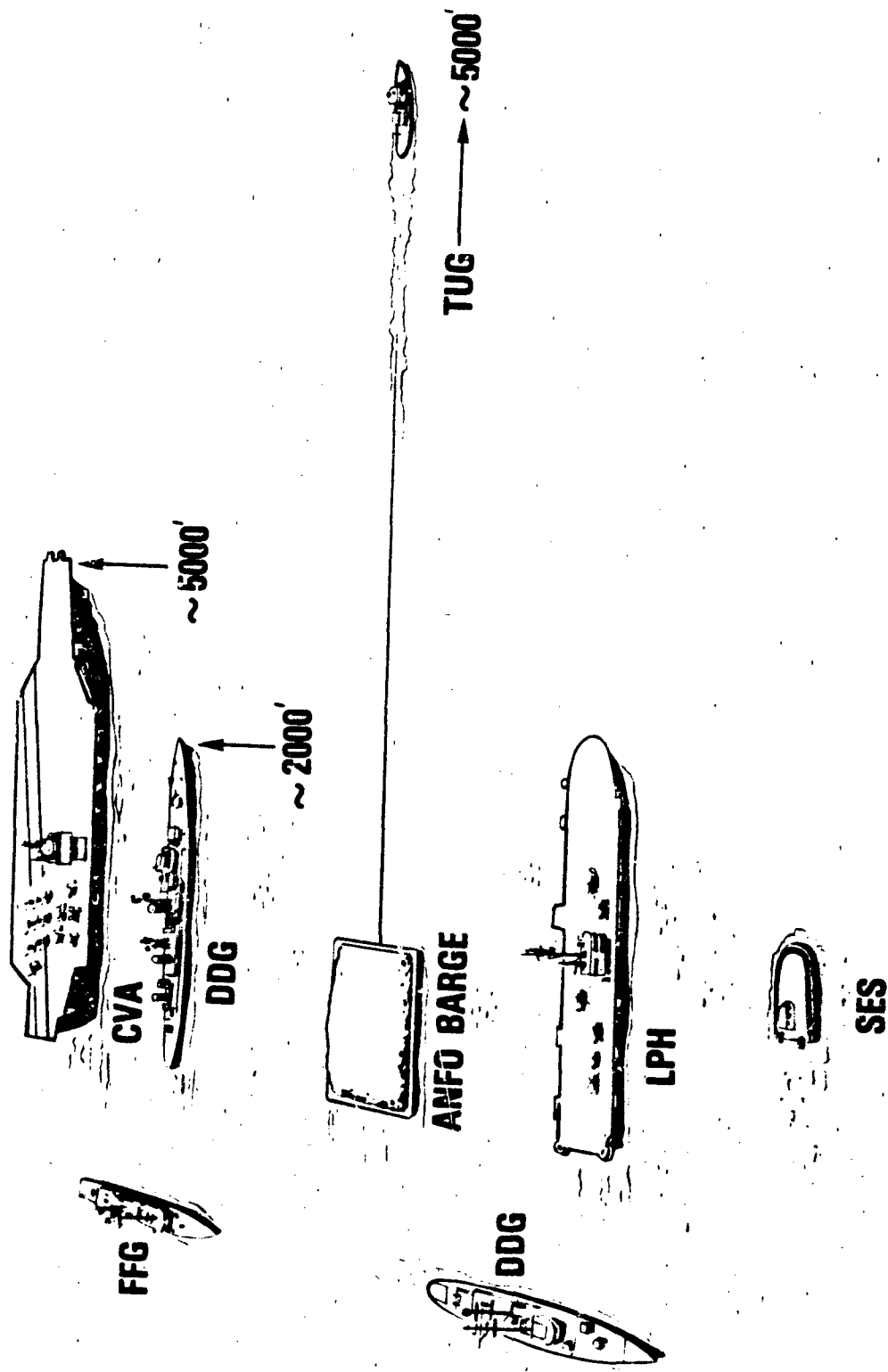


FIGURE 5-11. SEA TRIAL CONCEPT - AT ANCHOR OR UNDERWAY.



To be sure, there are some problems that have to be solved before such a test can be conducted. The blast field has to be determined around exploding ANFO in a barge configuration; the charge geometry will be almost like a semi-cylinder with its longitudinal axis coincident with bottom centerline of the barge. A 5- to 20-ton test would be sufficient to map this field; the scalability of ANFO detonations in any particular geometry has been demonstrated. The underwater shock waves generated by the explosion have to be assessed in terms of their effects on the ships. And the barge debris pattern has to be determined. At the airblast pressure levels of usual interest for ship structure and on-board equipment response studies, both underwater shock and debris effects may be minimal.

Conceptually, ANFO can be used at sea also for underwater shock testing of ships and submarines in situations where present explosive line charge techniques are inadequate. In this concept, at some port facility, bulk ANFO is loaded into a steel or rubber container of appropriate dimensions to hold hundreds of tons of the material. A 12 ft diameter, 42 ft long cylinder would hold about 500 tons. Because the bulk ANFO has a density that is less than that of water, depending on the container weight and the extent to which it is loaded, the loaded container may float and so can be towed to the test site. A positively buoyant charge can be weighted and anchored to give the required depth of burst; a negatively buoyant charge can be supported by buoys. For deep depths of burst, steel container fragments probably would not be of concern; however, for shallow depths, they may be a hazard. Fragment hazards can be avoided completely by using a flexible, bladder-like rubber container. Compression of the ANFO within this container will lead to an increase in bulk density; the greater the depth, the higher the density. At shallow depths this may not be a problem -- the ANFO should detonate reliably; at deeper depths, the problem should be studied in detail.

The experience gained in large underwater shots where an aluminized ammonium nitrate slurry was used as the explosion source can serve as a guide to charge construction, detonation and booster techniques, and field operations (References 4 and 5).

5.5 ANFO USES UNDERGROUND

Underground detonation of large quantities of explosives have been used to simulate nuclear weapons cratering and ground shock effects for both military and civilian purposes. During the 1960's particularly, Project PLOWSHARE was investigating the use of nuclear devices and high explosives for various excavation tasks such as would be suitable for digging a second Panama canal. TNT charges weighing up to 500 tons and nitromethane and ammonium nitrate slurry explosives were used with depths of burial from the surface down to 125 ft. These and other underground detonations were used also to study effects of interest to the military community. With continuing talk at international conference tables of a pact to ban all nuclear weapon testing, it may be that dependence will have to be placed on simulation tests to answer military problems.

ANFO may be a suitable explosion source for underground tests particularly if large quantities -- hundreds and thousands of tons -- are required. It is expected that ANFO will continue to enjoy a price advantage over TNT, nitromethane, and ammonium nitrate slurries or gels; where absolute cost figures rather than comparative ones are of concern, the price edge of ANFO may be important. However, as with other applications of ANFO, the water problem, if present, has to be avoided. This may be difficult and expensive in some cases; obviously, then, ANFO would not be a suitable choice.

5.6 ANFO FUTURE

ANFO has been used successfully on large scale DNA military response tests since 1976. It has proved to be more satisfactory in performance, safety, and cost than other explosives used in the past. But like any evolutionary process, ANFO may not be the end point in simulation sources; it's shortcomings invite continued research and exploration. It is troubled by anomalies which have no explanation. The sought-after homogeneity in charge material is difficult to attain. And its cost is continually increasing. Anomalies may be a fact of nature for large charges; any charge in the tens of tons size may produce them. Homogeneity of density and fuel oil content within limits may not be significant in terms of predictable airblast and ground shock effects. And cost appears to be more than competitive with other explosives.

The explosives community periodically should review the advances in explosives chemistry to seek a closer approximation than ANFO to all the desired, ideal characteristics. And test engineers and scientists should seek other experimental techniques to simulate nuclear proportioned nuclear weapon effects; large shock tubes appear to be a good avenue to follow. Until these other investigations prove fruitful, ANFO can be used with confidence for simulation purposes.

The development program from 1966 on through the test programs starting in 1976, have provided a good basis for future operations. As another inscription at the National Archives says, "Study the Past." This report hopefully provides a review of the past to guide the future.

REFERENCES

1. Reisler, R., "Air Blast Parameters from Pentolite Cylinders Detonated on the Ground in Various Operations," Ballistic Research Laboratories, Aberdeen, MD, BRL Report 2471.
2. Balcerzak, M.J., Johnson, M.R., and Kurz, F.R., "Nuclear Blast Simulation, Part I, Detonable Gas Explosion," General American Research Division, General American Transportation Corporation, 1966.
3. Guerke, G., and Scheklinski-Glueck, G., "Blast Parameters from Cylindrical Charges Detonated on the Surface of the Ground," Ernst Mach Institut, Freiburg, Germany, presented at the DDESB Explosive Safety Seminar, Norfolk, VA, August 1982.
4. Kos, D.W., and Kennedy, J.E., "Development of a System to Deliver and Detonate Large Explosive Charges Undersea," sponsored by The Advanced Research Projects Agency, ARPA Order No. 804, January 1969.
5. Hecht, R.J., Woolston, D.D., Weinstein, M.S., "IITRI 10 Ton 1968 Shot Series," Underwater Systems, Inc., Silver Spring, MD, July 1968.

DISTRIBUTION LIST

DEPARTMENT OF DEFENSE

Assistant to the Secretary of Defense
Atomic Energy
ATTN: Executive Assistant

Commander in Chief, Atlantic
ATTN: J7

Defense Advanced Rsch Proj Agency
ATTN: NMRO, G. Bulin
ATTN: Dir, Strat Tech Off
ATTN: NMRO
ATTN: PMO
ATTN: H. Winsor

Defense Communications Agency
ATTN: Code 510

Defense Electronic Supply Center
ATTN: DEFC-ESA

Defense Intelligence Agency
ATTN: DB-4C, Rsch, Phys Vuln Br
ATTN: DB-4C2, C. Wienle
ATTN: RTS-2A

Defense Nuclear Agency
ATTN: NATO
ATTN: STSP
ATTN: STRA
ATTN: SPTD
ATTN: SPSS
ATTN: STMA
ATTN: SPAS
ATTN: NASF
ATTN: RAAE, H. Fitz, Jr
ATTN: RAAE
4 cy ATTN: STTI/CA

Defense Technical Information Center
12 cy ATTN: DD

Dep Und Sec of Def, Comm, Cmd, Cont & Intel
ATTN: Principal DASD, C3I, M. Van Trees

Department of Defense Explo Safety Board
ATTN: Chairman

Field Command, DMA, Det 1
Lawrence Livermore National Lab
ATTN: FC-1

Field Command, Defense Nuclear Agency
ATTN: FCT
ATTN: FCTT
ATTN: FCTXE
ATTN: FCTT, W. Summa
ATTN: FCPR
ATTN: FCTEI

Field Command Test Directorate
ATTN: FCTC

Interservice Nuclear Weapons School
ATTN: TTV

DEPARTMENT OF DEFENSE (Continued)

Joint Chiefs of Staff
ATTN: GOSO, J-5 Force Plng & Prog Div
ATTN: J-5 Nuclear Div/Strategy Div
ATTN: SAGA

Joint Strat Tgt Planning Staff
ATTN: JLKC
ATTN: JLKS
ATTN: J.L.K., DNA Rep
ATTN: JPST

Under Secy of Def for Rsch & Engrg
ATTN: Engr Tech, J. Persh
ATTN: Strat & Space Sys (CS)

DEPARTMENT OF THE ARMY

Atmospheric Sciences Laboratory
ATTN: DELAS-EO

BMD Advanced Technology Center
ATTN: ATC-O, F Hoke
ATTN: ATC-T, M Capps
ATTN: ICRDABH-X

BMD Program Office
ATTN: DACS-BMZ
ATTN: DACS-BMT

BMD Systems Command
ATTN: BMDSC-HW

Chief of Engineers
ATTN: DAEN-RDL

Harry Diamond Laboratories
ATTN: DELHD-MW-RA, L. Belliveau, 22100
ATTN: DELHD-TA-L, 81100
ATTN: DELHD-MW-P, 20240
ATTN: DELHD-DTSD, 00103

US Army Armament Material Readiness Command
ATTN: Mm Library

US Army Armament Rsch Dev & Cmd
ATTN: DRDAR-LCW

US Army Ballistic Research Labs
ATTN: DRDAR-BLT, W. Schuman
ATTN: DRDAR-BLT, W. Taylor
ATTN: DRDAR-BLA-S
ATTN: DRDAR-BLT, J. Keefer

US Army Chemical School
ATTN: ATZN-CM-TPR

US Army Cold Region Res Engr Lab
ATTN: Technical Director

US Army Comb-Elec Engrg Instal Agency
ATTN: Tech Library

US Army Communications R&D Command
ATTN: DRDCO-COM RM, L. Dorkin

DEPARTMENT OF THE ARMY (Continued)

US Army Communications Command
ATTN: CC-OPS-WR, R. Nelson
ATTN: Tech Reference Div
ATTN: CC-OP-PD

US Army Electronics R&D Command
ATTN: DELET-ER

US Army Engineer Ctr & Ft Belvoir
ATTN: DT-LRC
ATTN: AT2A-DTE-ADM

US Army Engineer Div Huntsville
ATTN: HNDDE-CS, E. Williams
ATTN: HNDDE-SR

US Army Engineer Div Ohio River
ATTN: ORDAS-L

US Army Engr Waterways Exper Station
ATTN: WESSA, W. Flathau
ATTN: Library
ATTN: WESSE
ATTN: WESSS, J. Ballard

US Army Foreign Science & Tech Ctr
ATTN: DRXST-SO

US Army Materiel Dev & Readiness Cmd
ATTN: DRXAM-TL
ATTN: DRCDF-D

US Army Mobility Equip R&D Cmd
ATTN: DRDME-WC

US Army Nuclear & Chemical Agency
ATTN: MONA-WF
ATTN: Library
ATTN: MONA-OPS

US Army Tank Automotive R&D Command
ATTN: DRDTA-UL

US Army TRADOC Sys Analysis Actvy
ATTN: ATAA-TDC, R. Benson

US Army Training and Doctrine Comd
ATTN: ATORI-OP
ATTN: ATCD-T

US Army White Sands Missile Range
ATTN: STEWS-TE-AM, R. Nays
ATTN: STEWS-FE-R
ATTN: STEWS-TN-W, K. Cummings
ATTN: STEWS-TE-W, T. Arellanes

USA Missile Command
ATTN: DRSMI-RM
ATTN: DRSMI-MEA, D. Loney

DEPARTMENT OF THE NAVY

David Taylor Naval Ship R&D Ctr
ATTN: Code 142-3

Naval Air Systems Command
ATTN: AIR-360G JP-2, J. Schultz

DEPARTMENT OF THE NAVY (Continued)

Naval Coastal Systems Laboratory
ATTN: D. Sheppard

Naval Electronic Systems Command
ATTN: PME 117-21

Naval Facilities Engineering Command
ATTN: Code 048

Naval Material Command
ATTN: MAT 08T-22

Naval Research Laboratory
ATTN: Code 6770
ATTN: Code 2627
ATTN: Code 5584, E. Friebele
ATTN: 4700, W. Ali
ATTN: 4720, J. Davis
ATTN: Code 7780
ATTN: Code 5584, G. Sigel

Naval Surface Weapons Center
ATTN: Code E21
ATTN: Code X211
ATTN: Code R15, Mr Swisdak

Naval Surface Weapons Center
ATTN: Tech Library & Info Svcs Br
ATTN: W. Wishard

Naval Weapons Center
ATTN: Code 343, FKA6A2, Tech Svcs
ATTN: Code 3263, J. Bowen
ATTN: Code 266, C. Austin

Naval Weapons Evaluation Facility
ATTN: Code 10
ATTN: R. Hughes

Ofc of the Deputy Chief of Naval Ops
ATTN: NOP 654, Strat Eval & Anal Br

Office of Naval Research
ATTN: Code 474, M. Perrone

Strategic Systems Project Office
ATTN: NSP-43

DEPARTMENT OF THE AIR FORCE

Aeronautical Systems Division
ATTN: ASD/ENSSA

Air Force
ATTN: INT

Air Force Armament Laboratory
ATTN: DLYV, J. Collins

Air Force Institute of Technology
ATTN: Library

Assistant Chief of Staff, Intelligence
ATTN: IN

Sacramento Air Logistics Center
ATTN: MNEAE, R. Dallinger

DEPARTMENT OF THE AIR FORCE (Continued)

Air Force Weapons Laboratory
ATTN: NTES-C, R. Henny
ATTN: NTED, R. Matalucci
ATTN: NTE, M. Plamondon
ATTN: SUL
ATTN: DEX
ATTN: NTES-G

Ballistic Missile Office/DAA
ATTN: ENSN
ATTN: SYM

Deputy Chief of Staff
Research, Development & Acq
ATTN: AFRD

Foreign Technology Division
ATTN: NIS Library
ATTN: SOBF, S. Spring

Space Division
ATTN: YGD, L. Doan

Strategic Air Command
ATTN: DOWE
ATTN: DOCSO
ATTN: XPFS
ATTN: MRI/STINFO Library
ATTN: INAO

DEPARTMENT OF ENERGY

Department of Energy
Albuquerque Operations Office
ATTN: Tech Library

Department of Energy
Nevada Operations Office
ATTN: Doc Con for Tech Library

OTHER GOVERNMENT AGENCIES

Central Intelligence Agency
ATTN: OSWR/NEO

Department of Commerce National Bureau of Stnds
ATTN: Sec Ofc for R. Levine

Federal Emergency Management Agency
ATTN: Ofc of Rsch/NP, D. Bensen

OTHER

Brookhaven National Laboratory
ATTN: P. Levy

DEPARTMENT OF ENERGY CONTRACTORS

University of California
Lawrence Livermore National Lab
ATTN: L-14, W. Dickinson
ATTN: Tech Info Dept Library
ATTN: B. Hudson
ATTN: L-21, D. Oakley

Oak Ridge National Laboratory
ATTN: Central Rsch Library
ATTN: Civ Def Res Proj, Mr Kearny

DEPARTMENT OF ENERGY CONTRACTORS (Continued)

Los Alamos National Laboratory
ATTN: R. Brownlee
ATTN: MS/410, P. Lyons
ATTN: M. Pongratz
ATTN: R. Thorn
ATTN: Reports Library
ATTN: MS 218, P. Whalen
ATTN: C. Keller
ATTN: MS 670, J. Hopkins
ATTN: Librarian

Sandia National Laboratories
ATTN: Library & Security Classification Div

Sandia National Laboratories
ATTN: J. Walker
ATTN: Div 9722, J. Holmes
ATTN: Org. J. Bear
ATTN: Org 2330, B. Benjamin
ATTN: Org 7110, C. Broyles
ATTN: Div 1531, P. Adams
ATTN: J. Plimpton
ATTN: L. Anderson
ATTN: Tech Library 3141
ATTN: L. Vortman

DEPARTMENT OF DEFENSE CONTRACTORS

Acurex Corp
ATTN: J. Stockton

Aerospace Corp
ATTN: L. Selzer
ATTN: Library Acquisition M1/199

Applied Theory, Inc
2 cy ATTN: J. Trulio

ARTEC Associates, Inc
ATTN: D. Baum

AVCO Systems Division
ATTN: W. Reinecke
ATTN: Library A830
ATTN: A. Pallone

BDM Corp
ATTN: Corporate Library

Boeing Co
ATTN: Aerospace Library
ATTN: M/S 85/20, E. York
ATTN: R. Holmes

Boeing Co
ATTN: MS 86-01, A. Lunde
ATTN: M/S 42/37, K. Friddell
ATTN: MS 86-01, S. Durick

California Research & Technology, Inc
ATTN: F. Sauer

Carpenter Research Corp
ATTN: H. Carpenter

Charles Stark Draper Lab, Inc
ATTN: Tech Library

DEPARTMENT OF DEFENSE CONTRACTORS (Continued)

University of Dayton
ATTN: R. Servais
ATTN: B. Wilt
ATTN: D. Gerdeman
ATTN: N. Olson

University of Denver, Colorado Seminary
ATTN: Sec Officer for J. Wisotski

EG&E Wash Analytical Svcs Ctr, Inc
ATTN: Library

EG&G, Inc
ATTN: P. Zavaharo

Electro-Mech Systems, Inc
ATTN: R. Shunk

GARD
ATTN: G. Neidhardt

General Research Corp
ATTN: E. Bick
ATTN: R. Parisse

GEO Centers, Inc
ATTN: E. Marrae

Georgia Institute of Technology
ATTN: EES/EMSL/Solar Site, C. Brown

H&I Consultants, Inc
ATTN: W. Hall

H-Tech Labs, Inc
ATTN: B. Hartenbaum

Horizons Technology, Inc
ATTN: R. Kruger

IIT Research Institute
ATTN: Documents Library
ATTN: A. Longinow

Information Science, Inc
ATTN: W. Dudziak

JAYCOR
ATTN: L. Scott

Kaman Avidyne
ATTN: Library
ATTN: N. Hobbs

Kaman Sciences Corp
ATTN: Library

Kaman Sciences Corp
ATTN: E. Conrad

Kaman Tempo
ATTN: W. Chan
ATTN: DASIAC
ATTN: J. Shoutens

Karagozian and Case
ATTN: J. Karagozian

DEPARTMENT OF DEFENSE CONTRACTORS (Continued)

Kaman Tempo
2 cy ATTN: J. Petes
2 cy ATTN: R. Miller
2 cy ATTN: F. McMullan
5 cy ATTN: DASIAC

Lockheed Missiles & Space Co, Inc
ATTN: J. Bronko
ATTN: D. Kohler
ATTN: L. Chase
ATTN: S. Salisbury
ATTN: R. Smith
ATTN: T. Fisher
ATTN: R. Bardin

Lockheed Missiles & Space Co, Inc
ATTN: TIC-Library

Los Alamos Technical Associates, Inc
ATTN: C. Sparling
ATTN: P. Hughes
ATTN: J. Kimmerly

Magnavox Govt & Indus Electronics Co
ATTN: W. Richesor

Management Science Associates
ATTN: K. Kaplan

Martin Marietta Denver Aerospace
ATTN: D-607A, G. Freyer

Merritt Cases, Inc
ATTN: Library

Mission Research Corp
ATTN: Tech Library

National Academy of Sciences
ATTN: National Materials Advisory Board

University of New Mexico
ATTN: G. Lane
ATTN: E. Wang
ATTN: Tech Library
2 cy ATTN: D. Calhoun

New Mexico State University Board of Regents
ATTN: T. McConnell
ATTN: W. Stevens

Nichols Research Corp, Inc
ATTN: N. Byrn

Pacific-Sierra Research Corp
ATTN: H. Brode, Chairman SAGE

Pacifica Technology
ATTN: Tech Library

Physics Applications, Inc
ATTN: F. Ford

Physics International Co
ATTN: Tech Library
ATTN: J. Shee

DEPARTMENT OF DEFENSE CONTRACTORS (Continued)

R&D Associates

ATTN: Tech Information Center
ATTN: P. Rausch
ATTN: A. Kuhl
ATTN: D. Simons
ATTN: P. Haas
ATTN: C. Lee
ATTN: F. Field

R&D Associates

ATTN: B. Yoon

Rand Corp

ATTN: P. Davis

Rand Corp

ATTN: B. Bennett

Rockwell international Corp

ATTN: Library

S-CUBED

ATTN: R. Duff
ATTN: Library

Science & Engrg Associates, Inc

ATTN: B. Chambers III

Science Applications, Inc

ATTN: W. Plovs
ATTN: Tech Library

Science Applications, Inc

ATTN: J. McRary
ATTN: R. Deliberis

Science Applications, Inc

ATTN: Technical Library

TRW Electronics & Defense Sector

ATTN: P. Dai
ATTN: G. Hulcher

DEPARTMENT OF DEFENSE CONTRACTORS (Continued)

Science Applications, Inc

ATTN: W. Layson
ATTN: W. Chadsey
ATTN: W. Koehner
ATTN: G. Binninger
ATTN: R. Sievers
ATTN: M. Knasel
ATTN: J. Cockayne

Science Applications, Inc

ATTN: K. Sites

Southwest Research Institute

ATTN: W. Baker

SRI International

ATTN: A. Burns
ATTN: G. Abrahamson
ATTN: D. McDaniels
ATTN: D. Keough

Teledyne Brown Engineering

ATTN: J. Ravenscraft
ATTN: F. Leopard
ATTN: MS-12 Tech Library
ATTN: D. Ormond

Tetra Tech, Inc

ATTN: Library

TRW Electronics & Defense Sector

ATTN: N. Lipner
ATTN: B. Sussholtz
ATTN: J. Tambe
ATTN: R. Eastman
ATTN: Tech Info Center

Tech Reqs, Inc

ATTN: R. Flory

END

FILMED

4-85

DTIC